

SANNA SILJANDER

# Nanoarchitectonics of Nanocellulose-Carbon Nanotube Composites

From Dispersion to Functional Structures



SANNA SILJANDER

Nanoarchitectonics of Nanocellulose-  
Carbon Nanotube Composites  
From Dispersion to Functional Structures

ACADEMIC DISSERTATION

To be presented, with the permission of  
the Faculty of Engineering and Natural Sciences  
of Tampere University,  
for public discussion in the auditorium FA032 Pieni Sali 1  
of the Festia, Korkeakoulunkatu 8, Tampere,  
on 4<sup>th</sup> of November, at 12 o'clock.

ACADEMIC DISSERTATION  
Tampere University, Faculty of Engineering and Natural Sciences  
Finland

<i>Responsible supervisor and Custos</i>	Professor Jyrki Vuorinen Tampere University Finland	
<i>Supervisors</i>	Senior Research Fellow Tomas Björkqvist Tampere University Finland	Associate Professor Mikko Kanerva Tampere University Finland
<i>Pre-examiners</i>	Professor Kristiina Oksman Luleå University of Technology Sweden	Professor Orlando Rojas The University of British Columbia Canada
<i>Opponents</i>	Professor Kristiina Oksman Luleå University of Technology Sweden	Professor Eero Kontturi Aalto University Finland

The originality of this thesis has been checked using the Turnitin Originality Check service.

Copyright ©2022 Sanna Siljander

Cover design: Roihu Inc.

ISBN 978-952-03-2616-6 (print)

ISBN 978-952-03-2617-3 (pdf)

ISSN 2489-9860 (print)

ISSN 2490-0028 (pdf)

<http://urn.fi/URN:ISBN:978-952-03-2617-3>



Carbon dioxide emissions from printing Tampere University dissertations have been compensated.

PunaMusta Oy – Yliopistopaino  
Joensuu 2022

**To Miana**

**Creativity is intelligence having fun**

*- Albert Einstein*



# ACKNOWLEDGEMENTS

The research work presented in this thesis was conducted during 2016-2022 in the Faculty of Engineering and Natural Sciences unit of Material Science and Environmental Engineering and unit of Automation and Mechanical Engineering. This research was made possible by financial support from Tekes (the Finnish Funding Agency for Innovation), The Council of Tampere Region (Pirkanmaan liitto) and The European Regional Development Fund (ERDF).

Design Driven Value Chains in the World of Cellulose (DWoC) was a multidisciplinary research collaboration project. The project focused on finding new and innovative applications for cellulosic materials. The DWoC project combined design thinking and design-driven prototyping with strong competence in technology development. Collaboration during the project with professionals like Professor Ali Harlin, Kirsi Kataja and Professor Pirjo Kääriäinen I will value deeply for years to come.

ERDF funded Bio-based Intelligent Solutions Platform for Reinforcing Local Circular Economy (BioÄly) project focused on implementing novel technology demos and pilots for network collaborators and partners in the ecosystem. Aulis Lundell Oy CEO Leena Lundell and BioÄly team members are gratefully acknowledged.

First of all, I would especially like to thank Professor Jyrki Vuorinen for believing in me and giving me endless guidance in the world of composites. Without you, I would not even have started my Ph.D. studies. Thank you for this opportunity, now I can say that I truly master arts and crafts.

I also wish to express my gratitude to my supervisor Tomas Björkqvist for inviting me to work on the BioÄly project. I am thankful to you for your help, moral support, and all the great discussions about everything under the sun. I hope that we will work together in the future for it has been a true pleasure.

A warm thank you to all the co-authors and collaborators, Pasi Keinänen, Anna Rätty, Mikko Koivula, Jani Lehmonen, Anastasia Ivanova, Atsushi Tanaka, Karthik Ram Ramakrishnan, Vesa Kunnari, Antti-Juhana Mäki, Olli Tanhuanpää, Mari Honkanen, Alexander Efimov, Sampo Tuukkanen, Professor Pasi Kallio and Professor Mikko Kanerva for their contribution to my research and for the fruitful

collaboration. Nevertheless, the deepest gratitude I am giving to Pasi Keinänen who has been my guide and "partner in crime" during these years.

A very special thank you goes to Anne Skogberg for your friendship, innovative collaboration, and our enlightening discussions. Unexpected discoveries with you have truly ravaged my boat but luckily also provided a warm swimming ring.

Furthermore, I want to acknowledge all my current and former colleagues in the Composites and elastomer technology group, Automation technology unit, and Nanocellulose research group. Thanks also belong to my dear friends Katja, Sirke, Teemu and Karo who have been my support and had time to listen to me during these years as well as to my dear aunties Anneli, Marja and Tarja with their endless questions about what it actually is that I do.

I'd like to express my loving gratitude, with open arms, to my little brother Markus Kakkonen for his expertise and endless encouragement during the years we have worked together. My deepest gratitude I want to express to my parents Arja and Matti Kakkonen, for their love and support throughout my life and my studies.

Thanks to my beloved husband and soulmate Toni for being my everything. Finally, I dedicate this work to our child Miana. Thank you for your love, support, patience, and unwavering faith in my abilities during this thesis.

Pälkäne, 22.2.2022

*Sanna Siljander*



# ABSTRACT

The dissertation research seeks to identify parameters and phenomena that affect the properties of nanocellulose carbon nanotube (NC-CNT) composites, among others, on electrical conductivity. Nanocellulose provides the composite structure with an environmentally friendly, inexpensive, high-strength, dimensional, indigestible, non-toxic non-metallic matrix or it can serve as a carrier for other nanomaterials such as carbon nanotubes.

The properties of the NC-CNT composite being produced are strongly dependent on the quality of CNT dispersion, the length—width ratio of the nanotubes after the dispersion process, and the strength of the matrix, not forgetting the interactions between carbon nanotubes and nanocellulose matrix. When comparing electrical conductivities of cellulose-CNT composites reported in current scientific literature, it can be stated that several composite structures have an inefficient flow of current. First, conducting particles may not form an efficient percolation network, and second, inadequate distribution procedure results in a composite structure containing agglomerates of conductive particles. The main reason might still be that, in the formed composite structure, insulating matrix material is obstructing the flow of the electrons. These attributes are not thoroughly researched in current scientific literature and are addressed in this thesis.

The nanoarchitectonics concept, which utilizes several research fields and technologies to enable the creation of hybrid and composite material systems, has been chosen as an approach to the research. Nanoarchitectonics combines materials science, nanotechnology, and chemistry to overcome the challenges that arise when working with nanomaterials.

The research is divided into sections by examining two-, three-, and four-component systems, and identifying which parameters affect interactions between nanomaterials, as well as how the properties of nanocomposites can be further modified even after manufacturing. Throughout the entire dissertation study, a guideline aiming to use only a minimum amount of materials, chemicals, and energy in the manufacture of composites has been followed.

The main results include exemplary electrical conductivity of nano fibrillated cellulose (NFC) carbon nanotube composite films, the highest reported in the

literature at a comparatively low 16.7 w-% CNT concentration. This result was achieved by varying the concentration of different types of surfactants and looking at the effect of sonication energy, both on CNT dispersion quality and on the electrical conductivity of the film form composites made from NFC-CNT dispersion. In the processing of composite films, a manufacturing technique utilizing centrifugal force was used and the formed NFC-CNT composite was found to create a homogeneous and tightly compressed structure in the thickness direction of the film. Post processing of the prepared composite films, where surfactant assisting dispersing of nanomaterials was removed from interfaces, the electrical conductivity of the NFC-CNT composite was further increased.

In addition, the thesis study verified for the first time that cationic cellulose nanofibers (c-CNFs) can be used to disperse carbon nanotubes to form homogeneous and stable c-CNF-CNT dispersion. Notable results can also be attributed to the observation of the size distribution of nanocellulose relative to carbon nanotubes and its effects on electrical conductivity properties, and additionally the use of nanocellulose as a carrier of carbon nanotubes, e.g., in foam forming.

Based on the observations and results made during the dissertation study, the ambitious goal of the four component system manufacturing process was set and realized. Goal was to select the surfactant so that it would function both in the formation of stable homogeneous NFC-CNT dispersion and as a foam former in formation process. In this case, the amount of chemicals used is clearly reduced when they play multiple roles in the manufacturing process of flat and 3D composite structures.

This thesis research sets the foundation for future research of NC-CNT composite structures. Correlation between structure and functions was observed in this thesis, that especially size distribution of cellulose plays a crucial role in creating optimized conductivity with a limited amount of CNTs, while retaining the required mechanical strength characteristics of the conductive material. It can be expected that even higher electrical conductivity values can be achieved when nanocellulose aspect ratio is optimized to match the size of the CNTs so that NC surfaces are comprehensively coated with carbon nanotubes to form an electrically conductive percolation network. However, it should be noted that the research focused on achieving excellent electrical properties for NFC-CNT composite material, whereas the desire is to optimize, for example, mechanical properties of the composite material, the energy required to disperse used nanomaterials and the size ratios of those materials may differ considerably.

As an exception from the usual dissertation work, the results achieved in the study have been concretized when functional heating elements have been produced based on two different processes. The first heating element "Salmiakki" has been featured in several seminars and fairs in addition to media prominence. The second heating element solution got closer to the public from the research world when it was integrated into the Liune sliding door and presented at the "Pyörre" exhibition house of Lohja Housing Fair 2021.



# TIIVISTELMÄ

Väitöskirjatutkimuksessa pyrittiin selvittämään parametrejä ja ilmiöitä, mitkä vaikuttavat nanoselluloosa-hiilinanoputki (NC-CNT) komposiittien ominaisuuksiin mm. sähkönjohtavuuteen. Nanoselluloosa tarjoaa komposiittirakenteelle ympäristöystävällisen, edullisen, erittäin lujan, mittapysyvän, sulamattoman, myrkyttömän ei metallisen matriisin tai se voi toimia kantajana muille nanomateriaaleille, kuten hiilinanoputkille.

Valmistettavan NFC-CNT komposiitin ominaisuudet ovat kuitenkin vahvasti riippuvaisia CNT-dispersion laadusta, nanoputkien pituus-levyysuhteesta disperkointiprosessin jälkeen ja matriisin lujuudesta, unohtamatta hiilinanoputkien ja nanoselluloosan matriisin keskinäisiä vuorovaikutuksia. Kun tarkastellaan tieteellisessä kirjallisuudessa raportoitujen selluloosa-CNT-komposiittien sähkönjohtavuusarvoja, voidaan todeta, että komposiittirakenteissa sähkövirran liikkuminen on vajavaista. Ensimmäiseksi, sähkövirtaa johtava materiaali ei välttämättä muodosta tehokasta perkolaatioverkostoa, ja toiseksi, disperkointimenetelmä johtaa komposiittirakenteeseen, joka sisältää johtavan materiaalin muodostamia agglomeraatteja. Tärkein syy voi silti olla, että eristävä matriisimateriaali estää komposiittirakenteessa elektronien liikkeen kokonaan tai osittain. Näitä muuttujia ei tutkita perusteellisesti nykyisessä tieteellisessä kirjallisuudessa ja siksi niitä käsitellään tässä väitöskirjatutkimuksessa.

Tutkimuksen lähestymistavaksi on valittu nanoarkkitehtoniikka -konsepti, joka hyödyntää useita tutkimusaloja ja teknologioita, jotta hybridi- ja komposiittimateriaalisysteemien luominen mahdollistuu. Nanoarkkitehtoniikka yhdistää poikkitieteellisesti materiaalioppia, nanoteknologiaa ja kemiaa, jotta nanomateriaalien kanssa työskennellessä ilmenevät haasteet voidaan selättää.

Tutkimus on jaettu osiin tutkimalla kaksi-, kolme- ja neljäkomponenttisysteemejä, ja tunnistamalla mitkä parametrit vaikuttavat nanomateriaalien keskinäisiin vuorovaikutuksiin sekä miten valmistettavan nanokomposiitin ominaisuuksia voidaan edelleen muokata valmistuksen jälkeenkin. Läpi koko väitöskirjatutkimuksen on noudatettu ohjenuoraa, jonka tavoitteena on käyttää ainoastaan minimimäärä materiaaleja, kemikaaleja ja energiaa komposiittien valmistuksessa.

Keskeisimpiin tuloksiin lukeutuu nanofibrilloidun selluloosan (NFC)-hiilinanoputkikomposiitti-kalvojen hyvä sähkönjohtavuus, joka on korkein kirjallisuudessa ilmoitettu verrattain vähäisellä 16,7 p-% CNT-pitoisuudella. Tämä tulos saavutettiin varioimalla sekä CNT että NFC-CNT dispersion valmistusvaiheessa erityyppisten surfaktanttien pitoisuutta ja tarkastelemalla sonikaatioenergian vaikutusta, niin CNT dispersion laatuun kuin NFC-CNT dispersiosta valmistettujen kalvomuotoisten komposiittien sähkönjohtavuuteen. Komposiittikalvojen prosessoinnissa käytettiin keskipakovoimaa hyödyntävää valmistustekniikkaa ja muodostuneen NFC-CNT komposiitin havaittiin luovan kalvon paksuussuuntaan homogeenisen ja tiiviisti pakkautuneen rakenteen. Suorittamalla valmistetuille komposiittikalvoille jatkokäsittely, missä poistettiin nanomateriaalien rajapinnoilta disperkoinnissa apuna käytetty surfaktantti, saatiin NFC-CNT komposiitin sähkönjohtavuutta edelleen kasvatettua.

Lisäksi väitöskirjatutkimuksessa todennetaan ensimmäistä kertaa, että katinoitua nanoselluloosaa (c-CNF) voidaan käyttää hiilinanoputkien disperkoimiseen, jolloin muodostuu homogeeninen ja stabiili c-CNF-CNT dispersio. Merkittäviin tuloksiin voidaan myös lukea havainto nanoselluloosan kokojakaumasta suhteessa hiilinanoputkiin ja sen vaikutuksista sähkönjohtavuusominaisuuksiin, ja lisäksi nanoselluloosan käyttö hiilinanoputkien kantajana esim. vaahtorainauksessa.

Väitöskirjatutkimuksen aikana tehtyjen huomioiden ja tulosten pohjalta asetettiin sekä toteutettiin neljäkomponenttisysteemin valmistusprosessin kunnianhimoinen tavoite. Tavoitteena oli valita käytettävä surfaktantti niin, että se toimii sekä stabiilin homogeenisen NFC-CNT dispersion muodostuksessa kuin myös vaahtorainauksen vaahdonmuodostaja. Tällöin käytettävien kemikaalien määrä vähenee selvästi, kun niillä on useampi rooli tasamaisten sekä 3D-komposiittirakenteen valmistusprosessissa.

Tämä väitöskirjatutkimus asettaa perustan NC-CNT-komposiittirakenteiden tulevalle tutkimukselle. Tutkimuksessa havaittiin rakenteen ja funktionaalisuuden välinen korrelaatio, että erityisesti selluloosan kokojakaumalla on ratkaiseva rooli optimoidun johtavuuden luomisessa rajoitetulla määrällä hiilinanoputkia, säilyttäen samalla johtavan materiaalin vaaditut mekaaniset lujuusominaisuudet. Oletettavasti vielä korkeammat sähkönjohtavuusarvot voidaan saavuttaa, kun nanoselluloosan pituus-leveysuhde on optimoitu vastaamaan CNT:n kokoa siten, että NC-pinnat pinnoittuvat hiilinanoputkilla kattavasti muodostaen sähköjohtavan perkolaatioverkon. Huomioitavaa on kuitenkin, että tutkimus keskittyi saavuttamaan erinomaiset sähköiset ominaisuudet NFC-CNT komposiittimateriaalille. Jos taas halutaan optimoida esimerkiksi mekaaniset ominaisuudet, voi nanomateriaalien

disperkoimiseen tarvittava energia ja materiaalien keskinäiset kokosuhteet poiketa toisistaan huomattavasti.

Tavanomaisesta väitöskirjatutkimuksesta poiketen tutkimuksessa saavutetut tulokset on konkretisoitu, kun niiden pohjalta on valmistettu kahdella eri prosessilla toiminnalliset lämmityselementit. Ensimmäinen lämmityselementti "Salmiakki" on ollut esillä useissa seminaareissa ja messuilla medianäkyvyyden lisäksi. Toinen lämmityselementti pääsi tutkimusmaailmasta lähemmäksi kansaa, kun se implementoitiin osaksi Liune-liukuvaa väliovea ja esiteltiin Lohjan Asuntomessujen 2021 Pyörre -messutalossa.





# CONTENTS

1	Introduction .....	1
2	Material components and properties .....	5
	2.1 Carbon nanotubes.....	5
	2.2 Cellulosic materials .....	7
3	Nanoarchitectonics .....	13
	3.1 Self-assembly .....	14
	3.2 Nanocellulose functionalization .....	16
	3.3 Chemical manipulation using surfactants .....	17
4	Processing electrically conductive composites .....	21
	4.1 Two-component systems .....	23
	4.1.1 Nanocellulose as a dispersing agent .....	23
	4.1.2 Interactions between nanocellulose and surfactant.....	24
	4.1.3 Interactions between CNT and surfactant.....	24
	4.2 Three-component systems of NC-CNT surfactant.....	25
	4.2.1 Composite structure from three-component system.....	26
	4.3 Foam forming using NC-CNT surfactant dispersion with pulp .....	27
5	Recent research related to cellulose-CNT composites .....	29
6	The aims of this thesis.....	35
	6.1 Research questions .....	36
7	Experimental.....	37
	7.1 Materials .....	37
	7.2 Preparation of dispersions and composites.....	38
	7.2.1 Two-component system of MWCNT-surfactant dispersions.....	39
	7.2.2 Two-component system of CNF-MWCNT dispersions.....	39
	7.2.3 Three-component system of NFC-MWCNT-surfactant dispersions.....	41
	7.2.4 Four-component system of NFC-MWCNT surfactant and pulp .....	42
	7.3 Characterization .....	45

8	Results and discussion .....	47
8.1	Effect of sonication energy and surfactant type .....	47
8.1.1	Quality of CNT dispersion .....	47
8.1.2	Conductivity of NFC-CNT nanocomposite.....	48
8.2	Post-processing to enhance integrity of CNT percolation network.....	50
8.2.1	Mechanical strength of NFC-CNT pulp non-wovens.....	51
8.3	Dispersing action of c-CNF .....	52
8.3.1	Non-templated self-assembly .....	53
8.4	Effect of cellulose aspect ratio to electrical conductivity .....	54
8.4.1	NFC as a carrier for CNTs .....	57
8.5	Verification and validation of applicability .....	58
8.5.1	"Salmiakki" heating element .....	59
8.5.2	Bio-based heating element integrated into the sliding door.....	61
8.6	Affecting attributes to electrical conductivity in NC-CNT composites .....	65
9	Conclusions .....	67
9.1	Research question 1 .....	70
9.2	Research question 2 .....	70
9.3	Research question 3 .....	70
9.4	Research question 4 .....	71
9.5	Research question 5 .....	71
10	References.....	73

# ORIGINAL PUBLICATIONS AND DEMONSTRATION

**Publication I**                      **Optimized dispersion quality of aqueous carbon nanotube colloids as a function of sonochemical yield and surfactant/CNT ratio**

Keinänen, Pasi; Siljander, Sanna; Koivula, Mikko; Sethi, Jatin; Sarlin, Essi; Vuorinen, Jyrki; Kanerva, Mikko.

Heliyon, Vol. 4, No. 9, e00787, 2018

<https://doi.org/10.1016/j.heliyon.2018.e00787>

**Publication II**                      **Effect of surfactant type and sonication energy on the electrical conductivity properties of nanocellulose-CNT nanocomposite films**

Siljander, Sanna; Keinänen, Pasi; Rätty, Anna; Ramakrishnan, Karthik Ram; Tuukkanen, Sampo; Kunnari, Vesa; Harlin, Ali; Vuorinen, Jyrki; Kanerva, Mikko.

International Journal of Molecular Sciences, Vol. 19, No. 6, 1819, 2018

<https://doi.org/10.3390/ijms19061819>

**Publication III**                      **Self-assembled cellulose nanofiber–carbon nanotube nanocomposite films with anisotropic conductivity**

Skogberg, Anne; Siljander, Sanna; Mäki, Antti-Juhana; Honkanen, Mari; Efimov, Alexander; Hannula Markus; Lahtinen, Panu; Tuukkanen, Sampo; Björkqvist, Tomas and Kallio, Pasi

Nanoscale, 14, 448-463, 2022

<https://doi.org/10.1039/d1nr06937c>

**Publication IV****Conductive cellulose-based foam formed 3D shapes—  
from innovation to designed prototype**

Siljander, Sanna; Keinänen, Pasi; Ivanova, Anastasia;  
Lehmonen, Jani; Tuukkanen, Sampo; Kanerva, Mikko;  
Björkqvist, Tomas.

Materials, Vol. 12, No. 3, 430, 2019.

<https://doi.org/10.3390/ma12030430>

**Demonstration**

Bio-based heating element integrated into sliding Liune door. Presented at Housing Fair (Asuntomessut), 2021 Lohja in the Pyörre house.

<https://www.pyörre-talo.fi/liuneliukuovet>

<https://www.asuntomessut.fi/lohja-2021/kohteet/7-pyorre-talo>

# AUTHOR'S CONTRIBUTION

In Publications II and IV candidate Sanna Siljander was the main author and researcher. In publication III main author responsibility was equally divided with Anne Skogberg. Publication I was conducted with Pasi Keinänen and all other authors.

The candidate planned the experiments in publications I-IV and conducted most of the research work by preparing materials, dispersions, nanocomposites, and 3D structures in publications II and IV. The candidate carried out measurements with the support of Mikko Koivula and Anna Rätty in publications I and II. Analyses were performed mainly by the candidate and with Pasi Keinänen in publication I and with Anne Skogberg in publication III

Candidate wrote the manuscripts primarily in publications II and IV, and with the collaboration of Pasi Keinänen in publication I and with Anne Skogberg in publication III. Manuscripts were commented by supervisors prof. Jyrki Vuorinen, prof. Mikko Kanerva and Dr. Tomas Björkqvist. All the co-authors commented on the publications presented in this thesis.

Knowhow from Publications I, II and IV was utilized when the candidate fabricated three bio-based heating elements, which were integrated into the sliding Liune door and showcased at the housing fair at Lohja Finland 2021.



# 1 INTRODUCTION

Value-added "green" products provide a sustainable alternative to overcome the increasing demand for technological development by using non-fossil resources. Meanwhile, nano-sized multi-component materials are in the focus of cumulative interest because they can offer multi-functional characteristics such as excellent electrical conductivity and enhanced mechanical properties. This is because nanomaterials, such as nanocellulose (NC) and carbon nanotubes (CNT), possess unique physical and chemical characteristics due to their high surface area and nanoscale size (Dufresne 2013; Haghi 2012). The preparation of functional materials can be done by assembling a range of nanomaterials into hierarchical and organized structures. Their individual specific properties can be combined, resulting in advanced integrated systems, nanocomposites. In multiple application areas, such as batteries, supercapacitors, and solar cells, functional cellulose-based nanocomposite products are showing their great potential in means of excellent mechanical, chemical and physical properties.

The nanoarchitectonics utilizes several interdisciplinary research fields, methods, and techniques that are used to counter challenges rising from the nanoscale such as unexpected disturbances and fluctuations. These uncontrollable factors are rising from interactions between nanoscale components' atoms, molecules, and materials. Therefore, it is essential to control materials' organization, dimensions, compositions, and possible defects in the materials when they are used to assemble functional materials utilizing nanoarchitectonics concept. This approach is using controlled self-assembly, atomic or molecular manipulation, chemical manipulation, modeling, and external physical stimuli to harmonize and combine these techniques and their effects to resemble the process of architecting systems. (Ariga and Ebara 2018; Giese and Spengler 2019; Wang et al. 2019)

When manufacturing sustainable electrically conductive composites, considered aspects are the total cost, the level of the conductivity, chemical and physical stabilities, biodegradability, and the ease of the preparation (Du et al. 2017). To fulfill the required aspects, careful and systematic formulation of processing methods and materials will ultimately realize the desired properties in the composite structure.

Recent prospects on using nanocellulose and carbon nanotubes to manufacture electrically conductive structures have been highlighted in this study by using a minimum amount of energy, materials, and chemicals.

Electrically conductive materials are dependent on the mobility of electrons and the charge carrier concentration within their molecule structure. Generally, metals are materials where electrons can flow easily, but also some organic materials possess excellent electrical conductivity properties such as carbon nanotubes (CNTs) and graphene. Efficient percolation network should be formed, and its electrical conductivity needs to be more than 0.01 S/cm for material or composite to be considered conductive. Materials with a lower conductivity are used as antistatic and semiconducting materials (Huang 2002; Ma et al. 2010). Cellulose as an insulating material can form a template or support for conductive particles which can facilitate the electrical conductivity throughout the composite structure (Zhang, Dou, et al. 2019).

Cellulose-CNT composites have been reported to be applicable to supercapacitor electrodes (Kuzmenko et al. 2015; Lehtimäki et al. 2014; Tuukkanen et al. 2014), electromagnetic interference shielding devices (Lee, Lee, and Jeong 2016), chemical vapor sensors (Yun and Kim 2010), water sensors (Qi et al. 2015; Qi, Mäder, and Liu 2013), and pressure sensors (Wang et al. 2013). Cellulose-CNT nanocomposite films are also reported to have flame retardant properties with a shorter burn time and total heat release (Anderson et al. 2010).

Properties of cellulose-CNT composite are highly affected by the quality of the CNT dispersion, the aspect ratio of CNTs after a disaggregate treatment and the strength of the matrix, and interactions between carbon nanotubes and cellulose matrix (Bai and Allaoui 2003). Both CNT and its aggregate size are expected to play a very important role in the level of electrical conductivity. The dispersion phase of CNTs into an aqueous medium with cellulose and surfactant is a crucial step affecting, especially, the cellulose-CNT dispersion and composite preparation processes. The dispersing procedure is generally done in one or multistep processes. CNT dispersions are challenging since, when the surface area of particles increases, attractive forces between the aggregates increase as well (Vaisman, Wagner, and Marom 2006). High aspect ratio also enables the entanglement and bundling of CNTs (Rastogi et al. 2008). A common approach to non-covalently disperse CNTs in aqueous medium is to sonicate a mixture in the presence of surfactants.

The dissertation research seeks to identify ways, phenomena and which attributes affect the electrical conductivity in nanocellulose-carbon nanotube nanocomposite structures and how the attributes can be controlled and optimized using



nanoarchitectonics concept with minimum amount of energy, materials, and chemicals. The research is divided into sections by examining two-component, three-component, and four-component systems, and identifying which parameters and attributes affect interactions between nanomaterials, as well as how the properties of nanocomposites can be further modified even after manufacturing. In form of Venn diagram (Figure 1) is described how various component systems of the study are formed and in addition to the diagram four component system of nanocellulose-CNT-surfactant and pulp was also included in the study.

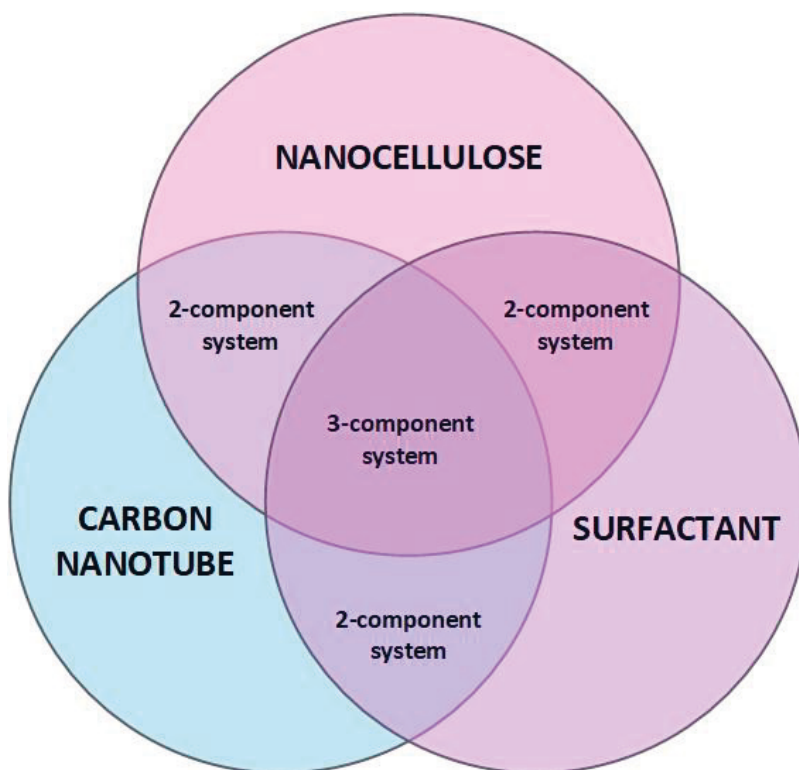


**Figure 1.** Venn diagram of nanocellulose, carbon nanotubes and surfactant forming two- and three-component systems. (Sanna Siljander 2022)

Efforts were made to reduce the amount of chemicals by using them in several roles during processing (Publication IV) as well as selecting e.g., surfactant type so that functionality, such as homogeneous dispersion, is achieved with minimal concentration (Publication I). Part of the research was also done completely without the surfactant chemical, with nanocellulose acting in a dual role (Publication III). Efforts were made to reduce energy but also working time by performing several

process steps simultaneously (Publications II, III and IV) such as dispersing nanocellulose and carbon nanotubes at the same time with or without presence of surfactant. In addition, exploring sonication energy in unit form kJ/g (Publications I-IV) allowed for more accurate use of energy.

The initial part of the dissertation covers literature based on materials (chapter 2), processing methods (chapter 4) and an overview of studies carried out by other research groups in the field of cellulose-CNT composites (chapter 5). Since the doctoral dissertation research has been done by utilizing approach of nanoarchitectonics, it is discussed in literature section (chapter 3). The aim and research questions which this thesis studies pursue to answer are presented in the chapter 6, followed by experimental section with results, discussion, and conclusions (chapters from 7 to 9). Part of conclusions chapter future perspectives are also discussed.

## 2 MATERIAL COMPONENTS AND PROPERTIES

When combining materials such as nanocellulose and carbon nanotubes together to form a composite structure, it is necessary to understand the characteristics of nanocellulose and carbon nanotubes themselves. This chapter describes material components and their properties which are used in this thesis.

### 2.1 Carbon nanotubes

Sumio Iijima discovered carbon nanotubes in 1991 (Iijima 1991). CNTs are formed by rolling a hexagonal grid of graphene sheets to the tube form. Nanotubes can consist of one layer of atoms (single-wall nanotubes SWNT) presented in Figure 2 or several nested tubes (few wall FWCNT, double-wall DWCNT, and multi-wall nanotubes MWCNTs). Carbon nanotubes have excellent electrical, mechanical, and thermal properties. However, these properties can vary depending on the processing method, defects, chirality, degree of graphitization, and aspect ratio (Haghi 2012). The MWCNTs used in this thesis studies have an average diameter of 9.5 nm, and their average length was 1.5  $\mu\text{m}$  according to the manufacturer's specifications. The current methods that produce CNTs, cause physically entangled carbon nanotubes. Furthermore, the characteristics of CNTs can be altered by changing the synthesis method and process conditions (Hilding et al. 2003).

CNT is a ballistic conductor, which means that it can ideally carry a charge without resistance. However, depending on the angle of folding (chirality), zigzag, armchair, or chiral (Figure 2 a,b,c), the carbon nanotubes can perform as a semiconductor, or the electrical conductivity can be as high as metals reaching  $10^7$  S/m (Hamedi et al. 2014; Wang and Weng 2018). In addition to a low electrical resistance, CNTs can carry the highest current density of any known material, for which the highest value is measured at  $10^9$  A/cm<sup>2</sup> (Haghi 2012).

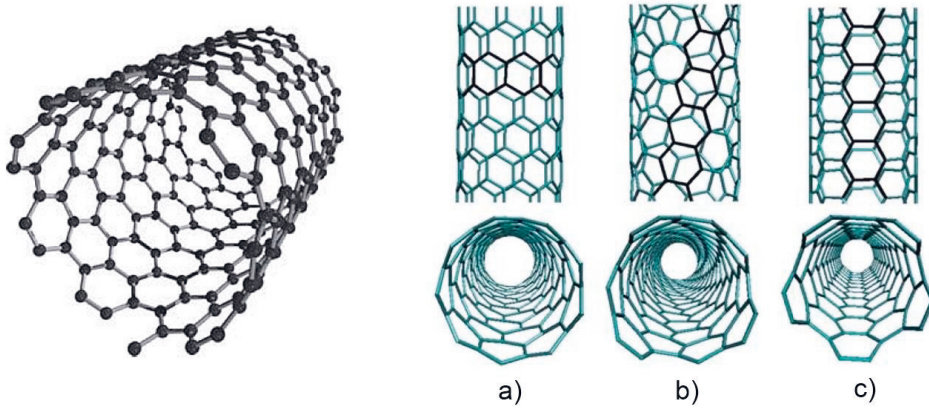


**Figure 2.** Single wall carbon nanotube (left) and three different chirality, the zigzag (a), chiral (b), and armchair (c) carbon nanotube structure (Reproduced from Galano 2010 with permission from the Royal Society of Chemistry; Roth and Carroll 2015, Copyright © 2015. John Wiley & Sons, Incorporated.).

The charge flow from CNT to CNT is powered by hopping and tunneling mechanisms. Certain activation energy needs to be applied so that electrons can travel through the CNT network. In the case of quantum mechanical tunneling, this activation energy defines the probability of electron movement from one CNT to another. The amount of current is following the Arrhenius equation and conductance generally increases with increasing temperature. This increases the activation energy and enables the thermal hopping mechanism. Due to these issues, the conductivity of the CNT network is limited by CNT-CNT contacts, and thus, the length of CNTs is crucial when optimizing the network conductivity.

Because of these characteristics, which were mentioned in the preceding paragraph, structure, characteristics of graphene, and high aspect ratio of CNTs, the formation of conducting network and attaining percolation threshold in an insulating cellulose matrix with a low CNT concentration is possible (Zhang et al. 2018). MWCNTs are generally considered metallic due to the electron energy state interactions between the nested layers, and they can last more mechanical stresses and allow more robust processing than SWCNTs. MWCNT production has recently increased because newly developed production technologies enable large quantities with relatively low prices.

Challenges of using carbon nanotubes in composites are to form controlled dispersion in the selected matrix by overcoming the strong van der Waals forces associated with the CNT aggregates. Commonly, SWCNTs form tightly packed

parallel bundles, whereas MWCNTs form entangled clusters with mesh configurations (Huang and Terentjev 2012). Each carbon nanotube must be separated, and clusters untangled to obtain an ideal conductive network. Dispersion homogeneity is maintained this way and single electrical contacts can form in the final product (Jung et al. 2008).

## 2.2 Cellulosic materials

Cellulose is an organic material containing carbon (C), hydrogen (H) and oxygen (O). Cellulose belongs in the group of polysaccharide and constructs from several hundred to thousands of  $\beta$ -linked D-glucose units. Being the most abundant organic polymer on Earth, cellulose is a main structural component of the primary cell wall in green plants and algae, reaching content of 40-50 % in wood and 90 % in cotton. In nature cellulose is found in the crystalline form of cellulose I, which consists of two polymorphs I $\alpha$  and I $\beta$ . The I $\alpha$  form is triclinic, while the I $\beta$  is monoclinic formation. Furthermore, ratio of these two crystalline forms is depending on the species meaning that I $\alpha$  is dominant in algae and I $\beta$  in plants such as wood (Dufresne 2012a).

Combining CNTs with cellulosic materials provides a conductive material network, where cellulose is an eco-friendly, low-cost, strong, dimension-stable, non-melting, non-toxic, and non-metal matrix, or carrier. The interest towards nano-sized cellulose has increased during the past years because of its excellent inherent mechanical, chemical, and physical properties.

Two approaches can be followed when manufacturing cellulosic nanomaterials: bottom-up involving biosynthesis to obtain bacterial cellulose (BC) (Iguchi, Yamanaka, and Budhiono 2000) and top-down method by disintegrating cellulosic biomass to a nanocellulose hydrogel with high water content (Turbak, Snyder, and Sandberg 1983). Cellulose-based micro and nanofibrils can be extracted from various types of plant fibers using mechanical forces, chemical treatments, enzymes, or combinations of these.

The most typical extraction method is however to process wood pulp and apply mechanical methods such as homogenization, micro-fluidization, micro-grinding, and cryocrushing. These processes expose cellulose material to high shearing and impact forces (Siró and Plackett 2010). The advantages of using wood-based cellulose are that existing infrastructure, machinery, and conventional technologies such as pulping, and bleaching can be partly used. Commonly starting materials for

nanocellulose are kraft pulp and dissolving pulp, where lignin, hemicellulose and impurities have been removed (Moon et al. 2011). Furthermore, nanocellulose is thought to be sustainable and beneficial in terms of energy consumption, production processes, environmental and safety issues when produced using wood-based biomass (Isogai 2013).

Finally, after fibrillation, the width of NC is typically between 3 and 100 nm and the length is several micrometers (International standard ISO 20477 2017). It means that this processing step has increased the ratio of surface area to volume dramatically (Gardner et al. 2008). Nanocelluloses have a diverse size range because of many combination possibilities in the top-down approach of pretreatments and mechanical fibrillation methods. Furthermore, nature, sequence and severity of these treatments highly affect the outcome (Dufresne 2012b). Multiple processing steps and additional enzymes and chemicals (e.g. TEMPO) will increase the cost of nanocellulose but result in smaller particles with a higher surface area (Zhang, Dou, et al. 2019). In Figure 3 is presented the hierarchical structure of wood cellulose from tree to molecule structure.

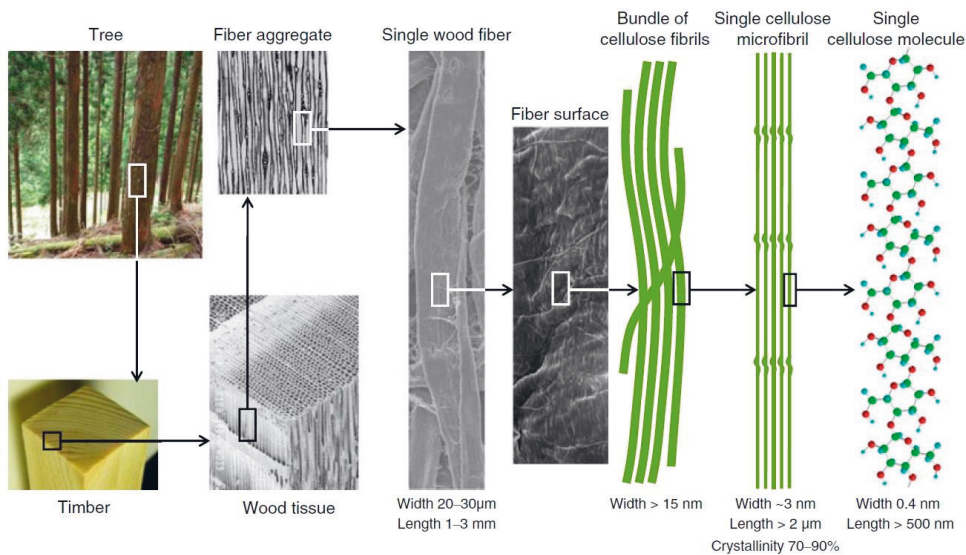


**Figure 3.** The hierarchical structure of wood cellulose from tree to molecule structure (Isogai 2013).

The standard (International standard ISO 20477 2017) on nanocellulose materials defines cellulose fibrils or fibril bundles with cross-section from some nanometers and length up to several micrometers as NC (Figure 4). Hereafter in the text, NC is used as a general term or when specific dimensions might not be known, and when talking about subordinate issues in a broader fashion. Nanocellulose produced using

mechanical means and utilized in publication II and IV is referred as nanofibrillated cellulose (NFC). Cellulose nanofibers (CNFs) used in publication III, refer to cellulosic material essentially of the same or smaller width as CNTs. Furthermore, the term CNF is used instead of NFC because in the study the nanocellulose material was fractionated and only the smallest fraction was studied. Micro fibrillated cellulose (MFC) refers to cellulosic material essentially larger in width than NFC, but smaller than the width of intact wood cellulose fibers (pulp, 20  $\mu\text{m}$ ). The size division between used terms is described below from the largest to the smallest.

Pulp > MFC > NFC > CNF > CNC

The morphological structure is uniform in nanocellulose, so its mechanical properties are better than those of the source biomass materials themselves. Morphology, crystalline structure, surface properties, chemical and physical properties, and properties in liquid suspension are significantly affecting the structure and properties of nanocellulose (Gardner et al. 2008). Mechanical properties of nanocellulose differ by its disordered and ordered regions of the molecule, meaning that amorphous regions contribute to flexibility and the plasticity of the bulk material, and crystalline contribute to the elasticity (Dufresne 2012b).

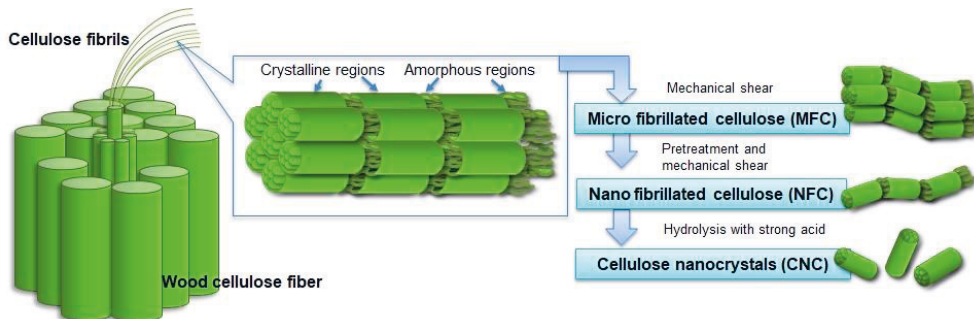


**Figure 4.** Visual comparison of pulp, MFC, NFC and CNC (Sampo Tuukkanen & Sanna Siljander 2021).

A distinguishing characteristic of nanocellulose is the high degree of hydroxylation along the polymer chain. As presented in Figure 5, nanocellulose has intra and intermolecular hydrogen bonds in the structure, which leads to a strong affinity to itself and toward materials containing hydroxyl groups such as  $-\text{OH}$  and  $-\text{COOH}$  (Moon 2011).

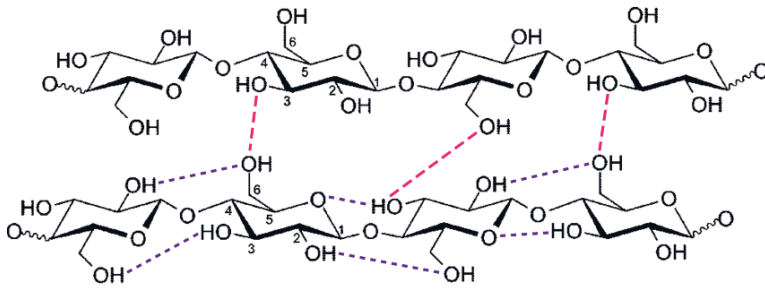


**Figure 5.** Intra (marked in purple) and intermolecular (marked in pink) hydrogen bonds in a cellulose molecule (Reprinted with permission from Pinkert *et al.* 2009, modified. Copyright 2009 American Chemical Society).

The deprotonation of these alcohol and carboxylic groups charges cellulose fibers negatively due to the presence of  $-O^-$  and  $-COO^-$  groups (Ho et al. 2011). These anionic charges on the surfaces of the cellulose fibers can repel other anionic materials such as carbon nanotubes and inorganic fillers which are commonly mixed with cellulose fibers to gain functional structures with enhanced electrical conductivity or barrier properties (Ho et al. 2011, 2012). Moreover, an entangled network, hydrogen bonding, and the gel-like structure of nanocellulose are affecting its mechanical and viscoelastic properties. Thus, in general, NC hydrogel has complex (shear thinning) rheological behavior even at low concentrations. (Hoeng, Denneulin, and Bras 2016; Moberg et al. 2017). In addition, the manufacturing technique and the resulting dimensions and surface properties significantly affect the rheology of the dispersions.

Used disintegration processing protocol has a significant impact also on the adhesion properties of nanocellulose and because of high surface area the adhesion properties are the most important parameter to control in nanocomposite applications (Gardner et al. 2008). NC is associated with a high aspect ratio since strong hydrogen bonds are forming between nanocellulose fibers. These bonds enhance mechanical properties and enable the formation of free-standing films (Hoeng et al. 2016). When manufacturing NC containing structures, a challenge is the shrinkage and distortion because of the faster evaporation rate on the surface than moisture transport within material. When this gradient occurs, it causes distortions because of local stresses (Baez, Considine, and Rowlands 2014; Gimåker et al. 2011). These challenges are typically overcome by selecting a base substrate that has adequate surface energy with casted nanocellulose to form a distortion-free film structure (Pammo et al. 2019; Tammelin, Hipp, and Salminen 2013).

The Young's modulus of casted nanocellulose films is reported to be 13.2 GPa and tensile strength is reported to be 214 MPa (Henriksson et al. 2008). Furthermore,



individual cellulose nanofibers' strength is reported to be up to 3 GPa, which is comparable to multi-wall carbon nanotubes (Saito et al. 2013). Mechanical properties of composites containing NC are reported in current literature to vary a lot because of the variations in the source material, pretreatment, component concentrations, and composite manufacturing method.



### 3 NANOARCHITECTONICS

The concept of nanoarchitectonics was first used by Masakazu Aono in the year 2000 at the 1<sup>st</sup> International Symposium on Nanoarchitectonics Using Suprainteractions in Tsukuba, Japan. (Aono 2011) Schematic visualization of nanoarchitectonics is presented in Figure 6.

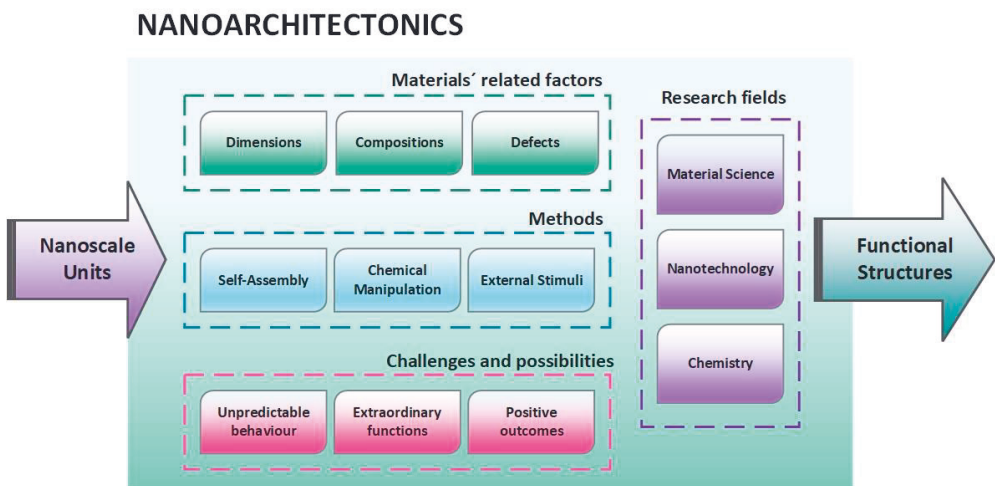


**Figure 6.** Nanoarchitectonics uses nanoscopic building blocks to create functional materials and systems with the knowhow of nanotechnology and various research fields. (Sanna Siljander 2021)

This concept utilizes several research fields and technologies so that hybrid material systems can be constructed. Individual fields are lacking methodology and only covering a restricted amount of information or analyses. In contrast to common nanomanufacturing strategies, the nanoarchitectonics is using nanoscale building units to fabricate advanced hybrid systems and architect functional materials. This concept utilizes several interdisciplinary research fields, methods, and techniques that are used to counter challenges emerging from nanoscale such as unexpected disturbances and fluctuations.

However, these challenges and uncontrollable factors can result in unpredictable behavior, extraordinary function, or positive outcome, which all are rising from interactions between component atoms, molecules, and materials. Therefore, it is essential to harmonize various actions, control materials' organization, dimension, compositions, and possible defects in the materials when they are used to assemble functional materials utilizing nanoarchitectonics. This approach is using controlled self-assembly, atomic or molecular manipulation, chemical manipulation, modeling, and external physical stimuli to harmonize and combine these effects and techniques to resemble the process of architecting systems, materials, and structures (Ariga and Ebara 2018; Giese and Spengler 2019; Wang et al. 2019). The goals utilizing nanoarchitectonics are listed below.

- i) Focus is to convert nanoscale units and nanomaterials to functional structures with a minimum amount of defects.
- ii) It should be noted that individual nano units are no key players when forming nanocomposites, but their interactions are.
- iii) To recognize unexpected functionalities rising from self-assembly and organization.

The emerging concept is utilizing the way to control, harmonize and modulate interactions between nanostructures, thus creating the possibility to fabricate macroscopic functional materials through understanding the arrangement and interactions of nanomaterials. Using not just a single tool of manufacturing but a total construction of architecture allows application of nanoarchitectonics to a variety of research and technology fields such as materials science, nanotechnology, and chemistry.

### 3.1 Self-assembly

Interfacial assembly is a process that occurs at the geometrical interface between two immiscible phases due to de-wetting instability, capillary forces, electrostatic interaction, and van der Waals forces (Maillard et al. 2000). Forming stable structures by linking these phenomena can be defined as an autonomous organization of the component towards the system's thermodynamic energy minimum. Modulating the concentration of certain additives such as ions or nanoparticles themselves can be used to affect the self-assembly process (Grzelczak et al. 2010). The nanoparticle

structures' properties when assembled are dependent on particle size, mass, spacing, surface properties, and the high-order structure of the individual components. Because self-assembly requires nanoparticles to be mobile, it usually takes place in liquid phases (Chen and Chi 2009; Whitesides and Grzybowski 2002). Therefore, the dispersion quality and stability are playing a key role. Furthermore, controlled, and optimized particle concentrations, as well as drying conditions, strongly influence the arrangement of the nanoparticles (Maillard et al. 2000).

Several forces and phenomena are influencing the stability of the dispersions including Brownian motion and van der Waals forces. Charged particles are influenced via electrostatic forces causing electrostatic repulsion or attraction dependent on the surface charges. It is suggested that the modifying the side chains of cellulose can further enhance self-assembly (Gardner et al. 2008). Gravity, magnetic and electric fields have also an influence on the dispersion stability. The total potential energy of interactions between colloidal particles is the sum of repulsion and attraction energies (Belgacem and Gandini 2008). The same forces affect the self-assembly of the molecular and meso or macroscopic objects (Whitesides and Grzybowski 2002).

Template-assisted assembly is considered as assembly guided by a modified substrate and it has been reported in many studies (Calahorra et al. 2018; Rycenga, Camargo, and Xia 2009; Xiong et al. 2017). Conversely, non-templated self-assembly has a composition simplicity and does not need any templates such as surface texture or binding molecules to drive the assembly (Grzelczak et al. 2010). Such more effortless non-templated self-organization, mainly based on droplet evaporation induced self-assembly (EISA) along the evaporating liquid boundary line is a recognized phenomenon with a variety of nanomaterials (Brinker et al. 1999) and has been reported for cellulose nanocrystals (CNC) (Mashkour et al. 2014), CNF (Mariani et al. 2020; Skogberg et al. 2017; Uetani and Yano 2013), carbon nanotubes (Zhang et al. 2010) and clay nanotubes (Zhao, Cavallaro, and Lvov 2015), to mention a few. Surface tension torques and capillary forces are hypothesized to have a role in the alignment of the fibrous nanoparticles along the evaporating droplet boundary line (Mashkour et al. 2014). In addition, it has been shown that particle concentration, length, surface charge, pH, salt concentrations, and temperature influence the alignment (Fall et al. 2011; Zhao et al. 2015).

## 3.2 Nanocellulose functionalization

Nanocellulose has a great potential to produce sustainable functional structures because of its mechanical and chemical properties and its colloidal stability in dispersions and suspensions for a wide range of salt concentrations and pH. Chemically added charged groups influence the physicochemical properties of NC (Fall et al. 2011) and can improve its processability and performance (Hammond 2004). A treatment with cations can be performed to render cellulose nanoparticles cationic by introducing positive charges on their surface. This strategy, applied to cellulose fibers, is largely used in the pulp and paper industry (Belgacem and Gandini 2008). Figure 7 presents a molecule structure of cationic cellulose with cationic groups in every third glucose unit.

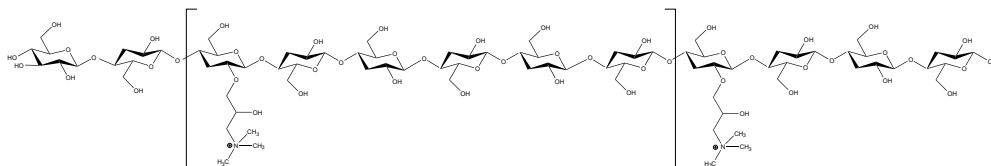


**Figure 7.** Molecule structure of cationic cellulose with the cationic group in every third glucose unit. (Anne Skogberg 2020)

CNT and nanocellulose form associated structures that are electrostatically stabilized through the charges of nanocellulose, and the dispersion limit can be further increased by increasing the surface charges of nanocellulose (Hajian et al. 2017). Cationic cellulose nanofibers can effectively adsorb negatively charged substances, such as nitrate, phosphate, fluoride, and sulfate containing molecules.

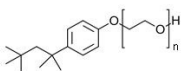
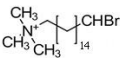
Adsorption capacity commonly increases with the surface charge density of nanocellulose (Voisin et al. 2017). Carbon nanomaterials show a tendency to establish stronger association onto nanocellulose surfaces that have a higher charge. During water removal in film formation, NC-CNT dispersion stays well dispersed that also strongly indicates the association between the NCs and CNTs is practically irreversible. Fluctuations of counterions on the surface of the nanocellulose induce polarization of electrons in the  $sp^2$  carbon lattice leading to an attractive interaction between the two nanomaterials (Hajian et al. 2017).

### 3.3 Chemical manipulation using surfactants

When dispersing solid particles in liquid, it has been described as a three-stage process: 1) wetting the solid particle such as powder, 2) de-aggregation of the particle clusters and 3) preventing reaggregation of dispersed particles (Rosen and Kunjappu 2012).

CNT dispersions are challenging. As the surface area of particles increases, it increases attractive forces between the aggregates as well (Vaisman, Wagner, et al. 2006) and also high aspect ratio enables the entanglement and bundling of CNTs (Rastogi et al. 2008). A common approach to non-covalently disperse CNTs to water medium is to sonicate a mixture in the presence of surfactant, which is a group of organic compounds that usually have a hydrophilic head and a hydrophobic tail. Surfactants are used as detergents, wetting agents, emulsifiers, foaming agents, and dispersants. The chemical structure, critical micelle concentration (CMC), and hydrophilic-lipophilic balance (HLB) values of surfactants used in this thesis are listed in Table 1.

**Table 1.** Surfactants used in this thesis.

	<b>Triton™ X-100</b>	<b>Pluronic® F-127</b>	<b>CTAB</b>	<b>SDS</b>
Type	Non-ionic	Non-ionic Polymeric	Cationic	Anionic
Name	Octylphenol Ethoxylate	Poloxamer	Hexadecyltri-methylammonium bromide	Sodium Dodecyl Sulfate
Chemical Structure		$H(OCH_2CH_2)_x(OCH_2CH(CH_3))_y(OCH_2CH_2)_zOH$		$CH_3(CH_2)_{10}CH_2O-SO_3^-Na^+$
Critical Micelle Concentration	0.2-0.9 mM (20-25 °C)	950-1000 ppm (25 °C)	0.92 mM (20-25 °C)	8.2 mM (25 °C)
HLB value	13.5	22	10	40

The presence of repulsive forces between the particles is presenting a dispersing effect. Surfactants' first function is to improve the wetting of the powder into a liquid medium. The second function is deagglomeration of the wetted particle agglomerates and aggregates by introducing repulsion. The basic idea is to enable surfactant molecules to be absorbed on the surface of CNTs via hydrophobic interactions,  $\pi$ - $\pi$  bonds, hydrogen bonds, or electrostatic interactions.

Surfactants can be characterized based on their characteristic behavior, absorption at interfaces, and self-accumulation into supramolecular structures (Vaisman, Wagner, et al. 2006). Their ability to function is dependent on the characteristics of dispersed particles, surfactant properties, and used solvent or medium (Vaisman, Marom, and Wagner 2006). Furthermore, the dispersing efficiency is linked to the length of the surfactant's alkyl chain, the presence of benzene ring, and the head group (Islam et al. 2003). In the case of non-ionic surfactants, a longer chain length is reported to be more effective due to increased steric repulsion. McDonald *et al.* found that surfactant's dispersion efficiency is also dependent on CNTs' diameters (McDonald et al. 2006), so the same type of surfactant does not support steady dispersion of SWCNTs and MWCNTs (Clark, Subramanian, and Krishnamoorti 2011). Surfactants should also have a long polar tail and the ability to form stable micelle structures around the dispersed particles. If the surfactant's tail is charged, then Coulombic repulsion interaction can prevent CNTs from re-agglomerating. This leads to favoring the usage of ionic surfactants (Wenseleers et al. 2004). In contrast, uncharged surfactants influence by the adsorption of chemical moieties onto the CNT surface via  $\pi$ - $\pi$  stacking interactions (Rastogi et al. 2008).

Not only the surfactant's nature and energy inserted into the dispersed system but also the concentration of surfactant has a vital role in the dispersion efficiency (Blanch, Lenehan, and Quinton 2010). Increasing surfactant concentration will enhance dispersibility until a plateau is reached. A too high surfactant concentration may have a negative effect on the physical properties, such as conductivity properties blocking off charge transport through the CNT network (Yu et al. 2007). Also, a too low surfactant concentration can cause re-agglomeration because a sufficient amount is needed to cover dispersed particle surfaces to prevent re-agglomeration (Islam et al. 2003; Yu et al. 2007). The optimum surfactant to dispersed particle mass ratio, in the case of CNTs, is reported to vary a lot, from 1:10 to 1:1 to 4:1 so that re-agglomeration is not happening after sonication (Islam et al. 2003; Vigolo et al. 2000; Yu et al. 2007).

In some cases, surfactant concentration is reported to be over the CMC, but micelle structures were not present in the dispersion. Presumably, most of the surfactant is adsorbed onto the carbon nanotube surfaces (Islam et al. 2003). It is believed that the efficient CNT dispersion is only possible when surfactant concentration is above the CMC value (Bai et al. 2010; Maillaud et al. 2013; Sun et al. 2008; Utsumi et al. 2007). The formed surfactant micelles can arrange themselves in different ways to the surface of the CNTs weakening the interactive forces



between CNTs and that way preventing aggregates from forming. It is reported that anionic sodium dodecyl sulfate (SDS) surfactant can arrange in half-cylinders, rings, or helices (Richard et al. 2003). In some cases, surfactants can prefer surfactant-surfactant interactions more than spreading to the carbon nanotube surface (Calvaresi, Dallavalle, and Zerbetto 2009). It is also reported that dispersing agents can form stable dispersions below and equal to their CMC limit (Angelikopoulos et al. 2010; Angelikopoulos and Bock 2008; Bonard et al. 1997; Bystrzejewski et al. 2010; Geng et al. 2008; Matarredona et al. 2003). It is also stated that the best result can be achieved with a concentration of 0.5 CMC and further increasing of the concentration of the surfactant has only a minor effect on the dispersion (Angelikopoulos et al. 2010).



## 4 PROCESSING ELECTRICALLY CONDUCTIVE COMPOSITES

A composite is a material where two or more different materials are combined and forming stronger alliance than those individual materials by themselves and still retain its own distinctive properties. Definition of composite is commonly described to be combination of materials which contain a continuous matrix constituent which acts as a binder for reinforcing constituent. However, when composite structure is optimized for other functional properties than structural, it can be produced from completely different constituent combinations (Miracle and Donaldson 2001).

Adjusting properties such as mechanical and electrical conductivity in the composite structures is challenging and is dependent on many different parameters. Selection starts by choosing components and their concentrations, followed by used methods to obtain a good nanocomponent dispersion and processing of the composite (Tkalya et al. 2012). Nanocomposite term refers to composite structure where one or several material components are in nanoscale. Furthermore, in current literature when NC-CNT combination is described, nanocomposite term is used and therefore it is used in this thesis.

Dispersion technology is crucial for realizing applications of cellulose, NC, and CNT composites. Especially when using carbon nanotubes in composite structures high strain rate methods must be used. This way the high performance can be ensured when aggregates are distributed (Miyashiro, Hamano, and Umemura 2020).

CNTs are bound together by van der Waals forces and the binding energy density is calculated to be 16 kPa for these aggregates, which has junctions approximately 100 nm apart (Huang and Terentjev 2012). Binding energy densities must be overcome by applied local shear stresses to disperse CNTs into an aqueous medium. Typical dispersion methods for CNTs are high shear mixing and pure sonication (Hu et al. 2009; Kuzmenko et al. 2015; Lee et al. 2016; Oya and Ogino 2008; Salajkova et al. 2013; Wang et al. 2013; Yoon et al. 2006; Yun and Kim 2010). In general, sonication is superior to shear mixing, especially for systems with low viscosity (Huang and Terentjev 2008), where conventional mixing does not create high enough strain rates required to disintegrate the CNT aggregates.

Sonication is based on ultrasonic waves that generate microscopic bubbles and inertial cavitation, which produces shearing action and can break bonds inside CNT aggregates. The soundwaves alternate cycles of high and low pressure that are dependent on the applied frequency. Cavitation phenomenon creates bubbles at the low-pressure cycle in the sonicated low viscosity medium. The bubbles will collapse violently during the high-pressure cycle. This results in liquid and suspended particles becoming intensely agitated (Loos 2015). The distribution of shearing forces is strongly influenced by the geometry of the sonicator tip and sonication parameters. Shearing forces being in the maximum value near the tip and gradiently decreasing (Huang and Terentjev 2012; Loos 2015). This means that also sample volume, concentration, viscosity, and vessel diameter are affecting the integrity of the sonication process.

Sonication and the cavitation phenomena can cause chemical functionalization, as well as structural defects and changes in CNT length, surface, and aspect ratio (Huang 2002; Lu and Hsieh 2010; Rossell et al. 2013; Yang, Rochette, and Sacher 2005). Yang *et al.* reported that sonication causes chemical changes, mainly oxidation of the  $-CH_n$  groups on the outer surface of the MWCNTs. Their analysis indicated that the functionalization happens not at their ends but along the whole length of the CNTs, leaving  $-OH$ ,  $-C=O$ , and  $-COOH$  reactive groups to the surface (Yang et al. 2005).

Non-inertial cavitation is related to surface damages of the tubes, whereas inertial cavitation is causing exfoliation of the nanotubes. (Sesis et al. 2013) In the case of MWCNTs, only the outer layer is contributing to carrying the current through the nanotube and the outmost layers' structure and condition is therefore affecting the electrical conductivity (Min et al. 2010). This will further affect the electrical and mechanical performance of CNT-based composites and their applications.

Commonly, it is stated that a long sonication time results in good CNT dispersion within certain limits (Kun et al. 2013). However, the dispersion quality is highly dependent on the sonication energy rather than sonication time, because the sample volume, mass and viscosity, CNT type, sonicator power, and sonicator tip diameter can vary, not to forget the surfactant type and amount (Publication I and II). Because of these factors, in this thesis, sonication energy per dry mass unit is used.

The energy to dry mass ratio indicates the total applied energy, not absorbed energy by dry mass. A part of the energy is used to heat the water and a part is used to disperse nanoparticles. Also, part of the energy is used to degrade the sonicator itself and the vessel, to cause defects to the nanoparticles, and some energy is used to cause several different sonochemical reactions, like disintegration and the

reorganization of water molecules (Koda et al. 2003, Publication I). Therefore, it is surprising that generally the sonication process is not accurately described, and the processing parameters have not been stated clearly in the current scientific literature.

## 4.1 Two-component systems

Two-component systems referred in this study are NFC-CNT, c-CNF-surfactant, and CNT-surfactant systems. Standard ISO 14887 can be used to determine prospective dispersing agents for both cellulose and carbon materials. A suitable dispersing agent type would be for example a polyethoxy alcohol (PEO/alcohol) for CNTs, and polyisopropoxy (PEO/PPO) copolymer for cellulosic materials. The standard denotes that one commercial PEO/PPO copolymer surfactant is Pluronic®. In the case of CNT, one example of an alkyl phenoxy PEO ethanol dispersing agent is Triton™ 100 (International standard ISO 14887 2000).

### 4.1.1 Nanocellulose as a dispersing agent

Nanocellulose is reported to disperse SWCNTs and MWCNTs in the form of cellulose nanocrystals and chemically oxidized cellulose nanofibers (Koga et al. 2013; Mougél et al. 2016). The presence of hydroxyl (-OH) groups in the cellulose molecular structure enables hydrophilicity (negatively charged) and -CH groups are responsible for hydrophobic characteristics, meaning that cellulosic surface contains two kinds of sides for adsorption. The existence of both groups permits nanocellulose to act as a dispersant (Li et al. 2015; Olivier et al. 2012). Olivier *et al.* suggested that hydrophobic faces of the cellulose nanocrystals can interact with hydrophobic CNTs by expelling water and thus stabilizing the dispersion. The limitation is that hydrophobic characteristics are present only in a part of cellulose surfaces (Olivier et al. 2012). However, hydrophobic interactions are the driving force dispersing particles, but also long-range electrostatic repulsion forces affect the stability of NC-CNT dispersion, especially due to negative sulfate groups introduced in the typical CNC preparation process (Mougél et al. 2016).

### 4.1.2 Interactions between nanocellulose and surfactant

Cellulosic materials' behavior with different types of chemicals is crucial to recognize so that their role in current and future applications can be ensured. Several attributes affect the surfactant adsorption to the cellulose surface, such as flexibility, crystallinity, and surface chemistry which is dependent on the isolation process of cellulose. Furthermore, a rise in the cellulose fibrillation level is affecting properties because of the increased surface area and narrowing size distribution. Enzymatic or hydrochloric acid hydrolysis does not produce negative charges to the cellulose structure, contrary to chemical oxidation. Negative charges can be a beneficial means of keeping fiber and fibrils homogeneously dispersed to the aqueous medium (Tardy et al. 2017). Because of cellulose molecules' hydrophilic and hydrophobic characteristics, the surfactant type is affecting the cellulose-surfactant interactions. Triton X-100 and other nonionic surfactants are reported to mostly adsorb onto cellulose's hydrophobic sites, contrary to nonionic surfactants, cationic surfactants such as CTAB is reported to adsorb onto the hydrophilic side (Paria, Manohar, and Khilar 2005a, 2005b).

### 4.1.3 Interactions between CNT and surfactant

To utilize the unique properties of nanoparticles, such as CNTs, they need to be spread into fluid dispersion in a way that entangled and aggregated morphologies are homogeneously dispersed (Hilding et al. 2003). A common approach is to non-covalently disperse CNTs into a water medium to homogenize the mixture with the presence of surfactants. Reasons for the usage of surfactants are their low price, handleability, and easy acquisition (Javadian et al. 2017).

This method is based on having surfactant molecules adsorbed to the CNT surface physically, when inserted sonication energy is temporarily forming gaps in the nanotube agglomerates. This means that a non-chemical reaction is taking place and has a minimum effect on the chemical or internal electronic structure of the carbon nanotube's graphitic walls (Bystrzejewski et al. 2010). Several studies have used this non-covalent method (Bonard et al. 1997; Geng et al. 2008; Javadian et al. 2017; Rausch, Zhuang, and Mäder 2010; Vaisman, Wagner, et al. 2006). This modification method is also often very simple, containing sonication with centrifugation or filtration processes (Bai et al. 2011). These modifying surfactant molecules are being adsorbed on the surface of CNTs via hydrophobic interactions,  $\pi$ - $\pi$  bonds, hydrogen bonds, covalent or sometimes electrostatic interactions (Bai et

al. 2011; Yang and Xing 2010). Selected molecules, surfactants, or dispersants should have properties that are beneficial to attaching to the surface of the CNTs to create a repulsive barrier and interacting with the selected medium.

CNT dispersions have been prepared using sodium dodecyl sulfate, SDS (Blanch et al. 2010; Borovskaya, Idiatullin, and Zueva 2016; Bystrzejewski et al. 2010; Chatterjee et al. 2005; Clark et al. 2011; Grossiord et al. 2008; Hertel et al. 2005; Islam et al. 2003; Jiang, Gao, and Sun 2003; McDonald et al. 2006; Moore et al. 2003; Poulin, Vigolo, and Launois 2002; Richard et al. 2003; Sun et al. 2008; Tan and Resasco 2005; Vigolo et al. 2000; Yu et al. 2007; Yurekli, Mitchell, and Krishnamoorti 2004), hexadecyl trimethyl ammonium bromide, CTAB (Blanch et al. 2010; Jiang et al. 2008; Poorgholami-Bejarpasi and Sohrabi 2015; Rausch et al. 2010; Ryabenko, Dorofeeva, and Zvereva 2004; Tan and Resasco 2005; Vijayaraghavan 2015), Polyoxyethylene octyl phenyl ether, Triton X-100, containing aromatic rings which are suggested to have relatively high efficiency for dispersing because of the interactions between  $\pi$ -stacking in the CNTs (Bai et al. 2010; Geng et al. 2008; Islam et al. 2003; Rastogi et al. 2008; Shim et al. 2002; Tan and Resasco 2005) and bi-functional polymer, Pluronic F-127 (Blanch et al. 2010). Also, some research is done related to surfactant mixtures (Javadian et al. 2017; Madni et al. 2010).

## 4.2 Three-component systems of NC-CNT surfactant

Cellulosic material is providing support or template for the CNT particles to form and maintain a conductive network that remains intact and is serving as a continuous contributor to current flow in NC-CNT composite structures. The main reason for this is that cellulose is relatively dimensionally stable, especially in the longitudinal direction (Larsson and Wågberg 2008), and the inherent crystalline nature can serve as a reinforcement.

However, when consolidating conductive and insulating materials together, there is an inherent risk of inefficient flow of current. The conducting particles may not form an efficient percolation network because of low a concentration, inadequate distribution, and dispersion aggregates and agglomerates. In the formed composite structure, an insulating matrix material is obstructing the flow of electrons. Furthermore, much-needed dispersion aides such as surfactants, which are used to homogenize the dispersion of conductive particles, can act as a barrier, and prevent particles from connecting and forming a percolation network. That can lead to a reduction of conductive and mechanical properties of these composite structures.

In principle, surfactant modification is heterogeneous and strongly affected by the interaction between materials and medium. The interfacial interactions' origin and magnitude correlate to the performance and the properties of the manufactured composite structures. Attention must be given to the selection of the right type of surfactant to maximize the dispersing effect. At the same time, the concentration must be selected so that the plasticizing effect to the mechanical properties and disruption to electrical conductivity is minimized.

Obtaining generally good quality dispersion with a mixture of both NC and CNTs the help of surfactants is needed. Surfactants lower the interfacial free energy between particles, but it is difficult to know in what molar ratios surfactants are needed in contrast to the amount of mass the samples hold. The increasing of the surface area when the dispersion process is progressing, also affects the outcome. Choosing the right parameters helps to increase the quality of the dispersion and, in addition, enhances the properties of the three-component composite.

#### 4.2.1 Composite structure from three-component system

The incorporation of cellulosic materials with CNTs into 3D structure could lead to multifunctional composite material if each nano-component is dispersed efficiently (Chen et al. 2018). There are different manufacturing methods for the fabrication of CNT-cellulose composites, but all the methods typically include: (i) a phase of dispersing CNTs into a solution, and (ii) an impregnation phase into the cellulose substrates (e.g., paper, filter paper) (Fugetsu et al. 2008; Hu et al. 2009; Imai et al. 2010; Lee et al. 2016; Oya and Ogino 2008; Yun and Kim 2010). Alternatively, the dispersion can be used as a wet component with bacterial cellulose (Toomadj et al. 2011; Yoon et al. 2006), with cellulose I and regenerated cellulose fibers (Kuzmenko et al. 2015; Liu et al. 2016; Qi et al. 2013) or in an aerogel form (Qi et al. 2015).

Commonly, the incorporation of NC and CNTs is done by either a coating or a blending method. The coating method was used by Hu *et al.* (Hu et al. 2013). They used a Meyer rod to spread CNTs on the surface of NFC film. The majority of research groups studying NC-CNTs have used blending to achieve conductive composites in one or multistep processes (Hamedi et al. 2014; Yoon et al. 2006). Filtering CNTs through filter paper results in non-homogeneous distribution of CNT particles in the thickness direction. For this reason, the blending approach is offering better spreading of particles with a high amount of CNTs and physically entrapping them to the nanocellulose network. Because conductive composites are



often manufactured using the blending approach, the level of electrical conductivity is mostly depending on other factors than just the incorporating materials together.

Because of the large variety of cellulose processing methods with different types of CNTs, it is not obvious what aspect ratio or size distribution of NC will form an efficient percolation network to the formed composite structure. Typically, small particle size or functionalized particles consume more energy and chemicals when manufactured, which leads to a higher cost of material. From an economical point of view, the target of this thesis studies, is to find a combination of high performance with minimum materials, chemicals, and energy consumption.

The comparison of electrical conductivities of different cellulose-CNT composites is difficult because of the large variety of material combination options, individual material properties, and different measurement techniques. This demonstrates the importance of understanding interface science, dispersion procedure and quality.

### 4.3 Foam forming using NC-CNT surfactant dispersion with pulp

Foam forming technology enables the production and combination of a vast variety of fiber-based materials and the application of molding technologies to form lightweight cellulosic 3D structures. Technology was applied in studies reported in the publication IV. In general, the foam forming technology utilizes aqueous foam instead of water as a carrier medium and the shear thinning behavior of the foam makes it an excellent transport medium for fibers and particles, and it enables an excellent formation of the product being produced (Kinnunen et al. 2013; Smith and Punton 1975). In addition, the air content of the carrier foam is 60-70% and it consists of air bubbles with a diameter below 100  $\mu\text{m}$ . As stated in an article (Härkäsalmi et al. 2017), an interest is growing in the use of the aqueous foam as a transporting medium of solid materials such as particles and fibers. By using the foam forming technology, a decrease in the cost of production and material savings can be achieved (Kinnunen et al. 2013). Furthermore, foam forming ensures structures that have excellent formation and, when combined with a molding technology, enable lightweight structures (Alimadadi and Uesaka 2016; Haffner et al. 2017; Madani et al. 2014) and completely new functional product opportunities.

One of the most used surfactants to form the foam in the foam-forming process is the anionic surfactant sodium dodecyl sulfate (SDS), which is used in many industrial applications, such as shampoos, toothpastes, and shaving creams. The

motive for the wide use is its relatively low price, foam stability, easy diffusion in water and it can be used in rapid foaming (Al-Qararah 2015). However, SDS might still not be the optimal surfactant since it has been shown that SDS as a surfactant of a water-CNT system does not disperse CNTs optimally to homogeneous dispersion. Not even if the higher sonication energy and concentration of surfactant are used (Publication I). The results in the cited study also clarify that, when surfactant Triton X-100 is used, stable homogeneous CNT-water dispersion can be achieved.

It has been reported in current literature that by using nanocellulose in papermaking processes has several advanced properties: it has a high aspect ratio, high strength along with good flexibility, an interaction potential via hydrogen bonding, and a tendency to form strong entangled networks. These properties mean that high a tensile strength is attainable at relatively low concentrations, lower than 5% relative to pulp content (Boufi et al. 2017; Kajanto and Kosonen 2012). Moreover, an increase in density has also been reported when NC is added to pulp. NC attaches to the fiber surfaces as a layer and in this way a large contact area is formed, which increases the number of hydrogen bonds (Brodin, Gregersen, and Syverud 2014).

The application of NC-CNT dispersions in the foam forming process enables the manufacturing of conductive 3D structures to almost any shape and size. Unfortunately, because of the nanoscale size of CNTs, the formation with cellulose pulp alone does not occur efficiently enough to form the conductive percolation network during the foam-forming process. When a dispersion is prepared efficiently to form a homogeneous dispersion without any aggregates present, the nanosized CNT particles flow through the cellulose fiber network in the vacuum assisted molding with the foam. In Publication IV, it is verified that nanocellulose can be used as a carrier for CNTs and, in this way an efficient percolation network is obtained in the foam-formed composite structure. It has been reported that NC can increase the strength of cellulose non-woven structures that are manufactured using the foam-forming process (Kinnunen et al. 2013). CNTs are a good candidate to replace copper and aluminum as an interconnect material in next-generation electric devices (Ragab and Basaran 2009).

## 5 RECENT RESEARCH RELATED TO CELLULOSE-CNT COMPOSITES

Cellulosic material and conductive particles have a key role to attain the resulting properties of electrically conductive composites. In addition, the interactions between the used materials have a crucial role. Table 2 lists various combinations of cellulose materials and CNTs, whose electrical conductivity values can be compared to each other due to the same measurement technique used. Moreover, as given in Table 2, there are the manufactured composite form and used CNT types. In addition, CNT concentration in composite, used surfactant type or brand and electrical conductivity is stated.

Hamedi *et al.* used multistep methods to process NFC and also NFC-SWCNT dispersions. They did not use any surfactant and counted on the dispersing power of NFC when manufacturing nanocomposite films, aerogels and microfibers by using NFC-SWCNT dispersion. Filtering and pressing method were used to produce composite films containing 10 w-% SWCNTs resulted in a relatively high conductivity of 3.23 S/cm. Microfiber attained conductivity of 207 S/cm when 43 w-% SWCNT concentration was used, and aerogel had conductivity  $1.4 \times 10^{-4}$  S/cm with 12 w-% SWCNT concentration. Surprisingly, Hamedi *et al.* stated that this reported processing procedure is a route for making cheap conductive NFC composites even when expensive SWCNTs were used (Hamedi et al. 2014).

Qi et al. researched electrically conductive aerogels composed of CNTs and cellulose for a vapor sensing application. Cotton linters were dissolved to NaOH, urea, or CNT dispersion with surfactant and regenerated to form hydrogel. Flash freezing was used to obtain aerogel with a CNT concentration of 3, 5 and 10 w-% and a maximum electrical conductivity was achieved with 10 w-%:  $2.2 \times 10^{-2}$  S/cm (Qi et al. 2015). Li *et al.* studied thermoelectric aerogels based on carboxylated nanocellulose fibers and carbon nanotubes. When electrical conductivity was measured by applying contracts to top and bottom of the specimen 0.1 S/cm conductivity was attained by using 20 w-% CNTs (Li et al. 2022).

**Table 2.** Recent research results related to cellulose-CNT composites.

Composite form	Cellulose type	CNT type	CNT concentration [w-%]	Surfactant Type or brand	Conductivity [S/cm]	Reference
Film	Nanocellulose	SWCNT	10	Not used	3.2	Hamedi 2014
Microfiber	Nanocellulose	SWCNT	43	Not used	207	Hamedi 2014
Aerogel	Nanocellulose	SWCNT	12	Not used	$1.4 \times 10^{-4}$	Hamedi 2014
Film	Nanocellulose	MWCNT	5	xylan	1.1	Yamakawa 2017
Film	Nanocellulose	MWCNT	17	Triton X-100, removed	8.4	Publication II
Film	Nanocellulose	MWCNT	17	Triton X-100	3.0	Publication II
Film	Nanocellulose	MWCNT	17	Pluronic F-127	5.4	Publication II
Film	Nanocellulose	MWCNT paste	20	Not used	1.8	Chen 2018
Film	Nanocellulose	MWCNT	10	CTAB	0.4	Zhang 2019
Film	TEMPO NC	SWCNT	?	Not used	10	Koga 2013
Nanopaper	TEMPO NC	MWCNT	17	NPPE	$1.0 \times 10^{-3}$	Salajkova 2013
Film	Cellulose nanocrystals	SWCNT	10	Not used	0	Nguyen 2019
Pellicle	Bacterial NC	MWCNT	10	CTAB	$1.4 \times 10^{-1}$	Yoon 2006
Membrane	Bacterial NC	MWCNT	0.1	CTAB	$2.7 \times 10^{-2}$	Jung 2008
Film	Bacterial NC	MWCNT	?	CTAB	1.6	Toomadj 2011
Membrane	Bacterial NC	MWCNT	4	Not used	$6.2 \times 10^{-3}$	Xiao 2013
Aerogel	Regenerated	MWCNT	10	Brij76	$2.2 \times 10^{-2}$	Qi 2015
Film	Regenerated	MWCNT	10	CTAB	$7.2 \times 10^{-2}$	Huang 2015
Film	Regenerated, gel	MWCNT paste	20	Not used	5.0	Chen 2018
Paper	Cellulose pulp	SWCNT	2	SDS	$2.7 \times 10^3$ ohm/sq	Oya 2008
Paper	Cellulose Pulp	MWCNT	17	anionic	6.7	Imai 2010
Paper	Cellulose pulp	MWCNT	13	SDBS	1.1	Lee 2016

Hajian *et al.* manufactured a CNT-NC composites using an extremely high concentration of SWCNTs up to 75 w-% and resulting in a conductivity of 515 S/cm. The obvious reason for attaining this high conductivity value is the high concentration SWCNTs, but also the compressing of the composite structure increased the conductivity. Surprisingly, they inform only in supporting information that they added salt (NaCl) to the CNT-NC dispersion that will knowingly affect the conductivity values increasingly. They performed conductivity measurements using a two-probe measuring device (Hajian et al. 2017). SWCNTs were also used in studies by Nguyen *et al.* Cellulose nanocrystal dispersion with SWCNTs were sonicated in bath-type sonicator without surfactant and CNC-CNT films from dispersion were fabricated by using casting method. Films with 10 w-% SWCNTs did not conduct electricity (0 S/cm) presumably because several insulating CNCs and critical percolation was not reach (Nguyen et al. 2019).

Flexible NC-CNT composite films were prepared by using vacuum filtration process and pressing and electrical conductivity of 0.38 S/cm was achieved when 10 w-% MWCNT concentration was used. Zhang *et al.* used CTAB as surfactant in their studies. (Zhang, Sun, et al. 2019)

Huang *et al.* reported the results of a multiphase process with a compressing step, which was used to accomplish a conductivity of 0.072 S/cm using MWCNT-doping at a 10 w-% concentration and 0.056 S/cm with 5 w-% doping of cotton linters and CTAB as surfactant. Huang *et al.* also dissolved cellulose and regenerated it to form a film structure (Huang et al. 2015).

The electrical conductivity of TEMPO-oxidized cellulose films with a 16.7 w-% concentration of MWCNTs was 0.001 S/cm, which is lower than the limit for a conductive material (Salajkova et al. 2013). Koga *et al.* also manufactured nanocomposite films using TEMPO-oxidized cellulose nanofibers but used SWCNTs. The related conductivity is reported to be as high as 10 S/cm, but it is difficult to compare the value because it is reported with respect to volume fraction of CNTs instead of weight (Koga et al. 2013).

By using comparable materials such as xylan as surfactant and applying a filtering method, Yamakawa *et al.* obtained a 1.1 S/cm electrical conductivity with a 5 w-% MWCNT loading (Yamakawa et al. 2017) and Chen *et al.* reached a 1.8 S/cm level at 20 w-% MWCNT. They were able to increase the conductivity up to a value of 5.0 S/cm using a chemical alkali treatment (Chen et al. 2018).

Jung *et al.* manufactured conductive bacterial cellulose-silk fibroin membranes by immersing them to the MWCNT dispersion. They reported an electrical conductivity of  $2.7 \times 10^{-2}$  S/cm when 0.1 w-% MWCNT dispersion was used. Unfortunately,

they do not inform the CNT concentration in the BC-silk-CNT membrane (Jung et al. 2008). Yoon *et al.* used bacterial cellulose as a matrix and obtained a conductivity of 0.14 S/cm with a 9.6 w-% MWCNT loading (Yoon et al. 2006) and Toomadj *et al.* attained a conductivity of 1.6 S/cm by infusing MWCNT/CTAB 30 ml of 2 mg/ml dispersion to bacterial cellulose. The focus of that research was to analyze how immersion time is affecting the BC/MWCNT composite's conductivity properties and they did not analyze the concentration of MWCNTs in the composite structure (Toomadj et al. 2011).

Chitosan-cellulose-MWCNT membranes were fabricated by using ionic liquid dissolution and regeneration by Xiao *et al.* The conductivity of these membranes exceeded  $6.2 \times 10^{-3}$  S/cm with a 4 w-% concentration of MWCNTs (Xiao et al. 2013). Regenerated cellulose was used by Lee *et al.* They used DMAc/LiCl to dissolve cellulose and manufactured composite films with an electrical resistivity of  $10^2$ - $10^1$  ohm/cm when MWCNT concentration was between 2.0-3.0 w-% (Lee and Jeong 2015).

In addition, studies of manufacturing conductive cellulose composites via coating of cellulosic filter paper with carbon-based dispersion have revealed rather good results, but the consistency of the materials is not homogeneous. CNF and MWCNT coated filter papers were fabricated with a simple dipping method. These composite structures obtained an electrical conductivity of 1.1 S/cm and 0.85 S/cm (Lee et al. 2016; Mondal et al. 2017). By attaining sandwich structure of CNT-NFC/NFC/CNT-CNF an anisotropic electrically conductive films were fabricated for supercapacitor application. Research groups Hou *et al.* altered weigh ratio of CNT-NFC in the conductive layers from 1:2 to 7:1 resulting the lowest surface resistance of 32.7 ohm/sq when ratio 5:1 was used (Hou et al. 2020).

Fugetsu *et al.* manufactured conductive cellulose-based composites using a traditional papermaking process with a 8.32 w-% CNT concentration and, finally, the conductivity of 1.87 S/cm was obtained (Fugetsu et al. 2008). Additional cationic fixer was used when Imai *et al.* manufactured MWCNT-cellulose conductive papers with different CNT concentrations. The highest conductivity was attained by using a 16.7 w-% concentration (Imai et al. 2010). Oya *et al.* used the washi paper production procedure to manufacture composite paper containing 2 w-% SWCNTs and the measured average resistance was  $2.74 \times 10^3$  ohm/sq (Oya and Ogino 2008).

When comparing different research groups' electrical conductivities for cellulose-CNT composites, it can be stated that several composite structures have an inefficient flow of current. First, conducting particles may not form an efficient percolation network, and second, inadequate distribution procedure results in a

composite structure containing agglomerates of conductive particles. The main reason might still be that, in the formed composite structure, insulating matrix material is obstructing the flow of the electrons.

Zhang *et al.* suggested two different approaches to explain the conductivity phenomenon or lack of it in the cellulose- CNT composite. First, large quantities of defects and gaps in the structure are causing a "weakest link" effect. Secondly, the "optimized agglomeration" theorem is explaining conductivity, because it is often favorable for conductivity point of view to have a large number of interconnections. However, severe levels of aggregates and agglomerates are unfavorable both to electrical and mechanical properties (Zhang, Dou, et al. 2019).





## 6 THE AIMS OF THIS THESIS

This thesis focuses on optimizing electrical conductivity properties and understanding interactions between nanocellulose and CNT in nanocomposite structures by the means of nanoarchitectonics. Furthermore, studies are conducted using a minimum amount of materials, chemicals, and energy.

Publications I and III are presenting two-component systems of CNT-surfactant and cationic CNF-CNT. Publication I focus on how the sonication energy, surfactant type, and the surfactant amount is affecting the quality of CNT-surfactant dispersion and Publication III studies self-assembly of cationic CNF-CNT nanocomposite. Furthermore, nanocellulose's dispersing action to CNTs and the effect of functionalization of nanocellulose are studied in the publication III.

Publications II and IV are focusing on three-component systems that are used to research the effect of sonication energy, surfactant type, and surfactant amount to the electrical conductivity of NFC-CNT nanocomposite structures. Post-processing of NFC-carbon nanotube composite films to enhance integrity of CNT percolation network was also studied in Publications II and IV. Finally, Publication IV is reporting about an electrically heating 3D-structure that can be obtained when NFC-CNT-surfactant dispersion is combined with pulp using foam-forming as the manufacturing process. Figure 8 presents the schematic flow of Publications I to IV.

The novelty of this thesis and publications related to it is undeniable since several findings, results, and procedures are reported for the first time. A cohesive study (Publication I) was conducted to determine dependencies between sonication energy, surfactant amount, and type to CNT dispersion quality for the first time. In Publication II post-processing of NFC-carbon nanotube composite films to enhance conductivity were published and non-templated self-assembly of anisotropic CNF-CNT films with cationic cellulose nanofibers acting as a dispersing agent for CNTs was reported in Publication III for the first time. Furthermore, in Publication IV a novel heating element was manufactured using only two processing steps and a patent application was filed.

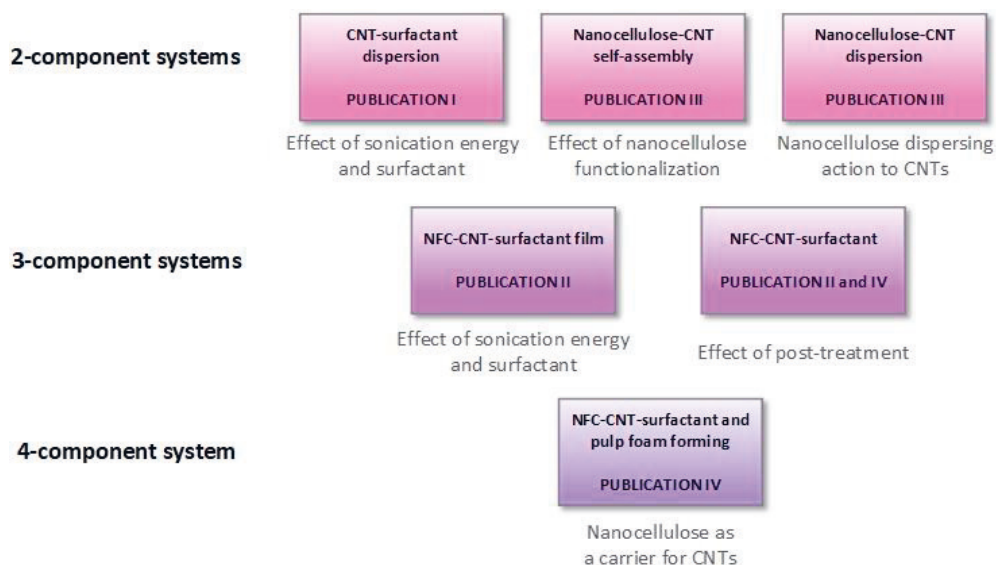


**Figure 8.** The aims of this thesis in a schematic form.

## 6.1 Research questions

The objectives of the thesis were to answer which attributes affect the electrical conductivity in nanocellulose-carbon nanotube nanocomposite structures and how their attributes can be controlled and optimized by using a minimum amount of energy, materials, and chemicals utilizing nanoarchitectonics.

1. Can composite structures' performance be enhanced after manufacturing?
2. Can cationic CNF act as a dispersing agent?
3. Is the nanocellulose aspect ratio to size distribution influencing the electrical conductivity in NC-CNT nanocomposites?
4. Which attributes are affecting the performance of NC-CNT nanocomposites' electrical conductivity?
5. How can cellulose-NC-CNT composites be manufactured using the minimum amount of energy, materials, and chemicals?

## 7 EXPERIMENTAL

This chapter introduces the materials and the methods used in the thesis. First, the materials of two, three, and four component systems are introduced followed by description of preparation and manufacturing processes. Furthermore, the characterization methods are described.

### 7.1 Materials

MWCNTs (Publications I-IV) (MWCNT, Nanocyl 7000, Nanocyl SA., Sambreville, Belgium) were purchased from Nanocyl Inc. The product was used in the state it was when received in all Publications. This type of CNTs is produced via catalytic chemical vapor deposition (CCVD). Nanocyl 7000 MWCNT was selected for the studies based on moderate price, availability, and good electrical conductivity characteristics.

In Publications II and IV, the nanofibrillated cellulose production was based on the mechanical disintegration of bleached hardwood kraft pulp (BHKP). Nanocellulose material which was selected for the studies because it is produced from kraft pulp and processed using mechanical disintegration method which is universally used approach. First, dried commercial BHKP produced from birch was soaked in ion-exchanged water at approximately 1.7 w-% concentration and dispersed using a high-shear Ystral dissolver for 10 min at 700 rpm. The chemical pulp was pre-refined in a Masuko grinder (Supermasscolloider MKZA10-15J, Masuko Sangyo Co., Tokyo, Japan) at 1500 rpm and fluidized with six passes through a Microfluidizer (Microfluidics M-7115-30, Microfluidics Corp., Newton, MA, USA) using a pressure of 1800 MPa. The final material appearance of NFC was a viscous and opaque hydrogel.

For Publication III, cationic CNF (c-CNF) was produced from bleached and never-dried cellulose kraft pulp. Cationization was conducted similarly as reported by Bendoraitiene *et al.* (Bendoraitiene et al. 2006). Material selection was done based on previous studies by Skogberg *et al.* (Skogberg et al. 2017).

The pulp was first concentrated in an oven to 63 % dry matter content. The reaction mixture was prepared from 140 ml of EPTMAC, 2 g of an aqueous solution of NaOH 5 %, and 2.3 ml of Milli-Q water. The ingredients were thoroughly mixed, and 50 ml of Milli-Q water was added to the mixture, which was warmed to 45°C. The pulp was added to the mixture, and it was stirred for 24 h at a high cellulose consistency ( $\approx 40$  %) with a CV Helicone Mix Flow (Design Integrated Technology Inc., Warrenton, USA) reactor. After the reaction, the cationic pulp was washed with 500 ml of ethanol, 500 ml of tetrahydrofuran (THF) (Sigma Aldrich, USA), and 1000 ml of Milli-Q water. Functionalized cellulose pulp was diluted to 2 w-% concentration and dispersed using a high-shear Ystral X50/10 Dispermix (Ystral GmH, Ballrechten-Dottingen, Germany) for 10 min at 2000 rpm. The pulp was then fibrillated using Microfluidics microfluidizer type M110-EH (Microfluidics, Westwood, USA) at 1800 bar pressure and inserted twice through two chambers with diameters of 400  $\mu\text{m}$  and 100  $\mu\text{m}$ . The fibrillated cationic CNF formed a highly viscous and transparent hydrogel with a final dry material content of 2 w-%. The degree of substitution was analyzed according to the method proposed by Bendoraitiene *et al.* (Bendoraitiene et al. 2006) and was 0.35.

The cellulosic fiber pulp material was responsible for forming bulk for foam formed 3D structures. Pulp used in the study of Publication IV was gently refined bleached kraft pulp (Scotch pine 3.7 % dry mass), as obtained from a Finnish pulp mill. Material selection was made based on the previous studies in the field of foam forming.

Four surfactants were chosen based on their ionic nature and standard: non-ionic Triton X-100 and Pluronic F-127, anionic sodium dodecyl sulfate (SDS), and cationic cetyl triammonium bromide (CTAB). Surfactants were purchased from Sigma-Aldrich (Merck KGaA, Darmstadt, Germany). All four types of surfactants were studied in Publication I and based on the results of Publication I three surfactants were selected to the studies of Publication II. In Publication IV surfactant Triton X-100 was used based on the findings of Publication II and the foaming ability.

## 7.2 Preparation of dispersions and composites

To observe the effect of sonication energy and the amount of surfactant on dispersion quality, CNT concentration in dispersions (Publication I) was kept constant at a 0.5 w-%. Also, in Publication II, concentration of CNTs was kept

constant at 0.05 w-% in NFC-CNT dispersion, meaning 16.7 w-% in the nanocomposite films, so the effects of sonication energy and surfactant type on the conductivity properties are more visible. For Publication III MWCNT concentration in dispersion was selected based on the findings in Publication II and varied from 21 to 34.5 w-% in self-assembled and isotropic nanocomposite films.

The sonication of the dispersion samples was performed for all Publications from I to IV with a tip horn ( $\phi$  12.7 mm) sonicator Q700 (QSonica LLC., Newton, CT, USA). The sonication amplitude of vibration (50 %) was kept constant. The power output remained between 60 and 70 W for every sonication. The system included a water bath to keep samples cool during the sonication so that the temperature would not rise above 30 °C. The water bath was cooled by circulating cooling glycerol through a chiller (PerkinElmer C6 Chiller, PerkinElmer Inc., Waltham, MA, USA). In Publication III, also SONICS Vibra Cell VCX 750 ultrasonic processor (Sonics and Materials, Inc., USA) was used for c-CNF with sonication parameters of 2 min at 20 % amplitude.

### 7.2.1 Two-component system of MWCNT-surfactant dispersions

Nanocyl NC 7000 MWCNTs' mass was kept constant (0.40 g, 0.5 w-%) in Publication I, and aqueous dispersions were prepared using four different surfactants with four different concentrations and sonicated using 10 different sonication energies, so that 160 samples were obtained. Each sample was weighed to a 100 ml glass beaker and diluted to a total of 80 g with deionized water. Selected surfactants were Triton X-100, Pluronic F-127, CTAB, and SDS. Surfactants were used with surfactant to MWCNT ratios of 1:4; 1:2; 1:1, and 2:1. The sonication of dispersions was conducted using sonication energies 0-1000 kJ/g (dry mass).

### 7.2.2 Two-component system of CNF-MWCNT dispersions

In Publication III, dispersing action of cationic cellulose nanofiber (c-CNF) material was investigated and reported for the first time. The control c-CNF MWCNT samples were prepared by sonicating the c-CNF supernatant and MWCNTs to form a homogeneous stable dispersion. The control samples contained the c-CNF supernatant with a concentration of 0.05 w-% of MWCNTs in an aqueous medium. The total dry mass for the control sample was 0.16 g. The resulting high-energy sonicated hes-c-CNF MWCNT dispersion was used to prepare control

nanocomposite films. A schematic illustration of dispersion and suspension preparation and nanocomposite manufacturing is described in Figure 9.

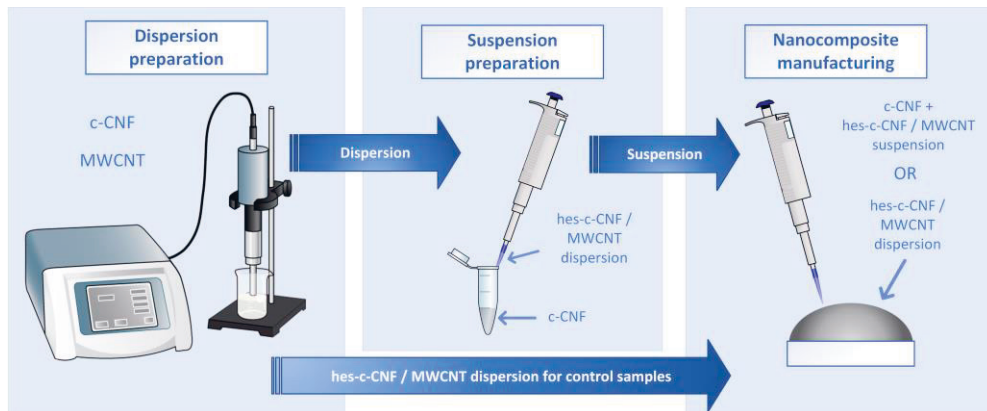


**Figure 9.** Schematic illustration of dispersion and suspension preparation, and nanocomposite manufacturing in Publication III.

The hes-c-CNF MWCNT dispersion was further suspended with different volume ratios of additional c-CNFs for the preparation of suspension samples. The nanocellulose used in S1 and S2 suspension is the 0.15 w-% c-CNF supernatant with concentrations of 37.5 v-% and 20 v-% while the nanocellulose in the S3 suspension was further sonicated with 625 kJ/g (dry mass) and marked hes-c-CNF. Thus, S1 and S2 differ in volume ratios of the dispersion and added c-CNFs, while S2 and S3 differ in the pretreatment of the added c-CNFs and hes-c-CNF, respectively, while the volume ratio is constant.

Polydimethylsiloxane (PDMS) substrates for nanocomposite manufacturing in Publication III were fabricated with a standard PDMS curing procedure in a Petri dish. A PDMS layer that was approximately 3 mm thick was prepared on a Petri dish surface and then cut into 10 mm diameter circular substrates using a 10 mm punch. The nanocomposite films were prepared by casting 250  $\mu$ L of the dispersion (control sample C) or suspension (samples S1, S2, S3) on the PDMS substrates and drying for five hours at 60 °C (UN55, Memmert GmbH + Co. KG, Schwabach, Germany) to obtain self-standing circular nanocomposite films with a 10 mm diameter and thickness between 0.007 and 0.011 mm.

### 7.2.3 Three-component system of NFC-MWCNT-surfactant dispersions

The NFC and MWCNT were sonicated simultaneously to prepare aqueous dispersions in Publication II and IV in presence of the surfactant, and after sonication, no centrifuge was used. This procedure utilizes the usage of a minimum amount of chemicals, materials, and processing phases so that energy consumption can be minimized.

NFC-CNT surfactant aqueous dispersions with a total of 80 g were prepared. The total dry mass for all the dispersions was kept constant at 0.24 g in Publication II so that the needed sonication energy per dry mass could be determined and this information was utilized in Publications III and IV.

In Publication II, one set contained NFC (0.25 w-%), CNTs (0.005 w-%), deionized water and one of the selected surfactants (Triton X-100, 0.25 w-%, Pluronic F-127, 0.09 w-% and 0.3 w-% and CTAB 0.30 w-%).

The samples for Publication II were sonicated with four different amounts of energies per dry mass, 166, 333, 500, 666, and 1000 kJ/g. Schematic visualization of the nanocomposite manufacturing (Publication II) is presented in Figure 10.

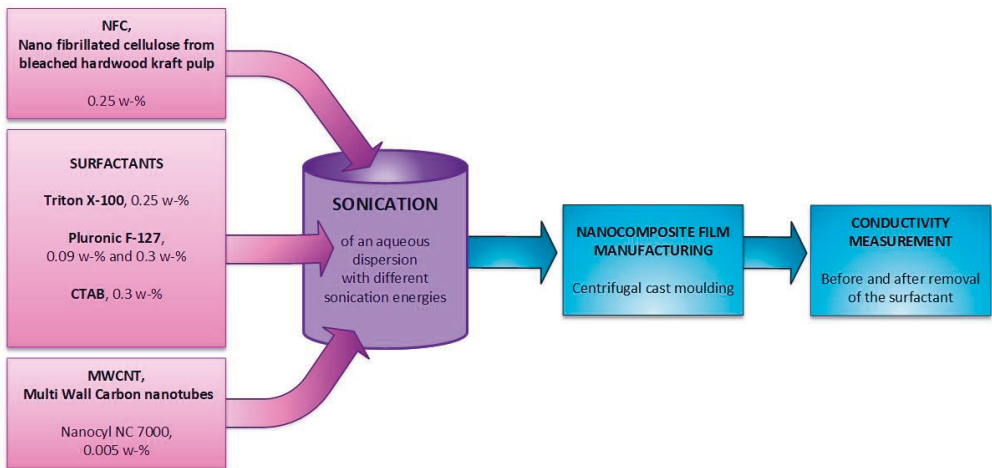


**Figure 10.** Schematic visualization of nanocomposite manufacturing procedure in Publication II.

Nanocomposite films were prepared by using centrifugal cast moulding in Publication II. A house-made equipment, which included a polyester vessel (Ikea Vispad) with a diameter of 22 cm and laboratory stirrer (Ika, Eurostar power) were used. The vessel set to rotate around a vertical axis with speed of 150 rpm to produce uniform and

well distributed films. Sonicated NFC-CNT-surfactant dispersion were poured into the vessel and rotated 24 h in RT.

Based on results obtained in Publication II, surfactant Triton X-100 and a sonication energy of 666 kJ/g were used in further studies reported in Publications III and IV.

#### 7.2.4 Four-component system of NFC-MWCNT surfactant and pulp

In Publication IV, NFC-MWCNT surfactant pulp non-woven composite structures in sheet and 3D form were manufactured using foam-forming process. The target was to use the selected surfactant type and surfactant amount in both the dispersion processing step and in the foam forming step. The concentration of surfactant must be sufficient to form stable and homogeneous dispersion, but it should also allow the formation of stable foam.

NFC and CNT were sonicated simultaneously and after sonication, no centrifuge was used so that the preparation of aqueous dispersions could be achieved using a minimum amount of processing steps. Two identical sets of NFC-CNT aqueous dispersions with a total volume of 1800 ml were prepared. One set contained NFC (0.15 w-%), CNTs (0.3 w-%), deionized water, and surfactant Triton X-100, (0.4 w-%). The total dry mass for the dispersions was 8.25 g.

In the foam-forming of non-woven composite structures, two sets of NFC-CNT dispersion were poured into the foam-forming systems' cylindrical tank that had the diameter of 32 cm. Followed by water and pulp, so that the total volume was 5.5 liters (Figure 11).





**Figure 11.** Laboratory scale foam forming equipment; (b) nanofibrillated cellulose-carbon nanotubes (NFC-CNT) dispersion, pulp, and water mixture before foaming in Publication IV.

When 3D form "Salmiakki" was processed, used material concentrations and methods were the same as in foam-forming the non-woven sheet form composite structures, only pulp concentration was increased to 85 g dry mass, meaning a concentration of 1.5 % in foam-forming. Mechanical mixing was conducted at a rotation speed of 3500 rpm for 3.5 min. The foaming time resulted in a 70 % air content in the foam, meaning that the total foam volume was 19 liters (Figure 12).

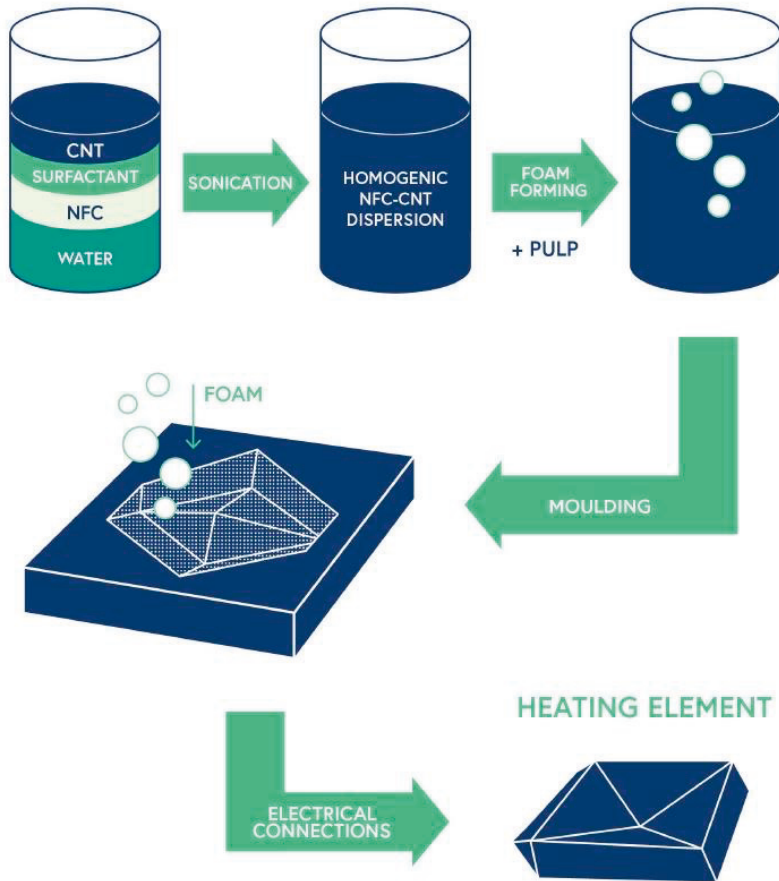


**Figure 12.** The manufacturing process of heating element prototype "Salmiikki", Publication IV.

The prepared foam containing NCF-CNT and pulp was poured into a planar or 3D mold, in the case of "Salmiikki" manufacturing, that had a perforated surface. The wet foam was removed using a 0.5 bar vacuum suction. A plastic film was placed on top of the foam column to maintain constant local suction. After vacuum assisted foam removal, the non-woven cellulosic fiber sheets and 3D structures were dried in a thermal cabinet at 70 °C for 12 hours until dry.

## 7.3 Characterization

UV-Vis spectrometric analyses were performed using Shimadzu UV-1800 spectrophotometer (Shimadzu Corp., Kyoto, Japan) in Publication I to determine the quality of the sonicated dispersions. Measurements were conducted at 500 nm, which is directly related to the concentration of CNTs in the dispersed state. A portion of each dispersion was collected, let settle for five days, and its supernatant was diluted to 1:300 with deionized water to get the solutions transparent. The opacity of the diluted dispersions was measured by using a spectrophotometer and plastic cuvettes with a 1 cm optical path length.

The electrical conductivity of nanocomposite films (Publication II), non-woven sheets, and 3D structures (Publication IV) were measured using a four-probe measuring procedure with a multimeter (Keithley 2002, Tektronix Inc.). With this method, it is possible to minimize the contact resistances and thus provide more accurate conductivity measurements than for commonly used two-terminal measurements. Probes were placed in line, with equal 3 mm spacing. The conductivity measurements were conducted using a 1 mA current and voltage was measured. Prepared nanocomposite films and foam formed non-woven sheet samples were cut to the size of 30 mm × 30 mm and conditioned according to the standard ISO 139 before conducting sheet resistance measurements. Similarly, measurements were conducted on 3D form without cutting samples. The measurements were conducted on the samples containing surfactant and, on the samples, where surfactant was removed by acetone or ethanol washing.

Infrared imaging in Publication III (IR-imaging, Fluke Ti400, Everett, WA, USA) was used to obtain the electrical anisotropy of the assembled c-CNF + hes-c-CNF/MWCNT films in comparison to the uniform conductivity of the control hes-c-CNF/MWCNT nanocomposite films at the macroscale. IR-imaging was performed by applying silver ink contact to the edge of the film samples, inserting a current through the film and recording sample heating. In Publication IV, IR-imaging was used to acquire the heating pattern of the 3D heating element "Salmiakki".

The mechanical testing was conducted to determine maximum breaking strength in Newtons of foam formed sheet samples in Publication IV. Objective was to research reinforcing effect of nanocellulose and carbon nanotubes on non-woven structure before and after removal of residual surfactant. Testing was done according to the standard EN 29073-3:1992 "Textiles. Test methods for non-wovens, Part 3: Determination of tensile strength and elongation" Used testing machinery was

Testometric M500-25kN (Testometric Co Ltd, Rochdale, UK). From the foam-formed non-wovens, ten sample pieces in total were cut (50 mm × 250 mm). Five of them were tested as such, while another set of five samples was washed in an appropriate amount of acetone in RT so that the remaining surfactant Triton X-100 was removed. In general, the removal of surfactants from various nanocomposites can enhance the mechanical and electrical properties (Keinänen et al. 2018, Publication II). All the non-woven composite samples were conditioned according to the standard ISO 139:2005 "Textiles- Standard atmospheres for conditioning and testing" before the tensile testing. The testing was performed by applying a constant displacement rate of extension of 100 mm/min.

Electron microscopy (FE-SEM, 3 kW, Zeiss ULTRAplus, Oberkochen, Germany) was used to characterize the nanomaterials and nanocomposite films in Publication II, III, and IV. The samples were attached to aluminum SEM stubs using carbon tape or carbon glue. The samples were either carbon or gold-coated to avoid charging during the SEM studies.

# 8 RESULTS AND DISCUSSION

The main results of this thesis are presented and discussed in this chapter. First, the effect of sonication energy, surfactant type, and amount to CNT dispersion quality is presented, followed by the conductivity of NFC-CNT nanocomposites in terms of sonication energy and surfactant type. Furthermore, the effect of NC aspect ratio to electrical conductivity in NC-CNT nanocomposites is discussed. Nanocellulose's carrying capability, dispersing action, and nanocomposites' post-processing to enhance conductivity, are also studied. Finally, affecting attributes to NC-CNT nanocomposites' electrical conductivity are listed and, verification and validation of applicability is reported.

## 8.1 Effect of sonication energy and surfactant type

CNT dispersion is challenging to manufacture because the internal energies of aggregates must be overcome. This can be done by using high shear forces obtained in sonication, but during processing, the integrity of the tubes is in jeopardy, which can negatively affect the NC-CNT and CNT-CNT interactions. Furthermore, surfactant type and the surfactant amount should also be optimized.

### 8.1.1 Quality of CNT dispersion

Studies published in Publication I were conducted because the CNT dispersions research field does not attain coherent results that inform the needed sonication energy in terms of kilojoule per material mass in grams (kJ/g). Sonication energy threshold can be achieved when surfactant concentration toward CNTs is at the right level.

It was reported in Publication I that SDS surfactant does not disperse MWCNTs efficiently and for that reason homogeneous dispersion does not form even if the sonication energy and surfactant concentration are increased. It is also stated in the study that suitable surfactant types to disperse MWCNTs are Triton X-100 and

Pluronic F-127 and CTAB. Figure 13 presents the UV-Vis spectrophotometry absorbance curves as a function of sonication energy for four different surfactant types with four concentrations. These curves are directly related to the quality of the sonicated carbon nanotube dispersions.

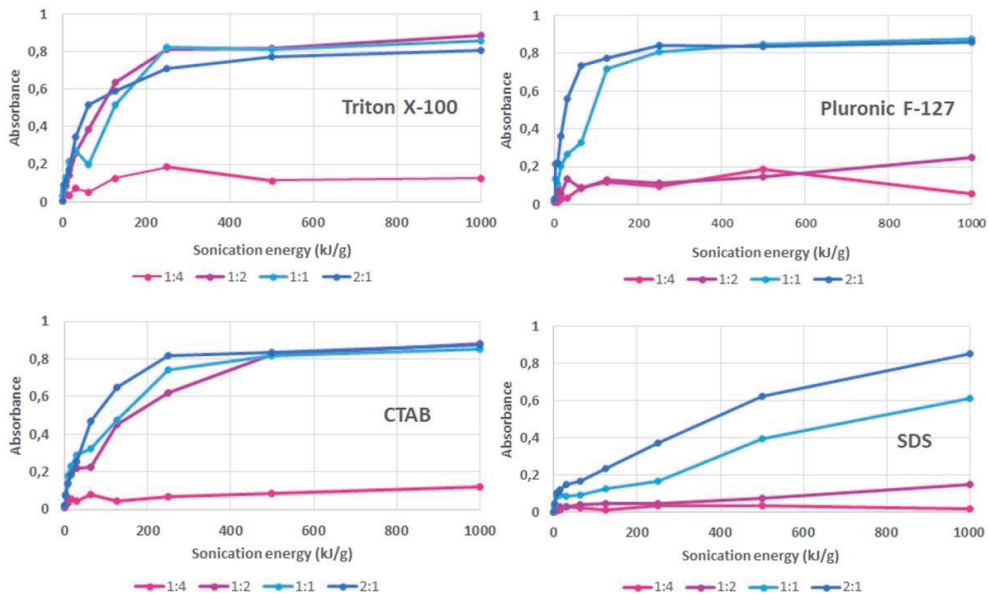


**Figure 13.** Absorbances as a function of sonication energy per mass (kJ/g) determined using surfactants Triton X-100, Pluronic F-127, CTAB and SDS with concentrations towards CNT mass 1:4; 1:2; 1:1 and 2:1. (Publication I)

Depending on the surfactant type, the concentration was studied for ranges of from 1:2 to 2:1 resulting in the fact that threshold was attained for a sonication energy of 100-200 kJ/g. In the case of Triton X-100, it can be also seen that increasing surfactant concentration to 2:1 had a negative effect on attaining homogenous dispersion. However, by using Triton X-100 the surfactant threshold can be obtained using a lower amount of chemicals and sonication energy than by using surfactants CTAB or Pluronic F-127.

### 8.1.2 Conductivity of NFC-CNT nanocomposite

In Publication II, coherent research was conducted focusing on how sonication energy, surfactant type and amount are affecting the electrical conductivity of NFC-

CNT composite films. Conductivity results as function of sonication energy (kJ/g) are presented in Figure 14 when Triton X-100, Pluronic F-127 and CTAB surfactants are used as a dispersing agent in the NFC-CNT composite films. The presented curves report the conductivity results for NFC-CNT films when used surfactant is still present in the composite structure (pristine) and after surfactant is removed away from the structure (washed). Overall, the shelf-life of the sonicated dispersion samples was significantly long, since the samples remained unchanged before the film preparation. Also, no sedimentation during centrifugal cast molding was detected since conductivity values were at the same level when measured from both sides of the nanocomposite films.

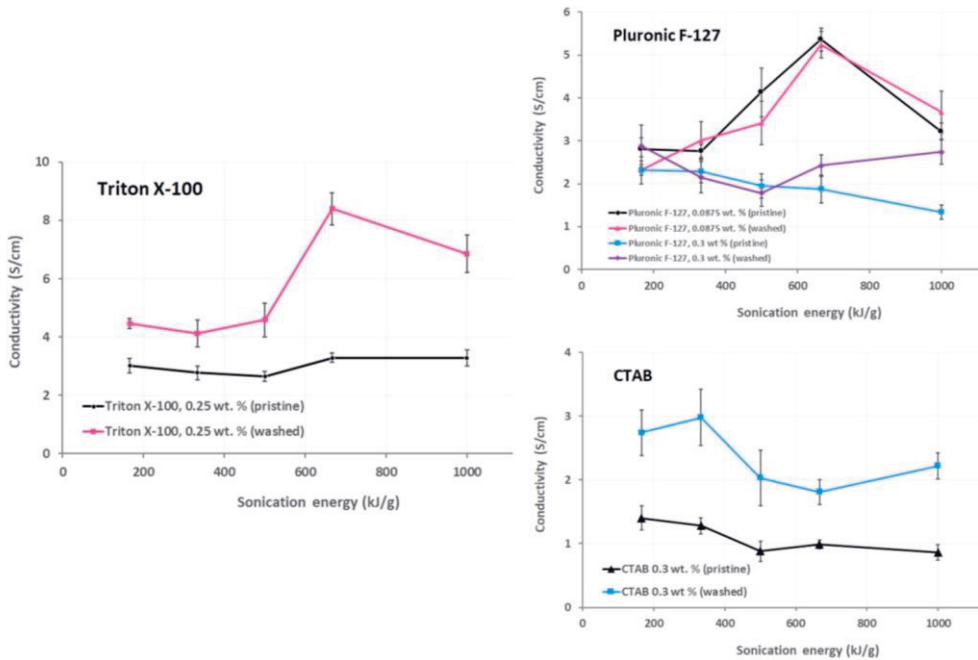


**Figure 14.** The conductivity of nanocomposite film before and after Triton X-100 surfactant removal, Pluronic F-127 surfactant removal, and CTAB surfactant removal. (Publication II)

According to the standard (International standard ISO 14887 2000), the hypothesis was that non-ionic surfactants would be the most promising surfactants to disperse the NFC-CNT mixture. This was clearly the case since the films made with surfactants Triton X-100 and Pluronic F-127 outperformed the films made with the ionic surfactant CTAB. The conductivity of films processed using CTAB decreased as the sonication energy kJ/g increased from almost 1.5 S/cm to less than 0.90 S/cm. The conductivity diagram of these films was different in its nature; the highest values

were measured with the lowest amount of sonication energy. By using surfactants Pluronic F-127 and Triton X-100, conductivity values of 5.36 S/cm and 3.0 S/cm, respectively, were achieved. These are high conductivity values with a relatively low CNT concentration of 16.7 w-% and using a minimum amount of processing steps, materials, and chemicals.

However, it should be noted that these results are only valid when using multiwall CNTs and in pursuit of good electrical conductivity. It is very likely that when optimizing the mechanical properties of NFC-CNT composites the maximum value can be achieved using different sonication energy relative to the drying mass (kJ/g).

## 8.2 Post-processing to enhance integrity of CNT percolation network

It is well known that surfactants can plasticize the structure of composites and interfere with conductivity properties by situating themselves at the interface between the conductive particles and the matrix. Furthermore, the much-needed surfactant is acting as a barrier and prevents particles from connecting and forming a percolation network which leads to reduction of conductive properties.

Publication II reported that Pluronic F-127 and Triton X-100 surfactants have resulted in good conductivity values when NFC-CNT dispersion is used to manufacture nanocomposite films with a relatively low CNT concentration. The conductivity values of the nanocomposite film can be further increased by removing the surfactant from the interfaces of NFC-CNT and CNT-CNT e.g., by acetone washing.

This effect was seen in samples that were dispersed using surfactant Triton X-100, but not in samples that were dispersed using Pluronic F-127 (Figure 14). The reason for this might be that Pluronic F-127 surfactant prefers NFC over CNTs and Triton X-100 prefers CNTs. The conductivity of 8.42 S/cm is the highest value reported to NFC-MWCNT composite films in the current literature using 16.7 w-% CNTs. Figure 15 presents the SEM imaging of NFC-CNT nanocomposite films' surface with sonication energies of 166 kJ/g and 666 kJ/g after the surfactant Triton X-100 removal.



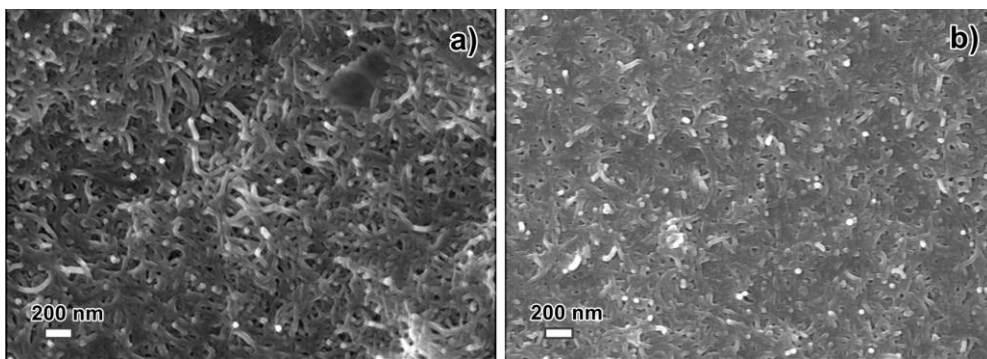


**Figure 15.** SEM imaging of NFC-CNT nanocomposite films' surface after surfactant (Triton X-100) removal with sonication energies of 166 kJ/g (a) and 666 kJ/g (b). (Publication II)

From the images, it can be observed that a sample of a high sonication energy (666 kJ/g, Figure 15b) is more compact and homogeneous in surface structure than the NFC-CNT nanocomposite film that has undergone a lower sonication energy (166 kJ/g, Figure 13a) treatment. The integrity of the structure has a beneficial effect on electrical conductivity since CNTs pack closer together to form a comprehensive percolation network. When post-processing to remove Triton X-100 surfactant is done for samples of lower sonication energy, electrical conductivity rises from 3.05 S/cm to a value of 4.47 S/cm meaning 47 % increase, while for a high sonication energy sample, the post-treatment resulted in a huge improvement in electrical conductivity by increasing it from 3.22 S/cm to 8.42 S/cm, an increase of 161 %.

Based on the results, it should be noted that, when post-processing of manufactured NFC-CNT films is possible with acetone washing, Triton X-100 surfactant should be selected as a dispersing agent to achieve excellent electrical conductivity. However, when surfactant removal is not an option, Pluronic F-127 should be selected.

### 8.2.1 Mechanical strength of NFC-CNT pulp non-wovens

In Publication IV, the effect of NFC-CNT surfactant dispersion on the mechanical strength of the foam-formed non-woven materials was tested and reported. The maximum breaking strength of the foam-formed non-woven NFC-CNT pulp surfactant composite structure was 121 N ( $\pm$  11.8 N). After the surfactant Triton X-100 was removed, the strength increased to a value of 142 N ( $\pm$  6.1 N). In comparison, the tensile strength for foam-formed reference non-woven made using

only the wood pulp fibers and surfactant, without NFC or CNTs, was 9.4 N ( $\pm 0.5$  N), and after acetone washing, to remove the surfactant, the value increased to 16.5 N ( $\pm 1.7$  N). This shows that NFC and CNTs increase the tensile strength of the non-woven composite structure and removal of the surfactant even higher values can be obtained.

Furthermore, the mechanical strength was expected to increase after the removal of the surfactant, due to the increased entanglement and interactions of NFC, CNTs and pulp. The effect of surfactant removal by acetone washing is marginal to conductivity values (7.7 S/m  $\rightarrow$  8.0 S/m) in the case of foam-formed NFC-CNT pulp composite structures. The reason for this might be that majority of the surfactant is already removed from the structure during the vacuum assisted molding process. Results also showed that adding NFC-CNT dispersion into the foam-forming process with wood pulp increased the tensile ultimate load values of the manufactured non-woven composite structures. This three-material system has over ten times higher tensile strength compared to one material system, pulp when residue surfactant is still present in the non-woven structure.

### 8.3 Dispersing action of c-CNF

The amphiphilic nature of the NC chain affects the solubility and the surface energy, which also affects the dispersibility, the hydrophobic interactions, and the aggregation tendency (Lindman, Karlström, and Stigsson 2010; Olszewska et al. 2011). During sonication, the applied energy affects intramolecular and intermolecular bonds, causing a different degree of fibrillation in the cellulose structure. The increased surface area and polar non-polar nature of cellulose aids the dispersion of hydrophobic MWCNTs in an aqueous environment. The high surface-to-length ratio of MWCNTs and the lack of functional groups determine that the chemistry of CNTs is dominated by dispersion type interactions. These extended  $\pi$ -conjugations, such as  $\pi$ - $\pi$  and cation- $\pi$ , enable non-covalent interactions with various substrates.

It is reported, in Publication III that cellulose and CNTs exhibit favorable interactions toward each other so that auto aggregation of both nanoparticles does not occur, and they form a strong entangled hybrid nanoparticle dispersion, where the cationic functional groups of c-CNFs point outwards from the hybrid structure, resulting in a stable dispersion. Findings in Publication III endorse that CNF and

CNTs have established robust connections at the molecular level and c-CNFs can be used to disperse MWCNTs.

When cationic CNF is used as a dispersing agent in CNF-CNT nanocomposites structure, CNTs are evenly distributed in the formed nanocomposite film (Figure 16).

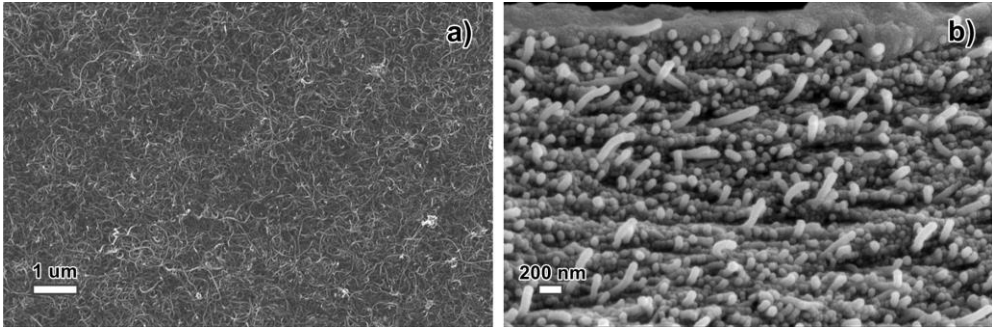


**Figure 16.** SEM imaging of c-CNF-CNT composite surface and cross-section showing evenly distributed CNTs. (Publication III)

Based on the findings, it can be confirmed that c-CNFs work as a dispersing and stabilizing agent. Publication III was the first publication to demonstrate the successful use of c-CNFs to disperse MWCNTs. However, further optimization for sonication energy per dry mass and materials' concentrations should be done because dispersion quality and stability are playing a key role lot of applications.

### 8.3.1 Non-templated self-assembly

Controlled nanomaterial assembly commonly requires extra time, high energy consumption, and expensive proprietary technologies and equipment. The method described in Publication III is simple, quick, efficient, and safe compared to current attempts to control the assembly of nanomaterials. Indeed, it was noted that in the assembled structures of high aspect ratio nanomaterials, the differences in the electric current parallel and perpendicular to the orientation results in conductivity anisotropy when additional c-CNF is added to hes-CNF-MWCNT dispersion.

An overview of the differences in the conductivity pattern between the isotropic control film and the self-assembled anisotropic films is visible in IR heat maps. The control film obtained from the sonicated stable homogeneous hes-c-CNF-MWCNT dispersion shows an even temperature and current flow across center of the film

when a constant voltage is applied on the film surface through the silver ink contacts. It is suggesting that the current follows the shortest route, as shown in the IR-image captured seconds after the beginning of heating before the heat has spread evenly across the film (Figure 17a).

Interestingly, when a solution containing additional free c-CNFs is suspended with the sonicated hes-c-CNF-MWCNT dispersion and the aqueous medium is evaporated, the resulting film possesses heat zones (Figure 17b). In the self-assembled films, the center area shows a lower temperature, indicating that the current is restricted to pass through the center line, which is the shortest path from terminal to terminal.

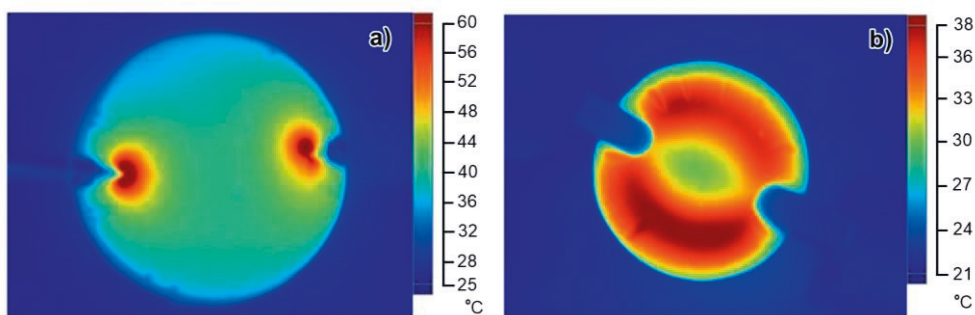


**Figure 17.** The difference in thermal conductivity between control and assembled films. IR-imaging of the isotropic control nanocomposite film (a) and self-assembled anisotropic nanocomposite film S1 (b) when a current is applied to the structure so that a heating phenomenon occurs. (Publication III)

The heat maps in Publication III confirm that evaporation of the aqueous medium from the hes-c-CNF-MWCNT dispersion results in a uniform electrically conductive nanocomposite films, while films that are evaporated from the suspensions (S1–S3) formed non-templated self-assembled nanocomposite films with anisotropic electrical conductivity. Furthermore, it was established that controlled, and optimized particle concentrations, as well as drying conditions, strongly influence the arrangement of the nanoparticles.

## 8.4 Effect of cellulose aspect ratio to electrical conductivity

An optimal “green” electrically conductive composite material can be obtained, when CNTs form electrically conductive tubular channels on the surfaces of

cellulose material with optimized size distribution. Different cellulose fibers and fibrils used in Publications II-IV revealed that, to form an efficient CNT percolation network in the composite structure, an optimum size and aspect ratio of cellulose material towards CNTs should be selected. This way formed composite material provides homogeneous electrical conducting pathways in the cellulose structure and wherein the CNT material is used in a material-efficient manner. In addition, sustainability and energy efficient processing principles can be achieved by using a minimum amount of processing steps, chemicals, and energy.

As noted, several research groups are aiming for using the smallest size of cellulose with CNTs, by utilizing chemical oxidation and multiple mechanical processing methods to produce nanocellulose. Results show that acquired electrical conductivity is at the level of semi conducting materials and usage is limited in real applications. It was observed in this thesis, that especially size distribution of cellulose plays a crucial role in creating optimized conductivity with a limited amount of CNTs, while retaining the required mechanical strength characteristics of the conductive material. Moreover, electrical conductivity can be further enhanced by removing the used surfactant from the composite structure by post-processing.

Publication III reported findings when c-CNF is sonicated with higher energy dosage and suspended with c-CNF-CNT dispersion, added c-CNFs increased the resistance, as indicated by the higher resistance of film S3 compared to that of film S2. This is likely due to the smaller size of the c-CNF in S3, which is a result of sonication. Thus, smaller c-CNFs seem to reduce conductive pathways more than larger c-CNFs in S2. In other words, the smaller c-CNFs of S3 cover MWCNTs better and therefore cause lower conductivity. Although, Publication III resulted that c-CNF can be used as a dispersing agent, the drawback of small size is that CNF is acting as a barrier between the CNT-CNT interfaces.

Figure 18 presents a schematic picture of the desirable carbon nanotube percolation network on the surface of cellulose fibrils. The ideal target is to manufacture sustainable NC-CNT composites with high electrical conductivity but also minimize the cost of manufacturing, amount of used materials and harmful chemicals. One option is to choose nanocellulose and CNT size distribution and CNT amount that are ideal for conductive CNT percolation network forming where NC does not situate in CNT-CNT interfaces by blocking movement of conductive electrons. NC has the potential to serve as a continuous or a branched template due to its relatively high aspect ratio, where conductive particles can be attached to the surface to form continuous conductive pathways in a hierarchical manner.

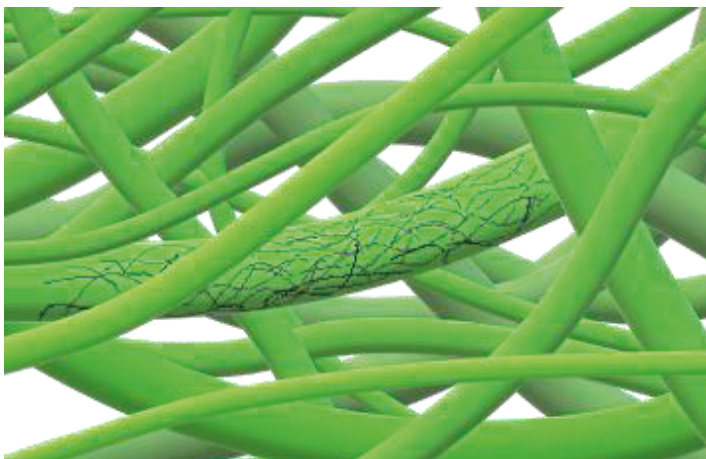


**Figure 18.** Desirable CNT percolation network on the surface of cellulose fibers. CNTs cover entirely the cellulose fiber surfaces but are here drawn exemplary only on part of the surfaces. (Sanna Siljander 2020)

The surface area of a cylindrical body is directly proportional to its diameter, but the volume is proportional to the square of diameter and, thus, the area-volume ratio decreases as the diameter increases. Since NC consists of elementary fibrils, without non-hollow volumes, such as the lumen volume in a complete wooden fiber, the mass of NC is directly proportional to the volume. Thus, a larger cylindrical body has a smaller surface area than smaller cylindrical bodies of corresponding joint mass. By choosing cellulose-based material with a larger diameter a structure is achieved, where the surface area of the NC material decreases compared to the surface area of the CNT material. At the same time, the number of CNTs becomes substantially higher than the number of NC particles, even when the mass portion of CNT is substantially lower than the mass portion of NC. This again enables NC to be coated with CNTs, which converts the NC's surface to become conductive, thanks to the formed CNT's percolation network on the NFC surfaces.

When these fully coated NCs form a hierarchical fiber network, there are connections between NC's conductive surfaces where no current preventing, insulating cellulose-based material is present. This solution not only prevents insulating material from being placed in the CNT's percolation network but allows multiple junctions in the internal CNT percolation network, which is particularly important because, while the CNTs are excellent conductors, a single junction conducts electricity only moderately. This CNT placing concentrating method utilizes the amount of CNT in an efficient way and optimized conductivity is achieved in relation to the amount of used CNT material.

A minimum amount of energy can only be used when fibrillating pulp to NC is done by using energy efficient apparatus. This approach lowers the energy and processing costs, and also utilizes the possibility to produce NC in a short period of time lowering the manufacturing costs even further. Thus, in contrast, to fibrillate NC to the smallest possible size, this presented solution utilized significantly larger NC in the preparation of cellulose-CNT composite materials to obtain conductivity.

#### 8.4.1 NFC as a carrier for CNTs

The hypothesis in Publication IV was that NFC acts as a carrier for CNTs. These hierarchical structures, where CNTs cover the surface of NFC or cellulose, can be used to for conductive structures.

Using NFC as a carrier for another material is mentioned in the patent filed by Tokushu Paper Manufacturing Co Ltd. They suggested using NFC in tinted papers as a carrier for a dye or pigment (Matsuda, Hirose, and Ueno 2001). Research group Hii *et al.* have reported in their article that micro fibrillated cellulose contributed to the bonding of calcium carbonate filler in the fiber network of paper (Hii et al. 2012). NFC is also suggested to be used as a biocarrier for controlled drug delivery. (Plackett et al. 2014)

In general, the foam forming technology utilizes aqueous foam instead of water as a carrier medium and the shear thinning behavior of the foam makes it an excellent transport medium for fibers and particles, and it enables the excellent formation of the product being produced. The application of NFC-CNT dispersions in the foam forming process enables the manufacturing of conductive 3D structures to almost any shape and size. Unfortunately, because of the nanoscale size of the CNTs, the formation with cellulose pulp alone does not occur efficiently enough to form the conductive percolation network during the foam forming process. When dispersion is prepared efficiently to form homogeneous dispersion without any aggregates present, the nanosized CNT particles flow through the cellulose fiber network in the vacuum assisted molding with the foam.

SEM imaging was used in Publication IV to investigate the CNT distribution in the foam formed non-wovens. The images have been taken from a dry sample and the NFC has generated a network where the dimensions for individual fibers are very difficult to determine. Two different magnifications in Figure 19 are illustrating the NFC and CNT nano-architecture, and the formation of a homogeneous CNT coverage over cellulose fibers.

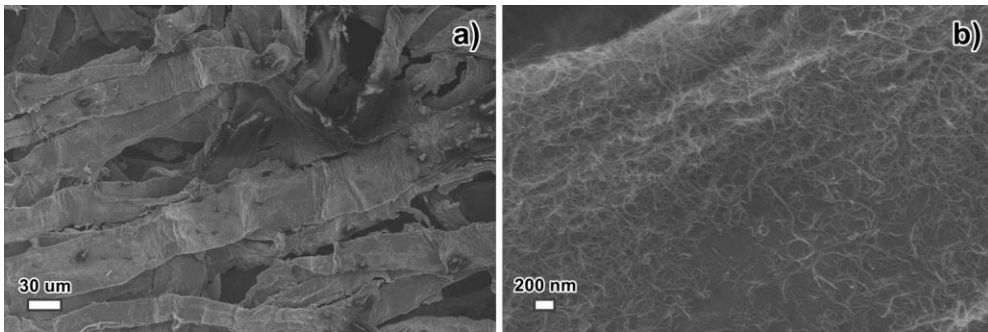


**Figure 19.** (a) Homogenous CNT coverage over cellulose fibers and (b) carbon nanotube percolation network on the surface of cellulose fiber. (Publication IV)

Figure 19 b shows a type of CNT coating on cellulose fibers: the coverage has an excellent distribution over the surface. This means that the dispersion process using the specific sonication parameters based on Publication II has been successful and a conductive percolation network of CNTs is formed.

## 8.5 Verification and validation of applicability

When conductivity reaches a certain level and an electric current is passing through the structure, which acts as a resistive conductor, the system starts to warm up due to its resistivity. This phenomenon is called resistive or Joule heating. Commonly, heating elements are manufactured by inserting a copper wire inside a seat heater or heating blanket. These types of multi-material structures are difficult to recycle, and heating occurs only near the conductive material.

By harnessing CNTs as a conductive material for heating elements, it is possible to manufacture structures that do not create hot spots. CNTs can act as a fire retardant and the entire volume of the heating element structure is functional (heating). When combining CNTs with cellulose matrix, recyclable light weight heating elements without internal conductive wires can be manufactured. Furthermore, it is possible to customize the maximum heating temperature of the heating element by adjusting the NFC-CNT dispersion quality, surfactant presence and concentration of CNTs in the formed structure. In addition to heating, such elements could be used to keep places dry, serve as an acoustic element or room divider, and have a decorative purpose. As well as in home interiors, it could be used inside boats, cars, campervans, or other spaces that are protected from direct contact with water.



In Publication III, it was introduced for the first time a method to manufacture cellulose based non-woven three-dimensional (3D) structures that are electrically conductive. The manufacturing of the conductive non-wovens is done using a minimum amount of processing steps, materials, and hazardous chemicals. Target was to use the selected surfactant type and amount in both the dispersion processing and in the foam forming step. Sufficient concentration of surfactant was established which can form stable and homogeneous dispersion of NFC-CNT, but it also allowed the formation of stable foam.

The pilot trial, in collaboration with Aulis Lundell Oy, three Liune sliding door integrable heating elements were manufactured. During the pilot trial also a fabrication method to emboss and impregnate cellulose substrate with NFC-CNT dispersion at one stage of work was developed by exploiting composite manufacturing methods. Outcomes of this pilot trial is examined further in chapter 8.5.2.

### 8.5.1 "Salmiakki" heating element

"Salmiakki", the heating element design is a result of close collaboration between materials research scientists Sanna Siljander (Tampere University) and Jani Lehmonen (VTT Technical Research Centre of Finland) and a designer Anastasia Ivanova (Aalto University). The funding and targets of the product prototype were a subtask in the multidisciplinary research collaboration Design Driven Value Chains in the World of Cellulose (DWoC) project ([www.cellulosefromfinland.fi](http://www.cellulosefromfinland.fi)). The objective was set to define the design of an electrical current-based heating element from a newly developed conductive material system (Publications II and IV), that highlights the advantageous properties and its production. "Salmiakki" prototype functionality was further improved in the ERDF funded Bio-based Intelligent Solutions Platform for Reinforcing Local Circular Economy (BioÄly) project.

When designing visual form of heating element paper mock-ups and digital modelling was used. Design was considered for its functional and perception attributes, resulting in the choice of a diamond-like shape that has got the name "Salmiakki" due to its resemblance in shape and black color to a traditional Finnish candy (Figure 20).

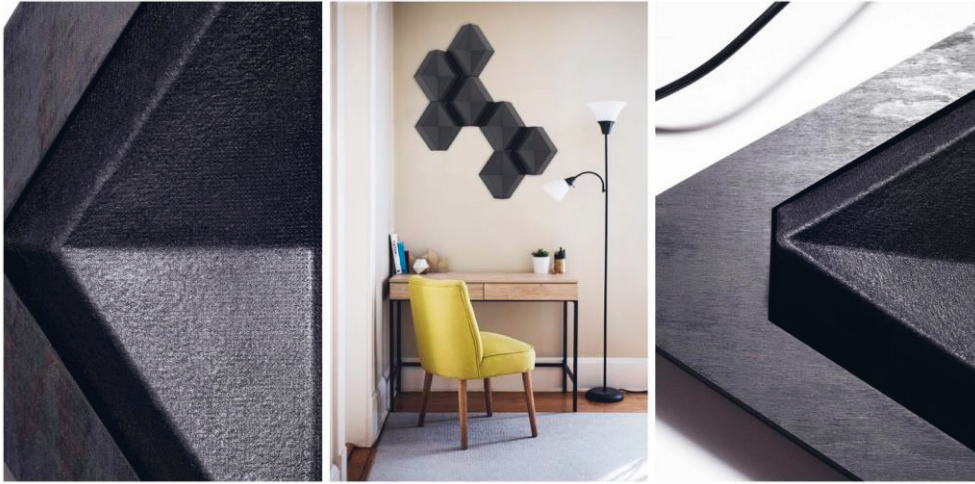


**Figure 20.** Visual design and digital rendering of heating element "Salmiakki". Photos by Eeva Suorlahti and digital rendering by Anastasia Ivanova.

The sheet resistivity of the manufactured 3D shape was measured using the four-probe method before and after removing surfactant from the structure by acetone washing. Average sheet resistances with standard deviation were, when measurements were performed from eight sample locations, 26.1 W/sq ( $\pm 2.7$  W/sq), and after acetone washing, 25.8 W/sq ( $\pm 2.0$  W/sq). Acetone washing did not decrease the resistivity much, meaning that there is a minimum amount of surfactant present in the structure that does not alter the conductivity of the carbon nanotubes significantly.

A post-treatment option was studied to enhance the visual features and the conductivity. The final 3D structure was coated with a spray of NFC-CNT dispersion that resulted darker, black finish and alongside, enhanced heating properties at a lower electrical voltage. If all the electric energy ( $P$ ) is converted into heat, then the heater temperature can be evaluated using Joule's first law of heating  $P = U^2R^{-1}$ , where  $U$  (electric voltage input, V) and  $R$  (resistance,  $\Omega$ ). Using the electric voltage input of 18.5 V with the resistivity of 25.8  $\Omega$ /sq, the electric power of the heating element is 13.2 W. After the post-treatment spray layer of NFC-CNT dispersion, the resistivity decreased to value 11.2  $\Omega$ /sq ( $\pm 0.9$   $\Omega$ /sq), meaning that the electric power of "Salmiakki" heating element is 30.6 W.

Finally, the cellulose fiber-based heating element was mounted in a plywood cover that was painted black using wood wax (Osmo Color 3169, Osmo Holz und Color GmbH & Co, Warendorf, Germany). The surface of the "Salmiakki" heating element was sprayed with varnish to gain a glossy surface (Dupli-color Lackspray,

Wolvega, Netherland) and electrical connections were installed. Copper tape forming the electrical connections are located on the opposing sides of the prototype "Salmiakki" and covers 18 cm<sup>2</sup> area per side. The distance between these copper connectors is 22 cm. As a power source "Salmiakki" is using 18.5 V, 3.5 A laptop charger (HP, Palo Alto, CA, USA).

In Figure 21, it can be observed that the temperature near copper tape conductors is 65–75 °C and a major part of the "Salmiakki" heating element is heated to a comfortable and steady 35–45 °C in RT.

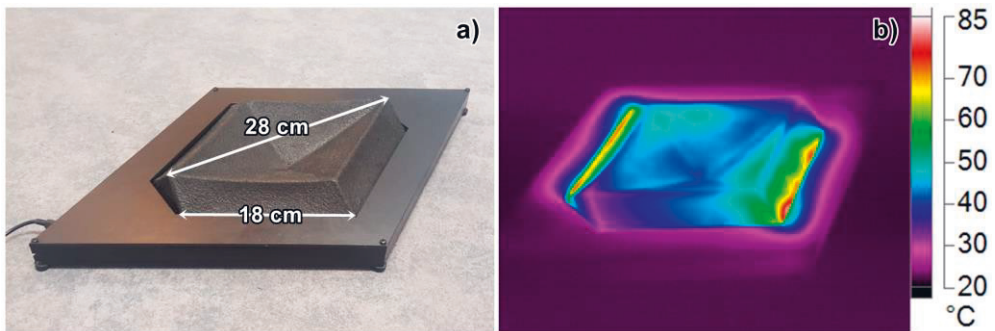


**Figure 21.** Plywood mounted 3D heating element "Salmiakki" with dimension (a) and IR-camera image of 3D heating element "Salmiakki" at steady state in room temperature (b) presented in Publication IV.

Because of rapid heating and cooling properties of CNTs, the heating response of the whole element to a steady state is in the order of minutes. When calculating the costs of manufacturing using the current pricing of raw materials, a "Salmiakki" element costs less than four euros (foaming plant investments not accounted for).

## 8.5.2 Bio-based heating element integrated into the sliding door

In the BioÄly project, a pilot trial was executed with Aulis Lundell Oy to produce new functions using biomaterial solutions in the Pyörre exhibition house by integrating bio-based heating elements into the Liune door structure. Aulis Lundell Oy manufactures spatial and structural solutions by bringing significant added value to its customers with steel structural solutions as well as reprocess profiles to elements. The Liune door, which is possible to slide hidden inside the wall, is Lundell's flagship product and Liune doors play an important role in the Pyörre exhibition house designed for Lohja housing fair 2021.

The pilot trial was started by completing an electrical safety survey to ensure safety requirements that dictate the manufacturing and usage of heating elements. Based on the survey the heating element "Salmiakki" and sliding door integrable heaters belong to the category of electric fitted and local heater. A maximum value of the AC voltage shouldn't be more than 42.4 V, or at DC 42.4 V or part should be separated from the voltage parts by a protective impedance. The efficiency of an electric space heater with a nominal thermal power of not more than 250 W shall have a minimum efficiency of 34 %. Because the working principle of "Salmiakki" and integrable heaters is that all electricity is converted to heat, the efficiency is 100 %.

The pilot trial, in collaboration with Aulis Lundell Oy, manufactured three heating elements integrable to the Liune sliding door. During the pilot trial also a manufacturing method to emboss and impregnate cellulose substrate with NFC-CNT dispersion at one stage of work was developed.

When preparing heating elements, 3D-modelled and 3D-printed structures in the shape of the desired embossed pattern are inserted into the prepared formwork frame (Figure 22a). A CNT-dispersion pre-impregnated cellulose substrate is then placed over them (Figure 22b) and covered with plastic film to form a vacuum sack. With the assistance of vacuum NFC-CNT dispersion is impregnated, which moistens the cellulose substrate, while creating the embossing patterns to the cellulose substrate (Figure 22c). CNT-dispersion with Triton X-100 surfactant, which was used in pre-impregnation, was obtained based on Publication I and NFC-CNT-Triton X-100 dispersion based on knowhow of Publications II and IV. In its entirety, three heating elements were produced, each with a unique pattern layout. Figure 22 presents steps of the heating element manufacturing process.

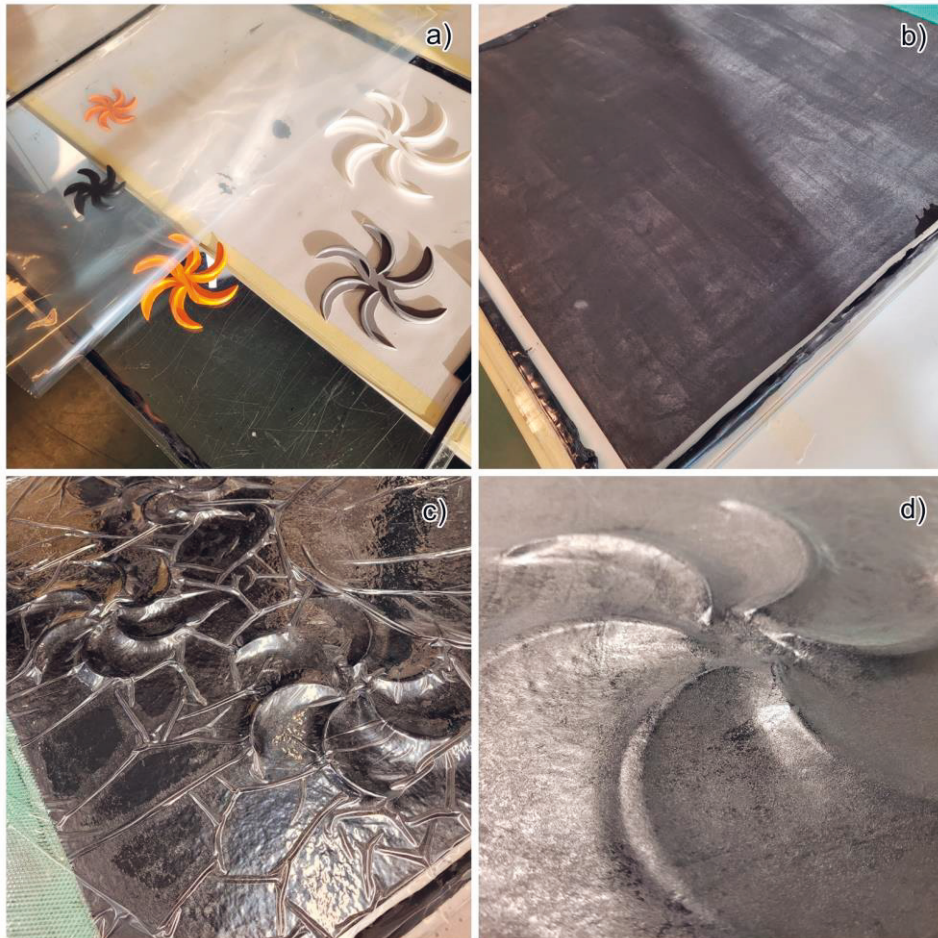


**Figure 22.** Manufacturing steps: Arranged 3D-printed structures (a), pre-impregnated cellulose substrate (b), cellulose substrate in vacuum sack impregnated with NFC-CNT dispersion and prepared heating elements' embossed pattern in close-up (d). (Sanna Siljander 2021)

After the prepared heating element dried, wires bent from a thin copper sheet were attached to the edges of the element, both at the top and bottom, and resistivity was measured. To gain a glossy surface, the heating element was spray coated with colorless varnish. These procedures were conducted for each of the heating elements.

When calculating the electric power of heating elements with a power source of 32-33 V, 2.4-2.5 A and resistivity of 13.2-13.3  $\Omega$ , obtained power values were 77-83 W meaning 240-280 W/m<sup>2</sup>. Figure 23 presents the rendered digital design models of the sliding door with three heating elements and finished heating elements installed to the Liune sliding door at Pyörre house.

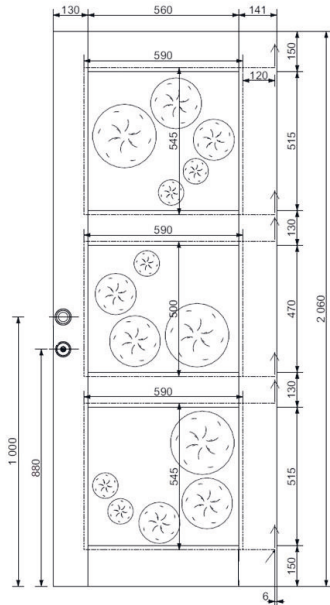


**Figure 23.** Rendered digital models of sliding door with the heating elements and installed heating elements in Liune sliding door at Pyörre house. (Aulis Lundell Oy and Leena Lundell 2021)

## 8.6 Affecting attributes to electrical conductivity in NC-CNT composites

When the goal is to form mechanically durable and electrically conductive material, it has been proven successful to combine NC and CNTs. In this hierarchical composite structure, the cellulose-based matrix acts as a mechanical support matrix and CNTs functionalize the materials' combination.

Common manufacturing methods and material combinations result in a heterogenic structure and conductivity is tuned to the targeted level by adding large amounts of CNTs, which will increase the cost of the composite structure. The main challenge is still with the insulating NC positioned between the electrically conductive CNT particles in the percolation network. This may prevent excellent conductivity when using modest amounts of CNTs to achieve mechanical strength and low price for the composite material. The trivial solution would be a material of pure CNTs aka bulky paper, but this material is too fragile in practice and the material cost is high.

Accordingly, there is still a need for low energy consumption processing methods and optimization of material combinations for producing electrically conducting composite materials in an eco-friendly way. Figure 24 sums up all the factors, which are affecting the electrical conductivity of cellulose-CNT composite structures. It is still undefined what is the exact importance of each factor.

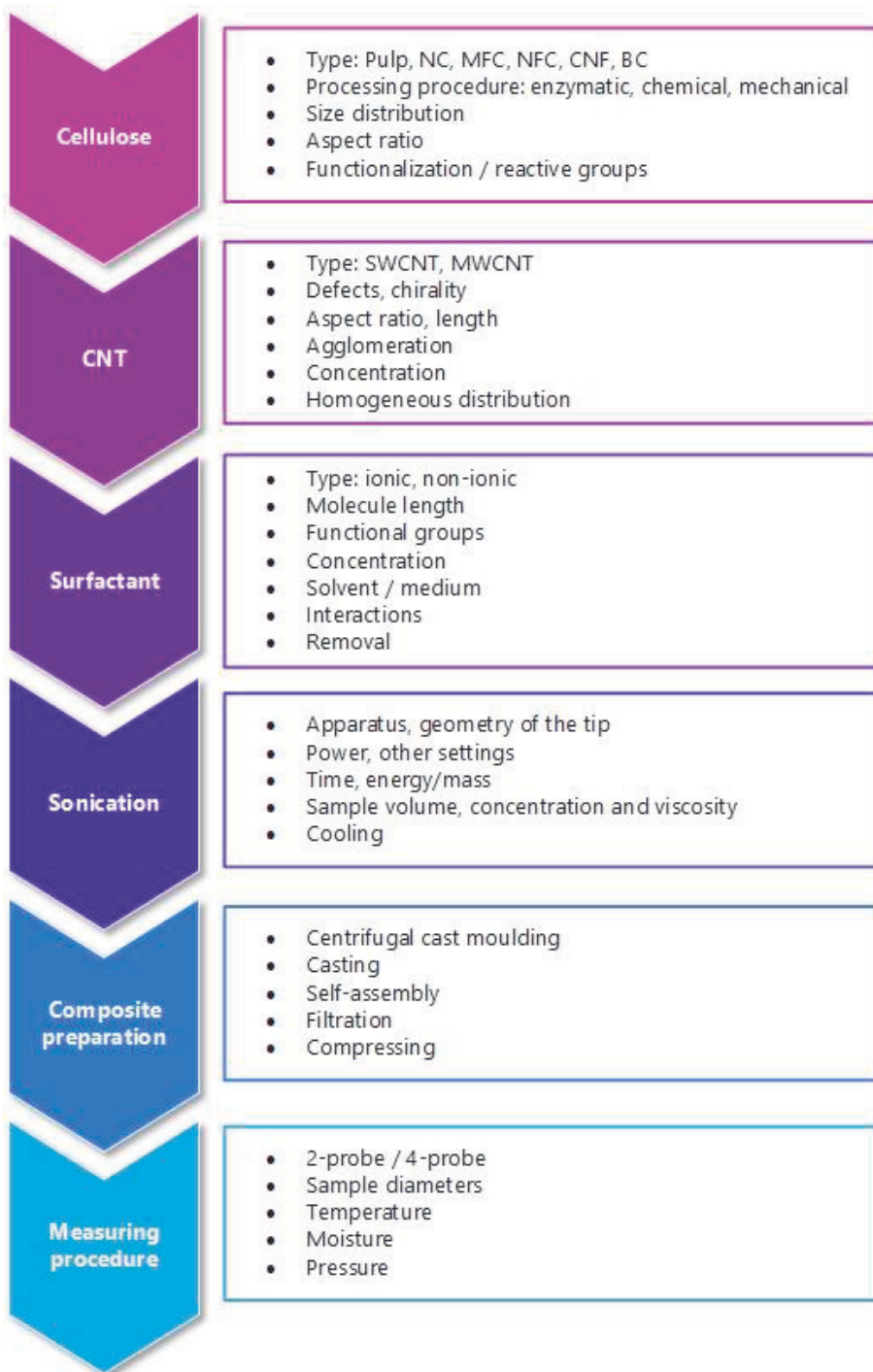


**Figure 24.** Factors affecting the conductivity of nanocellulose-CNT composite structures. (Sanna Siljander 2022)



## 9 CONCLUSIONS

The emerging concept of nanoarchitectonics provides a way to control, harmonize and modulate interactions between nanostructures, thus creating the possibility to fabricate macroscopic functional materials through understanding the arrangement and interactions of nanomaterials. Using not just a single tool of manufacturing but a total construction of architecture allows application of nanoarchitectonics to a variety of research and technology fields such as materials science, nanotechnology, and chemistry. Nanoarchitectonics concept was utilized in this thesis and several attributes were recognized to affect the NC-CNT composites' properties.

In the thesis studies challenges rising from nanoscale were encountered and functional materials were assembled successfully to hierarchical and organized structures. The thesis researched two-component, three-component, and four-component systems to identify process and material parameters that are affecting the interactions between nanomaterials. Throughout the entire dissertation study, a guideline has been followed, aiming to use only a minimum amount of materials, chemicals, and energy in the manufacture of composites. These value-added “green” products provide a sustainable alternative to overcome the increasing demand for technological development by using non-fossil resources.

With two-component systems' the sonication energy and surfactant concentration are strongly affecting the quality of the CNT aqueous dispersion and increasing surfactant amount can have negative effects on dispersion's homogeneousness (Publication I). By functionalizing CNFs and rendering it cationic, it was noted to have unique properties with CNTs when self-assembled anisotropic conductive structures were discovered. Additionally, cationic CNFs can be used as a dispersing agent for CNTs (Publication III).

Three component nanocomposite films with exemplary conductivity compared to reported research, were achieved by optimizing processing parameters and materials. The conductivity of 8.42 S/cm is the highest value reported to NFC-MWCNT composite films in the current literature using a 16.7 w-% CNTs (Publication II). The post-processing to enhance the integrity of CNT percolation network was studied (Publications II and IV) and significant differences between surfactant types were found. The reason for this phenomenon is that the Pluronic

F-127 surfactant prefers NC over CNTs and, respectively, Triton X-100 prefers CNTs (Publication II). Further research on the processing, materials, and their concentrations can lead to better dispersion of the CNTs and therefore even higher conductivity values of NC-CNT nanocomposite structures.

It was observed in this thesis, that especially size distribution of cellulose plays a crucial role in creating optimized conductivity with a limited amount of CNTs while retaining the required mechanical strength characteristics of the conductive material. When the size distribution and aspect ratio of NC and CNTs approaches equal dimensions, nanocellulose does not act as a carrier but situates between CNT-CNT interfaces and forms a barrier preventing CNTs to connect to one another. When aspect ratio is at right level, NC has the potential to serve as a continuous or a branched template due to its relatively high aspect ratio, where conductive particles can be attached to the surface to form continuous conductive pathways in a hierarchical manner.

By using NFC-CNT dispersion in the foam forming process with cellulose pulp (four component system), a higher mechanical strength can be achieved for non-woven conductive composite structure. The effect of removing the surfactant with an added acetone washing step was studied, but the effects were not significant on the measured mechanical strength and conductivity values. The reason for this might be that the majority of surfactant is removed already during the vacuum assisted molding process. These results mean that it is possible to manufacture conductive non-wovens and utilize the innovation using only two processing steps: sonication of the NFC-CNT dispersion and foam forming of the 3D structure (Publication IV).

Results reported in publications and in this thesis were obtained when nanoscale units and materials were converted to functional structures with minimum amount of defects. It should be noted that individual nanoscale units are not key players when forming nanocomposites, but their interactions are. Furthermore, self-assembly and organization related unexpected functionalities were recognized.

The applicability of the results of this thesis was verified and validated when functional heating elements were manufactured using two different processing methods. The idea of bio-based heating elements lies in the innovative production of comfort heat, which can be integrated into the interior of your home. The elements quickly warm up in their entire volume and are additionally fireproof. This heating technology with custom design option permits installation of heating elements to the household intermediate doors or design objects, rather than having heat sources only on the outer walls and in the floor.

The first heating element "Salmiakki" has been featured in several seminars and fairs in addition to media prominence. By using composite manufacturing procedures, a set of three heating elements with distinctive embossed patterns were prepared. This heating element solution was integrated into the Liune sliding door and presented at the Pyörre exhibition house of Lohja Housing Fair 2021. Since the housing fair, this functional technology solution has also been presented in interior program (Huvila ja Huussi) and in several articles and journals.

Future work is necessary to further minimize consumption of materials, chemicals, and energy when NC-CNT composite structures are fabricated. The thesis research achieved clear reductions in energy consumption as well as the amount of chemicals used when processing phases were combined, and chemicals were utilized for dual purposes. Further energy saving when manufacturing NC-CNT composite structures may be possible if more energy-efficient ways are used to fibrillate nanocellulose and possibly simultaneously homogenize carbon nanotubes with cellulose. Surfactant Triton and Pluronic were selected for the thesis studies when research performed by other research teams were analyzed and according to the standard recommendation. When working with a multimaterial solution, it may be possible that an even better result will be achieved by using a mixture of surfactants and through this approach it might be possible to reduce the amount.

In order to make it possible to concretize the findings and results of the thesis for commercial purposes, it is necessary to examine how to increase the size of the process. For example, same amount of energy per gram in sonication may not apply when sonicator size and batch volume are multiplied. Additionally, it is necessary to further clarify the importance of each material parameter in dispersion to be manufactured and processing parameters, which were identified in this study, to focus on optimizing the correct ones.

## 9.1 Research question 1

Answer to *the research question 1* “Can composite structures' performance be enhanced after manufacturing?”

The post-processing treatment with acetone washing was successfully utilized, and composites' mechanical and electrical conductivity performance was improved. Significant increase in conductivity was detected, when used Triton X-100 surfactant was removed away from NFC-CNT film structure in publication II. However, a comparable result was not seen in the case of foam-formed non-woven 3D-structures (publication IV). Reason for this is that majority of surfactant with dual function (dispersing agent and foaming agent) was already removed during vacuum assisted moulding process away from cellulose-NFC-CNT composite structure. Therefore, the post-processing of foam-formed composites has only a moderate effect on mechanical performance and the utility of the treatment should be carefully considered.

## 9.2 Research question 2

Answer to *the research question 2* “Can cationic CNF act as a dispersing agent?”

The application of sonochemical treatments to aqueous mixtures of cationic nanofibrillated cellulose and CNTs leads to even and relatively stable solutions of the assembled components, which can be easily formed to free-standing conductive nanocomposite films. It can be confirmed that c-CNF work as a dispersing/stabilizing agent for MWCNTs. However, further optimization for sonication energy per dry mass and materials' concentrations should be done.

## 9.3 Research question 3

Answer to *the research question 3* “Is the NC aspect ratio influencing electrical conductivity in NC-CNT nanocomposites?”

It can be determined that by choosing NC and CNT size distribution and amounts that are ideal for conductive CNT percolation network forming where NC does not situate in CNT-CNT interfaces but serves as a continuous or branched template, where conductive CNTs can be attached in a hierarchical manner, significant electrical conductivity can be achieved. When the size distribution and

aspect ratio of NC and CNTs approaches equal dimensions, NC does not act as a carrier but situates between CNT-CNT interfaces and forms a barrier preventing CNTs to connect to one another.

## 9.4 Research question 4

Answer to *the research question 4* “Which attributes are affecting the performance of NC-CNT nanocomposites' electrical conductivity?”

Nanomaterials were research in two-component, three-component, and four-component structures. The assumption was that there are numerous contributing factors (Figure 24), but the number of attributes rising from materials and processing procedure was substantial. In this thesis, its studies, it was recognized that material related attributes such as NC size and surfactant type and its' presence have considerable effect on the electrical conductivity. Furthermore, it was concluded in the studies that also sonication parameters and composite processing affect significantly and should be optimized. However, several factors can be controlled but still unexpected disturbances and fluctuations can occur when working with nanosized materials. It is still undefined what is the exact importance of each factor.

## 9.5 Research question 5

Answer to *the research question 5* “How can cellulose-NC-CNT composites be manufactured using minimum amount of energy, materials, and chemicals?”

It was uncovered in the thesis studies that materials could have a dual function when they are used as a dispersing agent as well as a foaming agent. This principle lowers consumption of chemicals, and it is a “greener” alternative to process composites. Chemicals, such as surfactants, can be selected so that dispersing effect is fulfilled with minimum amount and according to possibility to perform a post-processing step to manufactured composite structures. Furthermore, it was utilized that CNTs and NC can be sonicated simultaneously with or without presence of surfactant which lowers needed energy consumption, used processing steps and consumed chemicals.



## 10 REFERENCES

- Al-Qararah, Ahmad M. 2015. "Aqueous Foam as the Carrier Phase in the Deposition of Fibre Networks." Academic dissertation, University of Jyväskylä.
- Alimadadi, Majid, and Tetsu Uesaka. 2016. "3D-Oriented Fiber Networks Made by Foam Forming." *Cellulose* 23(1):661–71. doi: 10.1007/s10570-015-0811-z.
- Anderson, Robin E., Jingwen Guan, Michelle Ricard, Girjesh Dubey, Joseph Su, Gregory Lopinski, Gilles Dorris, Orson Bourne, and Benoit Simard. 2010. "Multifunctional Single-Walled Carbon Nanotube–Cellulose Composite Paper." *Journal of Materials Chemistry* 20(12):2400. doi: 10.1039/b924260k.
- Angelikopoulos, Panagiotis, and Henry Bock. 2008. "Directed Self-Assembly of Surfactants in Carbon Nanotube Materials." *Journal of Physical Chemistry B* 112(44):13793–801. doi: 10.1021/jp804891a.
- Angelikopoulos, Panagiotis, Andrei Gromov, Ailsa Leen, Oleg Nerushev, Henry Bock, and Eleanor E. B. Campbell. 2010. "Below the Cmc." *The Journal of Physical Chemistry C* 114(1):2–9. doi: 10.1021/jp905925r.
- Aono, Masakazu. 2011. "Focus on Materials Nanoarchitectonics." *Science and Technology of Advanced Materials* 12(4):10–12. doi: 10.1088/1468-6996/12/4/040301.
- Ariga, Katsuhiko, and Mitsuhiro Ebara. 2018. *Materials Nanoarchitectonics*. 1st ed. Wiley-VCH.
- Baez, Carlos, John Considine, and Robert Rowlands. 2014. "Influence of Drying Restraint on Physical and Mechanical Properties of Nanofibrillated Cellulose Films." *Cellulose* 21(1):347–56. doi: 10.1007/s10570-013-0159-1.

- Bai, J. B., and A. Allaoui. 2003. "Effect of the Length and the Aggregate Size of MWNTs on the Improvement Efficiency of the Mechanical and Electrical Properties of Nanocomposites - Experimental Investigation." *Composites Part A: Applied Science and Manufacturing* 34(8):689–94. doi: 10.1016/S1359-835X(03)00140-4.
- Bai, Yingchen, Daohui Lin, Fengchang Wu, Zhenyu Wang, and Baoshan Xing. 2010. "Adsorption of Triton X-Series Surfactants and Its Role in Stabilizing Multi-Walled Carbon Nanotube Suspensions." *Chemosphere* 79(4):362–67. doi: 10.1016/j.chemosphere.2010.02.023.
- Bai, Yu, Il Song Park, Sook Jeong Lee, Tae Sung Bae, Fumio Watari, Motohiro Uo, and Min Ho Lee. 2011. "Aqueous Dispersion of Surfactant-Modified Multiwalled Carbon Nanotubes and Their Application as an Antibacterial Agent." *Carbon* 49(11):3663–71. doi: 10.1016/j.carbon.2011.05.002.
- Belgacem, Mohamed Naceur, and Alessandro Gandini. 2008. *Monomers, Polymers and Composites from Renewable Resources*. 1 st. Elsevier Ltd.
- Bendoraitiene, Joana, Rasa Kavaliauskaite, Rima Kilmaviciute, and Algirdas Zemaitaitis. 2006. "Peculiarities of Starch Cationization with Glycidyltrimethylammonium Chloride." *Starch/Staerke* 58(12):623–31. doi: 10.1002/star.200600541.
- Blanch, Adam J., Claire E. Lenehan, and Jamie S. Quinton. 2010. "Optimizing Surfactant Concentrations for Dispersion of Single-Walled Carbon Nanotubes in Aqueous Solution." *Journal of Physical Chemistry B* 114(30):9805–11. doi: 10.1021/jp104113d.
- Bonard, Jean-marc, Thierry Stora, Jean-paul Salvetat, Fridiric Maier, Thomas Stockli, Claus Duschl, and Walt A. De Heer. 1997. "Purification and Size-Selection of Carbon Nanotubes." *Advanced Materials* (10):827–31.
- Borovskaya, A. O., B. Z. Idiatullin, and O. S. Zueva. 2016. "Carbon Nanotubes in the Surfactants Dispersion: Formation of the Microenvironment." *Journal of Physics: Conference Series* 690(1). doi: 10.1088/1742-6596/690/1/012030.
- Boufi, Sami, Israel González, Marc Delgado-Aguilar, Quim Tarrès, and Pere Mutjé. 2017. "Nanofibrillated Cellulose as an Additive in Papermaking Process." *Cellulose-Reinforced Nanofibre Composites: Production, Properties and Applications* 154(July):153–73. doi: 10.1016/B978-0-08-100957-4.00007-3.



- Brinker, C. Jeffrey, Yunfeng Lu, Alan Sellinger, and Hongyou Fan. 1999. "Evaporation-Induced Self-Assembly: Functional Nanostructures Made Easy." *Advanced Materials* 11(7):579–85. doi: 10.1557/mrs2004.183.
- Brodin, Fredrik Wernersson, Øyvind Weiby Gregersen, and Kristin Syverud. 2014. "Cellulose Nanofibrils: Challenges and Possibilities as a Paper Additive or Coating Material - A Review." *Nordic Pulp and Paper Research Journal* 29(1):156–66. doi: 10.3183/NPPRJ-2014-29-01-p156-166.
- Bystrzejewski, M., A. Huczko, H. Lange, T. Gemming, B. Büchner, and M. H. Rummeli. 2010. "Dispersion and Diameter Separation of Multi-Wall Carbon Nanotubes in Aqueous Solutions." *Journal of Colloid and Interface Science* 345(2):138–42. doi: 10.1016/j.jcis.2010.01.081.
- Calahorra, Yonatan, Anuja Datta, James Famelton, Doron Kam, Oded Shoseyov, and Sohini Kar-Narayan. 2018. "Nanoscale Electromechanical Properties of Template-Assisted Hierarchical Self-Assembled Cellulose Nanofibers." *Nanoscale* 10(35):16812–21. doi: 10.1039/c8nr04967j.
- Calvaresi, Matteo, Marco Dallavalle, and Francesco Zerbetto. 2009. "Wrapping Nanotubes with Micelles, Hemimicelles, and Cylindrical Micelles." *Small* 5(19):2191–98. doi: 10.1002/smll.200900528.
- Chatterjee, Tirtha, Koray Yurekli, Viktor G. Hadjiev, and Ramanan Krishnamoorti. 2005. "Single-Walled Carbon Nanotube Dispersions in Poly(Ethylene Oxide)." *Advanced Functional Materials* 15(11):1832–38. doi: 10.1002/adfm.200500290.
- Chen, Chuchu, Mengmin Mo, Wenshuai Chen, Mingzhu Pan, Zhaoyang Xu, Haiying Wang, and Dagang Li. 2018. "Highly Conductive Nanocomposites Based on Cellulose Nanofiber Networks via NaOH Treatments." *Composites Science and Technology* 156:103–8. doi: 10.1016/j.compscitech.2017.12.029.
- Chen, Xiaodong, and Lifeng Chi. 2009. *Interfacial Assembly of Nanoparticles into Higher-Order Patterned Structures*. Vol. 1. Elsevier Ltd.
- Clark, Michael D., Sachin Subramanian, and Ramanan Krishnamoorti. 2011. "Understanding Surfactant Aided Aqueous Dispersion of Multi-Walled Carbon Nanotubes." *Journal of Colloid and Interface Science* 354(1):144–51. doi: 10.1016/j.jcis.2010.10.027.

- Du, Xu, Zhe Zhang, Wei Liu, and Yulin Deng. 2017. "Nanocellulose-Based Conductive Materials and Their Emerging Applications in Energy Devices - A Review." *Nano Energy* 35(January):299–320. doi: 10.1016/j.nanoen.2017.04.001.
- Dufresne, Alain. 2012a. "Cellulose and Potential Reinforcement." Pp. 1–46 in *Nanocellulose*. De Gruyter Inc.
- Dufresne, Alain. 2012b. "Nanocellulose: Potential Reinforcement in Composites." Pp. 1–32 in *Natural Polymers, Volume 2: Nanocomposites*. Vol. 2, edited by J. Maya and S. Thomas. The Royal Society of Chemistry.
- Dufresne, Alain. 2013. "Nanocellulose: A New Ageless Bionanomaterial." *Materials Today* 16(6):220–27. doi: 10.1016/j.mattod.2013.06.004.
- Fall, Andreas B., Stefan B. Lindström, Ola Sundman, Lars Ödberg, and Lars Wågberg. 2011. "Colloidal Stability of Aqueous Nanofibrillated Cellulose Dispersions." *Langmuir* 27(18):11332–38. doi: 10.1021/la201947x.
- Fugetsu, Bunshi, Eiichi Sano, Masaki Sunada, Yuzuru Sambongi, Takao Shibuya, Xiaoshui Wang, and Toshiaki Hiraki. 2008. "Electrical Conductivity and Electromagnetic Interference Shielding Efficiency of Carbon Nanotube/Cellulose Composite Paper." *Carbon* 46(9):1256–58. doi: 10.1016/j.carbon.2008.04.024.
- Galano, Annia. 2010. "Carbon Nanotubes: Promising Agents against Free Radicals." *Nanoscale* 2(3):373–80. doi: 10.1039/b9nr00364a.
- Gardner, Douglas J., Gloria S. Oporto, Ryan Mills, and My Ahmed Said Azizi Samir. 2008. "Adhesion and Surface Issues in Cellulose and Nanocellulose." *Journal of Adhesion Science and Technology* 22(5–6):545–67. doi: 10.1163/156856108X295509.
- Geng, Yan, Ming Yang Liu, Jing Li, Xiao Mei Shi, and Jang Kyo Kim. 2008. "Effects of Surfactant Treatment on Mechanical and Electrical Properties of CNT/Epoxy Nanocomposites." *Composites Part A: Applied Science and Manufacturing* 39(12):1876–83. doi: 10.1016/j.compositesa.2008.09.009.
- Giese, Michael, and Matthias Spengler. 2019. "Cellulose Nanocrystals in Nanoarchitectonics-towards Photonic Functional Materials." *Molecular Systems Design and Engineering* 4(1):29–48. doi: 10.1039/c8me00065d.

- Gimåker, Magnus, Magnus Östlund, Sören Östlund, and Lars Wågberg. 2011. "Influence of Beating and Chemical Additives on Residual Stresses in Paper." *Nordic Pulp and Paper Research Journal* 26(4):445–51.
- Grossiord, Nadia, Joachim Loos, Lucas Van Laake, Maryse Maugey, Cécile Zakri, Cor E. Koning, and A. John Hart. 2008. "High-Conductivity Polymer Nanocomposites Obtained by Tailoring the Characteristics of Carbon Nanotube Fillers." *Advanced Functional Materials* 18(20):3226–34. doi: 10.1002/adfm.200800528.
- Grzelczak, Marek, Jan Vermant, Eric M. Furst, and Luis M. Liz-marza. 2010. "Directed Self-Assembly of Nanoparticles." 4(7):3591–3605.
- Haffner, Benjamin, Friedrich F. Dunne, Steven R. Burke, and Stefan Hutzler. 2017. "Ageing of Fibre-Laden Aqueous Foams." *Cellulose* 24(1):231–39. doi: 10.1007/s10570-016-1100-1.
- Haghi, A. K. 2012. "Carbon Nanotubes." Pp. 1–21 in *Advanced nanotube and nanofiber materials*, edited by A. K. Haghi and G. E. Zaikov. New York: Nova Science Publishers, Inc.
- Hajian, Alireza, Stefan B. Lindström, Torbjörn Pettersson, Mahiar M. Hamed, and Lars Wågberg. 2017. "Understanding the Dispersive Action of Nanocellulose for Carbon Nanomaterials." *Nano Letters* 17(3):1439–47. doi: 10.1021/acs.nanolett.6b04405.
- Hamed, Mahiar M., Alireza Hajian, Andreas B. Fall, Karl Hkansson, Michaela Salajkova, Fredrik Lundell, Lars Wgberg, and Lars A. Berglund. 2014. "Highly Conducting, Strong Nanocomposites Based on Nanocellulose-Assisted Aqueous Dispersions of Single-Wall Carbon Nanotubes." *ACS Nano* 8(3):2467–76. doi: 10.1021/nn4060368.
- Hammond, Paula T. 2004. "Form and Function in Multilayer Assembly: New Applications at the Nanoscale." *Advanced Materials* 16(15 SPEC. ISS.):1271–93. doi: 10.1002/adma.200400760.
- Härkäsalmi, Tiina, Jani Lehmonen, Jukka Itälä, Carlos Peralta, Sanna Siljander, and Jukka A. Ketoja. 2017. "Design-Driven Integrated Development of Technical and Perceptual Qualities in Foam-Formed Cellulose Fibre Materials." *Cellulose* 24(11):5053–68. doi: 10.1007/s10570-017-1484-6.

- Henriksson, Marielle, Lars A. Berglund, Per Isaksson, Tom Lindstrom, and Takashi Nishino. 2008. "Cellulose Nanopaper Structures of High Toughness." *Biomacromolecules* 9:1579–85.
- Hertel, Tobias, Axel Hagen, Vadim Talalaev, Katharina Arnold, Frank Hennrich, Manfred Kappes, Sandra Rosenthal, James McBride, Hendrik Ulbricht, and Emmanuel Flahaut. 2005. "Spectroscopy of Single- and Double-Wall Carbon Nanotubes in Different Environments." *Nano Letters* 5(3):511–14. doi: 10.1021/nl050069a.
- Hii, Collin, Øyvind W. Gregersen, Gary Chinga-Carrasco, and Øyvind Eriksen. 2012. "The Effect of MFC on the Pressability and Paper Properties of TMP and GCC Based Sheets." *Nordic Pulp and Paper Research Journal* 27(02):388–96. doi: 10.3183/NPPRJ-2012-27-02-p388-396.
- Hilding, Jenny, Eric Grulke, Z. George Zhang, and Fran Lockwood. 2003. "Dispersion of Carbon Nanotubes in Liquids." *Journal of Dispersion Science and Technology* 24(1):1–41. doi: 10.1081/DIS-120017941.
- Hoeng, Fanny, Aurore Denneulin, and Julien Bras. 2016. "Use of Nanocellulose in Printed Electronics: A Review." *Nanoscale* 8(27):13131–54. doi: 10.1039/C6NR03054H.
- Hou, Minjie, Yumeng Hu, Miaojun Xu, and Bin Li. 2020. "Nanocellulose Based Flexible and Highly Conductive Film and Its Application in Supercapacitors." *Cellulose* 27(16):9457–66. doi: 10.1007/s10570-020-03420-2.
- Hu, L., J. W. Choi, Y. Yang, S. Jeong, F. La Mantia, L. F. Cui, and Y. Cui. 2009. "Highly Conductive Paper for Energy-Storage Devices." *Proceedings of the National Academy of Sciences* 106(51):21490–94. doi: 10.1073/pnas.0908858106.
- Hu, Liangbing, Guangyuan Zheng, Jie Yao, Nian Liu, Ben Weil, Martin Eskilsson, Erdem Karabulut, Zhichao Ruan, Shanhui Fan, Jason T. Bloking, Michael D. McGehee, Lars Wågberg, and Yi Cui. 2013. "Transparent and Conductive Paper from Nanocellulose Fibers." *Energy Environ. Sci.* 6(2):513–18. doi: 10.1039/C2EE23635D.

- Huang, Hua Dong, Chun Yan Liu, Liang Qing Zhang, Gan Ji Zhong, and Zhong Ming Li. 2015. "Simultaneous Reinforcement and Toughening of Carbon Nanotube/Cellulose Conductive Nanocomposite Films by Interfacial Hydrogen Bonding." *ACS Sustainable Chemistry and Engineering* 3(2):317–24. doi: 10.1021/sc500681v.
- Huang, Jan Chan. 2002. "Carbon Black Filled Conducting Polymers and Polymer Blends." *Advances in Polymer Technology* 21(4):299–313. doi: 10.1002/adv.10025.
- Huang, Y. Y., and E. M. Terentjev. 2008. "Dispersion and Rheology of Carbon Nanotubes in Polymers." *International Journal of Material Forming* 1(2):63–74. doi: 10.1007/s12289-008-0376-6.
- Huang, Yan Yan, and Eugene M. Terentjev. 2012. "Dispersion of Carbon Nanotubes: Mixing, Sonication, Stabilization, and Composite Properties." *Polymers* 4(1):275–95. doi: 10.3390/polym4010275.
- Iguchi, M., S. Yamanaka, and A. Budhiono. 2000. "Bacterial Cellulose - a Masterpiece of Nature's Arts." *Journal of Materials Science* 35(2):261–70. doi: 10.1023/A:1004775229149.
- Iijima, Sumio. 1991. "Helical Microtubules of Graphitic Carbon." *Nature* 354(November):56–58.
- Imai, Masanori, Kousuke Akiyama, Tomo Tanaka, and Eiichi Sano. 2010. "Highly Strong and Conductive Carbon Nanotube/Cellulose Composite Paper." *Composites Science and Technology* 70(10):1564–70. doi: 10.1016/j.compscitech.2010.05.023.
- International standard ISO 14887. 2000. *Sample Preparation -- Dispersing Procedures for Powders in Liquids*.
- International standard ISO 20477. 2017. *Nanotechnologies — Standard Terms and Their Definition for Cellulose*.
- Islam, M. F., E. Rojas, D. M. Bergey, A. T. Johnson, and A. G. Yodh. 2003. "High Weight Fraction Surfactant Solubilization of Single-Wall Carbon Nanotubes in Water." *Nano Letters* 3(2):269–73. doi: 10.1021/nl025924u.

- Isogai, Akira. 2013. "Wood Nanocelluloses: Fundamentals and Applications as New Bio-Based Nanomaterials." *Journal of Wood Science* 59(6):449–59. doi: 10.1007/s10086-013-1365-z.
- Javadian, Soheila, Ali Motae, Maryam Sharifi, Hasti Aghdastinat, and Fariba Taghavi. 2017. "Dispersion Stability of Multi-Walled Carbon Nanotubes in Catanionic Surfactant Mixtures." *Colloids and Surfaces A: Physicochemical and Engineering Aspects* 531(July):141–49. doi: 10.1016/j.colsurfa.2017.07.081.
- Jiang, Linqin, Lian Gao, and Jing Sun. 2003. "Production of Aqueous Colloidal Dispersions of Carbon Nanotubes." *Journal of Colloid and Interface Science* 260(1):89–94. doi: 10.1016/S0021-9797(02)00176-5.
- Jiang, Mei Juan, Zhi M. Dang, Sheng Hong Yao, and Jinbo Bai. 2008. "Effects of Surface Modification of Carbon Nanotubes on the Microstructure and Electrical Properties of Carbon Nanotubes/Rubber Nanocomposites." *Chemical Physics Letters* 457(4–6):352–56. doi: 10.1016/j.cplett.2008.04.022.
- Jung, Rira, Hun-Sik Kim, Yeseul Kim, Soon-Min Kwon, Heon Sang Lee, and Hyoung-Joon Jin. 2008. "Electrically Conductive Transparent Papers Using Multiwalled Carbon Nanotubes." *Journal of Polymer Science Part B: Polymer Physics* 46(March):1235–42. doi: 10.1002/polb.21457.
- Kajanto, Isko, and Mika Kosonen. 2012. "The Potential Use of Micro- and Nanofibrillated Cellulose as a Reinforcement Element in Paper." *Journal of Science & Technology for Forest Products and Processes* 2(6):42–48.
- Keinänen, Pasi, Amit Das, and Jyrki Vuorinen. 2018. "Further Enhancement of Mechanical Properties of Conducting Rubber Composites Based on Multiwalled Carbon Nanotubes and Nitrile Rubber by Solvent Treatment." *Materials* 11(10):1806. doi: 10.3390/ma11101806.
- Kinnunen, Karita, Jani Lehmonen, Nikolai Beletski, Petri Jetsu, and Tuomo Hjelt. 2013. "Benefits of Foam Forming Technology and Its Applicability in High MFC Addition Structures." in *The 15th Pulp and Paper Fundamental Research Symposium*.
- Koda, Shinobu, Takahide Kimura, Takashi Kondo, and Hideto Mitome. 2003. "A Standard Method to Calibrate Sonochemical Efficiency of an Individual Reaction System." *Ultrasonics Sonochemistry* 10(3):149–56. doi: 10.1016/S1350-4177(03)00084-1.

- Koga, Hirotaka, Tsuguyuki Saito, Takuya Kitaoka, Masaya Nogi, Katsuaki Suganuma, and Akira Isogai. 2013. "Transparent, Conductive, and Printable Composites Consisting of TEMPO-Oxidized Nanocellulose and Carbon Nanotube." *Biomacromolecules* 14(4):1160–65. doi: 10.1021/bm400075f.
- Kun, Yang, Y. I. Zili, Jing Qingfeng, Y. U. E. Renliang, Jiang Wei, and L. I. N. Daohui. 2013. "Sonication-Assisted Dispersion of Carbon Nanotubes in Aqueous Solutions of the Anionic Surfactant SDBS: The Role of Sonication Energy." 58(17):2082–90. doi: 10.1007/s11434-013-5697-2.
- Kuzmenko, Volodymyr, Olga Naboka, Mazharul Haque, Henrik Staaf, Gert Göransson, Paul Gatenholm, and Peter Enoksson. 2015. "Sustainable Carbon Nanofibers/Nanotubes Composites from Cellulose as Electrodes for Supercapacitors." *Energy* 90:1490–96. doi: 10.1016/j.energy.2015.06.102.
- Larsson, Per A., and Lars Wågberg. 2008. "Influence of Fibre - Fibre Joint Properties on the Dimensional Stability of Paper." *Cellulose* 15(4):515–25. doi: 10.1007/s10570-008-9203-y.
- Lee, Tae Won, and Young Gyu Jeong. 2015. "Regenerated Cellulose/Multiwalled Carbon Nanotube Composite Films with Efficient Electric Heating Performance." *Carbohydrate Polymers* 133:456–63. doi: 10.1016/j.carbpol.2015.06.053.
- Lee, Tae Won, Sang Eui Lee, and Young Gyu Jeong. 2016. "Carbon Nanotube/Cellulose Papers with High Performance in Electric Heating and Electromagnetic Interference Shielding." *Composites Science and Technology* 131:77–87. doi: 10.1016/j.compscitech.2016.06.003.
- Lehtimäki, Suvi, Sampo Tuukkanen, Juho Pörhönen, Pasi Moilanen, Jorma Virtanen, Mari Honkanen, and Donald Lupo. 2014. "Low-Cost, Solution Processable Carbon Nanotube Supercapacitors and Their Characterization." *Applied Physics A: Materials Science and Processing* 117(3):1329–34. doi: 10.1007/s00339-014-8547-4.
- Li, Hongbing, Yudong Zong, Jia He, Qijun Ding, Yifei Jiang, Xia Li, and Wenjia Han. 2022. "Wood-Inspired High Strength and Lightweight Aerogel Based on Carbon Nanotube and Nanocellulose Fiber for Heat Collection." *Carbohydrate Polymers* 280(December 2021). doi: 10.1016/j.carbpol.2021.119036.

- Li, Yuanyuan, Hongli Zhu, Fei Shen, Jiayu Wan, Steven Lacey, Zhiqiang Fang, Hongqi Dai, and Liangbing Hu. 2015. "Nanocellulose as Green Dispersant for Two-Dimensional Energy Materials." *Nano Energy* 13:346–54. doi: 10.1016/j.nanoen.2015.02.015.
- Lindman, Björn, Gunnar Karlström, and Lars Stigsson. 2010. "On the Mechanism of Dissolution of Cellulose." *Journal of Molecular Liquids* 156(1):76–81. doi: 10.1016/j.molliq.2010.04.016.
- Liu, Yueyue, Dongyan Liu, Yuling Ma, and Guoxin Sui. 2016. "Characterization and Properties of Transparent Cellulose Nanowhiskers-Based Graphene Nanoplatelets/Multi-Walled Carbon Nanotubes Films." *Composites Part A: Applied Science and Manufacturing* 86:77–86. doi: 10.1016/j.compositesa.2016.04.002.
- Loos, Marcio. 2015. "Processing of Polymer Matrix Composites Containing CNTs." Pp. 171–88 in *Carbon nanotube reinforces composites*. CNR Polymer Science and Technology.
- Lu, Ping, and You Lo Hsieh. 2010. "Multiwalled Carbon Nanotube (MWCNT) Reinforced Cellulose Fibers by Electrospinning." *ACS Applied Materials and Interfaces* 2(8):2413–20. doi: 10.1021/am1004128.
- Ma, Peng Cheng, Naveed A. Siddiqui, Gad Marom, and Jang Kyo Kim. 2010. "Dispersion and Functionalization of Carbon Nanotubes for Polymer-Based Nanocomposites: A Review." *Composites Part A: Applied Science and Manufacturing* 41(10):1345–67. doi: 10.1016/j.compositesa.2010.07.003.
- Madani, A., S. Zeinoddini, S. Varahmi, H. Turnbull, A. B. Phillion, J. A. Olson, and D. M. Martinez. 2014. "Ultra-Lightweight Paper Foams: Processing and Properties." *Cellulose* 21(3):2023–31. doi: 10.1007/s10570-014-0197-3.
- Madni, Imtiaz, Chi Yong Hwang, Seong Dae Park, Yong Ho Choa, and Hee Taik Kim. 2010. "Mixed Surfactant System for Stable Suspension of Multiwalled Carbon Nanotubes." *Colloids and Surfaces A: Physicochemical and Engineering Aspects* 358(1–3):101–7. doi: 10.1016/j.colsurfa.2010.01.030.
- Maillard, M., L. Motte, a T. Ngo, and M. P. Pileni. 2000. "Rings and Hexagons Made of Nanocrystals: A Marangoni Effect." *The Journal of Physical Chemistry B* 104(50):11871–77. doi: 10.1021/jp002605n.



- Maillaud, Laurent, Cécile Zakri, Isabelle Ly, Alain Pénicaud, and Philippe Poulin. 2013. “Conductivity of Transparent Electrodes Made from Interacting Nanotubes.” *Applied Physics Letters* 103(26). doi: 10.1063/1.4858215.
- Mariani, Lisa M., Gnana Saurya Vankayalapati, John M. Considine, and Kevin T. Turner. 2020. “Characterization of Fiber Alignment and Mechanical Properties of Printed Cellulose Nanofibril Films.” P. 92 in *Mechanics of Biological Systems and Materials & Micro-and Nanomechanics, Volume 4*, edited by M. E. Grady. Springer.
- Mashkour, Mahdi, Tsunehisa Kimura, Fumiko Kimura, Mehrdad Mashkour, and Mehdi Tajvidi. 2014. “Tunable Self-Assembly of Cellulose Nanowhiskers and Polyvinyl Alcohol Chains Induced by Surface Tension Torque.” *Biomacromolecules* 15(1):60–65. doi: 10.1021/bm401287s.
- Matarredona, Olga, Heather Rhoads, Zhongrui Li, Jeffrey H. Harwell, Leandro Balzano, and Daniel E. Resasco. 2003. “Dispersion of Single-Walled Carbon Nanotubes in Aqueous Solutions of the Anionic Surfactant NaDDBS.” *The Journal of Physical Chemistry B* 107(48):13357–67. doi: 10.1021/jp0365099.
- Matsuda, Yuji, Mariko Hirose, and Katsuhiko Ueno. 2001. “United States Patent US 6183596 B1.”
- McDonald, Timothy J., Chaiwat Engtrakul, Marcus Jones, Garry Rumbles, and Michael J. Heben. 2006. “Kinetics of PL Quenching during Single-Walled Carbon Nanotube Rebundling and Diameter-Dependent Surfactant Interactions.” *Journal of Physical Chemistry B* 110(50):25339–46. doi: 10.1021/jp065281x.
- Min, Chunying, Xiangqian Shen, Zhou Shi, Lei Chen, and Zhiwei Xu. 2010. “The Electrical Properties and Conducting Mechanisms of Carbon Nanotube/Polymer Nanocomposites: A Review.” *Polymer - Plastics Technology and Engineering* 49(12):1172–81. doi: 10.1080/03602559.2010.496405.
- Miracle, Daniel, and Steven Donaldson. 2001. “Introduction to Composites.” Pp. 3–17 in *ASM Handbook*. Vol. 21.
- Miyashiro, Daisuke, Ryo Hamano, and Kazuo Umemura. 2020. “A Review of Applications Using Mixed Materials of Cellulose, Nanocellulose and Carbon Nanotubes.” *Nanomaterials* 10(2). doi: 10.3390/nano10020186.

- Moberg, Tobias, Karin Sahlin, Kun Yao, Shiyu Geng, Gunnar Westman, Qi Zhou, Kristiina Oksman, and Mikael Rigdahl. 2017. "Rheological Properties of Nanocellulose Suspensions: Effects of Fibril/Particle Dimensions and Surface Characteristics." *Cellulose* 24(6):2499–2510. doi: 10.1007/s10570-017-1283-0.
- Mondal, Subhadip, Sayan Ganguly, Poushali Das, Poushali Bhawal, Tushar Kanti Das, Lalatendu Nayak, Dipak Khastgir, and Narayan Ch Das. 2017. "High-Performance Carbon Nanofiber Coated Cellulose Filter Paper for Electromagnetic Interference Shielding." *Cellulose* 24(11):5117–31. doi: 10.1007/s10570-017-1441-4.
- Moon, Robert J., Ashlie Martini, John Nairn, John Simonsen, and Jeff Youngblood. 2011. *Cellulose Nanomaterials Review: Structure, Properties and Nanocomposites*. Vol. 40.
- Moore, Valerie C., Michael S. Strano, Erik H. Haroz, Robert H. Hauge, Richard E. Smalley, Judith Schmidt, and Yeshayahu Talmon. 2003. "Individually Wuspended Wingle-Walled Carbon Nanotubes in Various Surfactants." *Nano Letters* 3(10):1379–82. doi: 10.1021/nl034524j.
- Mougel, Jean Bruno, Coline Adda, Patricia Bertoncini, Isabelle Capron, Bernard Cathala, and Olivier Chauvet. 2016. "Highly Efficient and Predictable Noncovalent Dispersion of Single-Walled and Multi-Walled Carbon Nanotubes by Cellulose Nanocrystals." *Journal of Physical Chemistry C* 120(39):22694–701. doi: 10.1021/acs.jpcc.6b07289.
- Nguyen, Hoang Kha, Jaehan Bae, Jaehyun Hur, Sang Joon Park, Min Sang Park, and Il Tae Kim. 2019. "Tailoring of Aqueous-Based Carbon Nanotube-Nanocellulose Films as Self-Standing Flexible Anodes for Lithium-Ion Storage." *Nanomaterials* 9(4). doi: 10.3390/nano9040655.
- Olivier, Christophe, Céline Moreau, Patricia Bertoncini, Hervé Bizot, Olivier Chauvet, and Bernard Cathala. 2012. "Cellulose Nanocrystal-Assisted Dispersion of Luminescent Single-Walled Carbon Nanotubes for Layer-by-Layer Assembled Hybrid Thin Films." *Langmuir* 28(34):12463–71. doi: 10.1021/la302077a.

- Olszewska, Anna, Paula Eronen, Leena Sisko Johansson, Jani Markus Malho, Mikael Ankerfors, Tom Lindström, Janne Ruokolainen, Janne Laine, and Monika Österberg. 2011. "The Behaviour of Cationic NanoFibrillar Cellulose in Aqueous Media." *Cellulose* 18(5):1213–26. doi: 10.1007/s10570-011-9577-0.
- Oya, Takahide, and Toshio Ogino. 2008. "Production of Electrically Conductive Paper by Adding Carbon Nanotubes." *Carbon* 46(1):169–71. doi: 10.1016/j.carbon.2007.10.027.
- Pammo, A., H. Christophliemk, J. Keskinen, T. Bjorkqvist, S. Siljander, M. Mantysalo, and S. Tuukkanen. 2019. "Nanocellulose Films as Substrates for Printed Electronics." *Proceedings of MARSS 2019: 4th International Conference on Manipulation, Automation, and Robotics at Small Scales* 1–6. doi: 10.1109/MARSS.2019.8860931.
- Paria, Santanu, C. Manohar, and Kartic C. Khilar. 2005a. "Adsorption of Anionic and Non-Ionic Surfactants on a Cellulosic Surface." *Colloids and Surfaces A: Physicochemical and Engineering Aspects* 252(2–3):221–29. doi: 10.1016/j.colsurfa.2004.09.022.
- Paria, Santanu, C. Manohar, and Kartic C. Khilar. 2005b. "Kinetics of Adsorption of Anionic, Cationic, and Nonionic Surfactants." *Industrial and Engineering Chemistry Research* 44(9):3091–98. doi: 10.1021/ie049471a.
- Pinkert, André, Kenneth N. Marsh, Shusheng Pang, and Mark P. Staiger. 2009. "Ionic Liquids and Their Interaction with Cellulose." *Chemical Reviews* 109(12):6712–28. doi: 10.1021/cr9001947.
- Plackett, David V, Kevin Letchford, John K. Jackson, Helen M. Burt, John Jackson, and Helen Burt. 2014. "A Review of Nanocellulose as a Novel Vehicle for Drug Delivery." 29(January).
- Poorgholami-Bejarpasi, N., and B. Sohrabi. 2015. "Role of Surfactant Structure in Aqueous Dispersions of Carbon Nanotubes." *Fluid Phase Equilibria* 394:19–28. doi: 10.1016/j.fluid.2015.02.032.
- Poulin, Philippe, Brigitte Vigolo, and Pascale Launois. 2002. "Films and Fibers of Oriented Single Wall Nanotubes." *Carbon* 40(10):1741–49. doi: 10.1016/S0008-6223(02)00042-8.

- Qi, Haisong, Jianwen Liu, Jürgen Pionteck, Petra Pötschke, and Edith Mäder. 2015. "Carbon Nanotube-Cellulose Composite Aerogels for Vapour Sensing." *Sensors and Actuators, B: Chemical* 213:20–26. doi: 10.1016/j.snb.2015.02.067.
- Qi, Haisong, Edith Mäder, and Jianwen Liu. 2013. "Unique Water Sensors Based on Carbon Nanotube-Cellulose Composites." *Sensors and Actuators, B: Chemical* 185:225–30. doi: 10.1016/j.snb.2013.04.116.
- Ragab, Tarek, and Cemal Basaran. 2009. "Joule Heating in Single-Walled Carbon Nanotubes." *Journal of Applied Physics* 106(6). doi: 10.1063/1.3204971.
- Rastogi, Richa, Rahul Kaushal, S. K. Tripathi, Amit L. Sharma, Inderpreet Kaur, and Lalit M. Bharadwaj. 2008. "Comparative Study of Carbon Nanotube Dispersion Using Surfactants." *Journal of Colloid and Interface Science* 328(2):421–28. doi: 10.1016/j.jcis.2008.09.015.
- Rausch, Julius, Rong Chuan Zhuang, and Edith Mäder. 2010. "Surfactant Assisted Dispersion of Functionalized Multi-Walled Carbon Nanotubes in Aqueous Media." *Composites Part A: Applied Science and Manufacturing* 41(9):1038–46. doi: 10.1016/j.compositesa.2010.03.007.
- Richard, Cyrille, Fabrice Balavoine, Patrick Schultz, Thomas W. Ebbesen, and Charles Mioskowski. 2003. "Supramolecular Self-Assembly of Lipid Derivatives on Carbon Nanotubes." 300(May):775–79.
- Rosen, Milton J., and Joy T. Kunjappu. 2012. "Dispersion and Aggregation of Solids in Liquid Media by Surfactants." *Surfactants and Interfacial Phenomena* 368–91. doi: 10.1002/9781118228920.ch9.
- Rossell, Marta D., Christian Kuebel, Gabriele Ilari, Felix Rechberger, Florian J. Heiligtag, Markus Niederberger, Dorota Koziej, and Rolf Erni. 2013. "Impact of Sonication Pretreatment on Carbon Nanotubes: A Transmission Electron Microscopy Study." *Carbon* 61:404–11. doi: 10.1016/j.carbon.2013.05.024.
- Roth, S., and D. Carroll. 2015. *One-Dimensional Metals: Conjugated Polymers, Organic Crystals, Carbon Nanotubes and Graphene*. John Wiley & Sons, Inc.

- Ryabenko, A. G., T. V. Dorofeeva, and G. I. Zvereva. 2004. "UV-VIS-NIR Spectroscopy Study of Sensitivity of Single-Wall Carbon Nanotubes to Chemical Processing and Van-Der-Waals SWNT/SWNT Interaction. Verification of the SWNT Content Measurements by Absorption Spectroscopy." *Carbon* 42(8-9):1523-35. doi: 10.1016/j.carbon.2004.02.005.
- Rycenga, Matthew, Pedro H. C. Camargo, and Younan Xia. 2009. "Template-Assisted Self-Assembly: A Versatile Approach to Complex Micro- and Nanostructures." *Soft Matter* 5(6):1129-36. doi: 10.1039/b811021b.
- Saito, Tsuguyuki, Ryota Kuramae, Jakob Wohler, Lars A. Berglund, and Akira Isogai. 2013. "An Ultrastrong Nanofibrillar Biomaterial: The Strength of Single Cellulose Nanofibrils Revealed via Sonication-Induced Fragmentation." *Biomacromolecules* 14(1):248-53. doi: 10.1021/bm301674e.
- Salajkova, Michaela, Luca Valentini, Qi Zhou, and Lars A. Berglund. 2013. "Tough Nanopaper Structures Based on Cellulose Nanofibers and Carbon Nanotubes." *Composites Science and Technology* 87:103-10. doi: 10.1016/j.compscitech.2013.06.014.
- Sesis, Achilleas, Mark Hodnett, Gianluca Memoli, Andrew J. Wain, Izabela Jurewicz, Alan B. Dalton, J. David Carey, and Gareth Hinds. 2013. "Influence of Acoustic Cavitation on the Controlled Ultrasonic Dispersion of Carbon Nanotubes." *Journal of Physical Chemistry B* 117(48):15141-50. doi: 10.1021/jp410041y.
- Shim, Moonsub, Nadine Wong Shi Kam, Robert J. Chen, Yiming Li, and Hongjie Dai. 2002. "Functionalization of Carbon Nanotubes for Biocompatibility and Biomolecular Recognition." *Nano Letters* 2(4):285-88. doi: 10.1021/nl015692j.
- Siró, István, and David Plackett. 2010. "Microfibrillated Cellulose and New Nanocomposite Materials: A Review." *Cellulose* 17(3):459-94. doi: 10.1007/s10570-010-9405-y.

- Skogberg, Anne, Antti Juhana Mäki, Marja Mettänen, Panu Lahtinen, and Pasi Kallio. 2017. "Cellulose Nanofiber Alignment Using Evaporation-Induced Droplet-Casting, and Cell Alignment on Aligned Nanocellulose Surfaces." *Biomacromolecules* 18(12):3936–53. doi: 10.1021/acs.biomac.7b00963.
- Smith, M. K., and V. W. Punton. 1975. "Foam Can Improve Formation." *Pulp & Paper Canada* 76(1):55–58.
- Sun, Zhenyu, Valeria Nicolosi, David Rickard, Shane D. Bergin, Damian Aherne, and Jonathan N. Coleman. 2008. "Quantitative Evaluation of Surfactant-Stabilized Single-Walled Carbon Nanotubes: Dispersion Quality and Its Correlation with Zeta Potential." *J. Phys. Chem. C* 112(29):10692–99. doi: 10.1021/jp8021634.
- Tammelin, Tekla, Ulla Hippi, and Arto Salminen. 2013. "Method for the Preparation of NFC Films on Supports, WO2013/060934 A2."
- Tan, Yongqiang, and Daniel E. Resasco. 2005. "Dispersion of Single-Walled Carbon Nanotubes of Narrow Diameter Distribution." *Journal of Physical Chemistry B* 109(30):14454–60. doi: 10.1021/jp052217r.
- Tardy, Blaise L., Shingo Yokota, Mariko Ago, Wenchao Xiang, Tetsuo Kondo, Romain Bordes, and Orlando J. Rojas. 2017. "Nanocellulose–Surfactant Interactions." *Current Opinion in Colloid and Interface Science* 29:57–67. doi: 10.1016/j.cocis.2017.02.004.
- Tkalya, Evgeniy E., Marcos Ghislandi, Gijsbertus de With, and Cor E. Koning. 2012. "The Use of Surfactants for Dispersing Carbon Nanotubes and Graphene to Make Conductive Nanocomposites." *Current Opinion in Colloid and Interface Science* 17(4):225–32. doi: 10.1016/j.cocis.2012.03.001.
- Toomadj, F., S. Farjana, A. Sanz-Velasco, O. Naboka, P. Lundgren, K. Rodriguez, G. Toriz, P. Gatenholm, and P. Enoksson. 2011. "Strain Sensitivity of Carbon Nanotubes Modified Cellulose." *Procedia Engineering* 25:1353–56. doi: 10.1016/j.proeng.2011.12.334.
- Turbak, Albin, Fred Snyder, and Karen Sandberg. 1983. "Microfibrillated Cellulose, a New Cellulose Product: Properties, Uses, and Commercial Potential." *Journal of Applied Polymer Science: Applied Polymer Symposium* 37:815–27.

- Tuukkanen, S., S. Lehtimäki, F. Jahangir, A. P. Eskelinen, D. Lupo, and S. Franssila. 2014. "Printable and Disposable Supercapacitor from Nanocellulose and Carbon Nanotubes." *Proceedings of the 5th Electronics System-Integration Technology Conference, ESTC 2014*. doi: 10.1109/ESTC.2014.6962740.
- Utani, Kojiro, and Hiroyuki Yano. 2013. "Self-Organizing Capacity of Nanocelluloses via Droplet Evaporation." *Soft Matter* 9(12):3396–3401. doi: 10.1039/c3sm27822k.
- Utsumi, Shigenori, Mamiko Kanamaru, Hiroaki Honda, Hirofumi Kanoh, Hideki Tanaka, Takahiro Ohkubo, Hideki Sakai, Masahiko Abe, and Katsumi Kaneko. 2007. "RBM Band Shift-Evidenced Dispersion Mechanism of Single-Wall Carbon Nanotube Bundles with NaDDBS." *Journal of Colloid and Interface Science* 308(1):276–84. doi: 10.1016/j.jcis.2006.12.041.
- Vaisman, Linda, Gad Marom, and H. Daniel Wagner. 2006. "Dispersions of Surface-Modified Carbon Nanotubes in Water-Soluble and Water-Insoluble Polymers." *Advanced Functional Materials* 16(3):357–63. doi: 10.1002/adfm.200500142.
- Vaisman, Linda, H. Daniel Wagner, and Gad Marom. 2006. "The Role of Surfactants in Dispersion of Carbon Nanotubes." *Advances in Colloid and Interface Science* 128–130(2006):37–46. doi: 10.1016/j.jcis.2006.11.007.
- Vigolo, B., A. Penicaud, C. Coulon, C. Sauder, R. Paillet, C. Journet, P. Bernier, and P. Poulin. 2000. "Macroscopic Fibers and Ribbons of Oriented Carbon Nanotubes." *Science* 290(5495):1331–34. doi: 10.1126/science.290.5495.1331.
- Vijayaraghavan, D. 2015. "Aggregates of Single-Walled Carbon Nanotube Bundles in a Surfactant Solution." *Journal of Molecular Liquids* 209:440–46. doi: 10.1016/j.molliq.2015.05.063.
- Voisin, Hugo, Lennart Bergström, Peng Liu, and Aji P. Mathew. 2017. "Nanocellulose-Based Materials for Water Purification." *Nanomaterials* 7(3). doi: 10.3390/nano7030057.

- Wang, Miao, Ilya V. Anoshkin, Albert G. Nasibulin, Juuso T. Korhonen, Jani Seitsonen, Jaakko Pere, Esko I. Kauppinen, Robin H. A. Ras, and Olli Ikkala. 2013. "Modifying Native Nanocellulose Aerogels with Carbon Nanotubes for Mechanoresponsive Conductivity and Pressure Sensing." *Advanced Materials* 25(17):2428–32. doi: 10.1002/adma.201300256.
- Wang, Qianqian, Qian Yao, Jun Liu, Jianzhong Sun, Qianqian Zhu, and Honglei Chen. 2019. *Processing Nanocellulose to Bulk Materials: A Review*. Vol. 26. Springer Netherlands.
- Wang, Yang, and George J. Weng. 2018. "Electrical Conductivity of Carbon Nanotube- and Graphene-Based Nanocomposites." Pp. 123–56 in *Micromechanics and Nanomechanics of Composite Solids*, edited by S. A. Meguid and G. J. Weng. Springer.
- Wenseleers, Wim, Igor L. Vlasov, Etienne Goovaerts, Elena D. Obraztsova, Anatolii S. Lobach, and August Bouwen. 2004. "Efficient Isolation and Solubilization of Pristine Single-Walled Nanotubes in Bile Salt Micelles." *Advanced Functional Materials* 14(11):1105–12. doi: 10.1002/adfm.200400130.
- Whitesides, George M., and Bartosz Grzybowski. 2002. "Self-Assembly at All Scales." *Science* 295(5564):2418–21. doi: 10.1126/science.1070821.
- Xiao, Wenjun, Tinghua Wu, Jiajian Peng, Ying Bai, Jiayun Li, Guoqiao Lai, Ying Wu, and Lizong Dai. 2013. "Preparation, Structure, and Properties of Chitosan/Cellulose/Multiwalled Carbon Nanotube Composite Membranes and Fibers." *Journal of Applied Polymer Science* 128(2):1193–99. doi: 10.1002/app.38329.
- Xiong, Rui, Ho Shin Kim, Shuaidi Zhang, Sunghan Kim, Volodymyr F. Korolovych, Ruilong Ma, Yaroslava G. Yingling, Canhui Lu, and Vladimir V. Tsukruk. 2017. "Template-Guided Assembly of Silk Fibroin on Cellulose Nanofibers for Robust Nanostructures with Ultrafast Water Transport." *ACS Nano* 11(12):12008–19. doi: 10.1021/acsnano.7b04235.
- Yamakawa, Akira, Shiho Suzuki, Takeshi Oku, Kenta Enomoto, Motohide Ikeda, Joseph Rodrigue, Keita Tateiwa, Yoshinobu Terada, Hiroyuki Yano, and Shinichi Kitamura. 2017. "Nanostructure and Physical Properties of Cellulose Nanofiber-Carbon Nanotube Composite Films." *Carbohydrate Polymers* 171:129–35. doi: 10.1016/j.carbpol.2017.05.012.



- Yang, De-quan, Jean-Francois Rochette, and Edward Sacher. 2005. "Functionalization of Multiwalled Carbon Nanotubes by Mild Aqueous Sonication." *Journal of Physical Chemistry B* 109(16):7788–94. doi: 10.1021/jp045147h.
- Yang, K., and B. Xing. 2010. "Adsorption of Organic Compounds by Carbon Nanomaterials in Aqueous Phase: Polanyi Theory and Its Application." *Chemical Reviews* 110(10):5989–6008. doi: 10.1021/cr100059s.
- Yoon, Seok Ho, Hyung-Joon Jin, Moo-Chang Kook, and Yu Ryang Pyun. 2006. "Electrically Conductive Bacterial Cellulose by Incorporation of Carbon Nanotubes." *Biomacromolecules* 7(4):4. doi: 10.1021/bm050597g.
- Yu, Junrong, Nadia Grossiord, Cor E. Koning, and Joachim Loos. 2007. "Controlling the Dispersion of Multi-Wall Carbon Nanotubes in Aqueous Surfactant Solution." *Carbon* 45(3):618–23. doi: 10.1016/j.carbon.2006.10.010.
- Yun, Sungryul, and Jaehwan Kim. 2010. "Multi-Walled Carbon Nanotubes-Cellulose Paper for a Chemical Vapor Sensor." *Sensors and Actuators, B: Chemical* 150(1):308–13. doi: 10.1016/j.snb.2010.06.068.
- Yurekli, Koray, Cynthia A. Mitchell, and Ramanan Krishnamoorti. 2004. "Small-Angle Neutron Scattering from Surfactant-Assisted Aqueous Dispersions of Carbon Nanotubes." *Journal of the American Chemical Society* 126(32):9902–3. doi: 10.1021/ja047451u.
- Zhang, Hao, Chang Dou, Lokendra Pal, and Martin A. Hubbe. 2019. "Review of Electrically Conductive Composites and Films Containing Cellulosic Fibers or Nanocellulose." *BioResources* 14(3):7494–7542.
- Zhang, Hao, Xiaohang Sun, Martin A. Hubbe, and Lokendra Pal. 2019. "Highly Conductive Carbon Nanotubes and Flexible Cellulose Nanofibers Composite Membranes with Semi-Interpenetrating Networks Structure." *Carbohydrate Polymers* 222(March). doi: 10.1016/j.carbpol.2019.115013.
- Zhang, Haoruo, Xunwen Sun, Zhengguang Heng, Yang Chen, Huawei Zou, and Mei Liang. 2018. "Robust and Flexible Cellulose Nanofiber/Multiwalled Carbon Nanotube Film for High-Performance Electromagnetic Interference Shielding." *Industrial and Engineering Chemistry Research* 57(50):17152–60. doi: 10.1021/acs.iecr.8b04573.

Zhang, Shanju, Qingwen Li, Ian A. Kinloch, and Alan H. Windle. 2010. "Ordering in a Droplet of an Aqueous Suspension of Single-Wall Carbon Nanotubes on a Solid Substrate." *Langmuir* 26(3):2107–12. doi: 10.1021/la902642f.

Zhao, Yafei, Giuseppe Cavallaro, and Yuri Lvov. 2015. "Orientation of Charged Clay Nanotubes in Evaporating Droplet Meniscus." *Journal of Colloid and Interface Science* 440:68–77. doi: 10.1016/j.jcis.2014.10.050.

*"Reality is the murder of a beautiful theory by a gang of ugly facts."*

# PUBLICATIONS

- Publication I**      Optimized dispersion quality of aqueous carbon nanotube colloids as a function of sonochemical yield and surfactant/CNT ratio
- Keinänen, Pasi; Siljander, Sanna; Koivula, Mikko; Sethi, Jatin; Sarlin, Essi; Vuorinen, Jyrki; Kanerva, Mikko.
- Heliyon, Vol. 4, No. 9, e00787, 2018 <https://doi.org/10.1016/j.heliyon.2018.e00787>
- Publication II**      Effect of surfactant type and sonication energy on the electrical conductivity properties of nanocellulose-CNT nanocomposite films
- Siljander, Sanna; Keinänen, Pasi; Rätty, Anna; Rama-Krishnan, Karthik Ram; Tuukkanen, Sampo; Kunnari, Vesa; Harlin, Ali; Vuorinen, Jyrki; Kanerva, Mikko.
- International Journal of Molecular Sciences, Vol. 19, No. 6, 1819, 2018 <https://doi.org/10.3390/ijms19061819>
- Publication III**      Self-assembled cellulose nanofiber–carbon nanotube nanocomposite films with anisotropic conductivity
- Skogberg, Anne; Siljander, Sanna; Mäki, Antti-Juhana; Honkanen, Mari; Efimov, Alexander; Hannula Markus; Lahtinen, Panu; Tuukkanen, Sampo; Björkqvist, Tomas and Kallio, Pasi
- Nanoscale, 14, 448-463, 2022 <https://doi.org/10.1039/d1nr06937c>
- Publication IV**      Conductive cellulose-based foam formed 3D shapes—from innovation to designed prototype
- Siljander, Sanna; Keinänen, Pasi; Ivanova, Anastasia; Lehmonen, Jani; Tuukkanen, Sampo; Kanerva, Mikko; Björkqvist, Tomas.
- Materials, Vol. 12, No. 3, 430, 2019. <https://doi.org/10.3390/ma12030430>



# PUBLICATION

I

## **Optimized dispersion quality of aqueous carbon nanotube colloids as a function of sonochemical yield and surfactant/CNT ratio**

P. Keinänen, S. Siljander, M. Koivula, J. Sethi, E. Sarlin,  
J. Vuorinen and M. Kanerva

Heliyon 4.9 (2018), e00787

**10.1016/j.heliyon.2018.e00787**

**<http://urn.fi/URN:NBN:fi:tty-201810262483>**

**Publication reprinted with the permission of the copyright holders.**



Received:  
29 March 2018

Revised:  
6 July 2018

Accepted:  
11 September 2018

Cite as: Pasi Keinänen,  
Sanna Siljander,  
Mikko Koivula, Jatin Sethi,  
Essi Sarlin, Jyrki Vuorinen,  
Mikko Kanerva. Optimized  
dispersion quality of aqueous  
carbon nanotube colloids as a  
function of sonochemical  
yield and surfactant/CNT  
ratio.

Heliyon 4 (2018) e00787.  
doi: 10.1016/j.heliyon.2018.  
e00787



# Optimized dispersion quality of aqueous carbon nanotube colloids as a function of sonochemical yield and surfactant/CNT ratio

Pasi Keinänen<sup>a,\*</sup>, Sanna Siljander<sup>a</sup>, Mikko Koivula<sup>a</sup>, Jatin Sethi<sup>b</sup>, Essi Sarlin<sup>a</sup>,  
Jyrki Vuorinen<sup>a</sup>, Mikko Kanerva<sup>a</sup>

<sup>a</sup> Tampere University of Technology, Laboratory of Materials Science, P.O. Box 527, FIN-33101, Tampere, Finland

<sup>b</sup> University of Oulu, Fiber and Particle engineering research unit, P.O. Box 4300, FIN-90014, Oulu, Finland

\* Corresponding author.

E-mail address: pasi.keinanen@tut.fi (P. Keinänen).

## Abstract

In this paper, we propose and verify a theoretical model of the development of dispersion quality of aqueous carbon nanotube (CNT) colloid as a function of sonochemical yield of the sonication process. Four different surfactants; Triton X-100, Pluronic F-127, CTAB and SDS were studied. From these four SDS had the lowest dispersion performance which was surprising. Optical dispersion quality results fits well with proposed theoretical model.

Keywords: Physical chemistry, Materials science

## 1. Introduction

There is one significant feature requiring attention when it comes to CNT-nanocomposites and colloids; a dispersion quality. Dispersion quality, i.e. dispersed nanotubes divided by the total number of nanotubes, has a huge impact on the effective surface area of the interaction between the matrix and the filler. In

order to optimize the performance one needs to know how to control the dispersion quality during each step of the manufacturing process.

CNTs forming large agglomerates creates challenges to process and stabilize colloids made of them. To optimize a dispersion process, enough energy density needs to be generated to overcome internal forces holding the aggregates together. Typical methods are shear-mixing [1] and sonication [2]. Of these two methods, sonication is superior especially for low viscosity systems where conventional mixing methods cannot create the required high strains rates. The dispersion process using sonication is based on inertial cavitation where imploding microscopic cavities generate intensive streams of molecules with high energy densities inside the liquid. Cavities are known to preferably exist at the boundaries of different materials [3] which makes sonication a very effective and precise method for dispersing nanotubes. Prolonged sonication however can cause damages to the tubes and must be avoided [4].

After the CNTs have been detached from aggregates, there is a possibility of re-agglomeration. To stabilize the system in water based dispersions, different types of surfactants such as ionic (anionic and cationic), non-ionic, polymer based and their combinations have been used comprising current state-of-the-art [5,6,7,8,9,10,11,12,13,14,15,16,17,18,19,20,21,22,23,24,25,26,27,28]. The basic idea is to enable surfactant molecules to be adsorbed on the surface of CNTs via hydrophobic interactions,  $\pi$ - $\pi$  bonds, hydrogen bonds or electrostatic interactions [29,30].

The nanotube dispersing efficiency of surfactants is linked to the length of an alkyl chain of the surfactant, presence of benzene ring, and the functional (terminal) group [10], concentration [22] and charge [31]. An optimum surfactant-CNT weight ratio has been reported to vary, ranging from 1:1 to 1:10 [10,32]. It has been reported that an efficient CNT dispersion is possible only when the surfactant concentration is above the CMC value [27,33,34,35]. It has also been reported that dispersing agents can form stable dispersions below and equal to their CMC limit [5,7,12,36]. Moreover, it has been noted that the best result can be reached with a concentration of 0.5 CMC, and that any further increases in the concentration of the surfactant has only a minor effect [36]. Even with a absence of consensus using too high surfactant concentration may affect the properties of CNT network in the end product, using too low surfactant concentration can cause re-aggregation in colloid since a sufficient amount is needed to cover all CNT surfaces [32].

During the sonication, there is a dynamic equilibrium of concentrations between individual, surfactant coated nanotubes and nanotube agglomerates. As more energy is brought into the system, more nanotubes are being detached from the agglomerates and a dispersion quality is approaching unity. There are number of methods available for studying the quality of CNT-dispersions and they include; atomic force microscopy (AFM) [10], transmission electron microscopy (TEM) [32], Raman



spectroscopy [37] and UV–Vis spectroscopy [38]. Of these methods, UV–Vis spectroscopy has been shown to represent the most accessible and versatile method to determine the dispersion quality of CNT dispersions especially for liquid systems. In the method, the light passing through a sample of colloid experiences scattering and absorbance. Both of these phenomena scale linearly with the concentration of colloidal particles and, therefore, the opacity  $\alpha$  of the dispersion can be used to measure the number of nanotubes (individual tubes or dispersed small aggregates) in the supernatant [23]. At a fixed wavelength, UV–Vis spectroscopy can be used to determine the onset point of  $\alpha$  as a function of the applied acoustic sonication energy. At this point, the system is close to its optimal dispersion state and further sonication would only damage the nanotubes without improving the quality of the dispersion.

In the previous studies the parameters to describe sonication have been total energy and time [38,39]. These parameters work well with specific processes but are insufficient for comparing different studies since different sonication systems have different yields of transforming electrical energy to acoustic energy and individual systems also produce different amounts of inertial cavitation (vs. non-inertial). Inertial cavitation is mainly responsible of exfoliation of nanotubes whereas non-inertial cavitation is related to surface damages of the tubes [40]. In order to generalize all types of sonication systems parameter of sonochemical yield should be used; like first proposed by Koda et al. [41].

This article introduces theoretical framework for controlling the dispersion quality of aqueous carbon nanotube colloids during a sonication process. This framework is indifferent towards the sonication system, used energies and times.

## 2. Theory

We propose that for an ultrasound system, where the re-agglomeration of carbon nanotubes is inhibited by using surfactants the rate of opacity increase is related to effective acoustic energy in a following way:

$$\frac{d\alpha}{dE} = (\alpha_{max} - \alpha)f \quad (1)$$

where  $E$  is the effective acoustic energy divided by CNT mass,  $\alpha_{max}$  is the maximum achievable opacity of the system and  $f$  is a shape function. By separation we arrive to

$$\frac{d\alpha}{(\alpha_{max} - \alpha)} = f dE \quad (2)$$

Integration, rearrangement, and then using both sides as exponents  $e^x$  leads to

$$\alpha = \alpha_{max} - C e^{-\int f dE} \quad (3)$$

For a system where  $f$  is a positive constant, and by applying boundary conditions,  $\alpha(0) = 0$  and  $\lim_{E \rightarrow \infty} \alpha(E) = \alpha_{max}$ ,  $\alpha$  can be expressed as

$$\alpha(E) = \alpha_{max}(1 - e^{-\kappa E}) \quad (4)$$

where,  $\kappa$  is a system-specific constant related to the types and quantities of the chemical components in the colloid.

In order to generalize (4) for all types of sonication systems, sonochemical yield is used instead of energy. In our experiments we used the concentration of iodine-ions  $I_3^-$  divided by CNT mass,  $C_{I_3^-}$  as a parameter [42].

It is known that sonolysis of water produces hydrogen peroxide  $H_2O_2$  via hydroxyl and hydrogen radicals and it causes oxidation of  $2I^-$  to  $I_2$  from dissolved potassium iodide.  $I_2$  then reacts with  $I^-$  to produce  $I_3^-$ , which has a peak absorbance at 355 nm and which can be detected by using UV-vis spectroscopy. The method, also known as Weissler reaction, has been proposed to be used as a standard method for the calibration of sonication systems [41]. The chain of chemical reactions is induced only by inertial cavitation, which is mainly responsible of the de-agglomeration of CNT aggregates. Therefore, Weissler reaction can be used to measure and compare effective dispersive processes of different sonication systems.

Thus, using  $C_{I_3^-}$  with Equation (4), it leads to

$$\alpha(C_{I_3^-}) = \alpha_{max}(1 - e^{-\kappa C_{I_3^-}}) \quad (5)$$

where the value of  $C_{I_3^-}$  is determined based on an experimental graph of electrical energy  $E_e$  versus concentration of iodine-ions.

For determination of sonochemical yield of  $I_3^-$  versus electrical energy consumed by the sonicator concentrations of  $I_3^-$  were analyzed using the Beer-Lambert law

$$\alpha = \epsilon bc \quad (6)$$

where  $\alpha$  is the absorbance,  $\epsilon$  is the molar attenuation coefficient of  $I_3^-$ ,  $b$  is the length of the optical path (in cm), and  $c$  is the concentration of  $I_3^-$ . Linear fitting was used to interpolate  $I_3^-$  production as a function of electrical energy and slope of the fitting was used to calculate values for the sonochemical yield.

### 3. Materials & methods

#### 3.1. Materials

In this study, we used Nanocyl7000 multiwall carbon nanotubes (Nanocyl SA., Sambreville, Belgium) and four different surfactants: octyl phenol ethoxylate (Triton

X-100), polyoxyethylene-polyoxypropylene block co-polymer (Pluronic F-127), sodium dodecyl sulfate (SDS) and cetyltrimethylammonium bromide (CTAB), all from Sigma Aldrich (Merck KGaA, Darmstadt, Germany). For the Weissler reaction potassium iodide (KI) (Merck KGaA, Darmstadt, Germany) was used.

### 3.2. Weissler reaction

For determination of sonochemical yield of  $I_3^-$  versus electrical energy consumed by the sonicator, 200 ml of 0.1M KI solution was sonicated using different total energies and corresponding concentrations of  $I_3^-$  were detected by measuring  $I_3^-$  specific absorbance with Shimadzu UV-1800 spectrophotometer (Shimadzu Corp., Kyoto, Japan).

### 3.3. Dispersion of carbon nanotubes

160 samples with  $0.40 \pm 0.01$  g of Nanocyl NC 7000 multiwall carbon nanotubes, four different surfactants (Triton X100, Pluronic F-127, CTAB, and SDS) with four different surfactant masses ( $0.1 \pm 0.01$  g,  $0.2 \pm 0.01$  g,  $0.4 \pm 0.01$  g and  $0.8 \pm 0.01$  g) and deionized water were weighed in 100 ml glass beakers so that all samples weighted  $80 \pm 0.1$  g. Dispersions were sonicated using 10 different electrical energies with QSonica Q700 sonicator (Qsonica L.L.C, Newtown, USA). A 12.7 mm diameter titanium probe was used and the vibration amplitude of a sonotrode was set to 60  $\mu$ m. To guarantee identical sample preparation throughout the series, the tip was always placed in the same position inside the beaker ( $15 \text{ mm} \pm 2 \text{ mm}$  from the bottom) and an external cooling bath with c. 200 W cooling capacity was used to limit the temperature variations during the sonication. The applied acoustic energy was varied by controlling the sonication time and it was monitored by an internal calorimeter of the QSonica Q700 sonicator. A power reading given by the sonicator remained between 100–120 W for all the sonications. An opacity at 500 nm, directly related to the concentration of carbon nanotubes in the dispersed state, was used to measure the quality of the sonicated dispersions. A portion of each dispersion was collected, let settle for five days, and its supernatant was diluted with to 1:300 with deionized water to get the solutions transparent. The opacity of the diluted dispersions were measured by using Shimadzu UV-1800 spectrophotometer and plastic cuvettes with 1 cm optical path length.

### 3.4. Imaging

The CNT agglomerate size was evaluated by drying a droplet of the dispersions on a metal plate and characterizing them by scanning electron microscopy (FIB-SEM, Zeiss Crossbeam 540).

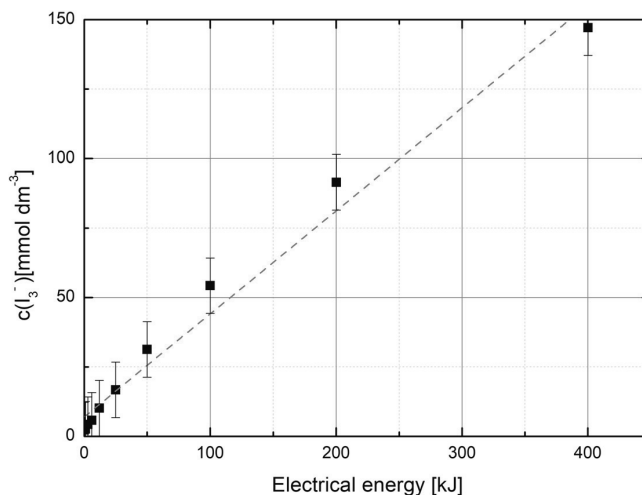


**Figure 1.** Concentration of  $I_3^-$  as a function of electrical energy  $E_{el}$  used by the sonicator. The sonochemical yield/energy for this particular sonication system was  $0.371 \text{ mmol dm}^{-3} \text{ kJ}^{-1}$ . An error from sample preparation and measurements were estimated to be  $\pm 10 \text{ mmol dm}^{-3}$ .

## 4. Results

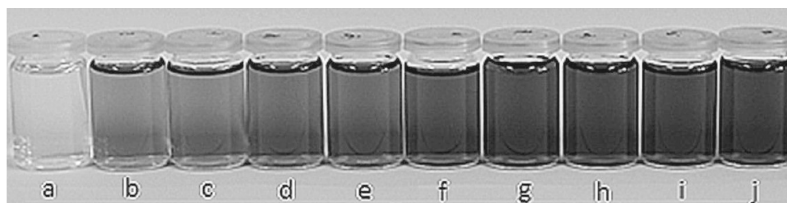
### 4.1. Weissler reaction

Figure 1 shows the development of  $I_3^-$  concentration as a function of electrical energy consumed by the sonicator. It can be observed that the production rate was higher in the beginning of the sonication. This is caused by the dissolved gases, which accelerate the hydrogen peroxide production by participating in the chemical reactions (oxygen) and by lowering the inertial cavitation threshold [43]. After dissolved gases have fully diffused and consumed by the process, the rate of  $I_3^-$  conversion slightly slows down. Linear fitting still gives a good approximation for  $C(I_3^-)$  versus  $E_e$  and was used in all future calculations.

### 4.2. Dispersion of CNTs

As the applied sonication energy gets higher, the supernatant of the dispersion becomes darker indicating an increase in the concentration of CNTs in dispersed state (Figure 2). The dark appearance was found to be stable up to several weeks.

Figure 3 shows that the opacity at 500 nm follows the proposed dependence on sonochemical yield (5). It can be seen that Triton X-100 and CTAB can disperse CNTs close to the maximum dispersion quality at a lower surfactant/CNT mass ratios compared to Pluronic F-127 and SDS. It is also evident that the acoustic energy required to disperse CNTs with SDS is significantly higher compared to others,



**Figure 2.** Series of diluted supernatants of CNT-dispersions corresponding different acoustic energies of sonication. Evolution of the dispersion quality can be seen from samples a to j. As solutions get darker, more individual nanotubes are being dispersed in to the liquid.

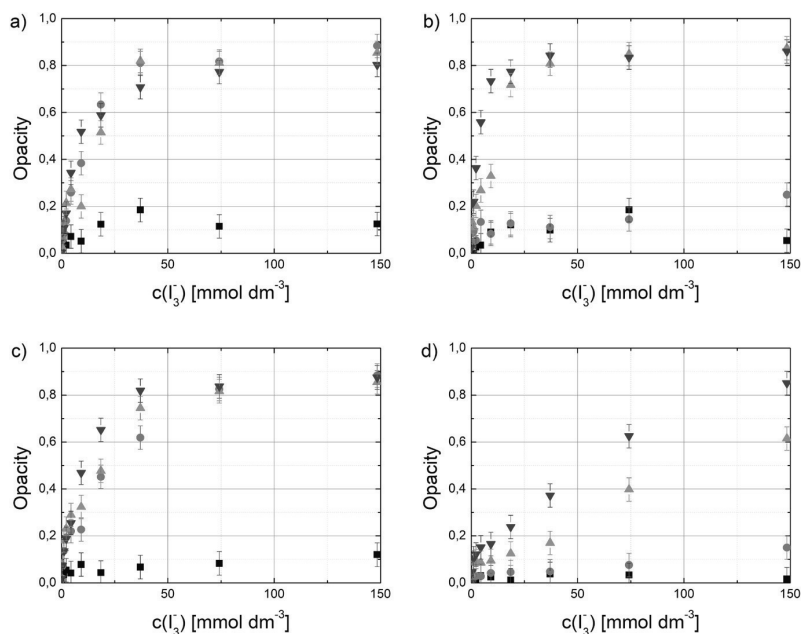


**Figure 3.** The development of opacity as a function of  $C(I_3^-)$  with different surfactant/CNT ratios: ■ 1:4, ● 1:2, ▲ 1:1 and ▼ 2:1 for a) Triton X-100, b) Pluronic F-127, c) CTAB and d) SDS.

and that the rate of development of dispersion quality is respectively lower. This is somewhat surprising since SDS is widely used in many of the reported studies and yet it seems to be more difficult to use in order to optimize the dispersion quality.

In Figure 4, a fitted opacity function (5) gives a theoretical asymptote for the maximum opacity,  $\alpha_{max}$ , with a theoretical infinite yield. Possible deviations from (5) with higher yields are due to the fracture (damage) of CNTs as the sonication progresses causing additional opacity, which is not related to the surfactant-assisted exfoliation of the aggregates.

In Figure 5 it can be seen that investigating dispersion quality with dried samples is rather challenging. One can say that larger agglomerates do disappear as a function

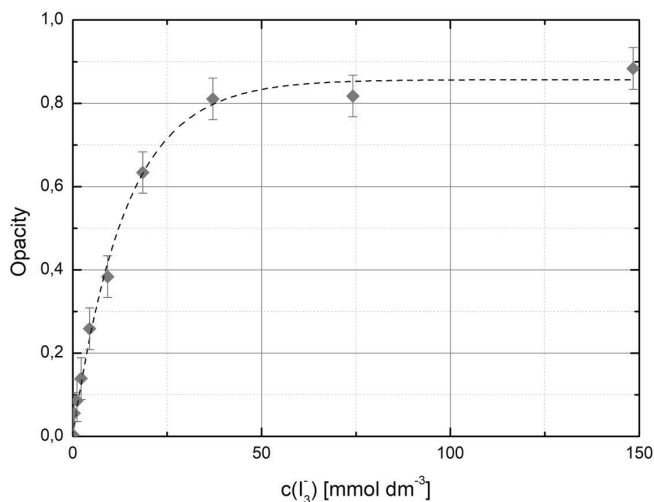


**Figure 4.** Measured opacity of sonicated 1:2 Triton X-100/CNT dispersion as a function of sonochemical yield of the sonicator together with a fitted opacity function (5).

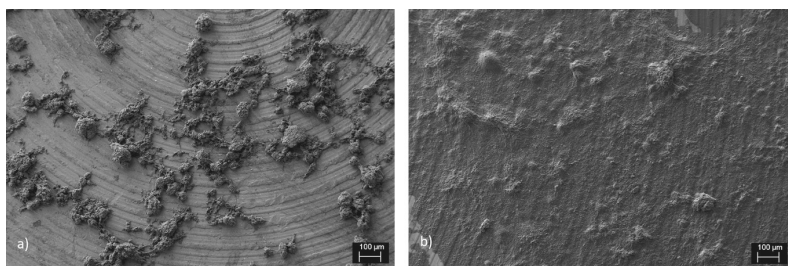


**Figure 5.** FIB images of dried 1:2 Triton X-100/CNT dispersions. a) Non-sonicated and b) sonicated with maximum opacity. It can be seen that most of the large agglomerates have been dispersed and the metal plate is coated with individual CNTs. Still some larger particles exist.

of sonochemical yield, but calculating a number describing the dispersion quality is basically impossible. Dried sample for FIB microscopy is not an accurate 2D presentation of the 3D situation. During the drying process the surface tension of water affects how 2D-structure is being formed. Therefore SEM or FIB microscopy is not optimal for studying dispersion quality of water based CNT colloids.

Variation of maximum absorbance can be seen for different surfactant/CNT ratios depending on the surfactant type (Figure 6). It is noticeable that there is a sharp change in the development of the maximum opacity as the surfactant/CNT ratio increases. Below this threshold value of surfactant/CNT ratio, the highest reachable opacity (indicating the maximum dispersion quality) is to be low. On the other hand, when the ratio matches the threshold value, the maximum opacity gets also rapidly reached and further increase in the ratio does not improve the dispersion. For applications where surfactant assisted dispersions are necessary, the determination

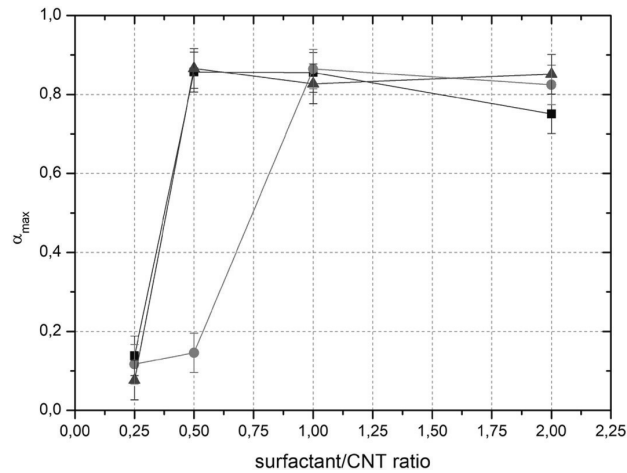


**Figure 6.** Measured maximum opacities as a function of surfactant/CNT ratio for three different surfactants: ■ Triton X-100, ● Pluronic F-127 and ▲ CTAB.

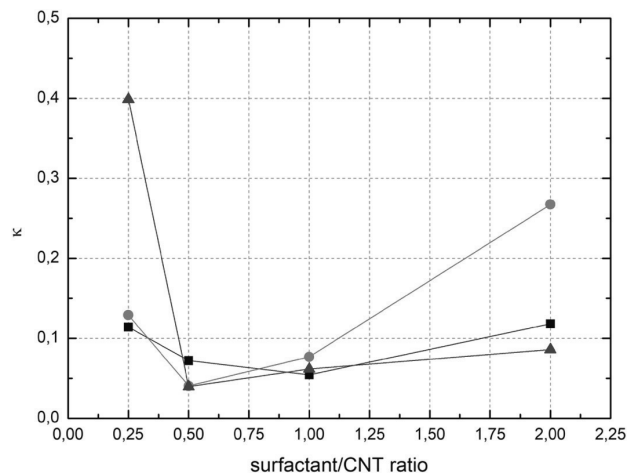


**Figure 7.** The factor  $\kappa$ , indicating a growth speed of the opacity as a function of surfactant/CNT for ■ Triton X-100, ● Pluronic F-127 and ▲ CTAB.

of an optimum surfactant ratio is critical since excess surfactant remaining, for example in a nanocomposite matrix, will diminish the physical properties. SDS is not included in Figure 6 since the applied acoustic energy range was not high enough to reach the saturation in the opacity. SDS was the only surfactant which did not reach saturation point of the opacity with used energies even with highest concentrations. All sonications except the lowest concentration of SDS were above critical micelle concentration.

The factor  $\kappa$  in Equation (5), indicating the rate of opacity increase as a function of acoustic energy, is implicitly dependent on the surfactant/CNT ratio (Figure 7).

$\kappa$  can be observed to have a different local minimum for different surfactants, which is most likely related to the adsorption mechanism of the surfactant on the CNT surface. Depending on surfactant concentration, the assembly on the CNT surface is different. The tendency to improve the dispersion along with the increase in the acoustic energy is weaker the stronger is the surfactant layers internal binding on the initial agglomerates. Also, the response in the acoustic energy transfer by the surfactant layer can hinder the CNT agglomerate dispersion yet it is challenging to theoretically verify the difference in this response between different surfactants.

## 5. Conclusions

A theoretical equation for a development of the dispersion quality of aqueous CNT colloid as a function of sonochemical yield was proposed. Sonication experiments with four different surfactant types and different surfactant/CNT ratios and inertial cavitation activities were performed. The inertial cavitation activity was determined using the Weessler reaction. It was shown that the proposed equation fits well with the performed measurements and that the maximum opacities, received via fitting the equations, follows an S-curve as a function of surfactant/CNT ratio. The revealed sonochemical yield-dispersion (SCY-D) relation indicates that there is a threshold for the minimum surfactant/CNT ratio to achieve the optimal dispersion quality for a CNT-surfactant system. Here, we determined the lower and upper values of the threshold region of surfactant/CNT ratios for three different surfactants, namely Triton X-100, Pluronic F-127, and CTAB.

## Declarations

### Author contribution statement

Pasi Keinänen – Conceived and designed the experiments; Performed the experiments; Analyzed and interpreted the data; Contributed reagents, materials, analysis tools or data; Wrote the paper.

Sanna Siljander – Conceived and designed the experiments; Performed the experiments; Wrote the paper.

Mikko Koivula, Essi Sarlin – Performed the experiments.

Jatin Sethi, Jyrki Vuorinen, Mikko Kanerva: Analyzed and interpreted the data.



## Funding statement

This research did not receive any specific grant from funding agencies in the public, commercial, or not-for-profit sectors.

## Competing interest statement

The authors declare no conflict of interest.

## Additional information

No additional information is available for this paper.

## References

- [1] R. Andrews, D. Jacques, M. Minot, T. Rantell, Fabrication of carbon multiwall nanotube/polymer composites by shear mixing, *Macromol. Mater. Eng.* 287 (6) (2002) 395–403.
- [2] Y. Huang, E. Terentjev, Dispersion and rheology of carbon nanotubes in polymers, *Int. J. Mater. Forming* 1 (2) (2008) 63–74.
- [3] I. Lavilla, C. Bendicho, Fundamentals of ultrasound-assisted extraction, in: *Water Extraction of Bioactive Compounds*, Elsevier, 2018, pp. 291–316.
- [4] D.-Q. Yang, J.-F. Rochette, E. Sacher, Functionalization of multiwalled carbon nanotubes by mild aqueous sonication, *J. Phys. Chem. B* 109 (16) (2005) 7788–7794.
- [5] J.-M. Bonard, T. Stora, J.-P. Salvetat, F. Maier, T. Stöckli, C. Duschl, L. Forró, W.A. de Heer, A. Châtelain, Purification and size-selection of carbon nanotubes, *Adv. Mater.* 9 (10) (1997) 827–831.
- [6] L. Vaisman, G. Marom, H.D. Wagner, Dispersions of surface-modified carbon nanotubes in water-soluble and water-insoluble polymers, *Adv. Funct. Mater.* 16 (3) (2006) 357–363.
- [7] Y. Geng, M.Y. Liu, J. Li, X.M. Shi, J.K. Kim, Effects of surfactant treatment on mechanical and electrical properties of CNT/epoxy nanocomposites, *Composites, Part A, Appl. Sci. Manuf.* 39 (12) (2008) 1876–1883.
- [8] J. Rausch, R.-C. Zhuang, E. Mäder, Surfactant assisted dispersion of functionalized multi-walled carbon nanotubes in aqueous media, *Composites, Part A, Appl. Sci. Manuf.* 41 (9) (2010) 1038–1046.

- [9] S. Javadian, A. Motae, M. Sharifi, H. Aghdastinat, F. Taghavi, Dispersion stability of multi-walled carbon nanotubes in cationic surfactant mixtures, *Colloids Surf. A, Physicochem. Eng. Asp.* 531 (2017) 141–149.
- [10] M. Islam, E. Rojas, D. Bergey, A. Johnson, A. Yodh, High weight fraction surfactant solubilization of single-wall carbon nanotubes in water, *Nano Lett.* 3 (2) (2003) 269–273.
- [11] T.J. McDonald, C. Engtrakul, M. Jones, G. Rumbles, M.J. Heben, Kinetics of PL quenching during single-walled carbon nanotube rebundling and diameter-dependent surfactant interactions, *J. Phys. Chem. B* 110 (50) (2006) 25339–25346.
- [12] M. Bystrzejewski, A. Huczko, H. Lange, T. Gemming, B. Büchner, M. Rummeli, Dispersion and diameter separation of multi-wall carbon nanotubes in aqueous solutions, *J. Colloid Interface Sci.* 345 (2) (2010) 138–142.
- [13] B. Vigolo, A. Penicaud, C. Coulon, C. Sauder, R. Pailier, C. Journet, P. Bernier, P. Poulin, Macroscopic fibers and ribbons of oriented carbon nanotubes, *Science* 290 (5495) (2000) 1331–1334.
- [14] M.J. O’connell, S.M. Bachilo, C.B. Huffman, V.C. Moore, M.S. Strano, E.H. Haroz, K.L. Rialon, P.J. Boul, W.H. Noon, C. Kittrell, Band gap fluorescence from individual single-walled carbon nanotubes, *Science* 297 (5581) (2002) 593–596.
- [15] P. Poulin, B. Vigolo, P. Launois, Films and fibers of oriented single wall nanotubes, *Carbon* 40 (10) (2002) 1741–1749.
- [16] L. Jiang, L. Gao, J. Sun, Production of aqueous colloidal dispersions of carbon nanotubes, *J. Colloid Interface Sci.* 260 (1) (2003) 89–94.
- [17] V.C. Moore, M.S. Strano, E.H. Haroz, R.H. Hauge, R.E. Smalley, J. Schmidt, Y. Talmon, Individually suspended single-walled carbon nanotubes in various surfactants, *Nano Lett.* 3 (10) (2003) 1379–1382.
- [18] K. Yurekli, C.A. Mitchell, R. Krishnamoorti, Small-angle neutron scattering from surfactant-assisted aqueous dispersions of carbon nanotubes, *J. Am. Chem. Soc.* 126 (32) (2004) 9902–9903.
- [19] T. Chatterjee, K. Yurekli, V.G. Hadjiev, R. Krishnamoorti, Single-walled carbon nanotube dispersions in poly (ethylene oxide), *Adv. Funct. Mater.* 15 (11) (2005) 1832–1838.
- [20] T. Hertel, A. Hagen, V. Talalaev, K. Arnold, F. Hennrich, M. Kappes, S. Rosenthal, J. McBride, H. Ulbricht, E. Flahaut, Spectroscopy of single-

- and double-wall carbon nanotubes in different environments, *Nano Lett.* 5 (3) (2005) 511–514.
- [21] N. Grossiord, J. Loos, L. Van Laake, M. Maugey, C. Zakri, C.E. Koning, A.J. Hart, High-conductivity polymer nanocomposites obtained by tailoring the characteristics of carbon nanotube fillers, *Adv. Funct. Mater.* 18 (20) (2008) 3226–3234.
- [22] A.J. Blanch, C.E. Lenehan, J.S. Quinton, Optimizing surfactant concentrations for dispersion of single-walled carbon nanotubes in aqueous solution, *J. Phys. Chem. B* 114 (30) (2010) 9805–9811.
- [23] M.D. Clark, S. Subramanian, R. Krishnamoorti, Understanding surfactant aided aqueous dispersion of multi-walled carbon nanotubes, *J. Colloid Interface Sci.* 354 (1) (2011) 144–151.
- [24] A. Ryabenko, L. Fokeeva, T. Dorofeeva, Spectroscopic study of suspensions of single-wall carbon nanotubes in polyaniline solutions in *N*-methylpyrrolidone in UV–Vis–NIR regions, *Russ. Chem. Bull.* 53 (12) (2004) 2695–2699.
- [25] M.-J. Jiang, Z.-M. Dang, S.-H. Yao, J. Bai, Effects of surface modification of carbon nanotubes on the microstructure and electrical properties of carbon nanotubes/rubber nanocomposites, *Chem. Phys. Lett.* 457 (4) (2008) 352–356.
- [26] R. Rastogi, R. Kaushal, S. Tripathi, A.L. Sharma, I. Kaur, L.M. Bharadwaj, Comparative study of carbon nanotube dispersion using surfactants, *J. Colloid Interface Sci.* 328 (2) (2008) 421–428.
- [27] Y. Bai, D. Lin, F. Wu, Z. Wang, B. Xing, Adsorption of triton x-series surfactants and its role in stabilizing multi-walled carbon nanotube suspensions, *Chemosphere* 79 (4) (2010) 362–367.
- [28] I. Madni, C.-Y. Hwang, S.-D. Park, Y.-H. Choa, H.-T. Kim, Mixed surfactant system for stable suspension of multiwalled carbon nanotubes, *Colloids Surf. A, Physicochem. Eng. Asp.* 358 (1) (2010) 101–107.
- [29] Y. Bai, I.S. Park, S.J. Lee, T.S. Bae, F. Watari, M. Uo, M.H. Lee, Aqueous dispersion of surfactant-modified multiwalled carbon nanotubes and their application as an antibacterial agent, *Carbon* 49 (11) (2011) 3663–3671.
- [30] K. Yang, B. Xing, Adsorption of organic compounds by carbon nanomaterials in aqueous phase: Polanyi theory and its application, *Chem. Rev.* 110 (10) (2010) 5989–6008.
- [31] W. Wenseleers, I.I. Vlasov, E. Goovaerts, E.D. Obraztsova, A.S. Lobach, A. Bouwen, Efficient isolation and solubilization of pristine single-walled nanotubes in bile salt micelles, *Adv. Funct. Mater.* 14 (11) (2004) 1105–1112.

- [32] J. Yu, N. Grossiord, C.E. Koning, J. Loos, Controlling the dispersion of multi-wall carbon nanotubes in aqueous surfactant solution, *Carbon* 45 (3) (2007) 618–623.
- [33] S. Utsumi, M. Kanamaru, H. Honda, H. Kanoh, H. Tanaka, T. Ohkubo, H. Sakai, M. Abe, K. Kaneko, RBM band shift-evidenced dispersion mechanism of single-wall carbon nanotube bundles with NaDDBs, *J. Colloid Interface Sci.* 308 (1) (2007) 276–284.
- [34] Z. Sun, V. Nicolosi, D. Rickard, S.D. Bergin, D. Aherne, J.N. Coleman, Quantitative evaluation of surfactant-stabilized single-walled carbon nanotubes: dispersion quality and its correlation with zeta potential, *J. Phys. Chem. C* 112 (29) (2008) 10692–10699.
- [35] L. Maillaud, C. Zakri, I. Ly, A. Pénicaud, P. Poulin, Conductivity of transparent electrodes made from interacting nanotubes, *Appl. Phys. Lett.* 103 (26) (2013) 263106.
- [36] P. Angelikopoulos, A. Gromov, A. Leen, O. Nerushev, H. Bock, E.E. Campbell, Dispersing individual single-wall carbon nanotubes in aqueous surfactant solutions below the cmc, *J. Phys. Chem. C* 114 (1) (2009) 2–9.
- [37] K. Shen, S. Curran, H. Xu, S. Rogelj, Y. Jiang, J. Dewald, T. Pietrass, Single-walled carbon nanotube purification, pelletization, and surfactant-assisted dispersion: a combined TEM and resonant micro-Raman spectroscopy study, *J. Phys. Chem. B* 109 (10) (2005) 4455–4463.
- [38] N. Grossiord, O. Regev, J. Loos, J. Meuldijk, C.E. Koning, Time-dependent study of the exfoliation process of carbon nanotubes in aqueous dispersions by using UV-visible spectroscopy, *Anal. Chem.* 77 (16) (2005) 5135–5139.
- [39] P. Alafogianni, K. Dassios, S. Farmaki, S. Antiohos, T. Matikas, N.-M. Barkoula, On the efficiency of UV–vis spectroscopy in assessing the dispersion quality in sonicated aqueous suspensions of carbon nanotubes, *Colloids Surf. A, Physicochem. Eng. Asp.* 495 (2016) 118–124.
- [40] A. Sesis, M. Hodnett, G. Memoli, A.J. Wain, I. Jurewicz, A.B. Dalton, J.D. Carey, G. Hinds, Influence of acoustic cavitation on the controlled ultrasonic dispersion of carbon nanotubes, *J. Phys. Chem. B* 117 (48) (2013) 15141–15150.
- [41] S. Koda, T. Kimura, T. Kondo, H. Mitome, A standard method to calibrate sonochemical efficiency of an individual reaction system, *Ultrason. Sonochem.* 10 (3) (2003) 149–156.

- [42] A. Weissler, H.W. Cooper, S. Snyder, Chemical effect of ultrasonic waves: oxidation of potassium iodide solution by carbon tetrachloride, *J. Am. Chem. Soc.* 72 (4) (1950) 1769–1775.
- [43] C. Petrier, M.-F. Lamy, A. Francony, A. Benahcene, B. David, V. Renaudin, N. Gondrexon, Sonochemical degradation of phenol in dilute aqueous solutions: comparison of the reaction rates at 20 and 487 kHz, *J. Phys. Chem.* 98 (41) (1994) 10514–10520.



# PUBLICATION II

## **Effect of surfactant type and sonication energy on the electrical conductivity properties of nanocellulose-CNT nanocomposite films**

S. Siljander, P. Keinänen, A. Rätty, K. R. Ramakrishnan, S. Tuukkanen,  
V. Kunnari, A. Harlin, J. Vuorinen and M. Kanerva

International Journal of Molecular Sciences 19.6 (2018), 1819

**10.3390/ijms19061819**  
**<http://urn.fi/URN:NBN:fi:ty-201807302026>**

**Publication reprinted with the permission of the copyright holders.**







Article

# Effect of Surfactant Type and Sonication Energy on the Electrical Conductivity Properties of Nanocellulose-CNT Nanocomposite Films

Sanna Siljander <sup>1,\*</sup>, Pasi Keinänen <sup>1</sup> , Anna Rätty <sup>1</sup>, Karthik Ram Ramakrishnan <sup>1</sup>, Sampo Tuukkanen <sup>2</sup> , Vesa Kunnari <sup>3</sup>, Ali Harlin <sup>3</sup>, Jyrki Vuorinen <sup>1</sup> and Mikko Kanerva <sup>1</sup>

<sup>1</sup> Laboratory of Materials Science, Tampere University of Technology, FI-33720 Tampere, Finland; pasi.keinanen@tut.fi (P.K.); anna.raty@tut.fi (A.R.); karthik.ramakrishnan@tut.fi (K.R.R.); jyrki.vuorinen@tut.fi (J.V.); mikko.kanerva@tut.fi (M.K.)

<sup>2</sup> BioMediTech, Tampere University of Technology, FI-33720 Tampere, Finland; sampo.tuukkanen@tut.fi

<sup>3</sup> VTT Research Center, FI-02044 Espoo, Finland; vesa.kunnari@vtt.fi (V.K.); ali.harlin@vtt.fi (A.H.)

\* Correspondence: sanna.siljander@tut.fi; Tel.: +358-50-3-555-777

Received: 15 May 2018; Accepted: 15 June 2018; Published: 20 June 2018



**Abstract:** We present a detailed study on the influence of sonication energy and surfactant type on the electrical conductivity of nanocellulose-carbon nanotube (NFC-CNT) nanocomposite films. The study was made using a minimum amount of processing steps, chemicals and materials, to optimize the conductivity properties of free-standing flexible nanocomposite films. In general, the NFC-CNT film preparation process is sensitive concerning the dispersing phase of CNTs into a solution with NFC. In our study, we used sonication to carry out the dispersing phase of processing in the presence of surfactant. In the final phase, the films were prepared from the dispersion using centrifugal cast molding. The solid films were analyzed regarding their electrical conductivity using a four-probe measuring technique. We also characterized how conductivity properties were enhanced when surfactant was removed from nanocomposite films; to our knowledge this has not been reported previously. The results of our study indicated that the optimization of the surfactant type clearly affected the formation of freestanding films. The effect of sonication energy was significant in terms of conductivity. Using a relatively low 16 wt. % concentration of multiwall carbon nanotubes we achieved the highest conductivity value of 8.4 S/cm for nanocellulose-CNT films ever published in the current literature. This was achieved by optimizing the surfactant type and sonication energy per dry mass. Additionally, to further increase the conductivity, we defined a preparation step to remove the used surfactant from the final nanocomposite structure.

**Keywords:** nanocellulose; carbon nanotubes; nanocomposite; conductivity; surfactant

## 1. Introduction

Conductive composite materials with micrometer and nanoscale fillers, like metallic powders, carbon black, graphite and carbon fibers, are used in many applications, such as antistatic films and electromagnetic interference (EMI) shielding. Electrical conductivity of 0.01 S/cm or higher is required for the composite to be considered conductive, while materials with lower conductivity can be used as antistatic and semiconducting materials. One of the drawbacks with most fillers is that the filler content ratio needs to be as high as 50 wt. % to achieve the percolation threshold (i.e., the critical concentration of filler that corresponds to the sharp rise of conductivity). However, this high filler content ratio might lead to a decrease in the resultant composite's mechanical properties [1,2]. Nanomaterials, such as carbon nanotubes (CNTs) and graphene, play a role in the development of future composite materials.

For example, CNTs and graphene have been used to toughen matrix polymers [3], to adjust barrier properties of nanocomposite films [4], and to form hierarchical reinforcements [5]. It is possible to attain the percolation threshold in the insulating polymer matrix at a low CNT concentration due to their excellent electrical, mechanical and thermal properties.

Individual CNTs are part of a group of the strongest and most conductive nanomaterials known [6]. Additionally, CNTs can carry higher current density than any other known material, with its highest measured value being 109 A/cm<sup>2</sup> [7,8]. However, to obtain an ideal conductive network, the carbon nanotubes have to be well separated and homogenous dispersion should be maintained in the final product. Without efficient dispersion, filler aggregates act as defect sites, which leads to lower mechanical performance [9,10]. As the most abundant polymer on earth, cellulose is a promising and well-known material that can be used as a matrix in nanocomposites.

Cellulose is environmentally conscious, low-cost, strong, dimension-stable, non-melting, non-toxic and is a non-metal matrix. The interest towards nanoscale cellulose has increased during the past few years because of its inherent properties, including its good mechanical properties, which are better than those of the respective source biomass material [11]. Cellulose-based micro-/nanofibrils (MFC/NFC) can be extracted from various types of plant fibers using mechanical forces, chemical treatments, enzymes or combinations of these. The most typical approach, however, is to apply wood pulp and mechanical methods such as homogenization, microfluidization, microgrinding and cryocrushing. Finally, after fibrillation, the width of NFC is typically between 5 and 20 nm, with a length of several micrometers. Nanocellulose (NFC) has hydroxyl groups in its structure and is therefore associated with high aspect ratio and strong hydrogen bonds formed between nanocellulose fibers [12]. These bonds enhance mechanical properties and enable the formation of free standing films. A combination of CNTs and cellulose I provides a conductive nanocomposite network. CNT-cellulose composites have been reported to be used as supercapacitor electrodes [13,14], electromagnetic interference shielding devices [15], chemical vapor sensors [16], water sensors [17,18], and pressure sensors [19].

There are different manufacturing methods for the fabrication of CNT-cellulose nanocomposites, but all the methods typically include (1) a phase of dispersing CNTs into a solution, and (2) an impregnation phase into the cellulose substrates (e.g., paper, filter paper) [15,16,20–23]. Alternatively, the dispersion can be used as a wet component with bacterial cellulose [24,25], with cellulose I and regenerated cellulose fibers [13,18,26] or in an aerogel form [17]. The processing of nanocellulose in an aqueous medium is the most common way due to its tendency to react with water, and strong affinity to itself and hydroxyl group containing materials [12]. Chen et al. [27] showed that NFCs and CNTs can form a three-dimensional conductive network structure in a gel-film morphology to achieve high electrical conductivity.

The properties of the nanocellulose-CNT composites are affected by the quality of CNT dispersion, amount of structural and oxidative defects in the graphitic structure of the CNTs, the aspect ratio of the CNTs after the disaggregate treatment, the strength of the matrix, and the interactions between the CNTs and the cellulose matrix. [28] The key challenge in numerous industrial applications is to achieve uniform and stable CNT dispersion. The homogenization phase is vital to maximize the excellent mechanical, electrical and thermal properties of the CNTs and the eco-friendly, strong and low-cost nanocellulose matrix. This is particularly important in the case of submicron- or nanometer-sized particles. In these scales, the surface chemistry plays an important role, managing the particle dispersion within the final product [29]. CNT dispersions are challenging because as the surface area of particles increases, the attractive forces between the aggregates [29] and the high aspect ratio enable the entanglement and bundling of CNTs [30]. There are two phenomena that affect CNT dispersions: nanotube morphology and the forces between the tubes. Entanglement of CNTs occurs due to tube morphology, as well as molecular forces, high aspect ratio, and high flexibility. Dispersing these entangled aggregates is difficult without damaging the nanotubes. Both CNT and aggregate size are expected to play a crucial role in the achieved level of electrical conductivity [31].

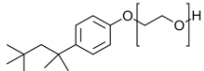
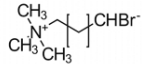
Two typical dispersion methods for CNTs include high shear mixing and pure sonication [13,15,16,19–21,24,32]. Sonication is based on ultrasonic waves that generate microscopic bubbles

or inertial cavitation, which produces a shearing action. This results in liquid and suspended particles becoming intensely agitated. Another common technique is to use a centrifuge in one of the processing steps to extract the unwanted agglomerates from the supernatant, but this additional phase takes time and effort and affects the concentration of dispersed particles in the dispersion. In general, sonication is superior to shear mixing, especially for low-viscosity systems [33], where conventional mixing does not create high enough strain rates to disintegrate the CNT aggregates.

Another issue in the manufacturing of films using NFC is the shrinkage and distortion of the structure because of faster evaporation rate on surface than the mass transport of moisture within the material. When strong enough gradient occurs, film distortions emerge because of local stresses [34,35].

One widely used method for CNT dispersion is the non-covalent method. In this method, chemical moieties are adsorbed onto the surface of CNTs, the CNTs are non-covalently dispersed in a water medium, and the resultant mixture is sonicated in the presence of the moieties, namely surfactants. Surfactants are a group of organic compounds that have a hydrophilic head and a hydrophobic tail, and they are commonly used as detergents, wetting agents, emulsifiers, foaming agents and dispersants. The advantage of the non-covalent method lies in the fact that it does not deteriorate the electronic structure of the CNTs' graphitic shells, maintaining their high electrical conductivity. Good dispersion can be achieved by having a mixture of both nanocellulose and carbon nanotubes with the help of surfactants, as the surfactants lower the interfacial free energy between the particles. Table 1 lists information about surfactants and their properties used in this study.

**Table 1.** Surfactants used in this study.

Product Name	Triton™ x-100	Pluronic® F-127	CTAB
Type	Non-ionic	Non-ionic Polymeric	Cationic
Name	Octylphenol Ethoxylate	Poloxamer	Hexadecyltri-methylammonium bromide
Chemical Structure		$H(OCH_2CH_2)_x(OCH_2CH(CH_3))_y(OCH_2CH_2)_zOH$	
Critical Micelle Concentration	0.2–0.9 mM (20–25) °C	950–1000 ppm (25 °C)	0.92 mM (20–25) °C
HLB value	13.5	22	10

In the current literature, there are several different types of surfactants used for dispersing nanocellulose and carbon nanotubes. Choosing a surfactant type for effective dispersion of nanotubes through surfactant adsorption is complicated, as the results in the published literature often give contradictory results. For example, some researchers [29] have suggested that ionic surfactants are preferable for creating aqueous dispersions. However, the non-ionic surfactant Triton X-100 was shown to be a better surfactant than the anionic surfactant SDS, which was attributed to the  $\pi$ - $\pi$  stacking ability of the former. The quality of the NFC-CNT dispersion is dependent on the nature of the surfactant, the concentration and the type of interactions between the surfactant and dispersing particles [36]. It has been stated that, for dispersing CNTs it is preferable for the surfactant to have a relatively high HLB (hydrophilic-lipophilic balance) value [29]. This assumption was proven false in our previous study [37]. Not only are the surfactant's nature and energy carried into the dispersed system, but the concentration of the surfactant also has a crucial role in the dispersion process [38]. Too high a surfactant concentration may negatively affect conductivity properties by blocking off the charge transport through the CNT network [39]. In addition, a low surfactant concentration can cause re-aggregation, because a sufficient amount is required to cover CNT surfaces to prevent re-aggregation [39,40]. It has been shown that an efficient CNT dispersion is only possible when the surfactant concentration is above the critical micelle concentration (CMC) value [41–44]. In some cases, the surfactant concentration is reported to be higher than the (CMC), but no micelle structures are

observed in the dispersion. Presumably, most of the surfactant has been adsorbed onto the surface of the CNTs [40]. In other cases, surfactants can prefer surfactant-surfactant interactions over spreading on the CNT surface [45]. It has also been reported that dispersing agents can form stable dispersions below and equal to their CMC limit [46–49]. Moreover, it has been noted that commonly, the best results can be reached with a concentration of 0.5 CMC and that any further increase in the concentration of surfactant has only a minor effect [48].

The ISO 14887:2000(E) standard can be used to determine prospective dispersing agents for both cellulose and carbon. We can categorize nanocellulose and CNTs as solids. In that case, when using water as liquid, the category of suitable dispersing agent would be a poly ethylene-oxide (PEO)/alcohol for CNT and PEO/poly propylene oxide (PPO) copolymer for nanocellulose. The standard also provides information about commercial surfactants that fall into the mentioned categories. PEO/PPO copolymer is a suitable surfactant for nanocellulose. The standard denotes that a commercial equivalent is Pluronic®. In the case of CNTs, one example of alkyl phenoxy PEO ethanol dispersing agent is Triton™.

The typical approach to the manufacturing of conductive cellulose-CNT films has been to increase CNT weight percentage without optimizing the dispersion procedure or the used surfactants. Also, the effect of the particular ratios of the cellulose, CNT and surfactant toward each other has not been fully investigated. Even though ultrasonication is widely used for the dispersion and stabilization of CNTs, there is not a standard procedure for the sonication process, and different research groups have applied different sonication treatments to their samples. Sonication can cause chemical functionalization but it can also cause defects and breakage of CNTs [1,50–52]. This will further affect the performance of CNT-based materials and their applications. It has been found in the current literature that sonication parameters such as sonicator type, sonication time and temperature control vary significantly, with reported sonication times ranging from 2 min with tip sonication to 20 h for bath sonication. Dassios et al. [53] attempted to optimize the sonication parameters for the dispersion of MWCNTs in an aqueous solution. Two critical questions concerning the homogeneity of aqueous suspensions of carbon nanotubes by ultrasonic processing were identified; namely, the dependence of dispersion quality on the duration and intensity of sonication and the identification of the appropriate conditions for retaining the highly desirable initial aspect ratio of the free-standing tubes in the dispersed state. Fuge et al. [54] studied the effect of different ultrasonication parameters (time, amplitude) on undoped and nitrogen-doped MWCNTs in aqueous dispersions and found a nearly linear decrease of the arithmetic mean average in MWCNT length with increasing ultrasonication time.

The aim of this study was to optimize the conductivity of NFC-CNT nanocomposite films using a minimum amount of processing steps (e.g., without centrifugal processing of dispersion or pressing of the film), materials and chemicals. In this paper, NFC and multiwall carbon nanotubes (MWCNT) were used to prepare composite films and study the effect of the sonication energy and surfactant type on the electrical conductivity of the nanocomposite. In addition, we investigated the removal of the surfactant from the nanocomposites and the subsequent effect on the electrical conductivity. To our knowledge this is a novel approach and has not been reported previously. The conductivity properties of the nanocomposites were studied as a function of the used sonication energy amount, as well as with and without the presence of surfactant.

## 2. Results

The impact of sonication energy on electrical conductivity was one of the processing parameters with the highest interest in this study. This was due to the lack of previous research in the current literature. Also, our results show that the surfactant type and sonication energy play a major role in achieving excellent conductivity. In addition to the previously mentioned parameters, removal of surfactant can enhance conductivity values toward levels never seen or reported.

Overall, the shelf-life of the sonicated dispersion samples was significantly long, since samples remained unchanged before the film preparation. Also, sedimentation was not detected, based on the fact that conductivity values were at the same level when measured from both sides of the

nanocomposite films. The appearance of the sonicated dispersion samples was identical; however, the consistency and visually inspected viscosity varied with increasing sonication energy. This was observed with Triton X-100 and Pluronic F-127 samples but not in cetyl trimethylammonium bromide (CTAB) surfactant-containing dispersions.

### 2.1. Conductivity of NFC-CNT Nanocomposite Films

Electrical conductivity of the even and uniform centrifugally cast films was measured using the four-probe measuring technique. With this method, it is possible to minimize the contact resistances and thus provide more accurate conductivity measurements than for the commonly used two-terminal measurement. The sheet resistances of prepared and cut nanocomposite films (size 30 mm × 30 mm) were measured using a four-point probe setup made in-house and a multimeter (Keithley 2002, Tektronix, Inc., Beaverton, OR, USA) in four-wire mode. The probes were placed in line, with equal 3 mm spacing. The four-probe setup is described elsewhere in detail [55]. The conductivity measurements were carried out using a 1 mA current and voltage was measured. Measurements were taken before and after removal of surfactant.

The selection of the most functional surfactant was an important aspect in this study. This selection was determined based on the sheet resistance measurements. The effect of different surfactants and sonication energy on conductivity is shown in Figure 1. From the conductivity diagrams, the effect of surfactant type can be visually observed and estimated.

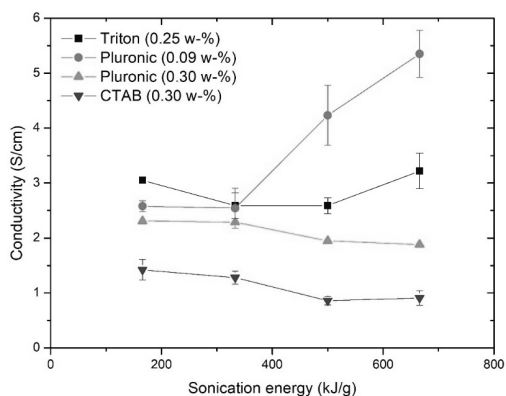


**Figure 1.** Conductivity of nanocomposite films processed using surfactants Triton X-100, Pluronic F-127 and cetyl trimethylammonium bromide. Concentration in weight percentages.

According to the standard, our assumption was that non-ionic surfactants would be the most promising surfactants. This was clearly the case, since the films made with surfactants Triton X-100 and Pluronic F-127 outperformed the films made with ionic surfactant CTAB.

Visual observations made with CTAB aqueous dispersion samples after sonication indicated that these samples did not gelate even with a higher amount of sonication energy per dry mass (666 kJ/g). This suggests that the dispersion process may not have been entirely successful, since samples had different consistencies and visually separate particles. The ionic surfactant (CTAB) was used to manufacture films at a 1 to 1 ratio of dry mass content of NFC and CNT. The conductivity of films processed using CTAB decreased as the sonication increased from almost 1.5 S/cm to less than 0.90 S/cm. The conductivity diagram of these films was different in its nature; the highest values were measured with the lowest amount of sonication energy.

Based on the standard Pluronic F-127, surfactant should be compatible with cellulosic materials. The first set of Pluronic F-127 nanocomposite films were done with a 1 to 1 ratio to dry mass content (0.30 wt. %). Results show that conductivity is decreasing as a function of sonication energy. Based on

this finding, another set of films was manufactured using a surfactant concentration below the CMC limit (0.09 wt. %). Conductivity results for this set of samples show higher conductivity values than films manufactured using a surfactant concentration higher than the CMC value (0.30 wt. %). Using Pluronic F-127 surfactant, the highest conductivity for nanocomposite films was achieved using a sonication energy of 666 kJ/g. When comparing values of films below and above CMC value the difference is sensational 5.36 S/cm (0.09 wt. %) versus 1.88 S/cm (0.30 wt. %).

For Triton, the highest conductivity value of 3.37 S/cm was achieved with 666 kJ/g sonication energy. It should be noted that almost the same conductivity result (3.02 S/cm) was achieved using just 166 kJ/g of sonication energy.

## 2.2. Effect of Surfactant Removal

Conductivity measurements were also carried out after the removal of the surfactant used in the dispersing phase. Triton X-100 and Pluronic F-127 films were acetone treated and CTAB films were treated with ethanol. It can be clearly seen in Figure 2 that removal of surfactant has a strong effect. Removal of surfactant from films made with CTAB increased the conductivity significantly; the maximum conductivity was 3.02 S/cm for 166 kJ/g sonication energy. However, the films expressed a decrease in conductivity at sonication energy similar to the films with the surfactants present. For Pluronic F-127 films (Figure 2c) made below the CMC limit of the surfactant, the removal of surfactant did not have a significant effect on the conductivity. Even though there was no clear trend, the film with surfactant had somewhat higher conductivity than the one where surfactant was not present. For Pluronic F-127 (0.30 wt. %), the shape of the diagram differed from other previous sets. The films initially exhibited a decrease in conductivity as a function of increasing sonication energy, and the highest values were measured for the samples sonicated at the least energy, but also for the highest amount of sonication energy. For the samples with high conductivity, the removal of the non-ionic surfactant increased the conductivity. The highest value obtained from these measurements was 2.88 S/cm for a sonication energy of 166 kJ/g. A dramatic increase was observed in conductivity values of films manufactured with surfactant Triton X-100 (Figure 2a): the conductivity increases from approximately 3.0 S/cm to a value of 8.42 S/cm when the non-ionic surfactant was removed (sample was sonicated at 666 kJ/g). It should be noted that the films containing the surfactant did not exhibit as strong a sensitivity to increasing sonication energy (as those without surfactant).

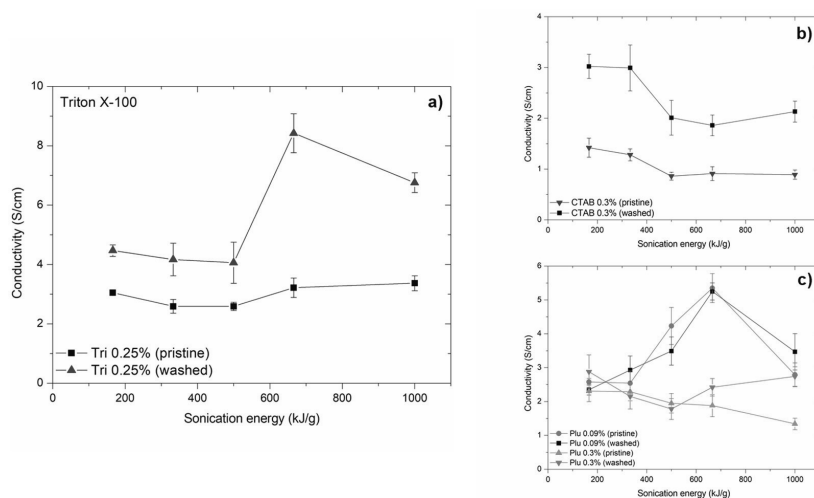


**Figure 2.** Conductivity of nanocomposite films before and after (a) Triton X-100 surfactant removal, (b) CTAB surfactant removal, and (c) Pluronic surfactant removal.

It is well known that surfactants can plasticize the structure of composites and interfere with conductivity properties by situating themselves at the interface between the conductive particles and matrix. This phenomenon was demonstrated when the properties of the nanocomposite films were compared in this study. Firstly, there was a clear increase in the conductivity of the films processed using the Triton X-100 and CTAB surfactants due to the removal of the surfactant. The diagrams (pristine vs. washed) were similar in their trend, and a clear increase in terms of conductivity was observed. When using the surfactant Pluronic F-127 for processing, a clear conclusion could not be made because the conductivity diagrams did not show a corresponding, monotonic trend due to surfactant removal. However, the results showed that, when the surfactant is present in the film structure, the effect of interference by Pluronic F-127 (concentration below CMC) on the electrical conductivity is at its minimum.

### 2.3. Comparison to Previous Results

When comparing our nanocomposite film's conductivity results to previous studies, we found that our results were superior to reported values. In Figure 3 are illustrated electrical conductivity results from studies that have used native NFC and manufactured homogenous nanocomposites from it. For non-ionic surfactants, the highest conductivity value found was 0.022 S/cm at a 10 wt. % CNT loading [17]. In our study, the highest value was 8.42 S/cm after removing Triton X-100 and, likewise, 5.35 S/cm with Pluronic F-127 still present in the film.

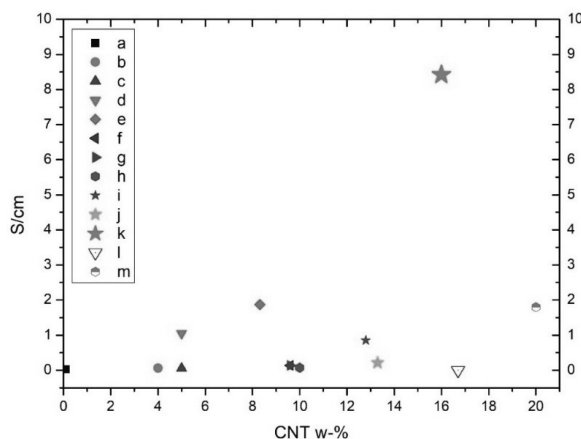


**Figure 3.** Comparison of obtained electrical conductivity of NFC-CNT nanocomposite films from the current literature. Pink star (letter k) refers to our data (Triton X-100), while other letters refer to a [9], b [56], c [57], d [58], e [22], f [9], g [24], h [57], i [59], j [15], l [32] and m [27].

Huang et al. [57] reported the results of a multiphase process which was used to accomplish a conductivity of 0.072 S/cm using MWCNT-doping at 10 wt. % and 0.056 S/cm with 5 wt. % doping with cotton linters and CTAB as a surfactant. CTAB surfactant was also used with bacterial nanocellulose and CNTs, where the conductivity was 0.027 S/cm (MWCNT 0.1 wt. %) [9]. Also, Yoon et al. [24] used bacterial cellulose as a matrix and obtained conductivity of 0.14 S/cm with 9.6 wt. % MWCNT loading. Electrical conductivity of TEMPO-oxidized cellulose films with 16.7 wt. % concentration of MWCNTs was 0.001 S/cm, which is lower than the conductive material limit [32]. For chitosan-cellulose-CNT membranes, Xiao et al. [56] accomplished conductivity of 0.062 S/cm with a 4 wt. % content of MWCNTs. By using comparable materials, but by applying a filtering method, Yamakawa et al. [58] obtained a 1.05 S/cm electrical conductivity with a 5 wt. % MWCNT loading and

Chen et al. 1.8 S/cm with 20 wt. % MWCNT. They were able to increase the conductivity to a value of 5.02 S/cm using a chemical alkali treatment.

In addition, studies about manufacturing conductive cellulose composites via coating cellulosic filter paper with a CNT dispersion have revealed rather good results, but the consistency of the materials is not homogeneous—not exactly an integral composite. Lee et al. [15] achieved conductivity of 1.11 S/cm using 13.3 wt. % MWCNT. Mondal et al. [59] reported conductivity values after using a dipping method, and they reached 0.85 S/cm with a 12.8 wt. % carbon nanofiber (CNF) content. Fugetsu et al. [22] manufactured conductive cellulose-based composites using a traditional paper making process with 8.32 wt. % CNT concentration and, finally, a conductivity of 1.87 S/cm was obtained.

#### 2.4. Characterization of Nanocomposite Structure

The surface and cross-section of the films processed using surfactant Triton X-100 was studied with SEM. Images were taken with Zeiss ULTRAPlus scanning electron microscope (SEM). The effect of sonication as well as the removal of surfactant were studied with the SEM images shown in Figure 4. Two samples were specifically chosen for this inspection: 166 kJ/g and 666 kJ/g sonication energy films containing surfactant (Figure 4a,c) and after removal of surfactant Triton X-100 by washing them in acetone (Figure 4b,d).

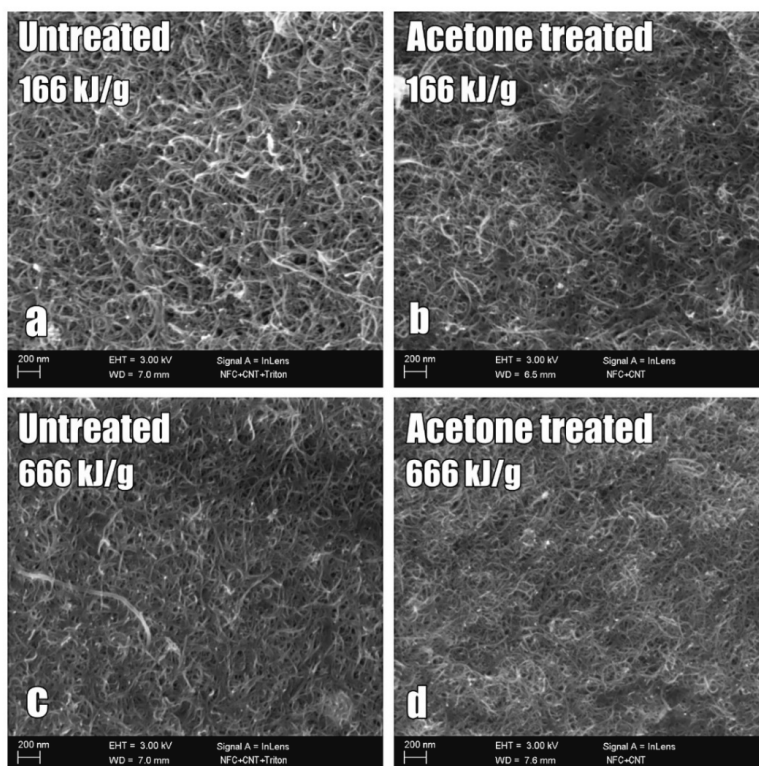


**Figure 4.** SEM imaging of NFC-CNT nanocomposite films surface (166 and 666 kJ/g) containing surfactant (a,c) and after removal of surfactant Triton X-100 by washing them in acetone (b,d).

In the top left (Figure 4a) image, some clusters of CNTs are present in the 166 kJ/g sonication energy sample, but not in the higher sonication energy 666 kJ/g sample. Both films have abundant



amount of CNTs in the surface. Here, the 166 kJ/g film has a more porous structure than the 666 kJ/g film. In addition, the CNTs form a more consistent network in the 666 kJ/g film after washing the surfactant away (Figure 4d).

The SEM images of the sonicated samples in Figure 4 showed that there were clusters present in the 166 kJ/g sonicated film, while the higher sonicated energy sample did not have similar kinds of clusters. This indicates that, for lower sonication energies, non-dispersed particles remain in the films. This is not preferred, since the purpose is to achieve good dispersion of all the particles in the dispersion and in the films manufactured. This is an indication that the sonication process and amount of energy used affect the extent of the dispersion of particles.

The through-thickness structure of the films was also generally studied using polished cross-sections of the films embedded in epoxy. The cross-section in Figure 5 shows the CNT ends (bright contrast spots) and their even distribution in the film (500 kJ/g), (Triton system) through the thickness. A slightly layered structure can be observed and concluded as a result of dispersion flow during the casting.

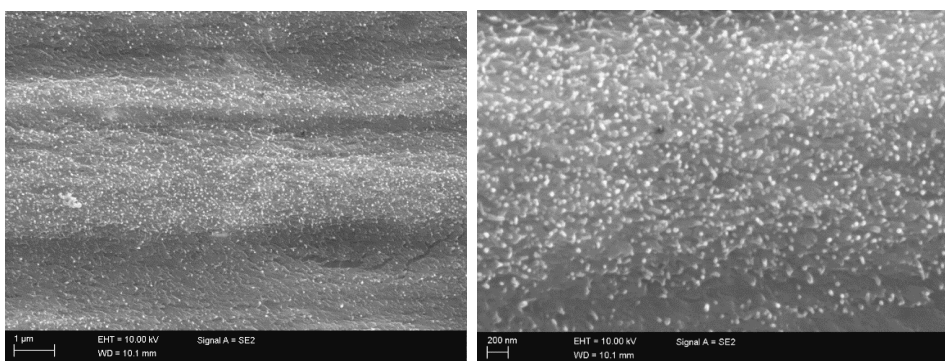


**Figure 5.** SEM imaging of the nanocomposite film (Triton X-100, 500 kJ/g) cross-section when embedded in epoxy: **Left** side: overall structure; **Right** side: magnification in the center of the film.

### 3. Discussion

Ultrasonication is a widely used process to manufacture aqueous CNT dispersions. However, how much it changes the properties of dispersed particles and the medium is often overlooked. It is known that sonication can, for example, generate hydrogen peroxide from water, degrade carbon nanotubes and ultimately destroy them. Therefore, it is important that the sonication process is optimized in terms of time and power. It also needs to be noted that the dispersion process is not linear, but follows an S-curve where temporal development of dispersion quality is related to quantity of un-dispersed solid.

Due to the re-agglomeration tendency of carbon nanotubes, it is necessary to use dispersion agents, i.e., surfactants, in manufacturing aqueous dispersions. If these dispersions are later used in conductive films, it is preferable to remove the surfactant to improve CNT network formation. Although carbon nanotubes are excellent conductors, CNT networks are not. This is due their high intertubular contact resistance. The contact points act essentially as a tunneling junction for electrons that is very sensitive to distance. The efficacy of surfactants is based on acting as a spacer between tubes, so any additional distance in a conductive network is detrimental to the conductivity itself.

### 4. Materials and Methods

Three-component systems containing nanocellulose, carbon nanotubes and surfactants are used in the strong, ecologically conscious nanocomposite films of this study. The CNTs add functionality

to the nanocellulose matrix and the surfactant enables percolation network to build and maximize conductivity properties.

In this study, the nanocellulose (NFC) production was based on mechanical disintegration of bleached hardwood kraft pulp (BHKP). First, dried commercial BHKP produced from birch was soaked in water at approximately 1.7 wt. % concentration and dispersed using a high-shear Ystral dissolver for 10 min at 700 rpm. The chemical pulp suspension was predefined in a Masuko grinder (Supermasscolloider MKZA10-15J, Masuko Sangyo Co., Tokyo, Japan) at 1500 rpm and fluidized with six passes through a Microfluidizer (Microfluidics M-7115-30, Microfluidics Corp., Newton, MA, USA) using 1800 MPa pressure. The final material appearance of NCF was a viscous and translucent gel.

Multiwall carbon nanotubes (MWCNT, Nanocyl 7000, Nanocyl SA., Sambreville, Belgium) were purchased from Nanocyl Inc. and the product was used in the state it was in when received. This type of nanotubes is produced via catalytic chemical vapor deposition (CCVD). Concentration of CNTs was kept constant at 16 wt. % in the nanocomposite films, so the effects of sonication energy and surfactant type to the conductivity properties are more visible.

Three surfactants were chosen based on their ionic nature and standard: non-ionic Triton X-100 and Pluronic F-127, and anionic cetyl triammonium bromide (CTAB). Surfactants were purchased from Sigma-Aldrich (Merck KGaA, Darmstadt, Germany). The surfactants were diluted in deionized water to form solutions with varying dissolutions (1, 2.5, 10 wt. %).

#### Preparation of NFC-CNT Aqueous Dispersion

The NFC and CNT were sonicated simultaneously and after sonication no centrifuge was used so that the preparation of aqueous dispersions could be achieved using a minimum amount of processing phases. NFC-CNT aqueous dispersions with a total volume of 80 mL were prepared. One set contained NFC (0.25 wt. %), CNTs (0.05 wt. %), deionized water and one of the selected surfactants (Triton X-100, 0.25 wt. %, Pluronic F-127, 0.09 wt. % and 0.3 wt. % and CTAB 0.30 wt. %). Details about preparation produce are showed as Figure 6.

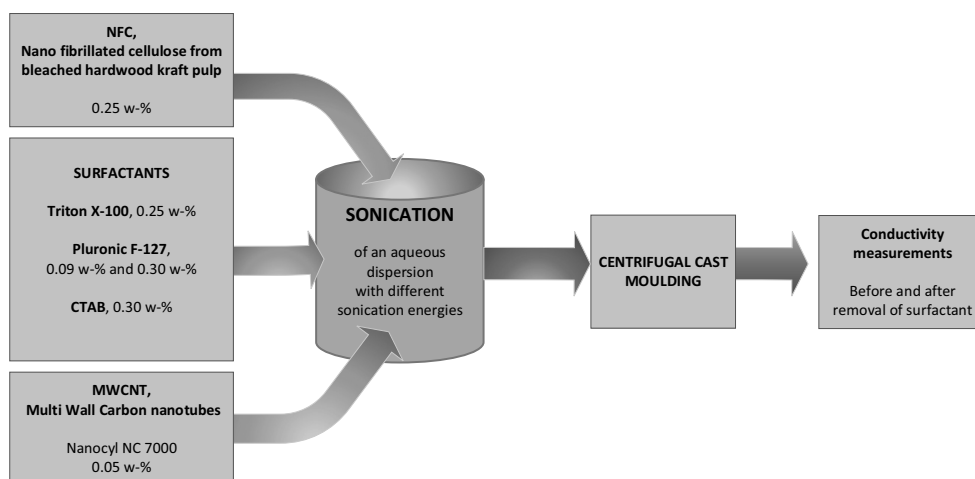


**Figure 6.** Preparation procedure of NFC-CNT dispersion and nanocomposite films.

The total dry mass for all the dispersions was 0.24 g. The sonication of the dispersion samples was performed with a tip horn ( $\varnothing$  12.7 mm) sonicator Q700 (QSonica LLC., Newton, CT, USA) in 100 mL glass beakers. The sonication amplitude of vibration (50%) was kept constant. The power output remained between 60 and 70 W for every sonication. The system included a water bath to keep

samples cool during the sonication so that temperature would not rise above 30 °C. The water bath was cooled by circulating cooling glycerol through a chiller (PerkinElmer C6 Chiller, PerkinElmer Inc., Waltham, MA, USA). Samples were sonicated for four different amounts of energies per dry mass, respectively 166, 333, 500 and 666 kJ/g, which corresponded to energies of 40, 80, 120 and 160 kJ. Unsonicated samples manufactured using all three surfactants were not homogenous, and this is why film formation was unsuccessful and not analyzed.

## 5. Conclusions

The typical approach to the manufacturing of conductive cellulose-CNT films has been to increase CNT weight percentage without optimizing the dispersion procedure. In this study, NFC and multiwall carbon nanotubes (MWCNT) were used to prepare composite films using a minimum number of processing phases (e.g., no centrifugal dispersion or pressing of the film were used), materials and chemicals. The amount of CNTs was 0.05 wt. % in dispersion and 16 wt. % in the film after the evaporation of water in ratio to dry mass content of NFC and CNT. The effect of surfactant type (Triton X-100, Pluronic F-127 and CTAB) and sonication energy on the electrical conductivity of NFC-CNT nanocomposite films was investigated to identify optimal processing conditions for high conductivity of the nanocomposite. A conductivity of 5.36 S/cm was achieved by using Pluronic F-127 surfactant and 666 kJ/g of sonication energy. In addition, removal of the surfactant from film and its effect on the electrical conductivity was studied. A dramatic increase in conductivity values from approximately 3.0 S/cm to a value of 8.42 S/cm was observed for films manufactured with surfactant Triton X-100. Conductivity diagrams of the nanocomposite films show that sonication affects the electrical performance of the films. SEM images of sonicated samples showed that the films sonicated at 166 kJ/g have a more porous structure than the films sonicated at higher energy. The imaging also showed that the CNTs form a more consistent network with a combination of high sonication energy and surfactant removal. It can be concluded that the following parameters significantly affect the conductivity of NFC-CNT nanocomposite films:

- (a) Surfactant type
- (b) Surfactant concentration
- (c) Sonication energy
- (d) Removal of the used surfactant
- (e) Film processing technique

To summarize, we manufactured nanocomposite films with exemplary conductivity in comparison to reported research and this was achieved by optimizing processing parameters and materials. Further research on the surfactant types and concentration can lead to better dispersion of the CNTs and therefore even higher conductivity.

**Author Contributions:** S.S. and P.K. conceived and designed the experiments; S.S. and A.R. performed the experiments and analyzed the data; V.K. and A.H. contributed materials; S.S., A.R., P.K., S.T. and K.R.R. wrote the paper. M.K. and J.V. coordinated the project aims in accordance to publication specific actions and delegation.

**Funding:** This research received no external funding.

**Acknowledgments:** This work was funded by Tekes (Finnish Funding Agency for Innovation) through a strategic opening entitled Design Driven Value Chains in the World of Cellulose (DWoC 2.0). We acknowledge the contributions of Jarmo Laakso and Essi Sarlin for SEM imaging.

**Conflicts of Interest:** The authors declare no conflict of interest.

## References

1. Huang, J.C. Carbon black filled conducting polymers and polymer blends. *Adv. Polym. Technol.* **2002**, *21*, 299–313. [CrossRef]
2. Ma, P.C.; Siddiqui, N.A.; Marom, G.; Kim, J.K. Dispersion and functionalization of carbon nanotubes for polymer-based nanocomposites: A review. *Compos. Part A Appl. Sci. Manuf.* **2010**, *41*, 1345–1367. [CrossRef]

3. Pereira, C.; Nóvoa, P.J.R.O.; Calard, V.; Forero, S.; Hepp, F.; Pambaguian, L. Characterization of Carbon Nanotube Papers Infused with Cyanate-Ester Resin. In Proceedings of the ICCM International Conference on Composite Materials, Edinburgh, UK, 27–31 July 2009.
4. Layek, R.K.; Das, A.K.; Park, M.J.; Kim, N.H.; Lee, J.H. Enhancement of physical, mechanical, and gas barrier properties in noncovalently functionalized graphene oxide/poly(vinylidene fluoride) composites. *Carbon N. Y.* **2015**, *81*, 329–338. [CrossRef]
5. Palola, S.; Sarlin, E.; Kolahgar Azari, S.; Koutsos, V.; Vuorinen, J. Microwave induced hierarchical nanostructures on aramid fibers and their influence on adhesion properties in a rubber matrix. *Appl. Surf. Sci.* **2017**, *410*, 145–153. [CrossRef]
6. Hamedi, M.M.; Hajian, A.; Fall, A.B.; Hkansson, K.; Salajkova, M.; Lundell, F.; Wgberg, L.; Berglund, L.A. Highly conducting, strong nanocomposites based on nanocellulose-assisted aqueous dispersions of single-wall carbon nanotubes. *ACS Nano* **2014**, *8*, 2467–2476. [CrossRef] [PubMed]
7. Tuukkanen, S.; Streiff, S.; Chenevier, P.; Pinault, M.; Jeong, H.J.; Enouz-Vedrenne, S.; Cojocar, C.S.; Pribat, D.; Bourgoin, J.P. Toward full carbon interconnects: High conductivity of individual carbon nanotube to carbon nanotube regrowth junctions. *Appl. Phys. Lett.* **2009**, *95*, 113108. [CrossRef]
8. Haghi, A.K.; Thomas, S. *Carbon Nanotubes: Theoretical Concepts and Research Strategies for Engineers*; Apple Academic Press: Waretown, NJ, USA, 2015.
9. Jung, R.; Kim, H.-S.; Kim, Y.; Kwon, S.-M.; Lee, H.S.; Jin, H.-J. Electrically Conductive Transparent Papers Using Multiwalled Carbon Nanotubes. *J. Polym. Sci. Part B Polym. Phys.* **2008**, *46*, 1235–1242. [CrossRef]
10. Haghi, A.K.; Zaikov, G.E. *Advanced Nanotube and Nanofiber Materials*; Nova Science Publishers, Inc.: New York, NY, USA, 2012; ISBN 978-1-62-081201-3.
11. Hoeng, F.; Denneulin, A.; Bras, J. Use of nanocellulose in printed electronics: A review. *Nanoscale* **2016**, *8*, 13131–13154. [CrossRef] [PubMed]
12. Gardner, D.J.; Oporto, G.S.; Mills, R.; Samir, M.A.S.A. Adhesion and surface issues in cellulose and nanocellulose. *J. Adhes. Sci. Technol.* **2008**, *22*, 545–567. [CrossRef]
13. Kuzmenko, V.; Naboka, O.; Haque, M.; Staaf, H.; Göransson, G.; Gatenholm, P.; Enoksson, P. Sustainable carbon nanofibers/nanotubes composites from cellulose as electrodes for supercapacitors. *Energy* **2015**, *90*, 1490–1496. [CrossRef]
14. Lehtimäki, S.; Tuukkanen, S.; Pörhönen, J.; Moilanen, P.; Virtanen, J.; Honkanen, M.; Lupo, D. Low-cost, solution processable carbon nanotube supercapacitors and their characterization. *Appl. Phys. A Mater. Sci. Process.* **2014**, *117*, 1329–1334. [CrossRef]
15. Lee, T.W.; Lee, S.E.; Jeong, Y.G. Carbon nanotube/cellulose papers with high performance in electric heating and electromagnetic interference shielding. *Compos. Sci. Technol.* **2016**, *131*, 77–87. [CrossRef]
16. Yun, S.; Kim, J. Multi-walled carbon nanotubes-cellulose paper for a chemical vapor sensor. *Sens. Actuators B Chem.* **2010**, *150*, 308–313. [CrossRef]
17. Qi, H.; Liu, J.; Pionteck, J.; Pötschke, P.; Mäder, E. Carbon nanotube-cellulose composite aerogels for vapour sensing. *Sens. Actuators B Chem.* **2015**, *213*, 20–26. [CrossRef]
18. Qi, H.; Mäder, E.; Liu, J. Unique water sensors based on carbon nanotube-cellulose composites. *Sens. Actuators B Chem.* **2013**, *185*, 225–230. [CrossRef]
19. Wang, M.; Anoshkin, I.V.; Nasibulin, A.G.; Korhonen, J.T.; Seitsonen, J.; Pere, J.; Kauppinen, E.I.; Ras, R.H.A.; Ikkala, O. Modifying native nanocellulose aerogels with carbon nanotubes for mechanoresponsive conductivity and pressure sensing. *Adv. Mater.* **2013**, *25*, 2428–2432. [CrossRef] [PubMed]
20. Oya, T.; Ogino, T. Production of electrically conductive paper by adding carbon nanotubes. *Carbon N. Y.* **2008**, *46*, 169–171. [CrossRef]
21. Hu, L.; Choi, J.W.; Yang, Y.; Jeong, S.; La Mantia, F.; Cui, L.-F.; Cui, Y. Highly conductive paper for energy-storage devices. *Proc. Natl. Acad. Sci. USA* **2009**, *106*, 21490–21494. [CrossRef] [PubMed]
22. Fugetsu, B.; Sano, E.; Sunada, M.; Sambongi, Y.; Shibuya, T.; Wang, X.; Hiraki, T. Electrical conductivity and electromagnetic interference shielding efficiency of carbon nanotube/cellulose composite paper. *Carbon N. Y.* **2008**, *46*, 1256–1258. [CrossRef]
23. Imai, M.; Akiyama, K.; Tanaka, T.; Sano, E. Highly strong and conductive carbon nanotube/cellulose composite paper. *Compos. Sci. Technol.* **2010**, *70*, 1564–1570. [CrossRef]
24. Yoon, S.H.; Jin, H.J.; Kook, M.C.; Pyun, Y.R. Electrically conductive bacterial cellulose by incorporation of carbon nanotubes. *Biomacromolecules* **2006**, *7*, 1280–1284. [CrossRef] [PubMed]

25. Toomadaj, F.; Farjana, S.; Sanz-Velasco, A.; Naboka, O.; Lundgren, P.; Rodriguez, K.; Toriz, G.; Gatenholm, P.; Enoxfsson, P. Strain sensitivity of carbon nanotubes modified cellulose. *Procedia Eng.* **2011**, *25*, 1353–1356. [CrossRef]
26. Liu, Y.; Liu, D.; Ma, Y.; Sui, G. Characterization and properties of transparent cellulose nanowhiskers-based graphene nanoplatelets/multi-walled carbon nanotubes films. *Compos. Part A Appl. Sci. Manuf.* **2016**, *86*, 77–86. [CrossRef]
27. Chen, C.; Mo, M.; Chen, W.; Pan, M.; Xu, Z.; Wang, H.; Li, D. Highly conductive nanocomposites based on cellulose nanofiber networks via NaOH treatments. *Compos. Sci. Technol.* **2018**, *156*, 103–108. [CrossRef]
28. Hilding, J.; Grulke, E.; George Zhang, Z.; Lockwood, F. Dispersion of Carbon Nanotubes in Liquids. *J. Dispers. Sci. Technol.* **2003**, *24*, 1–41. [CrossRef]
29. Vaisman, L.; Wagner, H.D.; Marom, G. The role of surfactants in dispersion of carbon nanotubes. *Adv. Colloid Interface Sci.* **2006**, *128–130*, 37–46. [CrossRef] [PubMed]
30. Rastogi, R.; Kaushal, R.; Tripathi, S.K.; Sharma, A.L.; Kaur, I.; Bharadwaj, L.M. Comparative study of carbon nanotube dispersion using surfactants. *J. Colloid Interface Sci.* **2008**, *328*, 421–428. [CrossRef] [PubMed]
31. Bai, J.B.; Allaoui, A. Effect of the length and the aggregate size of MWNTs on the improvement efficiency of the mechanical and electrical properties of nanocomposites—Experimental investigation. *Compos. Part A Appl. Sci. Manuf.* **2003**, *34*, 689–694. [CrossRef]
32. Salajkova, M.; Valentini, L.; Zhou, Q.; Berglund, L.A. Tough nanopaper structures based on cellulose nanofibers and carbon nanotubes. *Compos. Sci. Technol.* **2013**, *87*, 103–110. [CrossRef]
33. Huang, Y.Y.; Terentjev, E.M. Dispersion and rheology of carbon nanotubes in polymers. *Int. J. Mater. Form.* **2008**, *1*, 63–74. [CrossRef]
34. Gimåker, M.; Östlund, M.; Östlund, S.; Wågberg, L. Influence of beating and chemical additives on residual stresses in paper. *Nord. Pulp Pap. Res. J.* **2011**, *26*, 445–451. [CrossRef]
35. Baez, C.; Considine, J.; Rowlands, R. Influence of drying restraint on physical and mechanical properties of nanofibrillated cellulose films. *Cellulose* **2014**, *21*, 347–356. [CrossRef]
36. Rosen, M.J. *Surfactants and Interfacial Phenomena*; John Wiley & Sons, Inc.: Hoboken, NJ, USA, 2004; ISBN 978-0-47-147818-8.
37. Keinänen, P.; Siljander, S.; Koivula, M.; Sethi, J.; Vuorinen, J.; Kanerva, M. Optimized dispersion quality of aqueous carbon nanotube colloids as a function of sonochemical yield and surfactant/CNT ratio. *Heliyon* **2018**, in press.
38. Blanch, A.J.; Lenehan, C.E.; Quinton, J.S. Optimizing Surfactant Concentrations for Dispersion of Single-Walled Carbon Nanotubes in Aqueous Solution. *J. Phys. Chem. B* **2010**, *114*, 9805–9811. [CrossRef] [PubMed]
39. Yu, J.; Grossiord, N.; Koning, C.E.; Loos, J. Controlling the dispersion of multi-wall carbon nanotubes in aqueous surfactant solution. *Carbon N. Y.* **2007**, *45*, 618–623. [CrossRef]
40. Islam, M.F.; Rojas, E.; Bergey, D.M.; Johnson, A.T.; Yodh, A.G. High weight fraction surfactant solubilization of single-wall carbon nanotubes in water. *Nano Lett.* **2003**, *3*, 269–273. [CrossRef]
41. Utsumi, S.; Kanamaru, M.; Honda, H.; Kanoh, H.; Tanaka, H.; Ohkubo, T.; Sakai, H.; Abe, M.; Kaneko, K. RBM band shift-evidenced dispersion mechanism of single-wall carbon nanotube bundles with NaDDBS. *J. Colloid Interface Sci.* **2007**, *308*, 276–284. [CrossRef] [PubMed]
42. Sun, Z.; Nicolosi, V.; Rickard, D.; Bergin, S.D.; Aherne, D.; Coleman, J.N. Quantitative Evaluation of Surfactant-stabilized Single-walled Carbon Nanotubes: Dispersion Quality and Its Correlation with Zeta Potential. *J. Phys. Chem. C* **2008**, *112*, 10692–10699. [CrossRef]
43. Maillaud, L.; Zakri, C.; Ly, I.; Pénicaud, A.; Poulin, P. Conductivity of transparent electrodes made from interacting nanotubes. *Appl. Phys. Lett.* **2013**, *103*, 263106. [CrossRef]
44. Bai, Y.; Lin, D.; Wu, F.; Wang, Z.; Xing, B. Adsorption of Triton X-series surfactants and its role in stabilizing multi-walled carbon nanotube suspensions. *Chemosphere* **2010**, *79*, 362–367. [CrossRef] [PubMed]
45. Calvaresi, M.; Dallavalle, M.; Zerbetto, F. Wrapping nanotubes with micelles, Hemimicelles, and cylindrical micelles. *Small* **2009**, *5*, 2191–2198. [CrossRef] [PubMed]
46. Geng, Y.; Liu, M.Y.; Li, J.; Shi, X.M.; Kim, J.K. Effects of surfactant treatment on mechanical and electrical properties of CNT/epoxy nanocomposites. *Compos. Part A Appl. Sci. Manuf.* **2008**, *39*, 1876–1883. [CrossRef]

47. Bystrzejewski, M.; Huczko, A.; Lange, H.; Gemming, T.; Büchner, B.; Rummeli, M.H. Dispersion and diameter separation of multi-wall carbon nanotubes in aqueous solutions. *J. Colloid Interface Sci.* **2010**, *345*, 138–142. [CrossRef] [PubMed]
48. Angelikopoulos, P.; Gromov, A.; Leen, A.; Nerushev, O.; Bock, H.; Campbell, E.E.B. Below the CMC. *J. Phys. Chem. C* **2010**, *114*, 2–9. [CrossRef]
49. Bonard, J.; Stora, T.; Salvetat, J.; Maier, F.; Stockli, T.; Duschl, C.; De Heer, W.A.; Forró, L.; Châtelain, A. Purification and Size-Selection of Carbon Nanotubes. *Adv. Mater.* **1997**, *9*, 827–831. [CrossRef]
50. Lu, P.; Hsieh, Y. Lo Multiwalled carbon nanotube (MWCNT) reinforced cellulose fibers by electrospinning. *ACS Appl. Mater. Interfaces* **2010**, *2*, 2413–2420. [CrossRef] [PubMed]
51. Rossell, M.D.; Kuebel, C.; Ilari, G.; Rechberger, F.; Heiligtag, F.J.; Niederberger, M.; Koziej, D.; Erni, R. Impact of sonication pretreatment on carbon nanotubes: A transmission electron microscopy study. *Carbon N. Y.* **2013**, *61*, 404–411. [CrossRef]
52. Yang, D.; Rochette, J.-F.; Sacher, E. Functionalization of Multiwalled Carbon Nanotubes by Mild Aqueous Sonication. *J. Phys. Chem. B* **2005**, *109*, 7788–7794. [CrossRef] [PubMed]
53. Dassios, K.G.; Alafogianni, P.; Antiohos, S.K.; Leptokaridis, C.; Barkoula, N.M.; Matikas, T.E. Optimization of sonication parameters for homogeneous surfactant assisted dispersion of multiwalled carbon nanotubes in aqueous solutions. *J. Phys. Chem. C* **2015**, *119*, 7506–7516. [CrossRef]
54. Fuge, R.; Liebscher, M.; Schröfl, C.; Oswald, S.; Leonhardt, A.; Büchner, B.; Mechtcherine, V. Fragmentation characteristics of undoped and nitrogen-doped multiwalled carbon nanotubes in aqueous dispersion in dependence on the ultrasonication parameters. *Diam. Relat. Mater.* **2016**, *66*, 126–134. [CrossRef]
55. Rajala, S.; Tuukkanen, S.; Halttunen, J. Characteristics of piezoelectric polymer film sensors with solution-processable graphene-based electrode materials. *IEEE Sens. J.* **2015**, *15*, 3102–3109. [CrossRef]
56. Xiao, W.; Wu, T.; Peng, J.; Bai, Y.; Li, J.; Lai, G.; Wu, Y.; Dai, L. Preparation, structure, and properties of chitosan/cellulose/multiwalled carbon nanotube composite membranes and fibers. *J. Appl. Polym. Sci.* **2013**, *128*, 1193–1199. [CrossRef]
57. Huang, H.D.; Liu, C.Y.; Zhang, L.Q.; Zhong, G.J.; Li, Z.M. Simultaneous reinforcement and toughening of carbon nanotube/cellulose conductive nanocomposite films by interfacial hydrogen bonding. *ACS Sustain. Chem. Eng.* **2015**, *3*, 317–324. [CrossRef]
58. Yamakawa, A.; Suzuki, S.; Oku, T.; Enomoto, K.; Ikeda, M.; Rodrigue, J.; Tateiwa, K.; Terada, Y.; Yano, H.; Kitamura, S. Nanostructure and physical properties of cellulose nanofiber-carbon nanotube composite films. *Carbohydr. Polym.* **2017**, *171*, 129–135. [CrossRef] [PubMed]
59. Mondal, S.; Ganguly, S.; Das, P.; Bhawal, P.; Das, T.K.; Nayak, L.; Khastgir, D.; Das, N.C. High-performance carbon nanofiber coated cellulose filter paper for electromagnetic interference shielding. *Cellulose* **2017**, *24*, 5117–5131. [CrossRef]



# PUBLICATION III

## **Self-assembled cellulose nanofiber-carbon nanotube nanocomposite films with anisotropic conductivity**

Skogberg, A., Siljander, S., Mäki, A-J., Honkanen, M., Efimov, A.,  
Hannula, M., Lahtinen, P., Tuukkanen, S., Björkqvist, T. & Kallio, P.

Nanoscale, vol. 14, 2 (2022), 448-463

**10.1039/d1nr06937c**  
**<https://urn.fi/URN:NBN:fi:tuni-202201311717>**

**Publication reprinted with the permission of the copyright holders.**






 Cite this: *Nanoscale*, 2022, 14, 448

# Self-assembled cellulose nanofiber–carbon nanotube nanocomposite films with anisotropic conductivity†

 Anne Skogberg,<sup>‡</sup> Sanna Siljander,<sup>‡</sup> Antti-Juhana Mäki,<sup>‡</sup> Mari Honkanen,<sup>c</sup> Alexander Efimov,<sup>‡</sup> Markus Hannula,<sup>a</sup> Panu Lahtinen,<sup>e</sup> Sampu Tuukkanen,<sup>a</sup> Tomas Björkqvist<sup>‡</sup> and Pasi Kallio<sup>‡</sup>

In this study, a nanocellulose-based material showing anisotropic conductivity is introduced. The material has up to 1000 times higher conductivity along the dry-line boundary direction than along the radial direction. In addition to the material itself, the method to produce the material is novel and is based on the alignment of cationic cellulose nanofibers (c-CNFs) along the dry-line boundary of an evaporating droplet composed of c-CNFs in two forms and conductive multi-walled carbon nanotubes (MWCNTs). On the one hand, c-CNFs are used as a dispersant of MWCNTs, and on the other hand they are used as an additional suspension element to create the desired anisotropy. When the suspended c-CNF is left out, and the nanocomposite film is manufactured using the high energy sonicated c-CNF/MWCNT dispersion only, conductive anisotropy is not present but evenly conducting nanocomposite films are obtained. Therefore, we suggest that suspending additional c-CNFs in the c-CNF/MWCNT dispersion results in nanocomposite films with anisotropic conductivity. This is a new way to obtain nanocomposite films with substantial anisotropic conductivity.

 Received 20th October 2021,  
Accepted 28th November 2021

DOI: 10.1039/d1nr06937c

[rsc.li/nanoscale](https://rsc.li/nanoscale)

## Introduction

There is an increasing demand for thinner, cheaper, lighter, and more eco-friendly electrically conductive films and composites<sup>1</sup> with anisotropic properties<sup>2,3</sup> for applications including optics, sensors, actuators, aerogels, mechanical reinforcement of advanced materials, and growth guiding substrates including hydrogels for biomedical applications.<sup>2,3</sup> There are various motivations for material alignment in these applications, such as a need for anisotropic properties in adjusting the stiffness and strength of structural materials; optimizing the reinforcement efficiency in fiber-reinforced composites; and mimicking

the topography and architecture of native tissues in biomedical materials and applications, especially related to cell alignment *in vitro*.<sup>2</sup> The assembled oriented particles with a high aspect ratio generally exhibit anisotropic physical properties. If the particle is also conductive, an anisotropic conductivity may result, which is potentially useful in electronic components, capacitors, sensors, electromechanical actuators, *etc.* In the assembled structures of high aspect ratio nanomaterials, the differences in the electric current parallel and perpendicular to the orientation results in conductivity anisotropy.<sup>4</sup>

Cellulose nanofibers (CNFs) are an excellent candidate as a primary ingredient in such composites since they provide an eco-friendly and low-cost material alternative<sup>1</sup> with the potential to align and offer anisotropic properties for the resulting composite material.<sup>2</sup> CNF-based electrically conducting materials have been produced by coating, blending or doping CNFs with conductive nanoparticles such as carbon nanotubes (CNTs). CNFs act as a matrix and dispersant of the conductive CNT component.<sup>5–7</sup> These nanomaterials together provide a combination of their superior properties such as the film forming potential,<sup>8</sup> favourable mechanical and chemical properties, colloidal stability, cytocompatibility<sup>9–15</sup> and biocompatibility of CNFs,<sup>9–11</sup> and high mechanical strength, stiffness, and electrical and thermal conductivity of CNTs.<sup>16</sup>

Chemically added charged groups influence the physico-chemical properties of CNFs<sup>17</sup> and can improve their processa-

<sup>a</sup>BioMediTech Institute and Faculty of Medicine and Health Technology (MET), Tampere University, Korkeakoulunkatu 3, 33720 Tampere, Finland.

E-mail: anne.skogberg@tuni.fi

<sup>b</sup>Automation Technology and Mechanical Engineering, Faculty of Engineering and Natural Sciences, Tampere University, Korkeakoulunkatu 6, 33720 Tampere, Finland. E-mail: sanna.siljander@tuni.fi

<sup>c</sup>Tampere Microscopy Center, Tampere University, Korkeakoulunkatu 3, 33720 Tampere, Finland

<sup>d</sup>Chemistry, Faculty of Engineering and Natural Sciences, Tampere University, Korkeakoulunkatu 8, 33720 Tampere, Finland

<sup>e</sup>VTT Technical Research Center of Finland, Tietotie 4E, 02150 Espoo, Finland

† Electronic supplementary information (ESI) available: Additional experimental details and results. See DOI: 10.1039/d1nr06937c

‡ These authors contributed equally.

bility and performance.<sup>18</sup> Treatment with cations can be performed to render cellulose nanofibers cationic by introducing positive charges on their backbone. Cationic CNFs (c-CNFs) can be used in both high-end applications as nanocomposites and high volume applications,<sup>19</sup> and are gaining increasing attention as a potential novel nanomaterial with tailored properties in more specialized applications.<sup>20,21</sup> Cationic CNFs have the capability to align along the evaporating droplet boundary line by self-assembly mechanisms.<sup>22</sup> By dispersing carbon nanotubes with c-CNF, there is potential to form aligned structures also in electrically conductive composites. None of the previous studies have used c-CNFs in the dispersion of CNTs. In the current study, the use of cationic CNFs as a dispersing and stabilization agent is reported for the first time and their alignment is studied in nanocomposite films.

Superior CNF properties are often challenging to transfer into optimal macroscale performance. In plants, CNFs are naturally aligned into highly hierarchical structures. However, despite several attempts and extensive research, the realignment of disintegrated and fibrillated CNFs remains challenging.<sup>2</sup> While the alignment of CNFs alone is challenging as such, it is extremely challenging to align CNFs in composites.<sup>2</sup> Another challenge is dispersing CNTs because of their self-aggregation tendency especially in aqueous media,<sup>23</sup> which on the other hand is often a prerequisite for hydrophilic CNFs.<sup>24</sup> While CNT blending in aqueous media is poor due to strong self-aggregation, sonication treatments have been introduced to obtain homogeneous dispersions.<sup>6,25</sup>

Several research groups have reported the ability of CNFs to disperse CNTs in aqueous media using sonication and act as a stabilization agent in the CNF–CNT dispersion; furthermore, a stable dispersion can be obtained without the use of surfactants, which have been commonly used.<sup>7,26–28</sup> Chemical modifications of at least one of the nanomaterial components by the introduction of charged groups may enhance the dispersing effect. In addition, repulsive forces may prevent the re-agglomeration of the particles in the dispersion state resulting in a more stable dispersion.<sup>1</sup> It has been shown, *e.g.*, that anionic CNFs enhance the dispersion of CNTs.<sup>29</sup>

Sonication is one of the methods used for attaining the dispersion of nanoparticles in aqueous media. It is based on inertial cavitation where imploding cavities, which are known to exist at the boundaries of materials, generate intensive streams of molecules.<sup>30</sup> In sonication, a high energy density is introduced to the CNT–CNT interface, which is high enough to cause initial separation of the nanotubes by breaking non-covalent forces between tubes. However, the used amount of energy should be optimized such that only non-covalent forces are overcome and the carbon nanotube backbone remains intact. An overly high sonication energy can cause carbon bond breakage inside individual nanotubes, which deteriorates their ballistically conducting nature. The dispersion quality and functionalization obtained in sonication depend on the used sonication energy, medium, surfactant type, and surfactant amount.<sup>6,25,31</sup>

In this study, we present a method to produce self-assembled nanocomposite films with adjustable anisotropic thermal and electrical conductivity. The method uses sonochemical treatment and c-CNFs to disperse multiwall carbon nanotubes (MWCNTs). The resulting dispersion is assembled with the help of additional, suspended c-CNFs, which are based on the previously reported c-CNF alignment along an evaporating boundary line.<sup>22</sup> We also show how the alteration of the composition and pre-treatment of the two nanomaterials enable the fabrication of nanocomposite films with either isotropic or anisotropic properties. Controlled nanomaterial assembly commonly requires more time, high energy consumption, and expensive proprietary technology.<sup>32</sup> The method described in this article is simple, quick, efficient, and safe compared to current attempts to control the assembly of nanomaterials. Such novel nanocomposites could be used as a cell guidance material with cells that benefit from the mechanical improvements offered by MWCNTs or in applications in which anisotropic heat or current conductivity is essential. CNF-based electrically conductive composites have many advantages although many challenges remain, *e.g.* related to electrical connectivity. In our previous study, we have also shown that MWCNTs can be effectively dispersed with unmodified CNFs with the help of surfactants and form highly conductive nanocomposite films with a relatively low MWCNT concentration.<sup>6</sup> In the present article, we combine the advantages of these observed phenomena to create a totally new methodological concept: c-CNFs are used as an aid to disperse MWCNTs homogeneously to form a stable dispersion, and additional c-CNFs in the dispersion undergo interfacial self-assembly with the high energy sonicated (hes-) hes-c-CNF/MWCNT dispersion, resulting in a novel nanocomposite film with anisotropic properties.

## Results and discussion

### Theoretical assumption and modelling

In our previous study, we showed c-CNF alignment along an evaporating boundary line. In the present study, we studied if a conducting component (MWCNT) can be added, and still obtain anisotropic film properties. We also have studied dispersing MWCNTs using CNFs and sonication, and thus hypothesize that CNFs used as a dispersant form a stronger complex with MWCNTs, compared to CNFs that are added to the system by more gentle manual mixing. Based on our previous findings, we hypothesize as shown in Fig. 1, that an isotropic conductive film is obtained when water from the hes-c-CNF/MWCNT dispersion is evaporated and an anisotropic film is obtained when water is evaporated from a suspension composed of the hes-c-CNF/MWCNT dispersion and additional c-CNFs. Fig. 1 conceptually depicts the *hypothesis* for explaining the structural composition and the electrical conductivity of the films fabricated from a dispersion (control) or with suspended free c-CNFs. Sonochemical treatment of c-CNFs and MWCNTs is hypothesized to result in a stable dispersion.

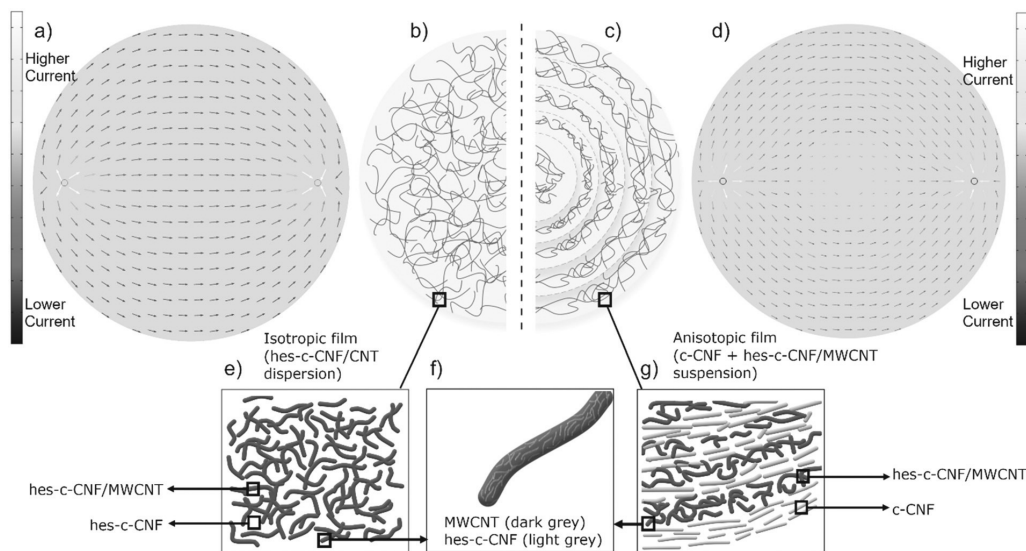


**Fig. 1** Conceptual images of the hypothesized structure of nanocomposite films (b, c, e, f, and g). Left side (b and e) represents the control film manufactured using the hes-c-CNF/MWCNT dispersion. Right side of (c and g) represents the assembled nanocomposite film manufactured using the c-CNF + hes-c-CNF/MWCNT suspension. The schematic represents simulations of electrical properties of an isotropic control (a) and anisotropic self-assembled (d) nanocomposite films using finite element method (FEM). Alignment direction of free assembling c-CNFs is shown in g. Light grey represents c-CNFs, while dark grey is MWCNTs. In the control film (e) dark grey MWCNTs are surrounded by the c-CNF matrix (white surroundings). During dispersion preparation, *i.e.* sonication, c-CNFs are fibrillated and degraded in length such that they cover the MWCNT surface (f). The added c-CNFs during suspension preparation are larger in size compared to hes-c-CNF. The repeating, alternating structure in (g) is an oversimplification. The illustrations are oversimplified and not in scale and do not try to show the actual sizes or actual structure of the assembled film but give an overview of the hypothesized repeating structure at the nanoscale, and show the difference between control and assembled films.

Nanocomposite films formed from this hes-c-CNF/MWCNT dispersion (control samples) are uniformly conducting in all directions (that is, isotropic films), as illustrated by the left-side schematic in Fig. 1(a and b). When free c-CNFs are added to the stable dispersion, a self-assembled structure is formed during evaporation, providing anisotropic electrical properties (that is, assembled films), as depicted in the right-hand-side schematic in Fig. 1(b and c). Fig. 1 shows simulations of electrical properties of isotropic control (a) and anisotropic assembled (d) nanocomposite films using the finite element method (FEM) using COMSOL Multiphysics® Version 5.4 (COMSOL, Inc. USA). Fig. 1e and g show a hypothesized structure at the nanoscale, highlighting the aligning component, which is suspended c-CNFs (Fig. 1g) in the assembled films, while the repeating, alternating structure in Fig. 1g is an oversimplification. The structure is believed to alter at the nanoscale, and the boundaries between aligning c-CNFs and more entangled hes-c-CNF/MWCNTs are not as clear as shown in Fig. 1g. We assume the increasing amount of c-CNFs between the “layers” from the edge towards the center (based on the resistance results presented in Fig. 3). A film manufactured from the hes-c-CNF dispersion exhibits even conduction. The high energy sonication treatment causes c-CNF fibrillation and chopping, resulting in smaller hes-c-CNFs (Fig. 1f) compared to the suspended c-CNFs that have not been high energy soni-

cated (Fig. 1g). Using thermal imaging and resistance measurement, we aim to confirm this presented *Hypothesis* of the assembled film with anisotropic conductivity. Furthermore, we performed micro- and nanostructural characterization to provide support for the *Hypothesis* of an assembled structure and the dispersal effect of c-CNFs. While the exact structure and alignment are challenging to show at the nanoscale, in the next sections we present a variety of results supporting the hypothesis in which the c-CNF alignment drives the formation of anisotropically conductive films.

#### Anisotropy characterization: electrical conductivity of nanocomposite films using heat maps

The heat map results confirm that evaporation of the aqueous medium from the dispersion results in uniform electrically conductive nanocomposite films, while that evaporated from the suspension (S1–S3) formed self-assembled nanocomposite films with anisotropic electrical conductivity. An overview of the differences in conductivity between the isotropic control film and the self-assembled anisotropic films is visible in IR heat maps (Fig. 2). The control film obtained from the sonicated stable homogeneous hes-c-CNF-MWCNT dispersion shows an even temperature across the film when a constant voltage is applied on the film surface through the silver ink contacts, suggesting that the current follows the shortest

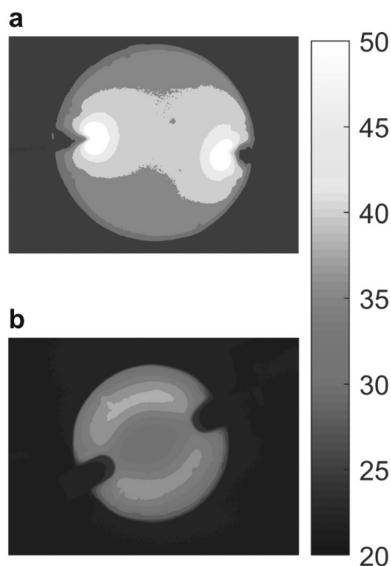


**Fig. 2** Difference in thermal conductivity between control and assembled films. IR-imaging of the isotropic control nanocomposite film (a) and self-assembled anisotropic nanocomposite film S1 (b) when a current is applied to the structure so that heating phenomenon occurs.

route, as shown in the IR-image captured soon after the beginning of heating (Fig. 2a), before heat has spread evenly across the film. Current flows through the centre of the film, as hypothesized for uniformly conducting films. The result is consistent with the results obtained with the finite element model illustrated in Fig. 1a. Interestingly, when a solution containing additional free c-CNFs is suspended with the sonicated hes-c-CNF-MWCNT dispersion and the aqueous medium is evaporated, the resulting film possesses heat zones (Fig. 2b) instead of homogeneous temperature distribution as in the control film (the fully heated control film is not shown here). In the infrared images shown in Fig. 2b, higher temperatures indicate the paths that the current passes through. In the self-assembled films, the centre area shows a lower temperature, indicating that the current is restricted to pass through the centre line, which is the shortest path from terminal to terminal.

#### Anisotropy characterization: electrical conductivity analysis using resistance measurement

The IR-imaging depicts the anisotropic electrical properties of the self-assembled films at the macroscopic scale. Resistances determined (Fig. 3 and Fig. S1 of ESI†) using the measurement protocol (Fig. 8) confirm the findings obtained with the IR-imaging: the control film shows isotropic behavior, while self-assembled films S1–S3 are electrically anisotropic.

The control films show relatively constant resistance throughout the film, as illustrated in Fig. 3. In contrast to the

control films, the self-assembled films S1–S3 show evident anisotropy. The resistance increases along the centre line towards the centre (measurements A and C, Fig. 3), while along the circle it essentially remains constant, measured from both circles 1 and 3 (measurements D and E, respectively, Fig. 3).

In measurement A, the measurement probes are moved along the centre line, maintaining a constant probe distance, depicting an increase in resistance when moving towards the centre, and a subsequent decrease in resistance when moving from the centre towards the edge of the film. The resistance increase is apparent in each measurement towards the centre, although the increase is larger closer to the centre.

Measurement B demonstrates an increase in resistance along the different circular zones, that is, circles when zones are located closer to the centre. Thus, the resistance continually increases even though the probe distance decreases. A difference in the isotropic control film is evident, where the resistance decreases with reduced probe distances, as is expected for an evenly conducting film. Measurement B includes radial line locations that correspond to the location at 180° in measurement D and E, further confirming lower resistances along a circular zone than along the centre line.

In measurement C, one probe remains in location 1 in all measurements, while the other probe is moved along the centre line, that is, the probe distance increases in the subsequent measurements. Measurement C again confirms the difference between the control and assembled films. The resistance in the control film increases slightly with an increasing probe distance, while in the self-assembled films S1–S3, the resistance increases significantly until the centre, with a subsequent decrease after the centre towards the opposite edge of the film. This is in accordance with the Hypothesis, which assumes the current passes through the conducting zones, that is, along the circles in the self-assembled S1–S3 films – instead of the shortest route across the centre, as in the control films.

The resistance measured along circle 1 and along circle 3 in measurements D and E, respectively, is consistent with the Hypothesis. In the control film, the resistance in circle 1 is slightly higher than that in circle 3. This is due to the longer probe distance in circle 1 than in circle 3. Thus, the result is compatible for a uniformly conducting film. Opposite to the control film, the self-assembled films (S1–S3) have a lower resistance in circle 1 than in circle 3, even though the probe distance decreases in circle 3. The result is in accordance with measurement B (Fig. 3), which demonstrated the increase in the resistance along the different circles when zones are located closer to the centre. Opposite results between the control films and films S1–S3 further confirm the Hypothesis of an anisotropic assembly in S1–S3. The increase in resistance of all the measured films (control, S1–S3) when moving along circles 1 or 3 results from the increasing probe distance.

The demonstrated anisotropy is stronger in S2 than in S1 because of a higher concentration of suspended free c-CNFs in S2 than in S1. The concentration of suspended free c-CNFs is

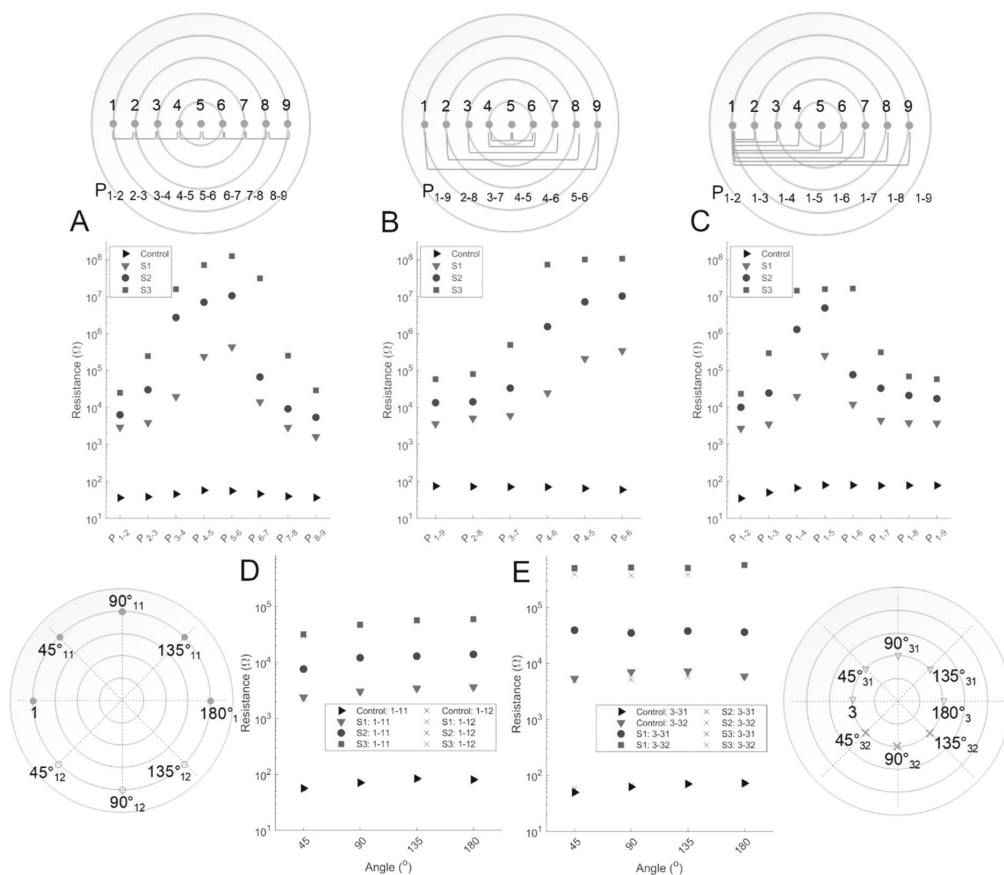


**Fig. 3** Resistance of the assembled (S1–S3) and control (C) films. Resistance measurement protocol (presented at the upper row). Results for films S1–S3 and control from locations along the radial line (measurements A–C presented at the middle row) and along circles 1 and 3 (measurements D and E, at the lower row). In measurements, locations  $n_n$ – $p_n$ ,  $n_n$  and  $p_n$  stand for negative and positive probe locations, respectively.

equal in S2 (supernatant) and S3 (supernatant sonicated  $625 \text{ kJ g}^{-1}$ ). Even though the concentration of suspended c-CNFs is equal in S2 and S3, the anisotropy is stronger in S3. Suspended c-CNFs are more fibrillated in S3 compared to S2, thus the nanofibrils in S3 are expected to be smaller in diameter.

When comparing resistances on approximately the same distance along circle 1 and along the radial line, that is, probe locations 1 –  $45^\circ_{11}$  (measurement D) and 1–4 (measurement C), respectively – the resistance is approximately 10-fold, 100-fold, and 1000-fold higher in the radial line compared to the resistance along circle 1 for S1, S2, and S3, respectively. Comparing the length of the radial line from the edge until the centre of the film – that is, locations 1–5 (measurement C) – and the corresponding distance on circle 1 – that is, locations 1 –  $90^\circ_{11}$  (measurement D) – the difference in the resistance along the centre line (from location 1 to location 5) is even higher, approaching 100-fold and 1000-fold in S1 and S2, respectively.

In S3, the resistance in the corresponding locations remains the same as between locations 1 and 4, that is, approximately 1000-fold. In all self-assembled films S1–S3, the highest resistance is found in the middle of the films and is approximately  $0.5 \text{ M}\Omega$  for S1 in locations 4–5, while approaching  $10 \text{ M}\Omega$  and  $100 \text{ M}\Omega$  in S2 and S3, respectively. Composites were subjected to an electric field for at least 11 min as the measurements were repeated three times for each film, to demonstrate the stability of the films. In addition, three parallel films were fabricated and measured in order to show the repeatability of the film manufacture. Parallel and repeat resistance measurement results are summarized in ESI Fig. S1† and the results indicating the stability of the films in the electric field are presented in ESI Fig. S1 and S2.†

#### Anisotropy characterization: topographical alignment

Scanning electron microscopy images were collected at different locations on the film to perform SEM image-based

orientation analysis. Cytospectre software<sup>33</sup> was used for the analysis to obtain the degree and direction of orientation from the assembled films or the lack of orientation from the control films. Using spectral analysis, two different values were obtained to confirm anisotropy from the SEM images of assembled films (Fig. 4). First, we use a parameter called the circular variance (CV) value to show the difference in the degree of orientation between assembled and control films. CV was determined from each image (Fig. 4a, b and h) in order to describe to degree of orientation. A CV value of 1 refers to perfect isotropy, while a value of 0 is perfect anisotropy. While the CV value of the isotropic control film is close to 1 (indicating isotropy), that of assembled films is

remarkably lower (indicating more anisotropic topography compared to control films), Fig. 4h.

In addition to the CV value, a mean orientation angle of each image location was determined in order to show the orientation direction along the evaporating boundary line. While CV only describes the degree of orientation – that is, isotropy or anisotropy – the mean orientation can be used to show if the orientation direction is according to our hypothesis; that is, along the evaporating dry-line boundary, and thus along the imaginary circles. For this purpose, the films were scanned on a specific surface location, and the scanning location (Fig. 4c) was compared with the mean orientation angle (Fig. 4e) of the analyzed images (Fig. 4a and b as an

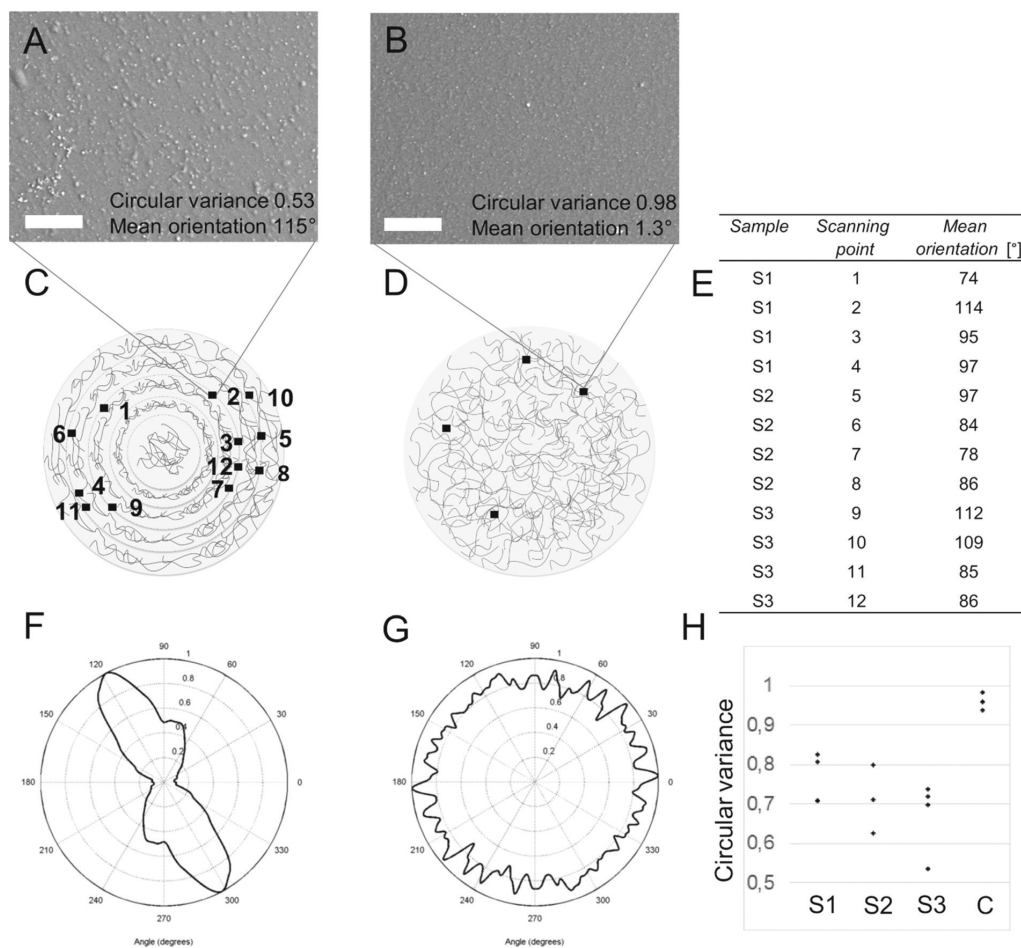


**Fig. 4** Low vacuum SEM scans from the surface of the S3 (a) and control (b) films. Scale bar in a and b is 50  $\mu\text{m}$ . Examples of scanning locations (c) and the corresponding mean orientation angles (e) of the assembled films. The mean orientation angles for the control films (d), so no primary alignment direction is expected. A graphical illustration (f) of the orientation describes the orientation direction in Scanning Point 2 (SEM image in (a)), while isotropy (g) is confirmed for the location seen in SEM image (b). Circular variances of the films S1, S2, S3 and control (h). Circular variance averages ( $n = 4$ ) or the films S1, S2, S3, and control are 0.76, 0.65, 0.67 and 0.96, respectively. Perfect isotropy corresponds to circular variance value 1, while 0 stands for perfect anisotropy.

example) and the expected orientation direction according to our hypothesis (Fig. 1). The mean orientation is presented only for assembled films, as the control films have no expected orientation according to the analyzed CV values. However, an example of the mean orientation angle for the control sample is shown in Fig. 4b for the scanning location shown in Fig. 4d.

The CV analysis (Fig. 4h) confirmed the expected higher degree of orientation of the assembled films compared to the control films, as discussed below. The degree of anisotropy is greater for assembled films than for control films with more isotropic CV values. As the film also contains isotropic MWCNT arrangement (Fig. S4a, e and i†), CV values are not expected to be close to zero. This is because only the added c-CNFs are expected to align along the dry-line boundary during evaporation. Thus, the average CV values ( $n = 4$ ) of the assembled films S1, S2, and S3 are 0.65–0.76 (Fig. 4h), compared to the previously determined 0.27,<sup>22</sup> of highly anisotropic pure c-CNF films. The average circular variance ( $n = 4$ ) of the control films is 0.96.

In summary, CV values show a higher degree of anisotropy for assembled films than control films do, while the mean orientation angles in specific locations show orientation along the circle. This indicates orientation along the dry-line boundary during the evaporation of the liquid.

When analyzing the low vacuum SEM surface scans (one example in Fig. S5†), it is evident that the hes-c-CNF fibrillates during sonication, as the larger fiber bundles that can be seen in S1 and S2 (Fig. S5a and b†) are missing in S3 (Fig. S5c†), in which the suspended component was hes-c-CNF. The decreased size of hes-c-CNF compared to c-CNFs is due to the high energy sonication treatment of the former. The sonication energy used in suspended hes-c-CNF in S3 is the same as that used to prepare the hes-c-CNF/MWCNT dispersion. The degree of orientation is significantly higher in the case of S3 (manufactured using hes-c-CNF + hes-c-CNF/MWCNT) compared to the control film (manufactured using hes-c-CNF/MWCNT). This confirms that the alignment is not dependent on the suspended c-CNF size, but the addition of the suspended c-CNFs.

### Nanocomposite film structure supporting the hypothesis

To confirm the basis behind the observed electric anisotropy, structural characterization of the films and their components was performed using scanning electron microscopy (SEM), (scanning) transmission electron microscopy ((S)TEM) and atomic force microscopy (AFM). According to SEM, (S)TEM, and AFM imaging, MWCNTs were in random orientation in all control and self-assembled (S1–S3) films. Thus, no alignment/orientation of MWCNTs was observed (Fig. 5c and S4a and e†). While it is challenging to observe topographical alignment from the densely packed film surface of low weight element components, SEM images were analyzed using spectral analysis in order to detect possible anisotropy and orientation direction. Spectral analysis (Fig. 4) was consistent with our hypothesis, that there is topographical anisotropy in the direction expected, *i.e.* parallel to the evaporating boundary line. In

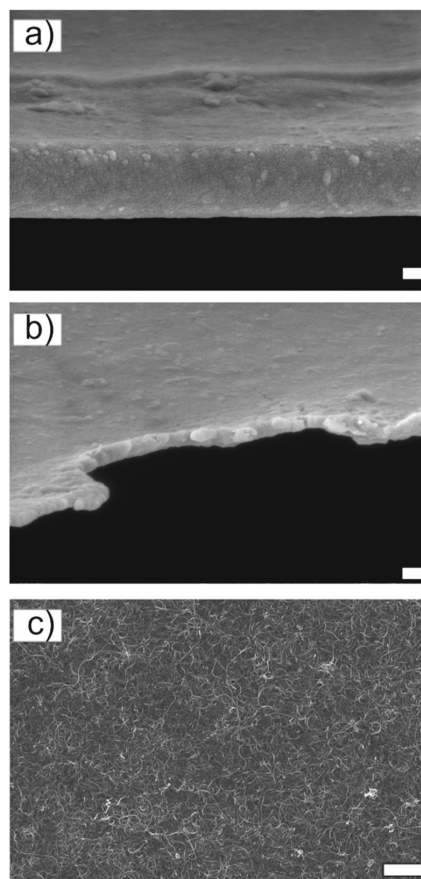
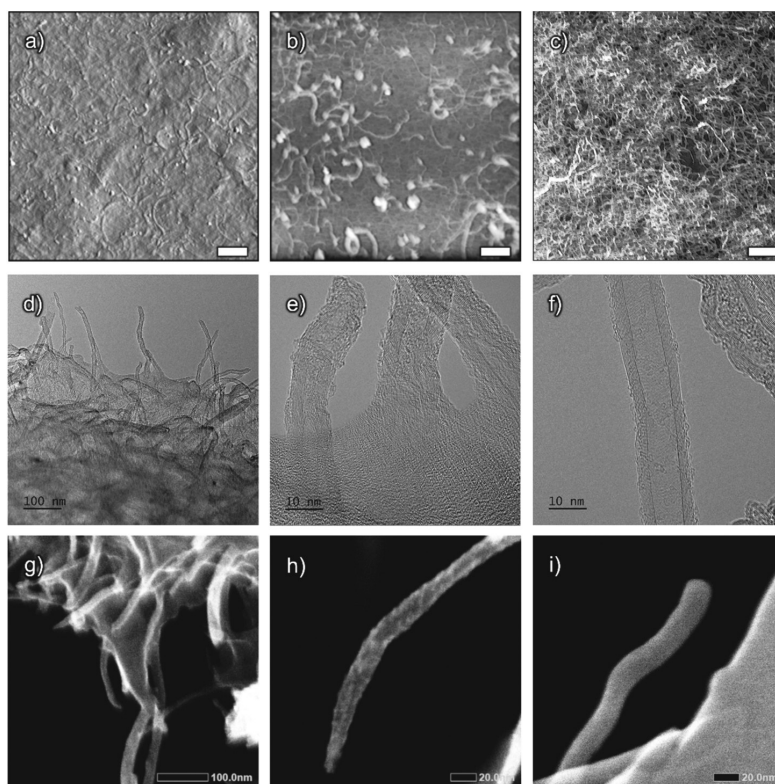


Fig. 5 SEM edge view of the intact assembled (a) and control (b) nanocomposite film. Surface scan with visible MWCNTs is presented in (c). More SEM images are presented in ESI file Fig. S4.† Scale bar sizes are as follows: 200 nm (a and b), and 1  $\mu\text{m}$  (c).

our previous study<sup>22</sup> the evaporation was studied and we showed c-CNF alignment along (parallel) the evaporating boundary line (from edge towards the center). This indicates that suspended c-CNFs are the aligning component and are the driving component of the self-assembly. Surface examination of a film prepared from the hes-c-CNF/MWCNT dispersion (control, Fig. S4i†) shows well-dispersed MWCNTs and no aggregates were observed. The edges of the control film (Fig. 5b) and the assembled film S1 (Fig. 5a) were observed because we previously reported that the self-assembly of c-CNFs begins on the droplet boundary line.<sup>22</sup> SEM characterization of the film edges (Fig. 5a and b) show that, in the control film (Fig. 5b), the edges are not as uniform as in the self-assembled films (Fig. 5a). MWCNTs can be seen on the edge of the control films, while no MWCNTs are visible in the edge of the self-assembled films.

According to the Hypothesis, we expect free c-CNF alignment on the evaporating boundary line; thus, the film edge should be relatively smooth, as demonstrated in Fig. 5a. In addition, the outmost film edge is slightly thickened in the case of the self-assembled films, which is consistent with our previous observation of droplet boundary line pinning in the beginning of evaporation<sup>22</sup> and accumulation of aligned fibers on the boundary edge. Therefore, a slight 'coffee ring' effect is expected in the very beginning of the evaporation, after which the evaporation progresses evenly as the nanosized fibers of the suspension align parallel to the boundary line. The droplet evaporates by shrinking towards the centre and allows more time for the assembly of c-CNFs in the beginning of droplet evaporation, that is, further from the droplet centre.<sup>22</sup> In the previous study, we investigated the droplet evaporation of free c-CNFs in more detail, and it is known that evaporation closer to the centre is faster due to the smaller droplet volume. This likely influences the film thickness, composition, and anisotropic properties. More structural characterization is presented in ESI file Sections 1.3 and 1.4.†

The dispersive effect of the c-CNFs on MWCNTs is visible in the AFM scan of the film surface (Fig. 6a), as well as of the dilute dispersion (Fig. 6b), with no visible MWCNT aggregates present. The dilute dispersion presents larger molecules, that is, MWCNTs. Hes-c-CNF in the dispersion (Fig. 6b) is smaller than c-CNFs in the supernatant (Fig. 6c) due to a higher degree of sonication. This is observed also from surface scans (ESI Fig. S5†), which confirms the presence of larger nanocellulose fibers in S1 and S2 films fabricated using supernatant c-CNFs, while S3 was fabricated using 625 kJ g<sup>-1</sup> sonicated hes-c-CNF in which larger fibers are not detected. The TEM images show the c-CNF matrix rigidly attached to individual MWCNTs (Fig. 6d and e) on a torn film boundary. For comparison, Fig. 6f shows the TEM image of pristine multi-wall carbon nanotubes. Similar to SEM imaging, the challenge of TEM is to distinguish individual cellulose nanofibrils from a densely packed matrix. (S)TEM (secondary electron imaging) was used to distinguish individual c-CNFs on top of MWCNTs (Fig. 6h), from a torn film boundary (Fig. 6g). Untreated MWCNTs were examined using STEM (Fig. 6i) for comparison.



**Fig. 6** Nanostructure comparison. AFM (a–c) and (S)TEM (secondary images) (d–i) of the film surface (a), torn film boundary (d, e and g), dilute dispersion (b), dilute c-CNF supernatant (c), untreated MWCNTs (f and i) and individual MWCNTs with c-CNFs on the surface (h) from a torn nanocomposite film. Scale bar sizes in (a–c) is 500 nm.



Based on the findings of SEM and AFM examination, we can confirm that c-CNFs work as a dispersing/stabilizing agent for MWCNTs. The present study is the first to demonstrate the successful use of c-CNFs to disperse MWCNTs. However, further optimization for sonication energy per dry mass and materials' concentrations should be done.

### Chemistry and interactions of the components: Interactions and chemical characterization

To attain more information regarding the effects of sonication treatments and interactions between cationic nanocellulose and carbon nanotubes, magic angle spinning (MAS) NMR spectroscopy is applied. The objectives are to examine possible chemical modification and to evaluate the interaction between c-CNFs and MWCNTs. The  $^1\text{H}$  NMR spectra in ESI Fig. S7† illustrate the hydrogen peaks of the untreated c-CNFs (Fig. S7a†) which were used as a reference for the examination of the effects of sonication treatments on the sonicated samples (Fig. S7b and c† for hes-c-CNFs, respectively, and Fig. S7d† for the hes-c-CNF-MWCNT dispersion and ESI 1.5† in more detail).

The intensity and the area of the signal peak at 2.1 ppm results from  $-\text{CH}_3$  groups of the functionalized hydroxypropyl-trimethylammonium side chain and remain relatively unchanged in c-CNF samples (Fig. S7a-c†), indicating that the functional group remains intact and relatively stable throughout the sonication treatments. Untreated c-CNFs and c-CNFs sonicated with  $625 \text{ kJ g}^{-1}$  provide the same signals. Thus, the effect of sonication on the chemical structure of c-CNF is assumed negligible. Evaluating the interaction between c-CNFs and MWCNTs during sonication is not straightforward from  $^1\text{H}$  NMR spectra (Fig. S7d†) as the analyte is merged and signals are broad and overlapping. However, when compared to the signals obtained from c-CNF alone, we can draw some conclusions on the organization of c-CNFs in the sample: the functional group is expected to point out from the entangled hes-c-CNF-MWCNT nanostructure. As the peaks in 5 ppm to 3.8 ppm are weak and broadened, the corresponding protons are not solvated, indicating strong interaction between those areas of c-CNFs with MWCNTs. The formed nanostructure is tightly packed, which prevents water from penetrating between the interaction sites. In summary, as the trimethyl protons of the cationic substituent remain unchanged in all samples, we can assume it is facing outward from MWCNTs, while the less solvated area refers to cellulose ring protons, in this case one of the H3–H5, which would be the location of the stronger interaction with MWCNTs. The result is presented in more detail in ESI 1.5.†

The NMR result is in accordance with the suggested interaction where hes-c-CNF is covering MWCNTs (Fig. 1f and 6h). The result also provides valuable information regarding the orientation of c-CNFs relative to MWCNTs, which we cannot obtain from other characterization methods. Thus, we can make assumptions regarding the dispersion chemistry that the free c-CNF encounters when suspended with the dispersion. According to NMR, there is no covalent chemical modification

of the dispersion components during rather heavy sonication treatment, as also supported by the ATR-FTIR results (ESI Fig. S8†).

We propose that additional free c-CNFs are accountable for the self-assembly of c-CNF-MWCNT nanocomposite films; and this conclusion is consistent with our previous studies on the droplet evaporation of c-CNFs.<sup>22</sup>

## Discussion

We demonstrated the fabrication of nanocomposite films with either isotropic or anisotropic conductivity. The Hes-c-CNF/MWCNT dispersion was used to obtain an isotropic film (control), while additional c-CNFs suspended in the dispersion drove the assembly during evaporation, resulting in an anisotropic (assembled) film. The difference between components in the control film and the assembled film is that in the latter film the dispersion and c-CNFs were suspended, while the control films were formed directly from the dispersion. Alignment observed in our previous paper<sup>22</sup> is consistent with these results. Thus, we postulate that the free c-CNFs are responsible for the assembly along the boundary line. The suggested assembly on the evaporating liquid boundary line is described in more detail elsewhere<sup>22,32</sup> and is consistent with the observations of Mariani *et al.*<sup>34</sup> Therefore, we suggest, according to the Hypothesis, that the formation of anisotropic conductivity is due to c-CNF driven assembly.

Fig. 1 is an oversimplification of the hypothesized structure of the film in which the nanocomponents are not in scale. The diameter and length of c-CNFs have been determined using AFM and they are on average 5(–15) nm and less than 2  $\mu\text{m}$ , respectively.<sup>35</sup> According to the MWCNT manufacturer, the diameter and length of MWCNTs are on average approximately 9.5 nm and 1.5  $\mu\text{m}$ , respectively. Thus, they are similar to those of untreated c-CNFs. Sonication treatment during dispersion preparation is expected to significantly fibrillate and cut the length of hes-c-CNF. AFM images of the dispersion components (Fig. 6b) and the untreated c-CNFs (Fig. 6c) are consistent with this hypothesis.

The amphiphilic nature of the nanocellulose chain affects the solubility and the surface energy, which also affects the dispersibility, the hydrophobic interactions and the aggregation tendency.<sup>19,36</sup> During sonication, applied energy affects intramolecular and intermolecular bonds, causing a different degree of fibrillation in the cellulose structure. The increasing surface area and polar/non-polar nature of cellulose aid the dispersion of hydrophobic MWCNTs in an aqueous environment. The high surface-to-length ratio of MWCNTs and the lack of functional groups determines that the chemistry of carbon nanotubes is dominated by dispersion type interactions. These extended  $\pi$ -conjugations, such as  $\pi$ - $\pi$  and cation- $\pi$ , enable non-covalent interactions with various substrates. Evidently, cellulose and CNTs exhibit favorable interactions toward each other so that auto aggregation of both nanoparticles does not occur, and they form a strong

entangled hybrid nanoparticle dispersion, where the cationic functional groups of c-CNFs point outwards from the hybrid structure, resulting in a stable dispersion. Findings in the SEM and NMR studies endorse that nanocellulose and carbon nanotubes have established robust connections at the molecular level and c-CNFs can be used to disperse MWCNTs.

The alignment mechanism of individual c-CNFs along the evaporating droplet boundary line is based on the theory introduced by Mashkour *et al.*,<sup>32</sup> and it is based on the capillary force gradient and surface tension torque (STT) near a dry-line boundary layer. The dry-line boundary layer is the air–suspension–substrate interface, which is also referred to as a triple line.

We suggest, that in the beginning of the assembly process of the assembled films S1–S3, c-CNF fibers align along the boundary line due to pinning of one fiber end and alignment of the fiber parallel to the dry boundary line due to surface tension torques and capillary forces.<sup>22,32</sup> Initiation of the alignment of an individual c-CNF involves surface tension torques, and the propagation of the fibre alignment, when the fibre is bent closer to the boundary line due to capillary forces, according to the alignment process described in the study of Mashkour *et al.*<sup>32</sup> A previous study showing alignment of c-CNFs suggested that the same alignment theory applies to c-CNF during droplet evaporation. The interaction between dispersed MWCNTs and c-CNFs, as well as between the additional free c-CNFs and the hes-c-CNF-MWCNT dispersion component, is assumed to be relatively strong. The c-CNFs in the hes-c-CNF-MWCNT dispersion can further interact with free c-CNFs, which is hypothesized to initiate the assembly, further dragging the c-CNF-MWCNT into circular zones during droplet evaporation. Even though hes-c-CNF is not free to align after dispersing MWCNTs, the excess of cationic groups on the cluster surfaces allows stronger capillary forces to take place during drying when interaction with free aligning c-CNFs can take place. Therefore, free aligning c-CNFs traps along the hes-c-CNF-MWCNT entangled dispersion and an assembled structure is formed. This results in aligned free c-CNFs during droplet evaporation and assembly of the hes-c-CNF-MWCNT entangled dispersion, resulting in alternating aligned c-CNFs and more entangled hes-c-CNF-MWCNTs. Sonication pre-treatment of suspended free c-CNFs increased the resistance, as indicated by the higher resistance of film S3 compared to that of film S2. This is likely due to the smaller size of the c-CNF in S3, which is a result of sonication. Thus, smaller c-CNFs seem to reduce conductive pathways more than larger c-CNFs in S2. In other words, the smaller c-CNFs of S3 may cover MWCNTs better, and therefore cause lower conductivity. It is worth highlighting, that the degree of orientation is significantly higher in the case of S3 (manufactured using hes-c-CNF + hes-c-CNF/MWCNT) compared to the control film (manufactured using hes-c-CNF/MWCNT). This confirms that the alignment is not dependent on the suspended c-CNF size, but the addition of the suspended c-CNFs. The dispersion consists of hes-c-CNF-MWCNT clusters in which cationic groups point outwards. Therefore, the added

c-CNFs can interact with these cationic groups and initiate the self-assembly at the evaporating boundary line. The added c-CNFs are expected to initiate the assembly process as described and result in alternating aligned c-CNFs and more entangled hes-c-CNF-MWCNT, shown in Fig. 1g. The anisotropic alignment is detected from the surface topography at a larger scale with image analysis, while the control films are more isotropic. Although individual aligned c-CNFs are not seen in SEM images, the detected larger scale anisotropy indicates tightly packed and aggregated aligned c-CNFs, similar to our previous study.<sup>22</sup> Anisotropy of the assembled films is a result of the added c-CNFs, while MWCNTs do not show alignment in the assembled films. When evaporation has proceeded close to the end towards the centre of the film, the evaporation rate is faster due to lower volume remaining, and there is no time for assembly along the liquid boundary line in the centre part of the film.

In the present study, the purpose of the resistance measurement was to indicate the difference in the electrical properties between the control film and the self-assembled films. Furthermore, the resistance measurement was used to characterize the level of anisotropic conductivity in the assembled films. Here, two-point measurement was used since it shows the conductivity exactly between two distinct points. Even though the usage of four-point measurement rules out the possible contact resistances between the metallic probes and the CNT network, it would require homogeneous surface conductivity and, is therefore not a suitable method for characterizing anisotropic films that have circle-shaped conducting pathways.

The distinct two-probe resistance measurement points along the centre line and along the circles were repeatedly defined using a designed measurement position template (see Fig. 8b). We noticed that along the circles (that is, the measurement locations in Fig. 8, measurements B, D, and E), the positive and negative probe locations could be switched without affecting the measured resistance. However, switching of the positive and negative probe locations along the centre line (that is, measurement locations in Fig. 8, measurement A and C) showed a significant difference on the measured resistance. This was further studied with IV-curves, which confirmed anisotropy along the centre line (that is, nonlinear IV-curves) in films S1–S3, while along the circular path in S1–S3 the curves were linear. Control films had linear IV-curves in both measured directions. As shown by the IR-images and resistance measurements, the conductivity of the assembled films is different along the radial direction compared to the circular zone direction. This is due to the aligned c-CNFs along the circle, while c-CNFs are packed next to each other along the neighbouring circles. Towards the centre, more and more CNFs are packed between the conducting MWCNT components, blocking the conductive pathways, and increasing resistance towards the centre. While this paper presents that the electrical properties are different along the zone and towards the centre due to c-CNF-driven assembly, the electrical properties along the radial direction should be studied further. Our observation indicates a resistive component along the

zone and a resistance coupled to a capacitive component along the radial line.

MWCNTs are often a better option for biomedical applications than SWCNTs due to more standardized methods of chemical functionalization and lower cytotoxicity.<sup>37</sup> The c-CNF cover on the MWCNT surface could provide even better biocompatibility while still providing the benefits of MWCNTs, for example, in biomedical applications such as multifunctional antimicrobial drugs, drug delivery vehicles, functional surfaces for cell growth and adhesion, and new therapies for diseases.<sup>38</sup> Furthermore, the c-CNF cover on the MWCNT surface could also provide safety for the user in terms of handling the materials. Thus, we expect that the presented cover of c-CNFs on the MWCNT surface resulting from sonochemical treatments is beneficial for the future use of MWCNTs. However, the cytocompatibility and health effects should be studied further.

Anisotropic materials are important functional materials in many fields. For instance, anisotropy in conductivity has been achieved in certain synthetic polymer systems.<sup>39,40</sup> However, it has been more difficult to create similar materials using biologically relevant matrices.<sup>39</sup> The size scale of c-CNFs in an anisotropic assembled substrate surface<sup>22</sup> is optimal for diverse biomedical applications that require protein adhesion. Previously, we have shown cell adhesion and growth on c-CNF-CNT-coated cellulose mesh substrates in our study,<sup>41</sup> in which the coating was prepared from the dispersion reported in the materials and methods section of the current paper. In addition, c-CNFs, either alone or as coating, have been shown to support cell growth, charge mediated adsorption, and cell alignment.<sup>22,42</sup>

Directionally conductive, engineered tissues have applications in a variety of fields, including stem cell biology, cardiac and neural tissue engineering, and biosensor development.<sup>39</sup> Models to mimic native tissues, such as anisotropic myocardial fiber architecture,<sup>43</sup> would benefit from adjustable platforms/substrates with both anisotropic and conductive properties, suggesting potential application areas for *in vitro* cell, tissue and disease models (organ on a chip, body on a chip, disease on a chip). In such *in vitro* platforms, electrical conductivity could serve to stimulate cell growth, differentiation, or drastically intentional damage to the cell, in the case of disease models or photodynamic therapies.<sup>41</sup> In addition, compartmentalized heating can be achieved with anisotropic films, as demonstrated with IR-imaging, and is adjustable by tuning film components. The demonstrated formation of assembled anisotropic conductivity is not limited to a specific substrate – that is, a circular film – nor to a specific application, but rather has potential in a variety of fields.

## Experimental

### Cationic cellulose nanofibers (c-CNFs) and multiwall carbon nanotubes (MWCNTs)

Cationic CNFs were produced from bleached and never-dried cellulose kraft pulp. Cationization was conducted similarly to

how it was reported by Bendoraitiene *et al.*,<sup>44</sup> who described the cationization of starch using EPTMAC (Raisacat, Chemigate, Finland) as a cationizing agent. The pulp was first concentrated in an oven to 63% dry matter content. The reaction mixture was prepared from 140 mL of EPTMAC, 2 g of aqueous solution of NaOH (5%), and 2.3 mL of Milli-Q water. The ingredients were mixed thoroughly and 50 mL of Milli-Q water was added to the mixture, which was warmed to 45 °C. The pulp was added to the mixture, which was then stirred for 24 h at a high cellulose consistency (~40%) with a CV Helicone Mix Flow (Design Integrated Technology Inc., Warrenton, USA) reactor. After the reaction, the cationic pulp was washed with 500 mL of ethanol, 500 mL of tetrahydrofuran (THF) (Sigma Aldrich, USA), and 1000 mL of Milli-Q water. The cationized pulp was soaked at 2% concentration of dry solids and dispersed using a high-shear Ystral X50/10 Dispermix mixer (Ystral GmH, Ballrechten-Dottingen, GER) for 10 min at 2000 rpm. The pulp suspension was then fibrillated using Microfluidics microfluidizer type M110-EH (Microfluidics, Westwood, USA) at 1800 bar pressure. The suspension was processed twice through two chambers, with diameters of 400 µm and 100 µm, respectively. The fibrillated cationic CNF formed a highly viscous and transparent hydrogel with a final dry material content of 2%. The degree of substitution was analyzed according to the method proposed by Bendoraitiene *et al.*<sup>44</sup> and was 0.35.

Multiwall carbon nanotubes (MWCNTs, Nanocyl 7000, Nanocyl SA., Sambreville, Belgium) were purchased from Nanocyl Inc. and the product was used in the state received. The MWCNTs are produced using catalytic chemical vapor deposition (CCVD).

### Preparation of c-CNF solution, hes-c-CNF/MWCNT dispersion, and hes-c-CNF/MWCNT + free c-CNF suspensions

The cationic CNF hydrogel (2.01 w%) was diluted to 0.15 w% (W/v) concentration with Milli-Q water and sonicated for 2 min at 20% amplitude using a SONICS Vibra Cell VCX 750 ultrasonic processor (Sonics and Materials, Inc., USA). The sonicated solution was centrifuged at 10 000g for 60 min (Thermo Scientific SL 8), and the supernatant with 0.145 w% was used for further processing. (The dry w% of the supernatant was determined from the freeze-dried product.)

The control hes-c-CNF/MWCNT samples were prepared by sonicating the c-CNF supernatant and the MWCNTs to form a homogeneous stable dispersion. The control samples contained the c-CNF supernatant with a concentration 0.05 w% of MWCNTs in aqueous medium. The total dry mass for the control sample was 0.16 g. The dispersion samples were sonicated using a tip horn sonicator Q700 (QSonica LLC, Newton, CT, USA) in 100 mL glass beakers. The amplitude of the sonication vibration was kept constant. The power output remained between 50 W and 60 W for every sonication. The sonication system included a water bath to keep samples cool during the sonication such that the temperature did not rise above 30 °C. The water bath was cooled by circulating cooling glycerol through a chiller (PerkinElmer C6 Chiller,

PerkinElmer Inc., Waltham, MA, USA). Samples were sonicated using a same amount of energy per dry mass, respectively  $625 \text{ kJ g}^{-1}$ . The sonication energy was chosen based on our previous studies.<sup>5,6</sup> The resulting hes-c-CNF/MWCNT dispersion was used to prepare control nanocomposite films (Fig. 7).

The hes-c-CNF/MWCNT dispersion was further suspended (Fig. 7) with varying volume ratios of additional c-CNFs for the preparation of suspension samples S1 (37.5% v/v), S2 (20% v/v) and S3 (20% v/v). The nanocellulose used in S1 and S2 suspension is the 0.15 w% c-CNF supernatant described previously, while the nanocellulose in the S3 suspension was further sonicated with  $625 \text{ kJ g}^{-1}$ , and is thus hes-c-CNF. Thus, S1 and S2 differ in volume ratios of the dispersion and added c-CNFs, while S2 and S3 differ in pretreatment of the added c-CNFs and hes-c-CNF, respectively, while the volume ratio is constant.

### Fabrication of nanocomposite films

To fabricate nanocomposite films, polydimethylsiloxane (PDMS) substrates were fabricated with a standard PDMS curing procedure in a Petri dish. A PDMS layer approximately 3 mm thick was prepared on a Petri dish surface, and then cut into 10 mm diameter circular substrates using a 10 mm punch. The nanocomposite films were prepared by casting 250  $\mu\text{L}$  of the dispersion (control sample C) or suspension (samples S1, S2, S3) on PDMS substrates and drying for 5 h at  $60 \text{ }^\circ\text{C}$  (UN55, Memmert GmbH + Co. KG, Schwabach, Germany) to obtain self-standing circular nanocomposite films with 10 mm diameter and thickness between 0.007 and 0.011 mm. The dispersion produces isotropic nanocomposite control films, while suspensions S1, S2, and S3 produce corresponding assembled anisotropic nanocomposite films. Thus, all films in this study are nanocomposite films, either isotropic or anisotropic. Later, the terms control film and assembled film are used, although when highlighting orientation, they

are referred to as isotropic (control) film and anisotropic (assembled) film, respectively.

### Characterization

The films were characterized using infrared imaging, resistance measurement, SEM, (S)TEM, AFM, micro-computed tomography (microCT), and nuclear magnetic resonance spectroscopy (NMR). Infrared imaging was used to illustrate the electrical anisotropy of the assembled films using heat maps, while the resistance measurement was used to demonstrate the difference between the control sample and assembled samples S1–S3 in more detail, and to investigate the electrical properties of the assembled samples. SEM, (S)TEM and AFM were used for structural characterization of the samples or their components to show or explain the assembly, as well as describe the interactions between the components. MicroCT was used for the thickness characterization of the films. Finally, NMR was performed in order to clarify the interaction between the dispersion components, as well as the effect of sonication treatments on the c-CNFs.

**Infrared imaging.** Infrared imaging (IR-imaging, Fluke Ti400, Everett, WA, USA) was used to obtain the electrical anisotropy of the assembled c-CNF + hes-c-CNF/MWCNT films in comparison to the uniform conductivity of the control hes-c-CNF/MWCNT nanocomposite films at the macroscale. IR-imaging was performed by applying silver ink contact to the edge of the film samples, inserting a current through the film and recording sample heating.

**Electrical measurement.** Resistances of nanocomposite film samples were determined according to the measurement plan shown in Fig. 8. The resistance was studied along (i) the centre line through the sample (measurements A–C) and (ii) along imaginary circles 1 and 3 (measurements D and E, Fig. 8a), later referred to as circle 1 and circle 3, respectively. The resistance between the measurement points was deter-

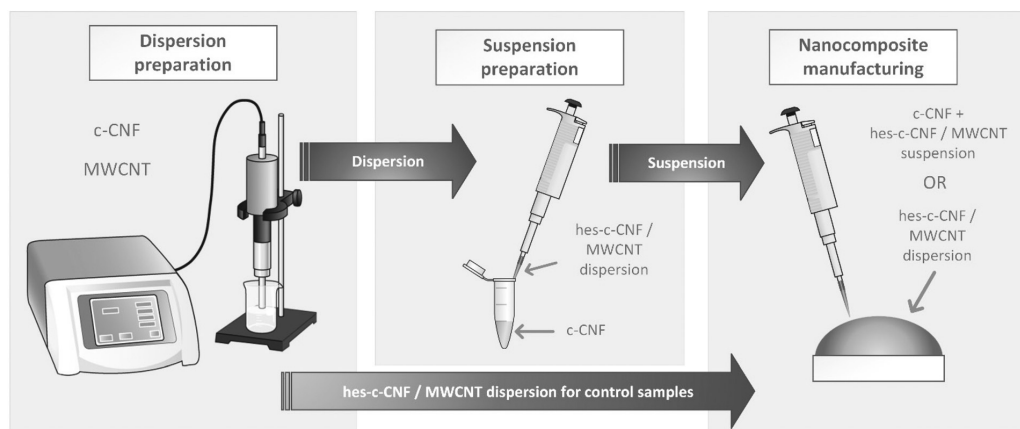
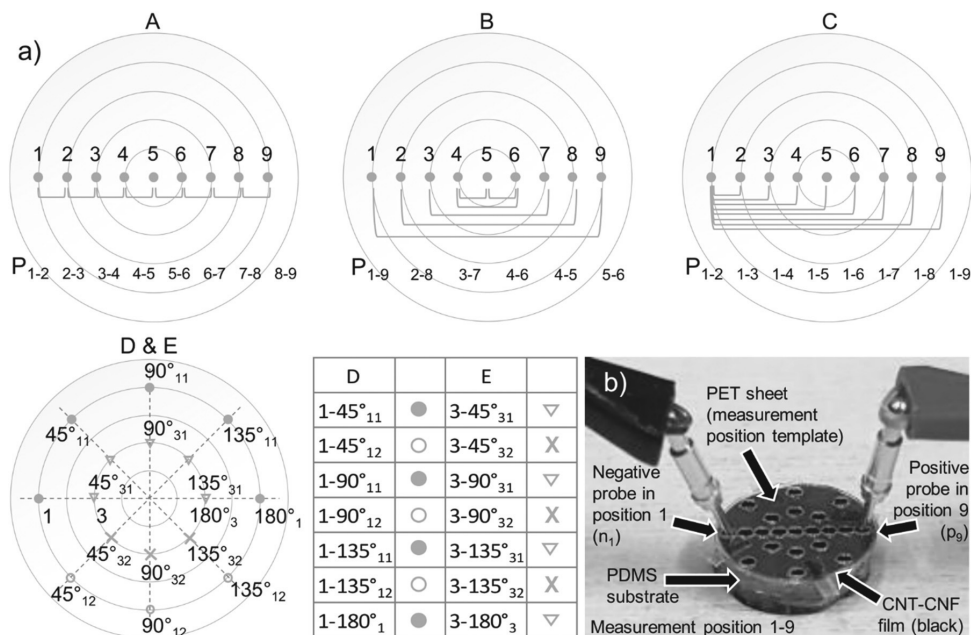


Fig. 7 The preparation of the dispersion and suspension, and the subsequent manufacture of the control isotropic and assembled anisotropic films using the dispersion and suspension, respectively.



**Fig. 8** Resistance measurement protocol (a) and measurement setup (b). Measurements A–C are performed along the centre line, while measurements D and E follow circle 1 (D) and circle 3 (E) according to the measurement protocol presented in measurements A–E (a), respectively. Measurement locations for measurements A–C are presented in the corresponding map, while the measurement locations for measurements D and E are shown in the table next to the D & E map.

mined from current outputs measured with a constant voltage 0.5 V using a using two-terminal measurement with a potentiostat (Iviumstat, Ivium Technologies B.V., Eindhoven, The Netherlands) in a chronoamperometry mode. An average of current value measured for 10 s from each measurement point was used in the resistance calculation ( $R = U/I_{avg}$ ). Three parallel sample films were measured, and the measurement was repeated 3–5 times for each individual sample film. Matlab was used for data analysis. To improve the repeatability of placing the measurement probes at the same locations on the parallel sample films, a mask was used. The mask (illustrated in Fig. 8b as a measurement template) was designed to include circular openings according to planned measurement locations. The openings are located along centre line in the radial direction, referred to as a radial line (locations from 1 to 9), as well as along circles 1 and 3 (locations 1, 45°<sub>11</sub>, 45°<sub>12</sub>, 90°<sub>11</sub>, 90°<sub>12</sub>, 135°<sub>11</sub>, 135°<sub>12</sub>, 180°<sub>1</sub> and 3, 45°<sub>31</sub>, 45°<sub>32</sub>, 90°<sub>31</sub>, 90°<sub>32</sub>, 135°<sub>31</sub>, 135°<sub>32</sub>, and 180°<sub>3</sub>, respectively). In the notation used in measurements A–C,  $n_n$ – $p_n$  (Fig. 8) represent the locations of the negative ( $n_n$ ) and positive ( $p_n$ ) probe, respectively, in which  $n$  stands for the location of either probe on the film (Fig. 8). During measurements A and B (Fig. 8), the location of both probes varies, while in measurements C–E (Fig. 8), the negative probe remained unchanged in location 1 (measurements C and D) and in location 3 (measurement E), while the location of the positive probe was changed onto the other locations on the

film. In the notation used in measurements D and E,  $a_{yn}^{\circ}$  (Fig. 8) represent the locations of the positive probe, in which  $a$  describes the angle between the lines formed along the location of the positive probe and the centre and along the location of the positive probe and the centre, while  $y$  stands for circle 1 or circle 3 and  $n$  stands for the location of the probe on the film on either one of the halves (<sub>1</sub> for the upper half and <sub>2</sub> for the lower half). Locations 180°<sub>1</sub> and 180°<sub>3</sub> correspond to the locations 9 and 7 at the radial line, respectively. The distance of the negative probe to the positive probe in the locations 1–45°<sub>11</sub> and 1–45°<sub>12</sub> are equal and are thus paired in the result chart.

**Electron microscopy.** Scanning electron microscopy (SEM) and (scanning) transmission electron microscopy ((S)TEM) were used to characterize the nanomaterials used and nanocomposite films. Front and side views of the nanocomposite films were characterized using SEMs (UltraPlus, Carl Zeiss, Oberkochen, Germany; JSM-IT500, Jeol Ltd, Tokyo, Japan). The samples were attached to aluminum SEM stubs using carbon tape or carbon glue. The front view was imaged on the surface of the nanocomposite films, while the side view was characterized from the torn film edges. Torn films were placed between a string and fixed on the SEM stub to obtain a cross-section and edge views of the films. The samples were either carbon or gold-coated to avoid charging during the SEM studies. (S)TEM (JEM-F200, Jeol Ltd, Tokyo, Japan) was used to characterize the

nanomaterials used and nanocomposite films. Untreated MWCNTs and small pieces of torn nanocomposite film edges were fixed on TEM grids with a holey carbon film.

**Alignment characterization.** SEM images were collected at different locations on the film to perform SEM image-based orientation analysis. Cytospectre software<sup>33</sup> was used for the analysis. A parameter called circular variance (CV) was determined from each image in order to describe to degree of orientation. A CV value of 1 refers to perfect isotropy, while a value of 0 is perfect anisotropy. In addition to the CV value, a mean orientation angle of each image location was determined in order to show the orientation direction along the evaporating boundary line. While CV only describes the degree of orientation – that is, isotropy or anisotropy – the mean orientation can be used to show if the orientation direction is according to our hypothesis; that is, along the evaporation boundary line, and thus along the imaginary circles.

**MicroCT.** Nanocomposite films were imaged with X-ray microtomography (microCT) using MicroXCT-400 (X-ray tube voltage of 40 kV and a current of 250  $\mu$ A; Carl Zeiss X-ray Microscopy, Inc., Pleasanton, CA, USA). The imaged sample area was 2.98 mm<sup>2</sup>. 3D microCT images were reconstructed from 1601 projections with a 10 s exposure time (20 $\times$  objective, binning 2, pixel size 1.048  $\mu$ m) using the microCT software tool XMReconstructor. 3D image stacks were manually thresholded for the 3D analysis. The mean film thickness with standard deviations from different locations of the films was calculated with the BoneJ Fiji plugin.<sup>45</sup> The data visualization was realized using Avizo 2019.3 software (Thermo Fisher Scientific, Waltham, MA, USA).

**Atomic force microscopy.** Atomic force microscopy scanning was performed in a tapping mode using a standard ACTA AFM probe with a resolution of 256  $\times$  256 pixels. Images were analyzed and postprocessed using AFM image processing software XEI (Park Systems, USA).

**Nuclear magnetic resonance spectroscopy (NMR).** The following samples were prepared and freeze-dried for NMR studies. The cationic CNF hydrogel (2.01 w%) was diluted to 0.15 w% (W/v) concentration in D<sub>2</sub>O (Sigma Aldrich), sample 1 (untreated c-CNF). Samples 2–4 were sonicated for 2 min at 20% amplitude using a SONICS Vibra Cell VCX 750 ultrasonic processor (Sonics and Materials, Inc., USA), with subsequent centrifugation at 10 000g for 60 min (Thermo Scientific SL 8). The resulting supernatant was sonicated using 625 kJ g<sup>-1</sup> or 1250 kJ g<sup>-1</sup> and a tip horn sonicator Q700 (QSonica LLC, Newton, CT, USA), resulting in samples 2 and 3 (c-CNF supernatant sonicated 625 kJ g<sup>-1</sup> or 1250 kJ g<sup>-1</sup>, respectively). Sample 4 (sonicated c-CNF-MWCNT dispersion) was prepared by sonicating the c-CNF supernatant (in D<sub>2</sub>O) and MWCNTs using 625 kJ g<sup>-1</sup>. Samples 1–4 were freeze-dried to remove excess moisture and used in NMR experiments.

NMR spectra were measured on a 500 MHz JEOL JNM-ECZ 500R spectrometer. Samples (approx. 50 mg) were packed into 3.2 mm diameter zirconia rotors with KelF caps as a tick suspension in D<sub>2</sub>O. The semi-solid state FG-MAS <sup>1</sup>H spectra were recorded at room temperature, with the high-resolution field

gradient FG-MAS probe at a spinning rate of 5 kHz. A water suppression pulse sequence was applied during the measurements.

## Conclusions

Application of sonochemical treatments to aqueous mixtures of cationic nanofibrillated cellulose and carbon nanotubes leads to even and relatively stable solutions of the assembled components, which can be easily formed as free-standing conductive nanocomposite films. Diverse characterization techniques confirm the strong interactions between c-CNFs and CNTs, mainly occurring through ionic and hydrophobic interactions, as well as hydrogen bonding induced by sonochemical treatments. Sonochemical treatment induces robust interactions between c-CNFs and MWCNTs in aqueous media, forming a strong entangled hybrid nanoparticle dispersion hes-c-CNF/MWCNT, where cationic functional groups of hes-c-CNFs point outwards from the hybrid structure. Drying of the dispersion results in evenly conducting films, while the incorporation of free c-CNFs (S1, S2) or hes-c-CNFs (S3) makes it possible to control the self-assembly of nanomaterials along the evaporating dry-line boundary and the simultaneous formation of conducting zones and thus the directional increase in resistance in the radial direction. The amount and composition of the added c-CNFs (or hes-c-CNFs) influence the conductivity differences in different directions. These films can be considered as free-standing self-assembled nanocomposite films displaying a tunable surface with functional properties such as adjustable conductivity. The novelty in the method described herein is that it produces adjustable directional conductivity and uses c-CNFs as a dispersing agent. The method is not limited to a specific application or to nanocomposite films as a substrate. Instead, the tunable composition, substrate preparation technique, and functionalization possibilities offer interesting possibilities in the fields of biomedical sciences and energy applications in general and should be studied further.

## Author contributions

The manuscript was written through contributions of all authors. All authors have given approval to the final version of the manuscript.

## Conflicts of interest

There are no conflicts of interest to declare.

## Acknowledgements

We acknowledge K. Tornberg for casting PDMS sheets for substrate preparation, M. Jokinen for his technical help related to

laser cutting of the measurement template, and M. Kakkonen for his technical help with IR imaging. SEM and (S)TEM studies were carried out at Tampere University using Tampere Microscopy Center facilities. We acknowledge P. Willberg-Keyriläinen (Senior Scientist, VTT) for the cationization of CNFs.

## References

- H. Zhang, C. Dou, L. Pal and M. A. Hubbe, *BioResources*, 2019, **14**, 7494–7542.
- K. Li, C. M. Clarkson, L. Wang, Y. Liu, M. Lamm, Z. Pang, Y. Zhou, J. Qian, M. Tajvidi, D. J. Gardner, H. Tekinalp, L. Hu, T. Li, A. J. Ragauskas, P. Youngblood and S. Ozcan, *ACS Nano*, 2021, **15**, 3646–3673.
- Q. Zhu, Q. Yao, J. Sun, H. Chen, W. Xu, J. Liu and Q. Wang, *Carbohydr. Polym.*, 2020, **230**, 115609.
- C. Zamora-Ledezma, C. Blanc, N. Puech, M. Maugey, C. Zakri, E. Anglaret and P. Poulin, *Phys. Rev. E*, 2011, **84**, 1–5.
- S. Siljander, P. Keinänen, A. Ivanova, J. Lehmonen, S. Tuukkanen, M. Kanerva and T. Björkqvist, *Materials*, 2019, **12**, 430.
- S. Siljander, P. Keinänen, A. Rätty, K. R. Ramakrishnan, S. Tuukkanen, V. Kunnari, A. Harlin, J. Vuorinen and M. Kanerva, *Int. J. Mol. Sci.*, 2018, **19**, 1–14.
- A. Hajian, S. B. Lindström, T. Pettersson, M. M. Hamed and L. Wäberg, *Nano Lett.*, 2017, **17**, 1439–1447.
- Z. Shi, G. O. Phillips and G. Yang, *Nanoscale*, 2013, **5**, 3194–3201.
- M. Bhattacharya, M. M. Malinen, P. Lauren, Y. R. Lou, S. W. Kuisma, L. Kanninen, M. Lille, A. Corlu, C. Guguen-Guillouzo, O. Ikkala, A. Laukkanen, A. Urtti and M. Yliperttula, *J. Controlled Release*, 2012, **164**, 291–298.
- Y.-R. Lou, L. Kanninen, T. Kuisma, J. Niklander, L. A. Noon, D. Burks, A. Urtti and M. Yliperttula, *Stem Cells Dev.*, 2014, **23**, 380–392.
- M. M. Malinen, L. K. Kanninen, A. Corlu, H. M. Isoniemi, Y. R. Lou, M. L. Yliperttula and A. O. Urtti, *Biomaterials*, 2014, **35**, 5110–5121.
- L. Alexandrescu, K. Syverud, A. Gatti and G. Chingacarrasco, *Cellulose*, 2013, **20**, 1765–1775.
- M. Čolić, D. Mihajlović, A. Mathew, N. Naseri and V. Kokol, *Cellulose*, 2015, **22**, 763–778.
- K. Hua, E. Ålander, T. Lindström, A. Mihranyan, M. Strømme and N. Ferraz, *Biomacromolecules*, 2015, **16**, 2787–2795.
- Z. Wang, D. O. Carlsson, P. Tammela, K. Hua, P. Zhang, L. Nyholm and M. Strømme, *ACS Nano*, 2015, **9**, 7563–7571.
- A. Lekawa-Raus, J. Patmore, L. Kurzepa, J. Bulmer and K. Koziol, *Adv. Funct. Mater.*, 2014, **24**, 3661–3682.
- A. B. Fall, S. B. Lindström, O. Sundman, L. Ödberg and L. Wågberg, *Langmuir*, 2011, **27**, 11332–11338.
- P. T. Hammond, *Adv. Mater.*, 2004, **16**, 1271–1293.
- A. Olszewska, P. Eronen, L. S. Johansson, J. M. Malho, M. Ankerfors, T. Lindström, J. Ruokolainen, J. Laine and M. Österberg, *Cellulose*, 2011, **18**, 1213.
- Y. Xue, Z. Mou and H. Xiao, *Nanoscale*, 2017, **9**, 14758–14781.
- V. Thakur, A. Guleria, S. Kumar, S. Sharma and K. Singh, *Mater. Adv.*, 2021, **2**, 1872–1895.
- A. Skogberg, A. J. Mäki, M. Mettänen, P. Lahtinen and P. Kallio, *Biomacromolecules*, 2017, **18**, 3936–3953.
- Y. A. J. Al-Hamadani, K. H. Chu, A. Son, J. Heo, N. Her, M. Jang, C. M. Park and Y. Yoon, *Sep. Purif. Technol.*, 2015, **156**, 861–874.
- C. Salas, T. Nypelö, C. Rodriguez-Abreu, C. Carrillo and O. J. Rojas, *Curr. Opin. Colloid Interface Sci.*, 2014, **19**, 383–396.
- P. Keinänen, S. Siljander, M. Koivula, J. Sethi, E. Sarlin, J. Vuorinen and M. Kanerva, *Heliyon*, 2018, **4**, e00787.
- M. M. Hamed, A. Hajian, A. B. Fall, K. Hkansson, M. Salajkova, F. Lundell, L. Wgberg and L. A. Berglund, *ACS Nano*, 2014, **8**, 2467–2476.
- J. B. Mougél, C. Adda, P. Bertoncini, I. Capron, B. Cathala and O. Chauvet, *J. Phys. Chem. C*, 2016, **120**, 22694–22701.
- C. Olivier, C. Moreau, P. Bertoncini, H. Bizot, O. Chauvet and B. Cathala, *Langmuir*, 2012, **28**, 12463–12471.
- H. Koga, T. Saito, T. Kitaoka, M. Nogi, K. Suganuma and A. Isogai, *Biomacromolecules*, 2013, **14**, 1160–1165.
- I. Lavilla and C. Bendicho, in *Water Extraction of Bioactive Compounds*, Elsevier Inc., 2017.
- D. Yang, J.-F. Rochette and E. Sacher, *J. Phys. Chem. B*, 2005, **109**, 7788–7794.
- M. Mashkour, T. Kimura, F. Kimura, M. Mashkour and M. Tajvidi, *Biomacromolecules*, 2013, **15**, 60–65.
- K. Kartasalo, R.-P. Pölönen, M. Ojala, J. Rasku, J. Lekkala, K. Aalto-Setälä and P. Kallio, *BMC Bioinf.*, 2015, **16**, 344.
- L. M. Mariani, G. S. Vankayalapati, J. M. Conisidine and K. T. Turner, in *Mechanics of Biological Systems and Materials & Micro-and Nanomechanics*, Springer, Cham, 2019.
- T. Pöhler, T. Lappalainen, T. Tammelin, P. Eronen, P. Hiekkataipale, A. Vehniäinen and T. Koskinen, in *TAPPI International Conference on Nanotechnology ForestProduct Industry*, 2010, pp. 437–458.
- L. Lindman, G. Karlström and L. Stigsson, *J. Mol. Liq.*, 2010, **156**, 76–81.
- G. Jia, H. Wang, L. Yan, X. Wang, R. Pei, T. Yan, Y. Zhao and X. Guo, *Environ. Sci. Technol.*, 2005, **39**, 1378–1383.
- V. Pérez-Luna, C. Moreno-Aguilar, J. L. Arauz-Lara, S. Aranda-Espinoza and M. Quintana, *Sci. Rep.*, 2018, **8**, 1–11.
- C. M. Voge, M. Kariolis, R. A. MacDonald and J. P. Stegemann, *J. Biomed. Mater. Res., Part A*, 2008, **86**, 269–277.
- P. S. Goh, A. F. Ismail and B. C. Ng, *Composites, Part A*, 2014, **56**, 103–126.
- L. Bacakova, J. Pajorova, M. Tomkova, R. Matejka, A. Broz, J. Stepanovska, S. Prazak, A. Skogberg, S. Siljander and P. Kallio, *Nanomaterials*, 2020, **10**, 1–32.

- 42 J. Pajorova, A. Skogberg, D. Hadraba, A. Broz, M. Travnickova, M. Zikmundova, M. Honkanen, M. Hannula, P. Lahtinen, M. Tomkova, L. Bacakova and P. Kallio, *Biomacromolecules*, 2020, **21**, 4857–4879.
- 43 D. Kai, M. P. Prabhakaran, G. Jin and S. Ramakrishna, *J. Biomed. Mater. Res., Part B*, 2011, **98**, 379–386.
- 44 J. Bendoraitiene, R. Kavaliauskaite, R. Klimaviciute and A. Zemaitaitis, *Starch/Staerke*, 2006, **58**, 623–631.
- 45 A. Palmroth, S. Pitkänen, M. Hannula, K. Paakinaho, J. Hyttinen, S. Miettinen and M. Kellomäki, *J. R. Soc., Interface*, 2020, **17**, 20200102.



# PUBLICATION IV

## **Conductive cellulose based foam formed 3D shapes – From innovation to designed prototype**

S. Siljander, P. Keinänen, A. Ivanova, J. Lehmonen, S. Tuukkanen,  
M. Kanerva and T. Björkqvist

Materials vol. 12.3 (2019), 430

**10.3390/ma12030430**



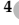

**<https://urn.fi/URN:NBN:fi:tuni-202205034296>**

**Publication reprinted with the permission of the copyright holders.**



Article

# Conductive Cellulose based Foam Formed 3D Shapes—From Innovation to Designed Prototype

Sanna Siljander <sup>1,\*</sup>, Pasi Keinänen <sup>1</sup>, Anastasia Ivanova <sup>2</sup>, Jani Lehmonen <sup>3</sup>, Sampo Tuukkanen <sup>4</sup>, Mikko Kanerva <sup>1</sup> and Tomas Björkqvist <sup>1</sup>

<sup>1</sup> Faculty of Engineering and Natural Sciences, Tampere University, P.O. Box 589, 33101 Tampere, Finland; pasi.keinanen@tuni.fi (P.K.); mikko.kanerva@tuni.fi (M.K.); tomas.bjorkqvist@tuni.fi (T.B.)

<sup>2</sup> Department of Design, Aalto University, P.O. Box 31000, 00076 Aalto, Finland; anastasia.ivanova@aalto.fi

<sup>3</sup> VTT Technical Research Centre of Finland Ltd, P.O. Box 1000, 02044 VTT, Finland; jani.lehmonen@vtt.fi

<sup>4</sup> Faculty of Medicine and Life Sciences, Tampere University; P.O. Box 589, 33101 Tampere, Finland; sampo.tuukkanen@tut.fi

\* Correspondence: sanna.siljander@tuni.fi; Tel.: +358-503555777

Received: 7 December 2018; Accepted: 18 January 2019; Published: 31 January 2019



**Abstract:** In this article, we introduce for the first time, a method to manufacture cellulose based electrically conductive non-woven three-dimensional (3D) structures using the foam forming technology. The manufacturing is carried out using a minimum amount of processing steps, materials, and hazardous chemicals. The optimized solution applies a single surfactant type and a single predefined portion for the two main processing steps: (1) the dispersing of nanocellulose (NC) and carbon nanotubes (CNT) and (2) the foam forming process. The final material system has a concentration of the used surfactant that is not only sufficient to form a stable and homogeneous nanoparticle dispersion, but it also results in stable foam in foam forming. In this way, the advantages of the foam forming process can be maximized for this application. The cellulose based composite material has a highly even distribution of CNTs over the NC network, resulting a conductivity level of 7.7 S/m, which increased to the value 8.0 S/m after surfactant removal by acetone washing. Also, the applicability and a design product case ‘Salmiakki’ were studied where the advantages of the material system were validated for a heating element application.

**Keywords:** nanocellulose; carbon nanotube; foam forming; conductivity; Salmiakki

## 1. Introduction

Scientific and industrial research communities are giving considerable attention to smart and functional materials that are based on renewable bio-based resources and are processed in eco-friendly ways. Cellulose is a very potential substance as it is a bio-based material and it can be used as a matrix when manufacturing functional structures. In addition, scientific and technological development is mature for the emergence of controlled multi-length materials that take advantage of different forms of cellulose applied in optimal ways. The added functionality requires developing new manufacturing processes and, especially, adjusting the colloid dispersion upon material production [1,2]. Our innovation is to use nanocellulose (NC) as a carrier for carbon nanotubes (CNT) in the foam forming process. In this article, we introduce for the first time a method to manufacture cellulose based non-woven three-dimensional (3D) structures that are electrically conductive. The manufacturing of the conductive non-wovens is done using a minimum amount of processing steps, materials, and hazardous chemicals. Our target is to use the selected surfactant type and amount in both the dispersion processing step and in the foam forming step. The concentration of surfactant must be sufficient to form stable and homogeneous dispersion, but it should also allow the formation of stable foam.

The foam forming process has been studied since it was invented in the 1970s [3,4]. VTT Technical Research Centre of Finland has been active in the upscaling of foam forming technology and the first dynamic foam forming studies of the upscaling process were carried out with a modified semi-pilot scale former [5]. The foam forming technology enables the production and combination of a vast variety of fibre-based materials and the application of moulding technologies to form lightweight cellulosic 3D structures. In general, the foam forming technology utilizes aqueous foam instead of water as a carrier medium and the shear thinning behaviour of the foam makes it an excellent transport medium for fibres and particles, and it enables the excellent formation of the product being produced [6,7]. In addition, the air content of the carrier foam is 60–70% and it consists of air bubbles with a diameter below 100 µm. As stated in an article [8], interest is growing in the use of aqueous foam as a transporting medium of furnishes. By using the foam forming technology, a decrease in the cost of production and material savings can be achieved [6]. Furthermore, foam forming ensures structures that have excellent formation and, when combined with moulding technology, enables lightweight structures [9–11] and completely new functional product opportunities.

The functional cellulose based matrix structure can be done by adding organic or inorganic nanostructured components. As one of the numerous options, carbon nanotubes (CNT) provide excellent electrical properties. CNTs have potential applications in electronics, for example, as interconnects [12] or energy storages [13]. The true conductivity potential of CNTs can be uncovered when the dispersing step to a liquid medium is performed properly to form a percolation network. Recent studies have revealed that the process of dispersing CNTs in a water-based system can be optimised so that the outcome functionality increases exponentially [14,15]. It is reported in those articles that, when using sonication as a dispersing process, the applied sonication energy to the dispersion and a properly selected surfactant play a key role when optimizing conductivity properties and dispersion quality. In the event, where cellulose pulp and NC-CNT dispersion are combined in the foam forming process, it is crucial to have the right concentration of surfactant to ensure there is enough air in the foam. Thus, a highly homogeneous dispersion of pulp fibres must be reached. The selection of the surfactant must be based on a systematic study to ensure that it will function as a dispersing aid in the sonication process but also form stable foam upon foam forming.

One of the most commonly used surfactants for foam forming is the anionic surfactant sodium dodecyl sulphate (SDS), which is used in many industrial applications, such as shampoos, toothpastes, and shaving creams. The motive for the wide use is its relatively low price, foam stability, easy diffusion in water and therefore it can be used in rapid foaming [16]. However, SDS might still not be the optimal surfactant, since it has been shown that SDS as a surfactant of a water-CNT system does not disperse CNTs optimally to homogeneous dispersion, even if the higher sonication energy and concentration of surfactant are used [15]. The results in the cited study also clarify that, when surfactant Triton X-100 is used, stable homogeneous CNT-water dispersion can be achieved.

When the target is to form stable and homogeneous dispersion of CNTs and nano-fibrillated cellulose, basically two alternatives of non-ionic surfactants exist, in addition to the basic case where nanocellulose itself acts as a dispersing agent [17]. Based on the current literature [14,18], Pluronic F-127 and Triton X-100 surfactants have resulted in good conductivity values when NC-CNT dispersion is used to manufacture nanocomposite films with relatively low CNT concentration. Actually, the conductivity values of the nanocomposite film can be further increased by removing the surfactant e.g., by acetone washing. This effect was seen in samples when NC and CNTs were dispersed while using surfactant Triton X-100, but not in samples that were dispersed using Pluronic F-127. The reason for this might be that Pluronic F-127 surfactant prefers nanocellulose over carbon nanotubes and, respectively, Triton X-100 prefers carbon nanotubes. Removing Triton X-100 surfactant from the interfaces improves the conductivity values.

Nanocellulose interactions with different surfactant types are reported comprehensively in the review article [19]. In general, interaction between nanocellulose and surfactant has a dependency on nanocellulose isolation procedure, which affects the surface charge and crystalline level of cellulose

structure, which results as mobility in the wet state. Surface modification is needed to achieve interaction between different phases but often this is done at the cost of a given environmental effect, which is reached using nanocellulose as a structural component in composite structures. Using nanocellulose in papermaking processes has several advanced properties: it has a high aspect ratio, high strength along with good flexibility, an interaction potential via hydrogen bonding, and a tendency to form strong entangled networks. These properties mean that a high tensile strength is attainable at relatively low concentrations, lower than 5% with respect to pulp content [20,21]. Moreover, an increase in density has also been reported when nanocellulose is added to pulp. Nanocellulose attaches to the fibre surfaces as a layer and in this way a large contact area is formed, which increases the number of hydrogen bonds [22]. Using nanocellulose as a carrier for another material is mentioned in the patent filed by Tokushu Paper Manufacturing Co Ltd. They suggested using nanocellulose in tinted papers as a carrier for a dye or pigment [23]. Research group Hii et al. have reported in their article that microfibrillated cellulose contributed to the bonding of calcium carbonate filler in the fibre network of paper [24]. Nanocellulose is also suggested to be used as a biocarrier for controlled drug delivery [25].

The application of NC-CNT dispersions in the foam forming process enables the manufacturing of conductive 3D structures to almost any shape and size. Unfortunately, because of the nanoscale size of the CNTs, the formation with cellulose pulp alone does not occur efficiently enough to form the conductive percolation network during the foam forming process. When dispersion is prepared efficiently to form homogeneous dispersion without any aggregates present, the nanosized CNT particles flow through the cellulose fibre network in the vacuum assisted moulding with the foam. Our hypothesis is that nanocellulose can be used as a carrier for carbon nanotubes. It has been reported that nanocellulose can increase the strength of non-wovens that are manufactured using the foam forming process [6] and CNTs are good candidate to replace copper and aluminium as an interconnect material in the next generation electric devices [26].

When conductivity is reached to a certain level and an electric current is passaged through the structure, which acts like a resistive conductor, the system starts to heat due to its resistivity. This phenomenon is called resistive or Joule heating. Commonly personal heating elements are manufactured by inserting copper wire inside a seat heater or heating blanket. These types of multi-material structures are difficult to recycle, and heating occurs only near the conductive material. By harnessing carbon nanotubes as a conductive material for heating elements, it is possible to manufacture structures that do not create hot spots, act as a fire retardant, and the entire volume of the structure is functional (heating). Furthermore, it is possible to customize a maximum heating temperature of the heating element by adjusting the NC-CNT dispersion quality and the amount of CNTs in the foam formed structure.

## 2. Materials and Methods

In this study, nanocellulose production was based on the mechanical disintegration of bleached hardwood kraft pulp (BHKP). First, dried commercial BHKP produced from birch was soaked in water at approximately 1.7 wt % concentration and dispersed using a high shear Ystral dissolver for 10 min at 700 rpm. The chemical pulp suspension was prerefined in Masuko grinder (Supermasscolloider MKZA10-15J, Masuko Sangyo Co., Kawaguchi, Japan) at 1500 rpm and then fluidized with eight passes through Microfluidizer (Microfluidics M-7115-30 Microfluidics Corp., Westwood, MA, USA) using 1800 MPa pressure. The final material appearance of NC was a viscous and opaque gel.

Multiwall carbon nanotubes were purchased from Nanocyl Inc. (MWCNT, Nanocyl 7000, Nanocyl SA., Sambreville, Belgium). CNTs were used as received, with-out pre-processing steps. This type of nanotubes is produced via catalytic chemical vapor deposition (CCVD).

The selection of used surfactant in this study was done based on the previous studies [14,15] and the requirement to reach an efficient foaming capability. Therefore, Triton X-100 was selected and it is a non-ionic surfactant that has a hydrophilic polyethylene oxide chain and an aromatic hydrophobic

group in its molecular structure. Triton X-100 was purchased from Sigma-Aldrich (Merck KGaA, Darmstadt, Germany).

The NC and CNT were sonicated simultaneously and after sonication no centrifuge was used so that the preparation of aqueous dispersions could be achieved using a minimum amount of processing steps. Two identical sets of NC-CNT aqueous dispersions with a total volume of 1800 mL were prepared. One set contained NC (0.15%), CNTs (0.3%), deionized water, and surfactant Triton X-100, 0.4% (Table 1). The total dry mass for the dispersions was 8.25 g. The sonication of the dispersions was performed using a tip horn ( $\varnothing$  12.7 mm) sonicator Q700 with 20 kHz frequency (QSonica LLC., Newton, CT, USA) in 2000 mL glass beakers. The sonication amplitude of vibration (50%) was kept constant. The power output remained between 50 and 60 W for both sonications. The system included a water bath to keep dispersion cool during the sonication so that temperature would not rise above 30 °C. The water bath was cooled by circulating cooling glycerol through a chiller (PerkinElmer C6 Chiller, PerkinElmer Inc., Waltham, MA, USA). Dispersions were sonicated with energy per dry mass, respectively 700 kJ/g dry mass. The energy/dry mass indicates the total applied energy, not absorbed energy by dry mass. Part of the energy is used to heat the water and part is used to disperse nanoparticles. Also, part of the energy is used to degrade the sonicator itself and the vessel, to cause defects to the nanoparticles, and some energy is used to cause several different sonochemical reactions, like disintegration and the reorganization of water molecules [15,27].

**Table 1.** Material concentrations in different processing steps.

Material	Dispersion	Foam Forming
NC	0.15%	0.1%
CNT	0.3%	0.2%
Surfactant Triton X-100	0.4%	0.25%
Pulp	-	0.35%
Total volume	1800 mL	5500 mL

The cellulosic fiber material used in this study was gently refined bleached kraft pulp (Scots pine 3.7% dry mass), as obtained from a Finnish pulp mill.

In the foam forming process, two sets of NC-CNT dispersion each volume of 1800 mL were poured in to the foam forming 32 cm diameter cylindrical tank (Figure 1a), followed by water and pulp, so that total volume was 5.5 litres (Figure 1b). Concentrations of materials are listed in Table 1. Mechanical mixing was carried out at a rotation speed of 3500 rpm for 3.5 min. Foaming time resulted in 70% air content to the foam, meaning that the total foam volume was 19 l. The prepared foam containing NC-CNT and pulp was poured into a planar mould that has a perforated surface with area of 0.19 m<sup>2</sup>, so that sheet formed 3D structure has a grammage of 100 g/m<sup>2</sup>. Wet foam was removed using 0.5 bar vacuum suction and for maintaining constant local suction plastic film was placed on the top of the foam column. After vacuum assisted foam removal the 3D cellulosic fiber sheet was dried in a thermal cabinet at 70 °C for 12 h until dry. Also, reference sheets using bleached kraft pulp and Triton X-100 surfactant were processed using the same procedure.



**Figure 1.** (a) Laboratory scale foam forming equipment; (b) nanocellulose-carbon nanotubes (NC-CNT) dispersion, pulp, and water mixture before foaming.

The electrical conductivity of the foam formed non-wovens were measured using the four-probe measuring technique. With this method, it is possible to neglect the effect of contact resistances and thus provide more accurate conductivity measurements than using two-terminal measurement. The sheet resistances of prepared and cut foam formed non-wovens (size 30 mm × 30 mm) were measured using a four-point probe setup made in-house and a multimeter (Keithley 2002, Tektronix, Inc., Beaverton, OR, USA) in four-wire mode. The probes were placed in line, with equal 3 mm spacing. The four-probe setup is described elsewhere in detail [28]. The conductivity measurements were carried out using a 1 mA current and voltage was measured. Measurements were taken before and after the remaining surfactant was removed from samples by washing them in appropriate amount of acetone in room temperature (RT).

The mechanical testing (Testometric M500-25kN, Testometric Co Ltd, Rochdale, UK) of foam formed samples was done according to the standard EN 29073-3:1992 “Textiles. Test methods for non-wovens, Part 3: Determination of tensile strength and elongation”. From the foam formed non-wovens, ten sample pieces in total were cut (50 mm × 250 mm). Five of them were tested as such, while another set of five samples was washed in an appropriate amount of acetone in RT, so that the remaining surfactant Triton X-100 was removed. In general, the removal of surfactants from various nanocomposites can enhance the mechanical and electrical properties [14,29]. All of the non-woven samples were conditioned according to the standard ISO 139 before the tensile testing. The testing was performed by applying a constant rate of extension of 100 mm/min.

### 3. Results and Discussion

SEM imaging (FE-SEM, 3 kW, Zeiss ULTRAplus, Oberkochen, Germany) was used to investigate the CNT distribution in the foam formed non-wovens. The SEM images have been taken from a dry sample and the NC has generated a network where the dimensions for individual fibers are very difficult to determine. Two different magnifications in Figure 2 are illustrating the NC and the CNT interaction, and the formation of a homogeneous CNT coverage over cellulose fibers. Figure 2b describes a type of CNT coating on NC: the coverage has excellent distribution over the surface. This means that the dispersion process using the specific sonication parameters has been successful and a conductive percolation network of CNTs is formed.

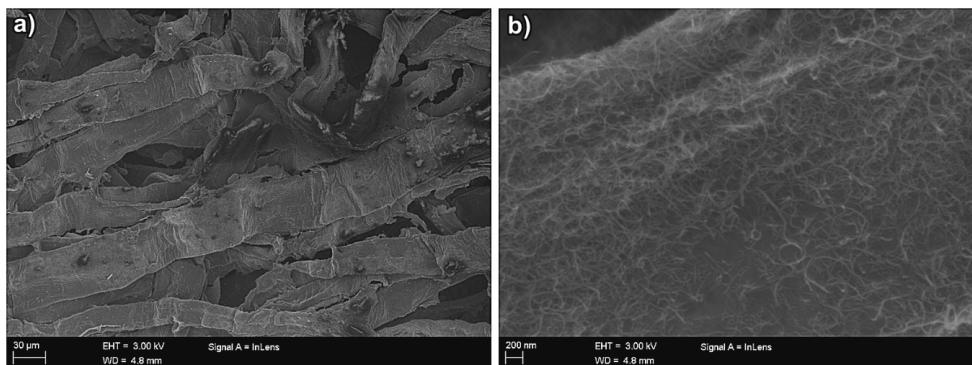


**Figure 2.** (a) Homogenous CNT coverage over cellulose fibers and (b) carbon nanotube percolation network on the surface of cellulose fiber.

The electrical conductivity and tensile testing of the foam formed non-woven material was measured before and after the removal of the surfactant. The non-woven material containing surfactant was determined to possess a conductivity of 7.7 S/m ( $\pm 1.32$ ). After the removal of the surfactant, conductivity increases to a value of 8.0 S/m ( $\pm 1.34$ ). The mechanical strength of the formed non-woven material is of essential importance for any practical application. Here, the tensile strength of the foam formed non-woven was 121 N ( $\pm 11.8$ ). After surfactant was removed, the strength increased to a value of 142 N ( $\pm 6.1$ ). In comparison, the tensile strength for foam formed reference non-woven made using the wood pulp, without nanocellulose or carbon nanotubes, is 9.4 N ( $\pm 0.5$ ), and after acetone washing, to remove the surfactant, the value increased to 16.5 ( $\pm 1.7$ ). This shows that nanocellulose and carbon nanotubes also increase the tensile strength of the non-woven composite structure. Also, the mechanical strength was expected to increase after removal of the surfactant, due to the increased entanglement and interactions of nanocellulose and carbon nanotubes.

The effect of surfactant removal by acetone washing is minimal to mechanical strength and conductivity values. The reason for this might be that a majority of the surfactant is already removed from the structure during the vacuum assisted moulding process. Results also show that adding NC-CNT dispersion in the foam forming procedure with wood pulp will increase the tensile values of the manufactured non-wovens. This three material system has over ten times higher tensile strength compared to one material pulp system when residue surfactant is still present in the non-woven structure.

The conductivity and mechanical performance of the final parameter set for the preparation led to results encouraging to the actual application verification. The high conductivity as well as mechanical strength mean that it is possible to manufacture conductive non-woven and utilize the innovated material system by using only two processing steps: (1) the sonication of the NC-CNT dispersion and (2) the foam forming of the final non-woven 3D structure.



#### 4. Verification and Validation of Applicability: Heating Element “Salmiakki”

The verification study was carried out to manufacture a conductive 3D structure of a selected prototype using foam forming. The collaboration between designer and materials scientists has undergone the following steps:

1. Design briefing and setting the objective: a heating element
2. Research: material properties, benchmarking
3. Product innovation: user profiling (business case), user experience scenarios, product ideas, initial sketching, evaluation discussion, decision on the product features—heating element for indoor use and a device of a portable size and modular structure
4. Product design development: further sketching and paper mock-ups, evaluation discussion, decision on the visual form, clarifying the material specifications, testing of the material properties needed for the prototype manufacturing, CAD modelling, mold development for the foam forming process
5. Manufacturing and testing the prototype
6. Realistic rendering images of CAD model in interior settings
7. Establishing the outcomes of the collaborative process

Salmiakki, the heating element design taking advantage of conductive cellulose-based composite, is a result of close collaboration between a designer (A. Ivanova) and materials research scientists (S. Siljander and J. Lehmonen). The funding and targets of the product were a subtask in the national Design Driven Value Chains in the World of Cellulose (DWOc 2.0) project ([www.cellulosefromfinland.fi](http://www.cellulosefromfinland.fi)). The objective was set to define the design of an electrical current-based heating element from newly developed conductive material that highlights the advantageous properties of this novel material and its production, provides a clear understanding of its future application possibilities, and emphasizes the local origin of raw materials that are used in the composite production. While features, such as high conductivity, no metal wires inside, temperature adjustability, mouldability, fire safety, light weight, soft material feeling, and recyclability make this material suitable for a variety of applications, several limiting factors, including restrictions in shape and color variations, needed to be considered to aim for the best performance and outlook.

Prior to the product ideation, a design research was conducted, which included benchmarking of existing indoor heating solutions, electrically-powered solutions, and solutions incorporating biomaterials. Benchmarking showed that a diverse variety of electrical interior heating designs are available on the market, however, biomaterials are seemingly not used for this type of applications. Based on a survey, no other product on the market offered bio-based, biodegradable indoor heating product solution with flexible temperature adjustment, and fabric-like tactile properties.

Product innovation was launched via creation of different user profiles. No in-depth user study was conducted prior to profile creation; the aim of profiles “personas”, was to serve as inspiration in the innovation and sketching the design process whilst helping to envision environments and situations where potential product’s users would benefit from the properties of conductive cellulose-based composite material. For instance, in addition to heating, such device could be used to keep places dry, serve as an acoustic element or room divider, and have a decorative purpose. As well as in home interiors, it could be used inside boats, cars, campervans, or other spaces that are protected from direct contact with water. Consequently, the decision was made to design a compact heating element of portable size and modular format, for indoor usage.

Visual design was initially carried out through the creation of sketches and scaled mock-ups, followed by full-scale paper models, which were discussed at the evaluation phase. Each paper model was considered for its functional and perceptual attributes, resulting in the choice of a diamond-like shape that has got the name “Salmiakki” due to its resemblance in shape and black color to a traditional Finnish candy.

For Salmiakki to be developed into a functional prototype, technical configurations of the material, direction of the electric current, and additional functional elements of the future heating device were outlined and observed when a CAD model was drawn. The CAD model was created for two major purposes: (1) to prepare a digital file for CNC-machinery of the mould for foam-forming process and (2) to create realistic 3D drawings to visualize the concept and plan modular compositions.

In order to manufacture the prototype a mould for foam forming process was sized and prepared. As a reference, the process of mould design for foam-formed cellulose fiber materials was considered, as described by Härkäsalmi et al. To ensure successful formability during the foam-forming process, the mould must have a sturdy structure withstanding the vacuum pressure (suction), and correct permeability allowing for water to pass through while capturing the cellulose fibers [8]. To achieve this, the structure was designed to consist of two parts, both being female moulds: load-bearing supporting structure machined from polystyrene foam and a smooth surface layer with micro-perforation, vacuum-formed from a polypropylene sheet with a 1.5 mm thickness. The prototype was manufactured at pilot plant of VTT Technical Research Centre of Finland located in the City of Jyväskylä.

Material concentrations and methods used were the same as in foam forming 3D sheets, only pulp concentration was increased to 85 g dry mass, meaning a concentration of 1.5% in foam forming. In Figure 3, a schematic flow of manufacturing of heating element Salmiakki is presented.

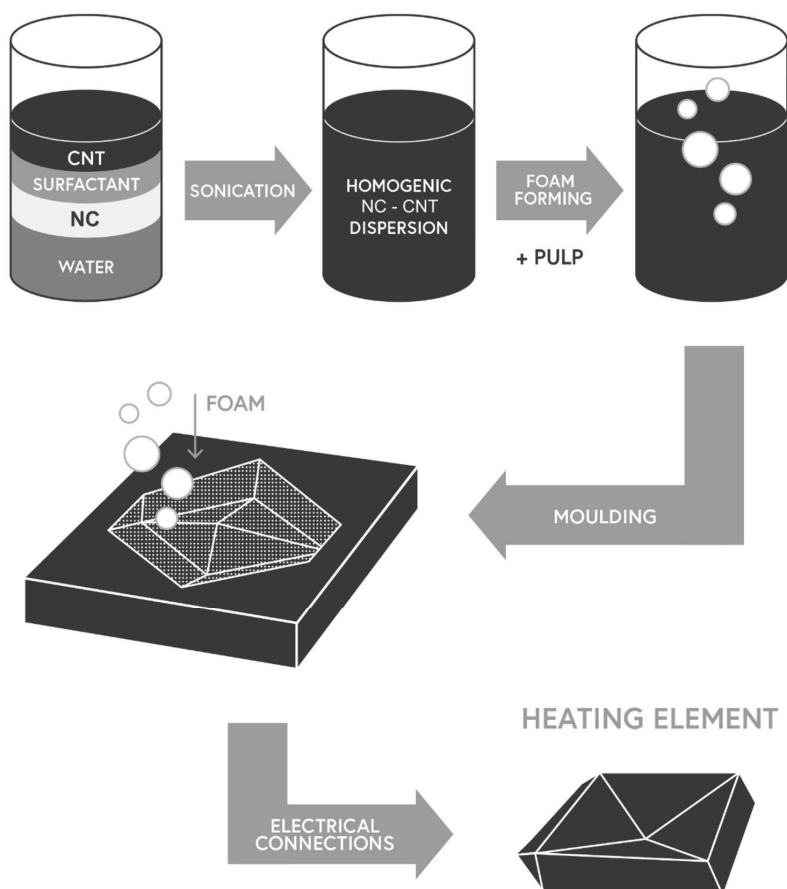


**Figure 3.** Manufacturing process of heating element prototype Salmiakki.

The sheet resistivity of the manufactured 3D shape was measured using the four-probe method before and after acetone washing. Average sheet resistances with standard deviation were, when measurements were performed from eight sample locations,  $26.1 \Omega/\text{sq}$  ( $\pm 2.7$ ), and after acetone washing,  $25.8 \Omega/\text{sq}$  ( $\pm 2.0$ ). Acetone washing did not decrease resistivity much, meaning that there is minimum amount of surfactant present in the structure that does not alter the conductivity of the carbon nanotubes. A post treatment option was studied to enhance the visual features and the conductivity. The final 3D structure was coated by the spray of NC-CNT dispersion that resulted darker, black finish and alongside, enhanced heating properties at a lower electrical voltage. If all electric energy  $P$  is converted into heat, then heater temperature can be evaluated using Joule's first law of heating  $P = U^2 \times R^{-1}$ , where  $U$  (electric voltage input, V) and  $R$  (resistance,  $\Omega$ ). Using the electric voltage input of 18.5 V with the resistivity of  $25.8 \Omega/\text{sq}$ , electric power of heating element is 13.2 W. After the post treatment spray layer of NC-CNT dispersion, the resistivity decreased to value  $11.2 \Omega/\text{sq}$  ( $\pm 0.9$ ), meaning that electric power is 30.6 W.

Finally, the cellulose fiber-based heating element was mounted in a plywood cover that was painted black using wood wax (Osmo Color 3169, Osmo Holz und Color GmbH & Co, Warendorf, Germany). The surface of the Salmiakki heating element was sprayed with varnish to gain glossy surface (Dupli-color Lackspray, Wolvega, Netherland) and electrical connections were installed. Copper tape forming the electrical connection are located on the opposing sides of the prototype Salmiakki and covering  $18 \text{ cm}^2$  area per side. The distance between these copper connectors is 22 cm. As a power source Salmiakki is using 18.5 V, 3.5 A laptop charger (HP, Palo Alto, CA, USA). Infrared camera imaging was performed using a thermal camera (Fluke Ti400, Everett, WA, USA). In Figure 4, it can be observed that the temperature near copper tape conductors is  $65\text{--}75 \text{ }^\circ\text{C}$  and a major part of Salmiakki heating element is heated to a comfortable  $35\text{--}45 \text{ }^\circ\text{C}$  temperature at steady state in room temperature. Because of rapid heating and cooling properties of CNTs, the heating response of the whole element to steady state is in the order of minutes.

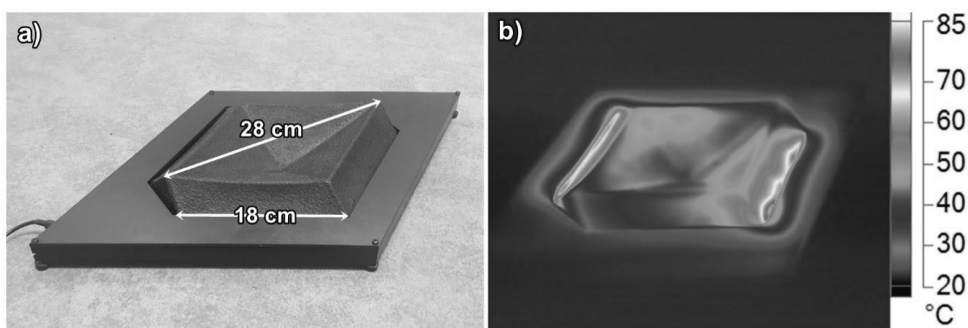


**Figure 4.** (a) Visual image of plywood mounted Salmiakki with dimensions and (b) Infrared camera image of heating element prototype Salmiakki at steady state in room temperature.

When calculated, based on the known pricing of raw materials', the total costs of Salmiakki heating element count less than four euros to manufacture the object (foaming plant investments not accounted for). In addition to the physical prototype, digital models that were rendered as realistic images of the heating element in use were produced to demonstrate how various modular compositions may be applied with various interior settings (see Figure 5).



**Figure 5.** Digital models of Salmiakki heating element.

The verification of the applicability via collaborative design, materials research, and prototype manufacturing process resulted in the following valid outcomes:

- Better understanding of application properties and overall possibilities of the novel conductive material
- Testing the foam-forming process of the conductive material into a complex three-dimensional object
- Effective dissemination of the research results for high technology readiness level (TRL) 6-7 through exhibiting of the physical prototype and sharing the digitally produced images.
- Deeper perspective of understanding the potential and possibilities of foam forming for producing functional 3D-structures.

## 5. Conclusions

This work focuses on the analysis of conductivity and mechanical strength of NC, CNT, and cellulose pulp based non-woven composite structure. Secondly, application of the foam forming process to prepare conductive non-woven sheets, where nanocellulose acts as a carrier for carbon nanotubes, is studied. Finally, the TRL 6-7 verification and validation programme is reported to establish industrial potential. The results show that it is possible to improve the surfactant selection, the sonication process of the NC-CNT dispersion, and foam forming to achieve the highly even coverage of CNT over the NC network, resulting in very high conductivity of 7.7 S/m. The effect of surfactant removal by acetone washing was studied, but the effects were not significant on the measured mechanical strength and conductivity values. Reason for this might be that the majority of surfactant is removed already during the vacuum assisted moulding process. The applicability and a design product case ‘Salmiakki’ were studied and the advantages of the material system were validated for a heating element application. The product case showed that it is possible to manufacture designed 3D heating element using a minimum amount of materials, processing steps, and hazardous chemicals.

These results mean that it is possible to manufacture conductive non-woven and utilize our innovation using only two processing steps: sonication of the NC-CNT dispersion and foam forming of the 3D structure. The whole process can be done using a minimum amount of materials and hazardous chemicals.

**Author Contributions:** S.S., P.K., A.I. and J.L. conceived and designed the experiments; S.S., P.K., A.I., J.L., and S.T. performed the experiments and analyzed the data; J.L. and A.I. contributed materials; S.S., P.K., A.I., J.L., S.T., M.K. and T.B. wrote the paper. M.K. and T.B. coordinated the projects aims in accordance to publication specific actions and delegation.

**Funding:** This work was funded by Tekes (Finnish Funding Agency for Innovation) through a strategic opening entitled Design Driven Value Chains in the World of Cellulose (DWoC 2.0) and Pirkanmaan liitto through project entitled BioÄly.

**Acknowledgments:** We acknowledge the contributions of Panu Lahtinen for cellulosic nanomaterial, Essi Sarlin for SEM imaging, Teija Joki for mechanical testing, Markus Kakkonen and Olli Tanhuanpää for all their help with manufacturing the heating element prototype “Salmiakki”.

**Conflicts of Interest:** The authors declare no conflict of interest.

## References

1. Klemm, D.; Schumann, D.; Kramer, F.; Hebler, N.; Koth, D.; Sultanova, B. Nanocellulose materials—Different cellulose, different functionality. *Macromol. Symp.* **2009**, *280*, 60–71. [CrossRef]
2. Du, X.; Zhang, Z.; Liu, W.; Deng, Y. Nanocellulose-based conductive materials and their emerging applications in energy devices—A review. *Nano Energy* **2017**, *35*, 299–320. [CrossRef]
3. Radvan, B.; Gatward, A.P.J. The Formation of wet-laid webs by a foaming process. *TAPPI J.* **1972**, *55*, 748.
4. Punton, V.W. The use of an aqueous foam as a fibre-suspending medium in quality papermaking. In *Proceedings of a Symposium Organized by the Society of Chemical Industry. Colloid and Surface Chemistry Group, and Held at Brunel University*; Society of chemical industry: London, UK, 1975.
5. Lehmonen, J.; Jetsu, P.; Kinnunen, K.; Hjelt, T. Potential of foam-laid forming technology in paper applications. *Nord. Pulp Pap. Res. J.* **2013**, 392–398. [CrossRef]
6. Kinnunen, K.; Lehmonen, J.; Beletski, N.; Jetsu, P.; Hjelt, T. Benefits of foam forming technology and its applicability in high MFC addition structures. In *Proceedings of the 15th Pulp and Paper Fundamental Research Symposium*, Cambridge, UK, 8–13 October 2013.
7. Smith, M.K.; Punton, V.W. Foam can improve formation. *Pulp Pap. Canada* **1975**, *76*, 55–58.
8. Härkäsalmi, T.; Lehmonen, J.; Itälä, J.; Peralta, C.; Siljander, S.; Ketoja, J.A. Design-driven integrated development of technical and perceptual qualities in foam-formed cellulose fibre materials. *Cellulose* **2017**, *24*. [CrossRef]
9. Madani, A.; Zeinoddini, S.; Varahmi, S.; Turnbull, H.; Phillion, A.B.; Olson, J.A.; Martinez, D.M. Ultra-lightweight paper foams: Processing and properties. *Cellulose* **2014**, *21*, 2023–2031. [CrossRef]
10. Alimadadi, M.; Uesaka, T. 3D-oriented fiber networks made by foam forming. *Cellulose* **2016**, *23*, 661–671. [CrossRef]
11. Haffner, B.; Dunne, F.F.; Burke, S.R.; Hutzler, S. Ageing of fibre-laden aqueous foams. *Cellulose* **2017**, *24*, 231–239. [CrossRef]
12. Tuukkanen, S.; Streiff, S.; Chenevier, P.; Pinault, M.; Jeong, H.J.; Enouz-Vedrenne, S.; Cojocar, C.S.; Pribat, D.; Bourgoin, J.P. Toward full carbon interconnects: High conductivity of individual carbon nanotube to carbon nanotube regrowth junctions. *Appl. Phys. Lett.* **2009**, *95*. [CrossRef]
13. Tuukkanen, S.; Välimäki, M.; Lehtimäki, S.; Vuorinen, T.; Lupo, D. Behaviour of one-step spray-coated carbon nanotube supercapacitor in ambient light harvester circuit with printed organic solar cell and electrochromic display. *Sci. Rep.* **2016**, *6*, 1–9. [CrossRef] [PubMed]
14. Siljander, S.; Keinänen, P.; Rätty, A.; Ramakrishnan, K.R.; Tuukkanen, S.; Kunnari, V.; Harlin, A.; Vuorinen, J.; Kanerva, M. Effect of surfactant type and sonication energy on the electrical conductivity properties of nanocellulose-CNT nanocomposite films. *Int. J. Mol. Sci.* **2018**, *19*. [CrossRef] [PubMed]
15. Keinänen, P.; Siljander, S.; Koivula, M.; Sethi, J.; Sarlin, E.; Vuorinen, J.; Kanerva, M. Optimized dispersion quality of aqueous carbon nanotube colloids as a function of sonochemical yield and surfactant/CNT ratio. *Heliyon* **2018**, *4*, e00787. [CrossRef] [PubMed]
16. Al-Qararah, A.M. *Aqueous Foam as the Carrier Phase in the Deposition of Fibre Networks*; University of Jyväskylä: Jyväskylä, Finland, 2015.
17. Hajian, A.; Lindström, S.B.; Pettersson, T.; Hamed, M.M.; Wågberg, L. Understanding the Dispersive Action of Nanocellulose for Carbon Nanomaterials. *Nano Lett.* **2017**, *17*, 1439–1447. [CrossRef] [PubMed]
18. Rätty, A. Electro-mechanical integrity of nanocellulose-carbon nanotube films. Master’s Thesis, Tampere University of Technology, Tampere, Finland, 2017.
19. Tardy, B.L.; Yokota, S.; Ago, M.; Xiang, W.; Kondo, T.; Bordes, R.; Rojas, O.J. Nanocellulose–surfactant interactions. *Curr. Opin. Colloid Interface Sci.* **2017**, *29*, 57–67. [CrossRef]
20. Boufi, S.; González, I.; Delgado-Aguilar, M.; Tarrès, Q.; Mutjé, P. Nanofibrillated Cellulose as an Additive in Papermaking Process. In *Cellulose-Reinforced Nanofibre Composites Production, Properties and Applications*; Elsevier: Amsterdam, Netherlands, 2017; ISBN 9780081009659.

21. Kajanto, I.; Kosonen, M. The potential use of micro- and nanofibrillated cellulose as a reinforcement element in paper. *J. Sci. Technol. For. Prod. Process.* **2012**, *2*, 42–48.
22. Brodin, F.W.; Gregersen, Ø.W.; Syverud, K. Cellulose nanofibrils: Challenges and possibilities as a paper additive or coating material—A review. *Nord. Pulp Pap. Res. J.* **2014**, *29*, 156–166. [CrossRef]
23. Matsuda, Y.; Hirose, M.; Ueno, K. Super microfibrillated cellulose, process for producing the same, and coated paper and tinted paper using the same. United States Patent US 6183596 B1, 7 April 1995.
24. Hii, C.; Gregersen, Ø.W.; Chinga-Carrasco, G.; Eriksen, Ø. The effect of MFC on the pressability and paper properties of TMP and GCC based sheets. *Nord. Pulp Pap. Res. J.* **2012**, *27*, 388–396. [CrossRef]
25. Plackett, D.V.; Letchford, K.; Jackson, J.K.; Burt, H.M.; Jackson, J.; Burt, H. A review of nanocellulose as a novel vehicle for drug delivery. *Nord. Pulp Paper Res. J.* **2014**, *29*, 105–118. [CrossRef]
26. Ragab, T.; Basaran, C. Joule heating in single-walled carbon nanotubes. *J. Appl. Phys.* **2009**, *106*. [CrossRef]
27. Koda, S.; Kimura, T.; Kondo, T.; Mitome, H. A standard method to calibrate sonochemical efficiency of an individual reaction system. *Ultrason. Sonochem.* **2003**, *10*, 149–156. [CrossRef]
28. Rajala, S.; Tuukkanen, S.; Halttunen, J. Characteristics of piezoelectric polymer film sensors with solution-processable graphene-based electrode materials. *IEEE Sens. J.* **2015**, *15*, 1–8. [CrossRef]
29. Keinänen, P.; Das, A.; Vuorinen, J. Further Enhancement of Mechanical Properties of Conducting Rubber Composites Based on Multiwalled Carbon Nanotubes and Nitrile Rubber by Solvent Treatment. *Materials (Basel)* **2018**, *11*, 1806. [CrossRef]



© 2019 by the authors. Licensee MDPI, Basel, Switzerland. This article is an open access article distributed under the terms and conditions of the Creative Commons Attribution (CC BY) license (<http://creativecommons.org/licenses/by/4.0/>).



